

ENVIRONMENTAL IMPACT STATEMENT

Nautilus Minerals Niugini Limited

Solwara 1 Project

Volume B
Appendices 8 - 15

September 2008
CR 7008_9_v4

ENVIRONMENTAL IMPACT STATEMENT

Solwara 1 Project

VOLUME B

APPENDICES 8 - 15

CR 7008_09_v4
September 2008



Project director	David Gwyther	
Project manager	Michael Wright	
Version:	Details:	Approved:
CR 7008_09_v1	Initial draft to client	July 2008
CR 7008_09_v2	Second draft to client	August 2008
CR 7008_09_v3	Third draft to client	September 2008
CR 7008_09_v4	Final for exhibition	September 2008

Appendices

- Appendices 1 to 3:
- 1 Baseline Environmental Study Eastern Manus Basin, Papua New Guinea – Module 1 Preliminary Scoping Study
 - 2 Baseline Environmental Study Eastern Manus Basin, Papua New Guinea – Module 2 Detailed Scoping Study
 - 3 Oceanography at Solwara 1
- Appendices 4 to 7:
- 4 Characterization and comparison of macrofauna at inactive and active sulphide mounds at Solwara 1 and South Su (Manus Basin)
 - 5 Macroinfauna of Active and Inactive Hydrothermal Sediments From Solwara 1 and South Su, Manus Basin, Papua New Guinea
 - 6 Quality Including Trace Elements of Sediments from the SuSu Knolls, Manus Basin, Bismarck Sea, Papua New Guinea
 - 7 Water and Sediment Characterisation and Toxicity Assessment for the Solwara 1 Project
- Appendices 8 to 15:
- 8 Juvenile Amphipod Whole Sediment Test Report
 - 9 Elutriate Testing Report Solwara 1 Project, Incorporating Phase 1: Effect of Holding Time; Phase 2: Effect of Temperature
 - 10 Biomass, Biodiversity and Bioaccumulation Desktop Study
 - 11 Modelling the Dispersion and Settlement of Sediment Removal Operation Prior to Mining at the Solwara 1 Mining Lease, Papua New Guinea
 - 12 Modelling the Dispersion of the Returned Water Discharge Plume from the Solwara 1 Seabed Mining Project Manus Basin, Papua New Guinea
 - 13 Prediction of underwater noise associated with a proposed deep-sea mining operation in the Bismarck Sea
 - 14 The Potential for Natural Disasters being Triggered by Mineral Extraction at the Solwara 1 Seafloor Hydrothermal Vent Site
 - 15 Stakeholder Consultation

Appendix 8

Juvenile Amphipod Whole Sediment Test Report



Juvenile Amphipod Whole Sediment Test Report MpL 020508

Client: Coffey Natural Systems
Project: Solwara
Test Performed: 10-day survival whole-sediment toxicity test using the juvenile amphipod *Melita plumulosa*

Test Method

This acute test measures the survival of juvenile amphipods (*Melita plumulosa*) following exposure to test sediments over a 10-day period. This test was carried out according to the protocols described in Simpson et al. (2005) and King et al. (2006). Sediments were homogenised immediately prior to being added to test beakers (38-40 g sediment per beaker, 5 replicates per sediment). Filtered seawater (30‰) was added, and each beaker was incubated at 21 °C with aeration overnight to allow sediments to settle. The following day, overlying water was replaced and 15 amphipods (7-14 days old) were randomly assigned to each beaker. Amphipods used in the tests were obtained from laboratory cultures. Treatments were fed 0.063 mg Sera micron fish food/juvenile every 3 days. Overlying water temperature, pH, salinity and dissolved oxygen were measured throughout the 10-day test. The number of surviving amphipods in each beaker was recorded after 10 days, and sediments were also stained to ensure full recovery of all surviving amphipods. Results are expressed as a percentage of the survival in the diluent control sediment. Also on day 10, three sub-samples were taken from each dilution, filtered (0.45 µm), acidified (2% Tracepure HNO₃) and analysed by ICP-AES for dissolved metals. A reference toxicant test (96-h water exposure to copper), using the same batch of juveniles, was carried out concurrently with the whole sediment tests. The median lethal concentration (LC50) and the 95% confidence limits were estimated by Maximum Likelihood Regression using Probit Analysis with Abbotts correction (Toxcalc, Version 5.0.23C).

Sample Preparation

Samples Collected:		
Samples Received:	13/03/2008	Test Initiated: 22/04/2008
CSIRO Sample No.	Sample Name	Sample Description
WQE08070	A10988	Dry silty sand

The sample was stored at 4°C and homogenised immediately prior to use in the test. Dilutions of the Solwara sediment were prepared by combining the dry 100% Solwara sediment (A10988) and the clean dry diluent sediment (sand) to achieve the required percentage by weight.

Results

Physico-chemical properties

Particle Size Distribution of the Solwara Sediment and the Dilutions

Test Material	Size Fractionation (%)			Comments
	< 63 µm	63-180 µm	>180 µm	
Diluent sediment	0	1	99	
1% Solwara Sediment	0	1	99	
5% Solwara Sediment	1	1	98	
10% Solwara Sediment	2	2	96	
33% Solwara Sediment	5	5	90	
100% Solwara Sediment	14	14	72	

10-day Survival of *M. plumulosa*

The Solwara sediment (A10988) was toxic to survival of *M. plumulosa* for all dilutions tested. The LC50 of the Solwara sediment was 4.3 (3.4-5.3) % and the NOEC was <1%.

Test Material	10-day Survival (% of Diluent Control)	Standard Error
Diluent sediment	100	0
1% Solwara sediment	84*	3
5% Solwara sediment	51*	3
10% Solwara sediment	28*	4
33% Solwara sediment	1*	1
100% Solwara sediment	1*	1
LC50 (95% CI)	4.3 (3.4 - 5.3)	

* Significantly different from the diluent control (p<0.05).

10-day Dissolved Metals in the Overlying Water

Dissolved copper concentrations in the overlying water from the 10, 33% and 100% Solwara sediment exceeded the 4-day Cu LC50 value of 221 µg/L for juvenile *M. plumulosa* in a water-only exposure, suggesting that release of copper (and potentially other metals) into the overlying waters may have contributed to the toxicity of the Solwara sediment.

Sample	Concentration (µg/L)											
	Ag	Al	As	Cd	Co	Cr	Cu	Fe	Mn	Ni	Pb	Zn
0% sediment	<3	<5	<10	<3	<3	<3	<3	<5	<3	<3	<10	<3
1% sediment	<3	<5	<10	<3	8.0	<3	65	<5	25	<3	<10	34
5% sediment	<3	<5	<10	4.3	34	<3	150	<5	42	<3	<10	170
10% sediment	<3	<5	<10	7.7	70	<3	290	<5	56	<3	<10	450
33% sediment	<3	<5	<10	22	160	<3	390	29	94	4.5	12	1200
100% sediment	<3	<5	<10	49	460	<3	1400	88	240	46	830	9500

For full dissolved metals analyses refer to 'Dissolved metals report for Solwara'.

Quality Assurance/Quality Control

Criteria	Range	Criterion Met?
≥80% survival in sediment control	100%	Yes
96-h reference toxicant LC50 (221 ± 46 µg Cu/L)	187 (158-218)	Yes
pH of overlying water in test beakers	8.0 ± 0.2	Yes
Salinity of overlying water in test beakers	30 ± 2‰	Yes
Dissolved oxygen in overlying water in test beakers	>80%	Yes
Temperature of overlying water in test beakers	21 ± 1°C	Yes

References

ANZECC/ARMCANZ (2000). Australian and New Zealand Guidelines for Fresh and Marine Water Quality. Volume 1. The Guidelines, Australian and New Zealand Environment and Conservation Council and Agriculture and Resource Management Council of Australia and New Zealand.

King, C.K., Gale, S.A. and Stauber, J.L. (2006) Acute toxicity and bioaccumulation of aqueous and sediment-bound metals in the estuarine amphipod *melita plumulosa*. *Environmental Toxicology*, 21, 489-504.

Simpson, S.L., Batley, G.E., Chariton, A.A., Stauber, J.L., King, C.K., Chapman, J.C., Hyne, R.V., Gale, S.A., Roach, A.C. and Maher, W.A. (2005). *Handbook for Sediment Quality Assessment* (CSIRO: Bangor, NSW). ISBN 0-643-09197-1.

Spadaro, D.A., Micevska, T., Simpson, S.L. (2008). Effect of nutrition on toxicity of contaminants to the epibenthic amphipod, *Melita plumulosa*. Archives of Environmental Contamination and Toxicology, (submitted).

ToxCalc. 1994. ToxCalc Users Guide. Comprehensive toxicity data analysis and database software, Version 5.0.23C. Tidepool Scientific Software, McKinleyville, CA, USA.

Testing and Reporting

Test carried out and report prepared by:

David Spadaro
Experimental Scientist (ph: 02 9710 6801)

Test report authorised by:

Dr Jenny Stauber
Senior Principal Research Scientist (ph: 02 9710 6808)

Date:

8/05/2008



Centre for Environmental Contaminants Research (CECR)

CSIRO Land and Water (CLW)
New Illawarra Road, Lucas Heights, NSW
Private Mail Bag 7, Bangor, NSW, 2234, Australia
Telephone 61 2 9710 6808 Fax 61 2 9710 6837

Page 1 of 4

Dissolved Metals in Waters: Analyses by ICP-AES

Subject: Dissolved metals in waters

Client: Anne-Maree Goldman, Coffey

Details: Dissolved metals in waters at end of toxicity tests (measured by ICP-AES)

Enquiries: Stuart Simpson
CSIRO Centre for Environmental Contaminants Research
New Illawarra Road, Lucas Heights,
Private Mail Bag 7, Bangor, NSW 2234
Tel. +61-2-9710-6807, Fax. +61-2-9710-6837
Email: Stuart.Simpson@csiro.au



Centre for Environmental Contaminants Research (CECR)

CSIRO Land and Water (CLW)
New Illawarra Road, Lucas Heights, NSW
Private Mail Bag 7, Bangor, NSW, 2234, Australia
Telephone 61 2 9710 6808 Fax 61 2 9710 6837

Page 2 of 4

Dissolved Metals in Waters: Analyses by ICP-AES

Metal analyses by inductively coupled plasma atomic emission spectroscopy

Trace metal concentrations in the final digest solutions were measured using inductively coupled plasma atomic emission spectroscopy (Spectroflame EOP, SPECTRO Analytical Instruments, Kleve, Germany) calibrated with commercially available standards (Plasma Chem, Farmingdale, NJ, USA).



Centre for Environmental Contaminants Research (CECR)

CSIRO Land and Water (CLW)
 New Illawarra Road, Lucas Heights, NSW
 Private Mail Bag 7, Bangor, NSW, 2234, Australia
 Telephone 61 2 9710 6808 Fax 61 2 9710 6837

Dissolved Metals in Waters: Analyses by ICP-AES

Quality Control:

Method blanks prepared using the standard procedure in the absence of sample.

Concentrations in µg/L

Blanks	Ag	Al	As	Cd	Co	Cr	Cu	Fe	Mn	Ni	Pb	Zn
Seawater blank 1	<3	<5	<10	<3	<3	<3	<3	<5	<3	<3	<10	9
Seawater blank 2	<3	<5	<10	<3	<3	<3	<3	<5	<3	<3	<10	11

Duplicates of field-collected samples

Concentrations in µg/L

Duplicates	Ag	Al	As	Cd	Co	Cr	Cu	Fe	Mn	Ni	Pb	Zn
5% 'sediment'	<3	<5	<10	4	33	<3	160	<5	41	<3	<10	180
5% 'sediment'	<3	<5	<10	4	33	<3	160	<5	41	<3	<10	180
5% 'sediment'	<3	<5	<10	5	35	<3	150	<5	42	<3	<10	180
10% 'sediment'	<3	<5	<10	8	70	<3	290	<5	56	<3	<10	450
10% 'sediment'	<3	<5	<10	8	68	<3	290	<5	56	<3	<10	450
10% 'sediment'	<3	<5	<10	8	72	<3	290	<5	56	<3	<10	450

Spike-recoveries for ICP-AES analyses

Samples (seawater) were spiked with to 35 µg/L mixed-metals solution and recoveries determined

Percent recovery, %

Sample	Ag	Al	As	Cd	Co	Cr	Cu	Fe	Mn	Ni	Pb	Zn
1% 'sediment'	100	100	100	100	100	100	106	100	111	100	100	123
5% 'sediment'	103	100	100	122	105	100	99	100	101	100	107	101



Dissolved Metals in Waters: Analyses by ICP-AES

Concentrations in µg/L

Sample	Ag	Al	As	Cd	Co	Cr	Cu	Fe	Mn	Ni	Pb	Zn
0% 'sediment'	<3	<5	<10	<3	<3	<3	<3	<5	<3	<3	<10	<3
1% 'sediment'	<3	<5	<10	<3	8.0	<3	65	<5	25	<3	<10	34
5% 'sediment'	<3	<5	<10	4.3	34	<3	150	<5	42	<3	<10	170
10% 'sediment'	<3	<5	<10	7.7	70	<3	290	<5	56	<3	<10	450
33% 'sediment'	<3	<5	<10	22	160	<3	390	29	94	4.5	12	1200
100% 'sediment'	<3	<5	<10	49	460	<3	1400	88	240	46	830	9500

Concentrations in µg/L

Field blanks	Ag	Al	As	Cd	Co	Cr	Cu	Fe	Mn	Ni	Pb	Zn
Method Blank	<3	<5	<10	<3	<3	<3	<3	<5	<3	<3	<10	<3
Method Blank	<3	<5	<10	<3	<3	<3	<3	<5	<3	<3	<10	<3

Appendix 9

**Elutriate Testing Report Solwara 1 Project,
Incorporating Phase 1: Effect of Holding Time; Phase 2: Effect of Temperature**

Elutriate Testing Report
Solwara 1 Project

Incorporating
Phase 1: Effect of holding time
Phase 2: Effect of Temperature

for

Coffey Natural Systems and Nautilus Minerals Niugini Limited

prepared by

David L. Parry
Tropical Futures: Mineral Program
Charles Darwin University

25 August 2008

Environmental Analytical Chemistry Unit,
Charles Darwin University, Darwin, NT 0909 Australia, CRICOS 00300K

Table of Contents

1.	Introduction	3
	Objectives of this study	
2.	Methodology	4
2.1	Phase 1: Effect of time experimental conditions	5
2.2	Phase 2: Effect of temperature experimental conditions	5
2.3	Seawater sample preparation	5
2.4	Analytical methods	6
3.	Results and Discussion	7
3.1	Characterisation of the centrifuged seawater	7
3.2	Characterisation of 0.45µm filtered seawater	11
3.3	Major cations in seawater elutriates	16
3.4	Dissolved organic carbon in seawater elutriates	16
3.5	Comparison to ANZECC/ARMCANZ (2000) water quality guidelines	20
4.	Conclusions	20
5.	References	22
Appendix 1:	Phase 1: Metal concentrations in 0.45 µm filtered seawater from 1:10 ore: seawater elutriates at 6°C. Note: Concentrations have been corrected for the Blanks and are therefore net concentrations for each time period.	
Appendix 2:	Phase 1: Metal concentrations in 0.45 µm filtered seawater (N/C sw 1 and 2) for elutriation experiments and seawater blanks.	
Appendix 3:	Phase 1: Quality control data for seawater metals analyses	
Appendix 4:	Phase 1: Normalised data for dissolved metals released from one gram of ore (ng/g ore) into 250ml seawater	
Appendix 5:	Phase 2: Metal concentrations in 0.45 µm filtered seawater from 1:10 ore: seawater 180 minute elutriation at 12°C and 24°C.	
Appendix 6:	Phase 2: Quality control data for seawater metals analyses.	
Appendix 7:	Phase 2: Net metals released and normalised data for dissolved metals released from one gram of ore (ng/g ore) into 250ml seawater at 12 and 24°C	
Appendix 8:	Metal concentrations in Nautilus ore sample used for Phase 1 and 2 experiments (Analysed by ALS)	

1. Introduction

The initial offshore phase of the Solwara 1 Project, which is located approximately 50km north of Rabaul, in the eastern extent of the Manus Basin – Bismarck Sea, New Ireland Province, Papua New Guinea, involves mining copper-, gold-, zinc- and silver-rich SMS deposits on the ocean floor at approximately 1,600m water depth. A subsea mining tool deployed from a mining support vessel will be used to mine the deposits and a riser and lift system, connected to the mining tool, will transport the ore to the surface vessel. Once on the surface vessel, the ore will be dewatered and transferred to a barge for shipping to an overseas concentrator and smelter. The processed water will be returned to the ocean approximately 25 m above the seafloor.

The CSIRO (Simpson et al, 2007) reported on water and sediment characterization in the vicinity of the SMS deposits at the Solwara 1 Prospect. They also reported on the toxicity of the ore dewatering water on aquatic organisms. In conjunction with this work they conducted elutriate tests to determine the potential for release of contaminants from ore in the dewatering plumes. The results of the elutriate tests showed metal release was high for As, Cu, Mn and Zn, but relatively low for Ag, Cd, Ni and Pb. Based on these results Simpson et al (2007) concluded that dilutions greater than 1,000 times may be necessary before concentrations of these metals would be below the 95% protection levels of the ANZECC/ARMCANZ (2000) water quality guidelines. These tests were conducted at room temperature in fully oxygenated seawater and using ore/sediment that may have been oxidized as a result of the storage methods used.

Coffey Natural Systems Pty Ltd engaged Charles Darwin University to carry out further elutriate tests based on the brief BE07008 (2008). The Brief was to conduct further elutriate tests for Nautilus Minerals Nugini Limited on an ore sample that would be extracted and subsequently discharged during an at sea ore de-watering process as part of the Solwara 1 project. The elutriate tests were to be conducted in three phases:

- Phase 1: Effect of holding time;
- Phase 2: Effect of temperature; and
- Phase 3: Effect of shaking.

These elutriate tests were designed to test a range of conditions to which the extracted metallurgical material may be exposed. On review of the data from Phases 1 and 2 Coffey Natural Systems advised Charles Darwin University that Phase 3 would not be required at this stage.

This report provides the results of Phases 1 and 2.

1.1 The objectives of this study:

- To test the effect of time and temperature on the degree to which contaminants are released to the water column from the ore dewatering process
- To determine the chemical composition of the contaminants released.
- To make recommendations regarding treatment of the ‘process’ water.

It was agreed in discussions with Coffey Natural Systems Pty Ltd that the original third objective: To determine the toxicity of the mined material and impact on benthic organisms, would not be included in this current study.

Phase 1 was to investigate the effect that the holding time onboard the vessel may have on the material, particularly with regards to contaminant release

Phase 2 was an investigation of the effect of temperature. The material will be mined at approximately 1,600 m where the temperature is approximately 2-3° C. It may take 3 to 6 minutes for the material to travel up the riser pipe where the temperature will be approximately 4°C (i.e., roughly a 1°C increase) before it reaches the surface. At the surface the material will be dewatered, during which time (duration varied and unknown), the temperature will rise. Finally the material is discharged back down the pipe (again 3 to 6 minutes), with the potential for cooling to occur during descent.

2. Methodology

Nautilus provided a ‘representative’ sample of ore (sample No. A10988), already crushed to 3.35 mm particle size, in vacuum sealed bags, which will exclude oxygen

and minimize air oxidation. However it is assumed that some exposure to air has occurred during the processing which would result in some surface oxidation. The ore was exposed to air prior to each set of experiments.

2.1 Phase 1: Effect of Time Experimental conditions:

Time series: 0, 5, 10, 15, 30, 60, 180, 420, 720 and 1,440 minutes.

- Experiment run in an incubator at 6°C in the dark .
- Solids:Seawater ratio of 1:10 (10%), 25g ore in 250 ml 0.45 µm filtered seawater.
- All samples were shaken for 5 minutes at 6°C in the dark at the beginning of the experiment before being placed in the incubator.
- After each time period bottles were allowed to settle a further 30 minutes at 6°C.
- 3 replicates were included for 0, 60 and 1,440 minute time periods with single samples for other time intervals. Blanks were included for 0, 60 and 1,440 minute time periods

The remaining ore from each time interval was shipped to ALS in Brisbane for geochemical characterisation.

2.2 Phase 2: Effect of Temperature Experimental Conditions:

- Samples incubated at 12 and 24°C for 180 minutes.
- Solids:Seawater ratio of 1:10 (10%), 25g ore in 250 ml 0.45 µm filtered seawater.
- All samples shaken for 5 minutes at the beginning of the experiment
- The bottles were kept in the dark during the course of the experiments.
- After the time period bottles were allowed to settle a further 30 minutes at the experimental temperature.
- 3 replicates and a blank were included for each temperature.

2.3 Seawater sample preparation:

1. Following the settling period, the supernatant was decanted and centrifuged.

2. An aliquot(s) of sample after centrifugation (2,500 rpm for 15 minutes) was taken for pH, Eh, temperature, conductivity, alkalinity, sulfide and dissolved oxygen measurements prior to filtration.
3. The remaining solution was filtered through a 0.45 μm acid-washed filter to remove particulates prior to chemical analysis. Chemical analysis of the supernatant included: organic carbon, sulfate, Au, Ag, Al, As, Ca, Cd, Co, Cr, Cu, Fe, Hg, K, Mg, Mn, Na, Ni, Pb, Sr and Zn.

2.4 Analytical methods:

pH

pH was measured with a TPS Aqua pH meter and Ionode pH electrode. The system was calibrated at pH 7 and 9 in accordance with the instrument manufacturer's instructions.

Redox (Eh)

Redox was measured with an Ionode ORP combination electrode and Aqua conductivity/pH meter. The system was calibrated in accordance with the manufacturer's instructions.

Dissolved oxygen

Dissolved oxygen was measured with a WP 82Y dissolved oxygen meter with a YSI Model 5739 dissolved oxygen probe. The system was calibrated in accordance with the manufacturer's instructions.

Conductivity

Conductivity was measured with a Cyberscan 200 conductivity meter and a Eutech Instruments conductivity probe. The system was calibrated in accordance with the manufacturer's instructions.

Alkalinity

Centrifuged samples (25 mL) were analysed by potentiometric titration with 0.01 M HCl to pH 2.5. A CyberScan pH 300 meter (Eutech Instruments) was used to monitor pH changes. Gran function plots of the titration data were used to determine alkalinity.

Sulfide

Sulfide concentration was measured using the methylene blue colorimetric method (Cline, 1969 and Fonselius, 1983). Sulfide was determined from the absorbance measured at 670nm.

Metal and sulfur analyses:

Quantitative analysis of dissolved (<0.45µm filtered sample) Al, V, Cr, Mn, Fe, Co, Ni, Cu, Zn, Ga, As, Mo, Ag, Cd, Hg, Au, Pb, U, Na, K, Mg, Ca and S was carried out by ICP-MS (Agilent 7500ce) analysis of seawater samples, diluted on-line 1/16, using collision cell H₂ and He gas for interference suppression.

Dissolved Organic Carbon

Filtered (<0.45µm) seawater samples were analysed for dissolved organic carbon by Australian Institute of Marine Science, Townsville, using a Shimadzu TOC-5000A analyser with sample acidification and sparging.

Quality Control

Quality control of laboratory analyses included procedural blanks, replicate analyses, spike additions and analyses of certified reference materials.

3. Results and Discussion

The incubator temperatures were logged every 10 minutes throughout the period of the experiments. The 6°C temperature ranged between 5.3 and 6°C, 12°C experiments averaged 12.1°C and 24°C experiments averaged 23.9°C.

3.1 Characterisation of the centrifuged seawater

pH, redox, conductivity and dissolved oxygen was measured at 6°C. The results are shown in Table 1.

Table 1: pH, redox (Eh), conductivity and dissolved oxygen of centrifuged seawater from 1:10 ore:seawater elutriation at 6°C

Sample	pH	Redox mv	Conductivity mS/cm	Dissolved oxygen %
Sea water	8.39	268	48.5	65.3
0 min Blank	8.46	264	49.4	76.9
0 min Dup 1	7.81	237	49.4	76.0
0 min dup 2	7.85	215	50.4	73.6
0 min Dup 3	7.82	210	50.8	70.5
5 min	7.85	216	47.6	70.0
10 min	7.81	207	48.8	64.4
15 min	7.78	215	48.0	64.9
30 min	7.87	216	49.7	71.6
60 min Blank	8.41	212	49.1	70.9
60 min Dup 1	7.86	213	50.3	73.1
60 min Dup 2	7.79	237	47.3	67.9
60 min Dup 3	7.80	223	48.3	68.1
180 min	7.79	214	47.5	78.6
420 min	7.77	237	52.6	63.9
720 min	7.71	227	51.4	70.5
1440 min Blank	8.36	269	49.7	66.2
1440 min Dup 1	7.66	213	52.1	60.1
1440 min Dup 2	7.67	216	52.5	59.4
1440 min Dup 3	7.63	218	52.8	57.9
Sea water	8.32	270	51.7	74.7

pH showed an initial decrease at time zero of approximately 0.6 pH units. The pH did not drop below that value over the first 420 minutes. There was a drop of another 0.1 pH units at 1440 minutes. This decrease in pH is most probably due to the surface oxidation of sulfide. The oxidation of the ore is also reflected in the decrease in redox and dissolved oxygen. Conductivity remained unchanged throughout the 24 hours.

Table 2: pH, redox (Eh), conductivity and dissolved oxygen of centrifuged seawater from 1:10 ore:seawater 180 minute elutriation at 12°C and 24°C

Sample	pH	Redox mv	Conductivity mS/cm	Dissolved oxygen %
Sea water	8.13	223	50.1	84.9
12 C Blank	8.13	228	49.2	89.4
12C Dup 1	7.39	217	50.3	85.1
12C Dup 2	7.36	241	50.2	79.5
12C Dup 3	7.3	243	50.3	80.7
24C Blank	8.17	240	50.1	55.8
24C Dup 1	7.19	248	50.9	47.3
24C Dup 2	7.11	253	50.5	47.5
24C Dup 3	7.36	242	50.5	50.9
Sea water	8.09	268	49.9	55.4

Table 2 shows that the pH decreased further at the higher temperatures of 12 and 24°C compared to 6°C. Figure 1 shows the decrease in pH of the elutriates at 6, 12 and 24°C after 180 minutes. The 6°C data is from the Phase 1 experiment, but it is the ore sample was used for both experiments and all other conditions were the same.

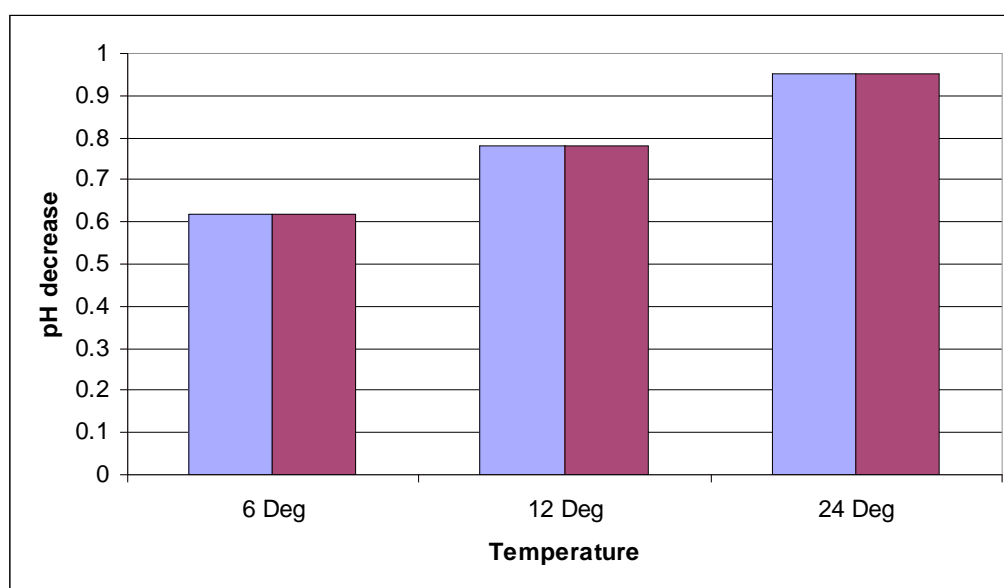


Figure 1: Decrease in centrifuged seawater pH from 1:10 ore:seawater 180 minute elutriation at 6°C, 12°C and 24°C. Note 6°C data from Phase 1 experiment.

The decrease in pH with temperature shows the temperature dependence of the oxidation of the sulfide ore under these conditions.

The Phase one experiment showed the alkalinity decreased by approximately 12% between 0 and 60 minutes compared to the control seawater which is consistent with the observed decrease in pH (Table 3). There was a further decrease in alkalinity at

1440 minutes which is also consistent with the further decrease in pH at this time interval.

Table 3: Alkalinity (centrifuged), dissolved organic carbon (0.45 µm filtered) and sulfide (centrifuged) in seawater from 1:10 ore:seawater elutriation at 6°C.

Sample	Alkalinity (mg/L as CaCO ₃)			DOC mg/L			Sulfide mg/L
	Value	Average	Stdev	Value	Average	Stdev	
NC sw	111.5			1.0			<0.5
Blk 0 min A	108.9			1.18			<0.5
0 min-1 A	97.2			1.44			<0.5
0 min-2 A	97.8	97.3	0.40	1.48	1.39	0.13	<0.5
0 min-3 A	97.0			1.24			<0.5
Blk 60 min A	110.4			0.92			<0.5
60 min-1 A	94.6			1.34			<0.5
60 min-2 A	99.1	97.1	2.27	1.32	1.35	0.04	<0.5
60 min-3 A	97.6			1.39			<0.5
Blk 1440 min A	110.9			0.88			<0.5
1440 min -1 A	92.8			1.23			<0.5
1440 min-2 A	93.2	92.7	0.46	1.21	1.25	0.06	<0.5
1440 min-3 A	92.3			1.32			<0.5

Table 4 shows that alkalinity in the seawater elutriates decreased in relation to the decreasing pH, although the decrease between 12 and 24°C is not significant .

Table 4: Alkalinity (centrifuged), and sulfide (centrifuged) in seawater from 1:10 ore:seawater 180 minute elutriation at 12°C and 24°C.

Sample	Alkalinity (mg/L as CaCO ₃)			Sulfide mg/L
	Value	Average	Stdev	
NC sw	106			<0.5
12C Blk	111			<0.5
12C Dup 1	91.9			<0.5
12C Dup 2	90.7	91.0	0.7	<0.5
12C Dup 3	90.5			<0.5
24C Blk	107			<0.5
24C Dup 1	90.4			<0.5
24C Dup 2	88.2	90.1	1.8	<0.5
24C Dup 3	91.8			<0.5

Sulfide was not detected in any of the centrifuged seawater samples (detection limit 0.5 mg/l) (Tables 3 and 4). The oxic conditions of these experiments (Tables 1 and 2) would have resulted in rapid oxidation of sulfide to sulfate.

3.2 Characterisation of 0.45 µm filtered seawater samples from elutriation

Metals concentration data for the Phase 1 experiment, effect of elutriation time at 6°C is shown in Appendices 1 and 2 with associated quality control data sets in Appendix 3. Appendix 4 shows the Phase dissolved metals data normalised to ng metal/g of ore. Phase 1 results showed the metals that were substantially elevated above background seawater were Co, Cu, Cd, Mn, Pb and Zn. Silver was elevated but was still below the ANZECC/ARMCANZ (2000) 95% protection level. Figures 2 and 3 show the concentrations of Co, Cu, Cd, Pb and Zn over the 1,440 minutes of the elutriation experiments at two different scales to accommodate the relatively higher concentration of Zn compared to the other metals.

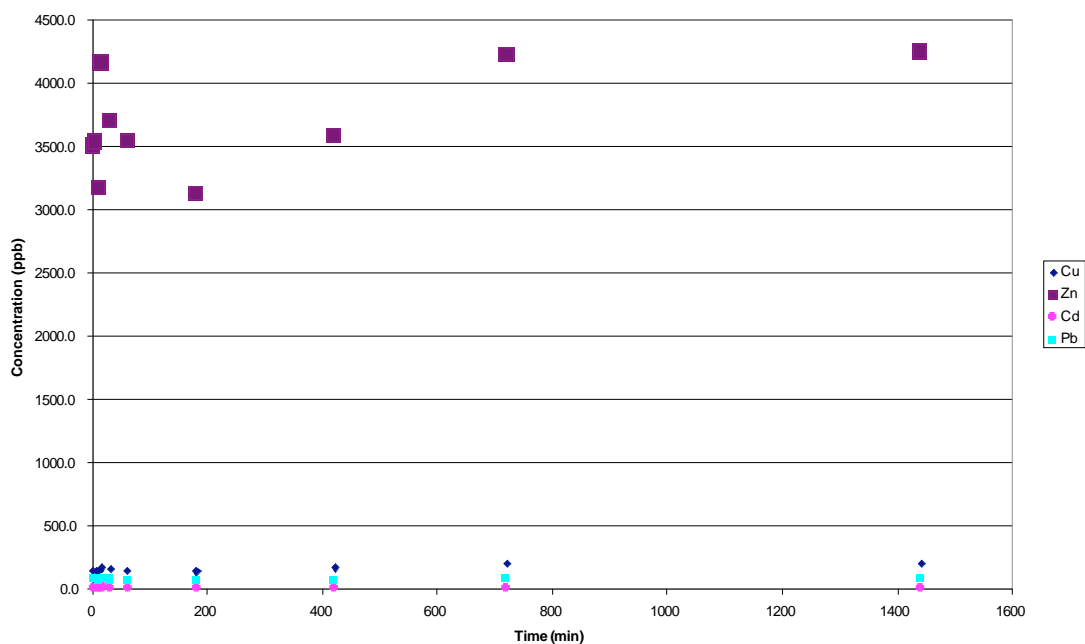


Figure 2: Concentration (ppb) of Cd, Cu, Pb and Zn in 0.45 µm filtered seawater from 1:10 ore:seawater elutriation at 6°C

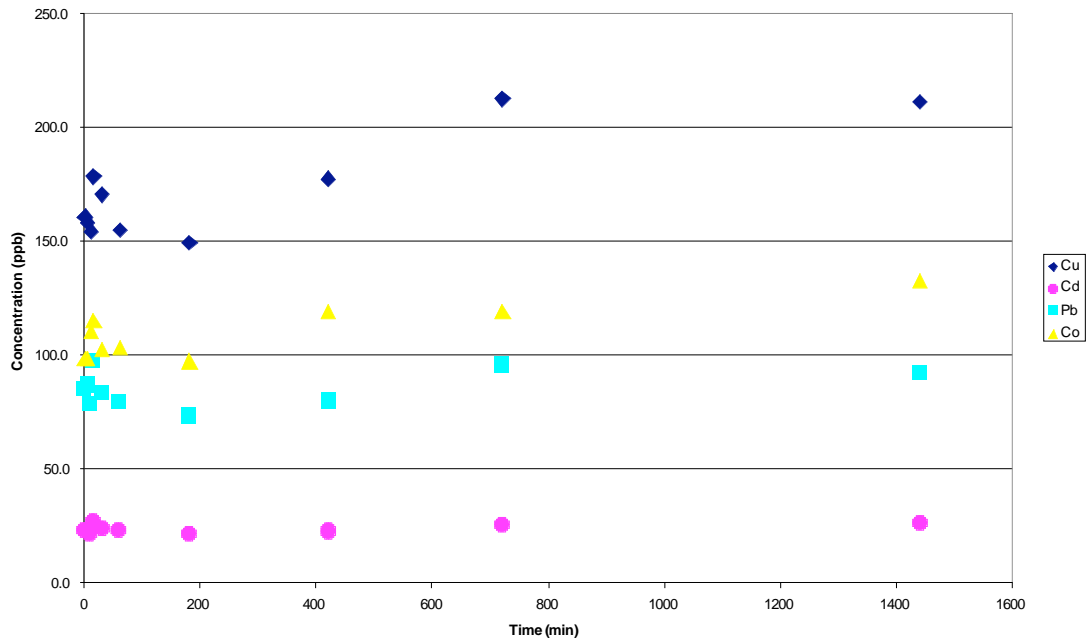


Figure 3: Concentration (ppb) of Cd, Co, Cu and Pb in 0.45 µm filtered seawater from 1:10 ore:seawater elutriation at 6°C

All five metals show similar trends with an initial rapid release of metals followed by a decrease in dissolved concentration to a minimum at 180 minutes and then a slow increase in concentration to 720 minutes. Between 720 and 1,440 minutes an equilibrium appears to have been achieved with little or no increase in concentration over that time. This result shows that the metal release in the oxic seawater is being largely controlled by sulfide oxidation and the dissolution of the oxidation products (see Batterham, 1999 and references therein).

Metal concentrations in filtered seawater from the Phase 2 experiment, effect of temperature at 12 and 24°C, is shown in Appendix 5 with associated QC data in Appendix 6. As observed in the Phase 1 experiment the metals that were substantially elevated above background seawater were Co, Cu, Cd, Mn, Pb and Zn. Silver was elevated and was above the ANZECC/ARMCANZ (2000) 95% protection level by a factor of approximately 2.5.

Figure 4 shows there was a substantial increase in metal dissolution at 12 and 24°C compared to 6°C. The concentration of Zn released was more than order of magnitude higher than any other metals. Figure 4 shows there was no substantial

difference in metal dissolution between 12 and 24°C. This result may indicate that there was further air oxidation of the ore between the Phase 1 and Phase 2 experiment which would result in enhanced dissolution. However the stability of metal sulfides is known to be affected by temperature (Tsang and Parry, 2004) and therefore an increase with temperature would not be unexpected.

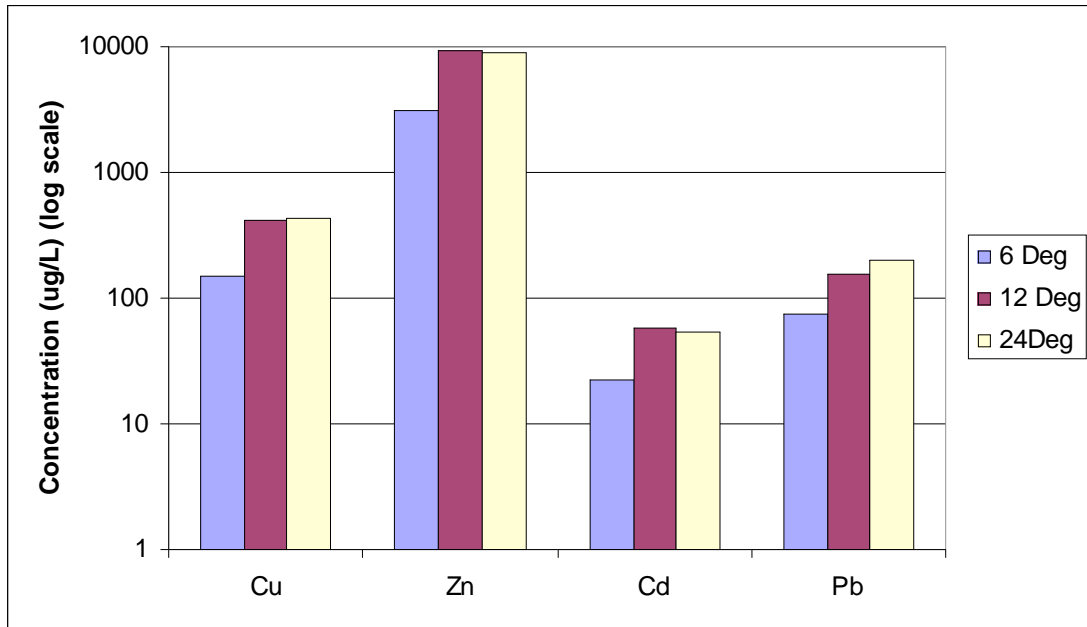


Figure 4: Concentration (ppb) of Cd, Cu, Pb and Zn in 0.45 µm filtered seawater from 1:10 ore:seawater 180 minute elutriation at 6°C, 12°C and 24°C (note 6°C results are from the Phase 1 experiment).

Figure 5 shows the mass of metal dissolved into the seawater per kg of ore at 6, 12 and 24°C. This data is derived from the seawater concentration data and therefore shows the same trends. Appendices 4 and 7 shows the net metals released from the ore and the resulting mass of metals released per mass of ore.

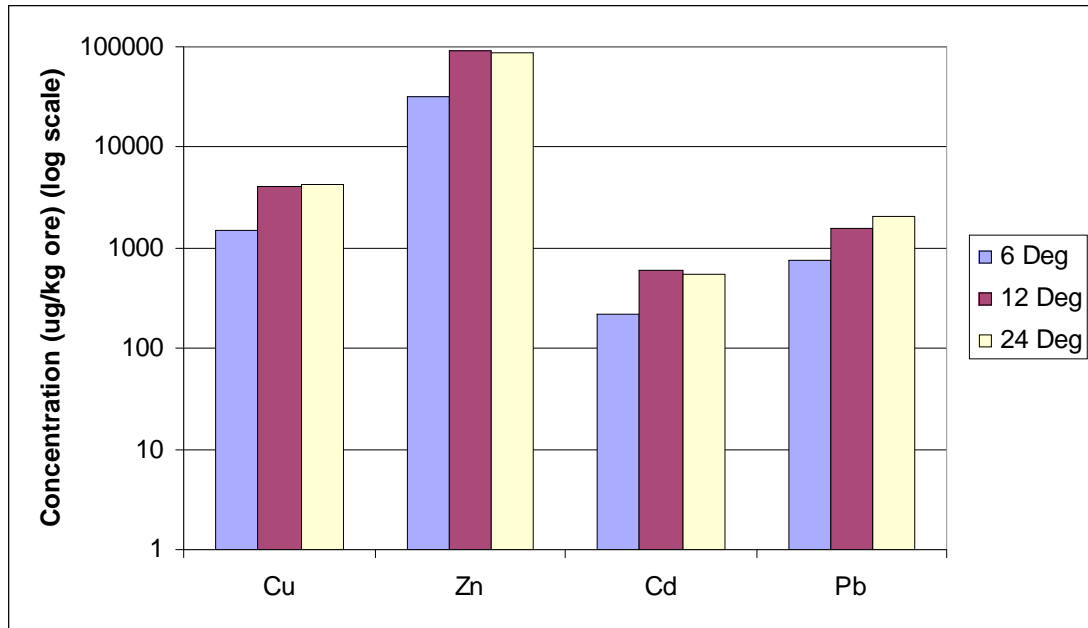
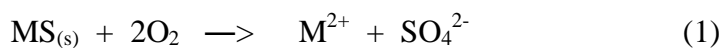


Figure 5: Mass of metal (μg) dissolved per kg of ore at 6, 12 and 24°C (note 6°C data from Phase 1 experiment).

Metal sulfides are generally very insoluble, but they are thermodynamically unstable in the presence of oxygen and water, undergoing complex oxidation/reduction reactions (Richardson, 1995, Tsang and Parry, 2004). The result of the oxidation is the production of sulfate and mobilization of metals. The overall oxidation of metal sulfides can be described by equation 1, but this is an oversimplification of a complex multi-step reaction.



The results from these elutriation experiments clearly show the mobilization of metals and concomitant release of sulfate (Table 5 and 6 and Figure 6). The Phase 1 experiment showed that virtually all the sulfate was released at time zero with little increase over time (Table 5). This would indicate that there was an existing oxidized surface on the ore sample. Figure 6 shows there is an increase in release of sulfur with temperature, however the substantial increase at 24°C is largely due to one of the replicates being approximately 100mg/L higher than the other 2 (Table 6).

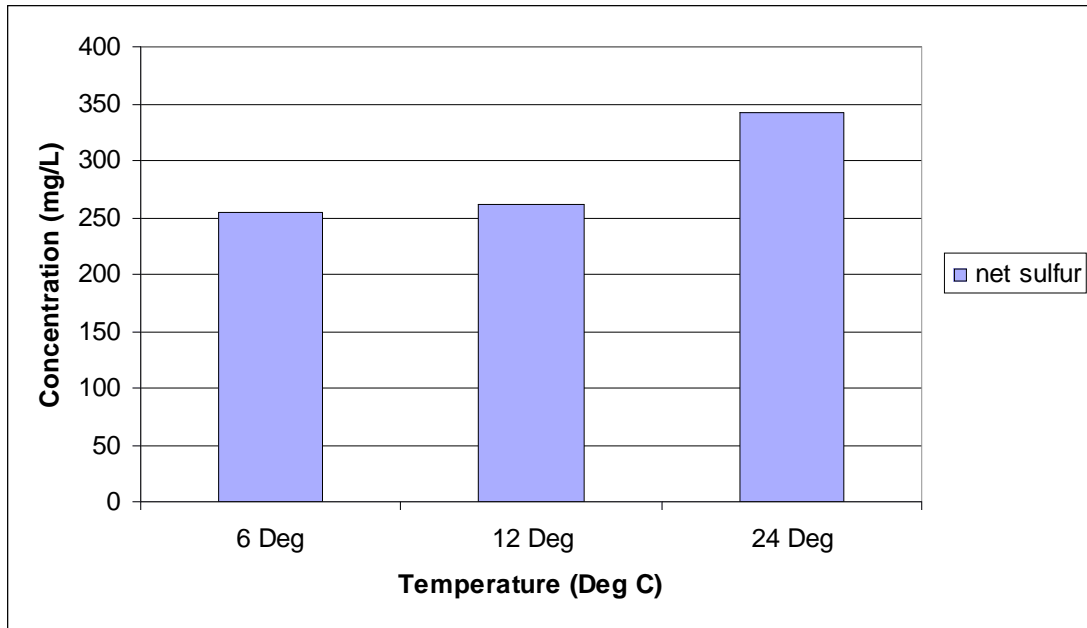
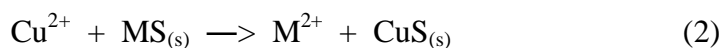


Figure 6: Net sulfur released (sulfur concentration in elutriate – sulfur in blank seawater) from 180 minute elutriation at 6, 12 and 24°C (note 6°C data from Phase 1 experiment).

In the Phase 1 experiment there was a decrease in dissolved metal concentrations between 15 and 180 minutes, most probably due to readsorption to the ore surface and/or precipitation as metal hydroxides and carbonates (Figures 2 and 3).

The slow increase in dissolved metal concentrations between 180 and 720 minutes reflects surface controlled dissolution which will be a combination of oxidation, the distribution of active ore surface defect sites (steps, kinks and pits) and lattice exchange reactions.

The metal analysis of the ore shows that Cu is the predominant mineral, more than an order of magnitude higher concentration than Zn. Although Cu is the predominant metal in the ore dissolved Zn is an order of magnitude higher and Cd and Pb are at similar concentrations to Cu. This is a result of the fact that copper forms the most insoluble sulfide and readily undergoes lattice exchange reactions with Pb, Zn and Cd sulfides (equation 2).



(M = Pb, Zn or Cd)

Zinc sulfide is the most soluble of all these metal sulfides and therefore will undergo exchange reactions with all these metals to enhance Zn mobilization (Batterham, 1999; Tsang and Parry, 2004 and references therein).

3.3 Major cations in seawater elutriates

Dissolved Na, K and Mg concentrations remained unchanged from background seawater concentrations throughout the 1,440 minutes of the Phase 1 experiment and the Phase 2 temperature experiments (Tables 5 and 6, respectively). In the time course experiment of Phase 1 calcium concentration showed an initial rapid increase in concentration of approximately 60%, paralleling the rapid initial metal release (Table 5). Figure 7 shows an increase in dissolution with increasing temperature which corresponds to the trend of decreasing pH with increasing temperature (Figure 1). This would suggest the presence of a readily soluble Ca mineral phase in the ore (no mineralogy was available for this ore sample).

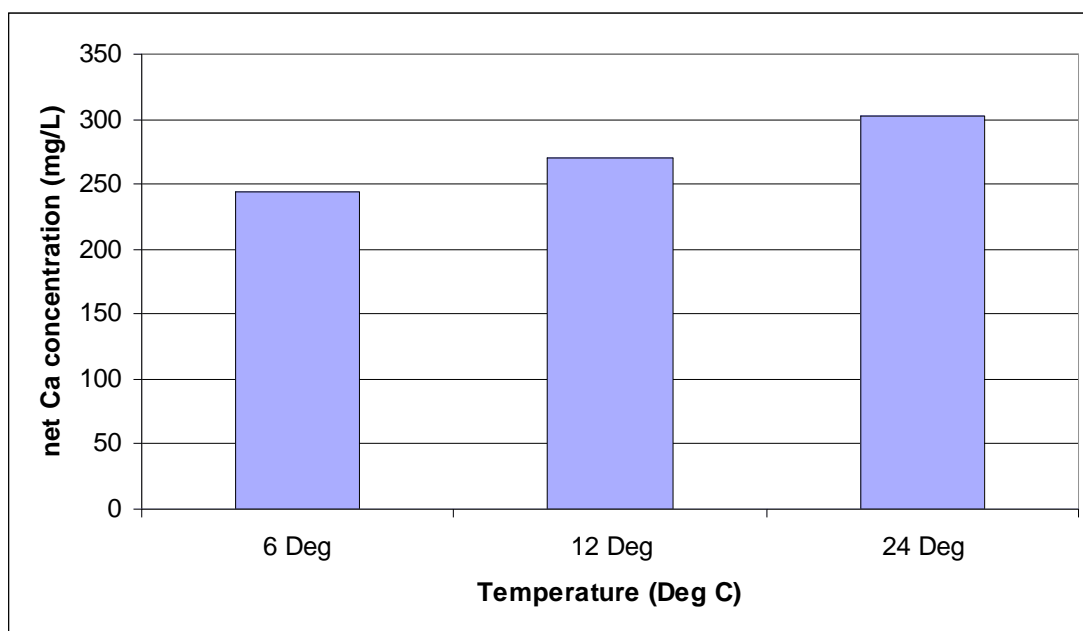


Figure 7: Net Ca concentration in filtered seawater from 180 minute elutriation at 6, 12 and 24°C. (Note: 6°C data from Phase 1 experiment).

3.4 Dissolved organic carbon in seawater elutriates

Dissolved organic carbon in Phase 1 experiment showed an initial increase in concentration of approximately 30% compared to the blank seawater (Table 3). The organic carbon may act as a ligand to complex some of the dissolved metals,

depending on the actual chemical form of the organic carbon. Organic ligands may also promote dissolution via surface complexation of metals such as Cu and Pb (Batterham, 1999). These organic complexes, if relatively inert, would reduce the bioavailability of the dissolved metals. The dissolved metal concentrations reported in this study would include organic complexes.

Dissolved organic carbon is not yet available for the Phase 2 experiment as there was an instrument failure.

Table 5: Major ions in 0.45 µm filtered seawater from 1:10 ore:seawater elutriation at 6°C

Sample	Na mg/L	Mg mg/L	K mg/L	Ca mg/L	Sulfur mg/L	Sulfate mg/L
BLK 0 min	9250	1200	378	395	880	2641
BLK 60 min	9380	1190	380	408	899	2698
BLK 1440 min	9270	1190	384	389	901	2703
0-1 min	9350	1190	379	662	1146	3437
0-2 min	9220	1170	377	643	1157	3472
0-3 min	9430	1190	381	659	1159	3477
5 min	9450	1190	381	657	1167	3501
10 min	9510	1200	385	651	1175	3525
15 min	9470	1190	383	713	1228	3684
30 min	9360	1190	370	645	1140	3421
60 min -1	9530	1200	375	664	1143	3429
60 min -2	9440	1190	376	636	1130	3390
60 min -3	9440	1200	378	664	1172	3515
180 min	9550	1200	378	652	1165	3494
420 min	9610	1200	378	682	1184	3551
720 min	9450	1200	374	689	1216	3648
1440 min -1	9400	1190	368	689	1207	3622
1440 min -2	9610	1070	377	653	1207	3622
1440 min -3	9650	1190	383	733	1214	3643
Reporting Limit						
Seawater	350	25.0	150	10.0	25	
Freshwater	0.35	0.025	0.15	0.01		
Quality Control						
SLRS-4 ¹ certified	1.92 ± 0.2 2.4 ± 0.2	1.56 ± 0.03 1.6 ± 0.1	0.672 ± 0.001 0.68 ± 0.02	5.99 ± 0.14 6.2 ± 0.2		
SLRS-3 ¹ certified	2.13 2.3 ± 0.2	1.54 1.6 ± 0.2	0.702 0.7 ± 0.1	5.78 6.0 ± 0.4		
SLEW-3 ² SLEW-3 (value)**	4420 (4620)**	619 (627)**	190 (204)**	208 (216)**		
NASS-5 ³ NASS-5 (value)**	8510 ± 245 (9360)**	1090 ± 15 (1270)**	347 ± 15 (413)**	365 ± 5 (437)**		
CASS-4 ³ CASS-4 (value)**	8800 ± 238 (9450)**	1100 ± 9 (1290)**	354 ± 21 (409)**	372 ± 7 (433)**		
Ref 3154# Ref 3154 (value)					437 ± 34 515	
¹ : National Research Council Canada - River water Reference Material ² : National Research Council Canada - Estuarine water Reference Material ³ : National Research Council Canada - Seawater Reference Material (#)**: Information only #: Sulfur solution; National Institute of Standards and Technology						

Table 6: Major ions in 0.45 µm filtered seawater from 1:10 ore:seawater 180 minute elutriation at 12°C and 24°C.

Sample:	Na (mg/L)	Mg (mg/L)	K (mg/L)	Ca (mg/L)	S (mg/L)	Sulfate (mg/L)
Reporting limit (R.L.)	0.164	0.00277	0.0136	0.0282	10	
Nightcliff filtered sw	10400	1150	377	411	990	2970
12oC 180 min blank	10500	1140	385	418	975	2925
12oC 180 min dup 1	10500	1080	370	629	1220	3660
12oC 180 min dup 2	10700	1130	380	678	1240	3720
12oC 180 min dup 3	10800	1150	385	697	1250	3750
24oC 180 min blank	10500	1150	384	428	935	2805
24oC 180 min dup 1	10500	1100	376	725	1250	3750
24oC 180 min dup 2	10700	1110	383	760	1340	4020
24oC 180 min dup 3	10900	1170	388	709	1240	3720
Quality control						
Spike recoveries						
24oC 180 min blank ave	10500	1150	384	428		
24oC 180 min blank stdev	272	16.3	10.4	6.55		
24oC 180 min blank spike	13200	1600	882	973		
Experimental spike	27.0	4.50	4.98	5.45		
Spike value	25.0	5.00	5.00	5.00		
Spike recovery (%)	108	90.0	99.6	109		
24oC 180 min dup 1 average	10500	1100	376	725		
24oC 180 min dup 1 stdev	777	110	22.9	83.3		
24oC 180 min dup 1 spike	13900	1650	901	1320		
Experimental spike	34.0	5.50	5.25	5.95		
Spike value	25.0	5.00	5.00	5.00		
Spike recovery (%)	136	110	105	119		
Certified reference materials and in house reference materials						
Sample:						
NASS-5 ave	8800	956	320	332		
NASS-5 stdev	343	40.2	12.8	8.76		
NASS-5 certified	(9360)*	(1270)*	(413)*	(437)*		
CASS-4 ave	9340	1020	338	370		
CASS-4 stdev	223	11.5	2.08	11.1		
CASS-4 certified	(9450)*	(1290)*	(409)*	(433)*		
ICP 200.7-6 ave	16.8	18.3	93.5	21.9		
ICP 200.7-6 stdev	1.24	1.10	2.22	1.52		
ICP 200.7-6 value	20.0	20.0	100	20.0		
eriss std ave	94.3	92.4	94.5	100		
eriss std stdev	4.93	4.11	2.19	5.23		
eriss std value	100	100	100	100		
SLRS-4 ave	1.53	1.43	0.608	5.70		
SLRS-4 stdev	0.161	0.0480	0.0126	0.278		
SLRS-4 certified	2.4 ± 0.2	1.6 ± 0.1	0.68 ± 0.02	6.2 ± 0.2		
SLRS-3 ave	2.21	1.48	0.635	5.71		
SLRS-3 stdev	0.175	0.0361	0.0193	0.146		
SLRS-3 certified	2.3 ± 0.2	1.6 ± 0.2	0.7 ± 0.1	6.0 ± 0.4		
Ref 3154					463 ± 8.4	
Ref 3154 certified					515	

NASS-5: National Research Council Canada - seawater reference material
 CASS-4: National Research Council Canada - seawater reference material
 SLRS-3 and 4: National Research Council Canada - River water reference material
 ICP 200.7-6: Commercial mixed metal standard containing 20 ppm metals (100 ppm K)
 eriss std: 100 ppm Na, Mg, K, Ca
 Ref 3154: National Institute of Standards and Technology sulfur solution

3.5 Comparison to ANZECC/ARMCANZ (2000) water quality guidelines

The dissolved concentrations of Co, Cu, Zn, Cd and Pb exceed the ANZECC/ARMCANZ (2000) guideline values for 95% protection level at all three temperatures (see Appendices 1 and 5). At 6°C zinc exceeded the guideline value by approximately 250 times, with Co, Cu, Cd and Pb exceeding the Guideline values by approximately 100, 120, 4 and 20 times, respectively. Therefore, if the ore slurry was maintained at 6°C a 300 fold dilution would reduce all metal concentrations to below the guideline level for 95% protection, a more conservative dilution of 500 fold would reduce all metal concentrations to below the guideline value for 99% protection, except for Co. However, the Co value of 0.005 µg/l is actually below the natural background levels for Co in coastal environments of northern Australia (Munksgaard and Parry, 2001).

The temperature experiment resulted in higher concentrations of metals at 12 and 24°C with Zn exceeding the ANZECC/ARMCANZ (2000) guideline value for 95% protection by approximately 600 times. Cobalt, Cu, Cd and Pb exceeded the guideline values by approximately 220, 300, 10 and 34-45 (12 and 24°C, respectively). Therefore a minimum of 600 fold dilution would reduce all metal concentrations below the ANZECC/ARMCANZ (2000) guideline values for 95% protection level.

4. Conclusions

The results of both the Phase 1 and 2 experiments indicate that there is an existing oxidized surface layer on the ore sample resulting in the rapid release of Mn, Co, Cu, Zn, Cd, Pb and sulfate. The Phase 1 experiment at 6°C showed that after the initial dissolution of this oxidized layer substantially slower dissolution from the exposed metal sulfide surface commenced. If the oxidized layer was due to air oxidation the results obtained in these experiments may represent a worst case scenario. The ore being mined in situ will mix with oxygenated seawater, not air, and this will result in substantially slower rates of metal sulfide oxidation (see Batterham, 1999) and concomitantly lower rates of metal dissolution.

Batterham (1999) removed the oxidized surface from a mixed metal sulfide ore concentrate and showed that the initial rate of dissolution for Cd, Cu and Zn in oxic

seawater was very slow. Lead still showed substantial rates of dissolution which reflects the rapid oxidation of galena, reported to initiate in minutes (Kim et al, 1994).

The Phase 2 experiment showed that there appears to be a temperature effect on dissolution of metals with a concomitant decrease in pH, increase in Ca dissolution and increase in sulfur as sulfate. While it has been reported that metal sulfides are less stable at higher temperatures (Tsang and Parry, 2004) the magnitude of increase measured in these experiments may be higher than expected due to air oxidation of the ore that may have occurred between the two experiments.

Acknowledging that these experiments may represent a worst case scenario, as a result of air oxidation of the ore, the results for the quality of elutriate water show that at least a 300 fold dilution will be required at 6°C and 600 fold dilution if the slurry will be between 12 and 24°C, to produce a discharge water quality that would be considered to have minimal if any environmental impact. A more conservative dilution of 1000 fold would reduce metal concentrations to below the ANZECC/ARMCANZ (2000) guideline values for 99% protection level for most metals even at 24°C, except for Co. This dilution would also reduce Ca and sulfate levels and increase pH and alkalinity to background levels. This assumes that the slurry will be processed within 180 minutes as there is no data for dissolution at 12 or 24°C beyond 180 minutes.

The required dilution could be readily achieved by initially mixing the processed seawater 1:10 with background seawater and pumping that back into the ocean at depth through a diffuser. A diffuser should be able to achieve a further 100 fold dilution within meters of the diffuser depending on currents.

These conclusions are based on the two sets of experiments that addressed the variables of temperature and time, but did not address turbulent mixing directly. However all experiments included a 5 minute shaking period at the beginning which may represent the mixing that will occur when the slurry is pumped to the surface.

5. References

ANZECC/ARMCANZ (2000). Australian and New Zealand Guidelines for Fresh and Marine Water Quality. Volume 1. The Guidelines, Australian and New Zealand Environment and Conservation Council and Agriculture and Resource Management Council of Australia and New Zealand.

Batterham, G. 1999. Mobilisation of heavy metals from metal sulfide concentrate in the marine environment – McArthur River region, Australia. PhD Thesis. Charles Darwin University. 310pp.

Cline, J.D. 1969. Spectrophotometric determination of hydrogen sulfide in natural waters. *Limnol Oceanogr* **14**, 454-458.

Coffey Natural Systems Pty Ltd. 2008. Further Elutriate and Toxicity Tests: Solwara 1 Project. BE07008 Brief Further Elutriate Test generic.

Fonselius, S.H. 1983. Determination of hydrogen sulfide. In: Methods of Seawater Analysis, Grasshoff, K., Ehrhardt, M. and Kremling, K. (eds.), Verlag Chemie, Weinheim, pp73-80.

Kim, B.S., Hayes, R.A., Prestidge, C.A., Ralston, J. and Smart, R. St. C. 1994. Scanning tunneling microscopy studies of galena: the mechanism of oxidation in air. *Appl. Surf. Sci.* **78**, 385-397.

Munksgaard, NC and Parry, DL. 2001. Trace metals, arsenic and lead isotope ratios in dissolved and particulate phases of north Australian coastal and estuarine seawater. *Marine Chemistry*, **75**, 165-184.

Richardson, P.E. 1995. Surface chemistry of sulfide flotation. In: Mineral surfaces, No. 5, Mineralogical Society Series, Vaughn, D.J. and Patrick, R.A.D. (eds.), Chapman & Hall, London. Pp 261-302.

Simpson, S, Angel, B, Hamilton, I, Spadaro, D and Binet, M. 2007. Water and sediment characterization and toxicity assessment for the Solwara 1 Project. CSIRO Land and Water Science Report 68/07. Report to Coffey Natural Systems Pty Ltd.

Tsang, J.J. and Pary, D.L. 2004. Metal mobilization from complex sulfide ore concentrate: effect of light and pH. *Aust. J. Chem.* **57**, 971-978.

Acknowledgements

Dr Jeffrey Tsang, Mr Dylan Campbell and Ms Françoise Foti carried out the experimental and analytical work

Appendix 1: Phase 1: Metal concentrations in 0.45 µm filtered seawater from 1:10 ore: seawater elutriates at 6°C. Note: Concentrations have been corrected for the Blanks and are therefore net concentrations for each time period.

Sample	Al (µg/L)	V (µg/L)	Cr (µg/L)	Mn (µg/L)	Fe (µg/L)	Co (µg/L)	Ni (µg/L)	Cu (µg/L)	Zn (µg/L)	Ga (µg/L)	As (µg/L)	Mo (µg/L)	Ag (µg/L)	Cd (µg/L)	Hg (µg/L)	Au (µg/L)	Pb (µg/L)	U (µg/L)
Reporting Limit (R.L.)	0.320	0.300	0.180	0.120	2.94	0.0300	0.0900	0.470	0.610	0.0200	0.480	0.380	0.070	0.020	0.150	0.310	0.070	0.500
Filtered seawater	<R.L.	<R.L.	<R.L.	<R.L.	<R.L.	<R.L.	<R.L.	<R.L.	<R.L.	<R.L.	<R.L.	<R.L.	<R.L.	<R.L.	<R.L.	0.380	0.070	<R.L.
Blank 0 min	<R.L.	0.350	0.240	0.290	<R.L.	<R.L.	<R.L.	0.630	<R.L.	<R.L.	<R.L.	<R.L.	<R.L.	<R.L.	<R.L.	<R.L.	<R.L.	<R.L.
Blank 60 min	<R.L.	<R.L.	<R.L.	<R.L.	<R.L.	<R.L.	<R.L.	<R.L.	<R.L.	<R.L.	<R.L.	<R.L.	<R.L.	<R.L.	<R.L.	0.380	0.070	<R.L.
Blank 1440 min	2.59	<R.L.	<R.L.	<R.L.	<R.L.	<R.L.	<R.L.	<R.L.	<R.L.	<R.L.	<R.L.	<R.L.	<R.L.	<R.L.	<R.L.	<R.L.	0.070	<R.L.
0 min-1	7.84	<R.L.	<R.L.	119	<R.L.	101	140	163	3560	0.110	3.27	16.1	1.10	23.5	<R.L.	<R.L.	86.6	2.99
0 min-2	3.53	<R.L.	<R.L.	112	<R.L.	96.8	106	168	3430	0.110	1.17	14.3	1.02	22.5	<R.L.	<R.L.	79.9	2.74
0 min-3	2.23	<R.L.	<R.L.	119	<R.L.	100	104	163	3540	0.150	<R.L.	14.9	1.01	24.7	<R.L.	<R.L.	88.7	3.01
5 min	6.66	<R.L.	<R.L.	112	3.03	99.2	112	159	3540	0.140	2.23	18.2	1.09	23.6	<R.L.	3.13	87.3	3.23
10 min	3.41	<R.L.	<R.L.	107	5.37	111	11.1	155	3180	0.200	<R.L.	16.3	1.06	21.5	<R.L.	2.61	78.8	2.86
15 min	8.99	<R.L.	<R.L.	133	5.91	116	15.7	179	4170	0.230	2.01	19.1	1.26	27.3	<R.L.	1.96	97.8	3.14
30 min	<R.L.	<R.L.	<R.L.	115	3.55	103	12.1	171	3700	0.160	2.39	15.5	1.00	23.9	<R.L.	1.30	83.8	2.86
60 min-1	5.85	<R.L.	<R.L.	116	3.88	108	11.4	159	3670	0.180	1.82	15.3	0.92	24.6	<R.L.	1.09	88.5	2.74
60 min-2	0.980	<R.L.	<R.L.	104	3.88	95.8	10.2	144	3270	0.130	<R.L.	16.4	0.79	21.4	<R.L.	1.14	71.8	2.36
60 min-3	7.87	<R.L.	<R.L.	117	6.10	108	11.6	164	3760	0.120	<R.L.	15.0	0.92	24.1	<R.L.	0.670	79.1	2.87
180 min	2.28	<R.L.	<R.L.	106	5.73	97.9	9.30	160	3130	0.150	<R.L.	13.4	0.74	21.9	<R.L.	1.00	73.8	2.53
420 min	0.420	<R.L.	<R.L.	113	7.32	120	11.3	178	3590	0.130	1.22	16.3	0.82	22.9	<R.L.	0.670	80.1	3.12
720 min	3.61	<R.L.	<R.L.	140	7.43	120	12.6	213	4230	0.130	1.18	15.9	0.94	25.6	<R.L.	0.430	96.0	3.46
1440 min-1	3.86	<R.L.	<R.L.	135	8.52	135	14.9	212	4430	0.200	2.66	15.3	0.90	26.2	<R.L.	1.39	95.3	3.18
1440 min-2	5.14	<R.L.	<R.L.	122	8.58	128	13.1	206	4000	0.130	3.86	18.8	0.82	24.3	<R.L.	0.730	85.1	2.88
1440 min-3	7.64	<R.L.	<R.L.	133	12.7	137	16.0	217	4330	0.210	0.630	14.3	0.87	28.2	<R.L.	0.540	96.1	3.30
PNG Marine WQ Std	ngv	ngv	ngv	2,000	1,000	ngv	ngv	30	5,000	ngv	50	ngv	ngv	1	0.2	ngv	4	ngv
ANZECC 2000 95% level	ngv	100	4.4 (C(V))	ngv	ngv	1.0	700	1.3	15	ngv	ngv	ngv	1.4	5.5	0.4	ngv	4.4	ngv
ngv = no guideline value																		

Appendix 2: Phase 1: Metal concentrations in 0.45 µm filtered seawater (N/C sw 1 and 2) for elutriation experiments and seawater blanks.

Sample	Al (µg/L)	V (µg/L)	Cr (µg/L)	Mn (µg/L)	Fe (µg/L)	Co (µg/L)	Ni (µg/L)	Cu (µg/L)	Zn (µg/L)	Ga (µg/L)	As (µg/L)	Mo (µg/L)	Cd (µg/L)	Au (µg/L)	Pb (µg/L)	U (µg/L)
Reporting Limit (R.L.)	0.320	0.300	0.180	0.120	2.94	0.0300	0.0900	0.470	0.610	0.0200	0.480	0.580	0.0200	0.310	0.0100	0.500
N/C sw 1	2.74	1.83	<R.L.	0.960	<R.L.	<R.L.	0.180	<R.L.	<R.L.	<R.L.	1.14	10.3	<R.L.	<R.L.	<R.L.	2.66
N/C sw 2	1.72	1.85	<R.L.	1.30	<R.L.	<R.L.	0.180	<R.L.	<R.L.	<R.L.	1.38	9.74	<R.L.	<R.L.	0.0100	2.52
Blank 0 min	1.20	1.89	<R.L.	0.950	<R.L.	<R.L.	0.350	<R.L.	<R.L.	<R.L.	1.36	10.2	<R.L.	<R.L.	<R.L.	2.66
Blank 60 min	1.83	1.87	<R.L.	0.970	<R.L.	<R.L.	0.320	<R.L.	<R.L.	<R.L.	1.23	10.6	<R.L.	<R.L.	0.0100	2.71
Blank 1440 min	2.13	1.98	<R.L.	0.970	<R.L.	<R.L.	0.300	<R.L.	<R.L.	<R.L.	1.38	10.5	<R.L.	<R.L.	<R.L.	2.68

Appendix 3: Phase 1: Quality control data for seawater metals analyses

Sample	Al (g/L)	V (g/L)	Cr (g/L)	Mn (g/L)	Fe (g/L)	Co (g/L)	Ni (g/L)	Cu (g/L)	Zn (g/L)	Ga (g/L)	As (g/L)	Mo (g/L)	Ag (g/L)	Cd (g/L)	Hg (g/L)	Au (g/L)	Pb (g/L)	U (g/L)
0 min -3 Ave	2.23	<R.L.	<R.L.	119	<R.L.	100	10.4	163	3540	<R.L.	<R.L.	14.9	<R.L.	24.7	<R.L.	<R.L.	88.7	
0 min -3 Stdev	2.89	<R.L.	<R.L.	<R.L.	<R.L.	1.01	1.04	1.90	46.0	<R.L.	<R.L.	<R.L.	<R.L.	0.190	<R.L.	0.440	0.550	
0 min -3 spike	486	515	527	643	501	688	522	700	4060	526	526	508	526	529	1140	1140	600	
Experimental spike #	48.4	51.5	52.7	52.4	50.1	50.8	51.1	53.7	52.4	52.6	52.6	49.4	52.6	50.5	114	114	51.2	
Spike value	50.0	50.0	50.0	50.0	50.0	50.0	50.0	50.0	50.0	ns	50.0	50.0	ns	50.0	ns	100	50.0	
Spike recovery(%)	98.8	103	105	105	100	102	102	107	105	105	105	98.8	105	101	114	114	102	
1440 min -3 Ave	7.64	<R.L.	<R.L.	133	12.7	137	16.0	217	4330	<R.L.	0.630	14.3	<R.L.	28.2	<R.L.	0.540	86.1	
1440 min -3 Stdev	9.59	<R.L.	<R.L.	1.38	<R.L.	1.47	1.06	2.08	14.0	<R.L.	1.22	1.12	<R.L.	0.0700	<R.L.	0.540	609	
1440 min -3 spike	505	521	539	660	515	654	538	763	4860	530	530	525	530	539	1030	1030	609	
Experimental spike #	49.8	52.1	53.9	52.7	50.2	51.7	52.2	54.6	63.6	53.0	53.0	51.0	53.0	51.0	103	103	51.2	
Spike value	50.0	50.0	50.0	50.0	50.0	50.0	50.0	50.0	50.0	ns	50.0	50.0	ns	50.0	ns	100	50.0	
Spike recovery(%)	99.6	104	108	105	100	103	104	109	127	106	106	102	106	102	103	103	102	

Experimental spike # = (spike - ave)/(dilution factor= 10)

Certified reference materials and checks for analysis

Sample	Al (g/L)	V (g/L)	Cr (g/L)	Mn (g/L)	Fe (g/L)	Co (g/L)	Ni (g/L)	Cu (g/L)	Zn (g/L)	Ga (g/L)	As (g/L)	Mo (g/L)	Ag (g/L)	Cd (g/L)	Hg (g/L)	Au (g/L)	Pb (g/L)	U (g/L)
NASS5 result/av.	<R.L.	1.20	<R.L.	0.920	<R.L.	<R.L.	0.250	<R.L.	<R.L.	<R.L.	1.27	9.80	<R.L.	0.0200	<R.L.	<R.L.	0.0100	2.60
std dev	N/A	0.100	N/A	0.0400	N/A	N/A	0.0300	N/A	N/A	N/A	0.160	0.190	N/A	0.0100		N/A	0.00	0.170
NASS5 certified	nv	(1.2)*	1.10 ± 0.015	0.919 ± 0.057	0.207 ± 0.035	0.11 ± 0.003	0.253 ± 0.028	0.297 ± 0.046	1.102 ± 0.039	nv	1.27 ± 0.12	9.6 ± 1.0	nv	0.023 ± 0.003		nv	0.008 ± 0.005	(2.6)*
CASS-4	1.86	1.15	<R.L.	2.87	<R.L.	<R.L.	0.250	0.550	<R.L.	<R.L.	1.19	9.82	0.02	0.0200	2.440	<R.L.	0.0100	2.62
CASS4 certified	nv	1.18 ± 0.16	1.44 ± 0.029	2.78 ± 0.19	0.713 ± 0.058	0.26 ± 0.003	0.314 ± 0.03	0.592 ± 0.055	0.381 ± 0.057	nv	1.11 ± 0.16	8.78 ± 0.86	nv	0.026 ± 0.003	nv	nv	0.098 ± 0.003	(3)*
bbref new on107 +20ppb	100	22.4	20.4	239	932	196	19.8	20.5	22.1	20.0	223	31.0	20.0	20.1	19.1	20.8	22.1	23.5
Value	82.9	22.2	20.8	225	82.1	20.3	20.3	21.4	18.9	20.4	19.2	30.9	20.0	20.3	20.0	22.1	22.1	24.4
10ppb Au																9.17		
Value																10.0		

Appendix 4: Phase 1: Normalised data for dissolved metals released from one gram of ore (ng/g ore) into 250ml seawater

Sample	Al	V	Cr	Mn	Fe	Co	Ni	Cu	Zn	Ga	As	Mo	Ag	Cd	Hg	Au	Pb	U
0min ave	455	<R.L.	<R.L.	1170	<R.L.	999	117	1620	36300	1.24	223	152	10.5	237	<R.L.	<R.L.	856	293
0 min stdev	29.1	N/A	N/A	21.3	N/A	6.45	19.3	2.23	131	0.220	14.5	7.38	0.4	8.17		N/A	32.9	1.04
5 min	67.9	<R.L.	<R.L.	1140	30.9	100	114	1620	36100	1.43	227	185	11.1	240	<R.L.	31.9	889	32.9
10 min	34.6	<R.L.	<R.L.	1090	54.6	1130	113	1570	32300	2.03	<R.L.	166	10.8	218	<R.L.	26.5	801	29.1
15 min	92.6	<R.L.	<R.L.	1370	60.9	1200	162	1840	49000	2.37	207	197	13.0	281	<R.L.	20.2	1010	32.4
30 min	<R.L.	<R.L.	<R.L.	1190	36.7	1070	125	1770	36300	1.66	247	160	10.3	247	<R.L.	13.4	867	29.6
60min ave	48.9	<R.L.	<R.L.	1150	47.5	1070	113	1600	36400	1.47	18.4	160	9.0	239	<R.L.	9.89	817	27.2
60 min stdev	38.9	N/A	N/A	77.0	13.9	73.5	8.14	115	3150	0.310	N/A	7.56	0.8	17.3		2.55	78.4	2.85
180 min	231	<R.L.	<R.L.	1070	58.0	890	94.1	1520	31700	1.52	<R.L.	136	7.5	221	<R.L.	10.1	746	25.6
420 min	4.17	<R.L.	<R.L.	1120	72.7	1190	112	1770	36600	1.29	121	152	8.1	227	<R.L.	6.65	795	31.0
720 min	36.5	<R.L.	<R.L.	1420	75.1	1210	127	2150	48800	1.31	11.9	161	9.5	259	<R.L.	4.36	971	35.0
1440 min ave	57.1	<R.L.	<R.L.	1330	102	1370	150	2170	48600	1.85	250	166	8.9	269	<R.L.	9.05	945	31.3
1440 min stdev	20.6	N/A	N/A	66.8	26.0	53.2	15.7	74.0	2080	0.450	16.9	24.6	0.4	21.9		4.39	62.4	3.40

Appendix 5: Phase 2: Metal concentrations in 0.45 µm filtered seawater from 1:10 ore: seawater 180 minute elutriation at 12°C and 24°C.

Sample:	Al (µg/L)	V (µg/L)	Cr (µg/L)	Mn (µg/L)	Fe (µg/L)	Co (µg/L)	Ni (µg/L)	Cu (µg/L)	Zn (µg/L)	Ga (µg/L)	As (µg/L)	Mo (µg/L)	Ag (µg/L)	Cd (µg/L)	Hg (µg/L)	Au (µg/L)	Pb (µg/L)	U (µg/L)
Baseline (RI)	0.676	0.401	0.104	0.083	0.323	0.0160	0.107	0.283	1.11	0.0102	0.324	0.48	0.01	0.025	0.20	0.720	0.011	0.192
NC sw (clean hb)	3.41	2.13	<RL	0.510	<RL	0.06100	0.480	<RL	<RL	<RL	1.52	10.3	<RL	<RL	<RL	<RL	0.0400	2.67
12xC 180 min blank	2.28	1.98	<RL	0.970	0.490	0.09100	0.240	3.55	4.72	<RL	1.24	10.5	<RL	<RL	<RL	<RL	0.380	2.77
12xC 180 min dup 1	6.27	<RL	<RL	145	1.91	202	17.5	405	8950	0.0900	2.61	18.9	2.65	55.2	<RL	0.750	149	5.37
12xC 180 min dup 2	5.97	<RL	<RL	137	1.51	218	15.8	329	8960	0.110	3.16	21.0	2.68	60.2	<RL	<RL	147	5.71
12xC 180 min dup 3	5.15	<RL	<RL	150	1.76	205	17.4	508	9560	0.100	3.26	18.4	3.27	61.1	<RL	<RL	166	5.66
24xC 180 min blank	1.67	1.93	<RL	1.36	<RL	<RL	0.210	0.630	<RL	<RL	0.980	10.7	<RL	<RL	<RL	<RL	<RL	2.75
24xC 180 min dup 1	10.9	<RL	<RL	158	2.17	226	19.0	488	9520	0.110	4.13	22.8	3.99	57.3	<RL	<RL	242	5.76
24xC 180 min dup 2	12.0	<RL	<RL	147	2.26	233	15.6	393	8890	0.120	4.15	28.1	3.51	54.1	<RL	<RL	192	6.03
24xC 180 min dup 3	14.0	<RL	<RL	132	1.98	193	16.8	393	8880	0.120	3.75	22.4	3.27	51.5	<RL	<RL	177	5.65

Appendix 6: Phase 2: Quality control data for seawater metals analyses.

Sample:	Al (g/L)	V (g/L)	Cr (g/L)	Mn (g/L)	Fe (g/L)	Co (g/L)	Ni (g/L)	Cu (g/L)	Zn (g/L)	Cs (g/L)	As (g/L)	Mo (g/L)	Ag (g/L)	Cd (g/L)	Hg (g/L)	Au (g/L)	Pb (g/L)	U (g/L)
24cC180 nm blank ave	1.67	1.93	<RL	1.36	<RL	2.17	276	488	920	<RL	4.13	278	3.99	<RL	<RL	<RL	<RL	2.75
24cC180 nm blank stdev	0.570	0.180	0.0200	0.0400	0.020	0.450	0.650	577	186	0.0100	0.180	0.170	0.0300	0.730	0.160	0.160	1.02	0.0300
24cC180 nm blank spike	63.3	52.1	53.1	48.4	48.9	52.1	72.0	538	9570	483	555	728	529	101	55.1	270	270	52.4
Experimental spike	61.7	51.2	50.2	51.7	48.2	50.1	53.1	46.7	51.7	492	51.4	50.0	48.9	43.8	55.7	28.7	28.7	46.6
Spike value	50.0	50.0	50.0	50.0	50.0	50.0	50.0	50.0	50.0	50.0	50.0	50.0	50.0	50.0	50.0	50.0	50.0	50.0
Spike recovery (%)	123	102	100	103	98.5	97.7	104	102	105	97.7	116	106	126	102	93	102	102	98.4
24cC180 nm dup 1 average	10.9	<RL	<RL	163	2.17	276	19.0	488	920	<RL	4.13	278	3.99	<RL	<RL	<RL	242	5.76
24cC180 nm dup 1 stdev	0.0200	0.0400	0.00	2.06	0.450	3.08	0.650	577	186	0.0100	0.180	0.170	0.0300	0.730	0.160	0.160	1.02	0.0300
24cC180 nm dup 1 spike	63.1	52.1	52.2	479	53.4	276	72.0	483	9570	483	555	728	529	101	55.1	270	270	52.4
Experimental spike	52.2	52.0	52.2	50.8	51.2	50.1	53.1	46.7	51.7	492	51.4	50.0	48.9	43.8	55.7	28.7	28.7	46.6
Spike value	50.0	50.0	50.0	50.0	50.0	50.0	50.0	50.0	50.0	50.0	50.0	50.0	50.0	50.0	50.0	50.0	50.0	50.0
Spike recovery (%)	104	104	104	102	102	100	106	99.5	103	98.4	103	100	97.8	87.5	111	111	57.5	93.2

Experimental spike = (spike - ave)/(dilution factor = 1).

Certified reference materials and checks for analysis

Sample:	Al (g/L)	V (g/L)	Cr (g/L)	Mn (g/L)	Fe (g/L)	Co (g/L)	Ni (g/L)	Cu (g/L)	Zn (g/L)	Ga (g/L)	As (g/L)	Mo (g/L)	Ag (g/L)	Cd (g/L)	Hg (g/L)	Au (g/L)	Pb (g/L)	U (g/L)
NSSS ave	<RL	1.20	0.110	0.920	<RL	<RL	0.250	0.300	<RL	<RL	1.27	9.60	<RL	<RL	<RL	<RL	<RL	2.60
NSSS stdev	0	0.13	0.0300	0.0300	0.110	0.0100	0.0400	0.0800	0.110	0.160	0.10	0.160	<RL	0.023	IV	IV	0.008	0.0300
NSSS certified	0	1.2	0.11	0.919	0.087	0.011	0.263	0.287	0.102	IV	1.27	9.6	IV	0.023	IV	IV	0.008	2.6
CSSS-Lave	1.56	1.30	0.140	2.96	0.710	0.0200	0.290	0.560	<RL	<RL	1.24	9.8	0.0100	0.0300	<RL	<RL	<RL	2.62
CSSS-Lstdev	0.470	0.160	0.0100	0.120	0.0100	0.00	0.0300	0.0500	0.140	0.140	0.140	0.210	0.01	0.00	<RL	<RL	0.0100	0.0300
CSSS-L certified	IV	1.08 ± 0.16	0.144 ± 0.029	IV	0.713 ± 0.068	0.026 ± 0.003	0.314 ± 0.03	0.592 ± 0.035	0.381 ± 0.057	IV	1.11 ± 0.16	8.78 ± 0.86	IV	0.026 ± 0.003	IV	IV	0.008 ± 0.0036	IV
SLEW3	<RL	2.37	0.110	1.62	<RL	0.0300	1.29	1.44	<RL	<RL	1.31	4.85	<RL	0.0500	<RL	<RL	<RL	1.41
SLEW3 certified	IV	2.57 ± 0.31	0.183 ± 0.019	1.61 ± 0.22	0.598 ± 0.059	0.042 ± 0.010	1.23 ± 0.07	1.55 ± 0.12	0.201 ± 0.037	IV	1.36 ± 0.09	(6.1)*	(0.009)*	0.048 ± 0.004	IV	IV	0.0090 ± 0.0014	(1.9)*
bb ref + 20ppb	101	22.0	19.6	24.4	99.8	19.4	20.4	20.0	21.0	19.1	22.7	33.0	4.72	20.6	<RL	<RL	21.5	24.3
bb ref + 20ppb value	82.9	22.2	20.8	22.5	82.1	20.5	20.3	20.5	21.0	20.4	19.2	30.9	5.00	20.6	IV	IV	22.1	24.4
In House sw/AG Clean + 20 ppb Al & Ag																		
In House sw/AG Clean + 20 ppb Al & Au value																		

CSSS: National Research Council Canada - Nearshore Seawater Reference Material for Trace Metals
 NSSS: National Research Council Canada - Seawater Reference Material for Trace Metals
 SLEW3: National Research Council Canada - Estuarine Water Reference Material for Trace Metals
 bb ref + 20 ppb: Seawater containing 20 ppb trace metals (5 ppb Ag)
 In House sw/AG Clean + 20 ppb Al & Ag: Clean Seawater containing 20 ppb Al and Ag
 (*): Information only

Appendix 7: Phase 2: Net metals released and normalised data for dissolved metals released from one gram of ore (ng/g ore) into 250ml seawater at 12 and 24°C

Net metals released from ore

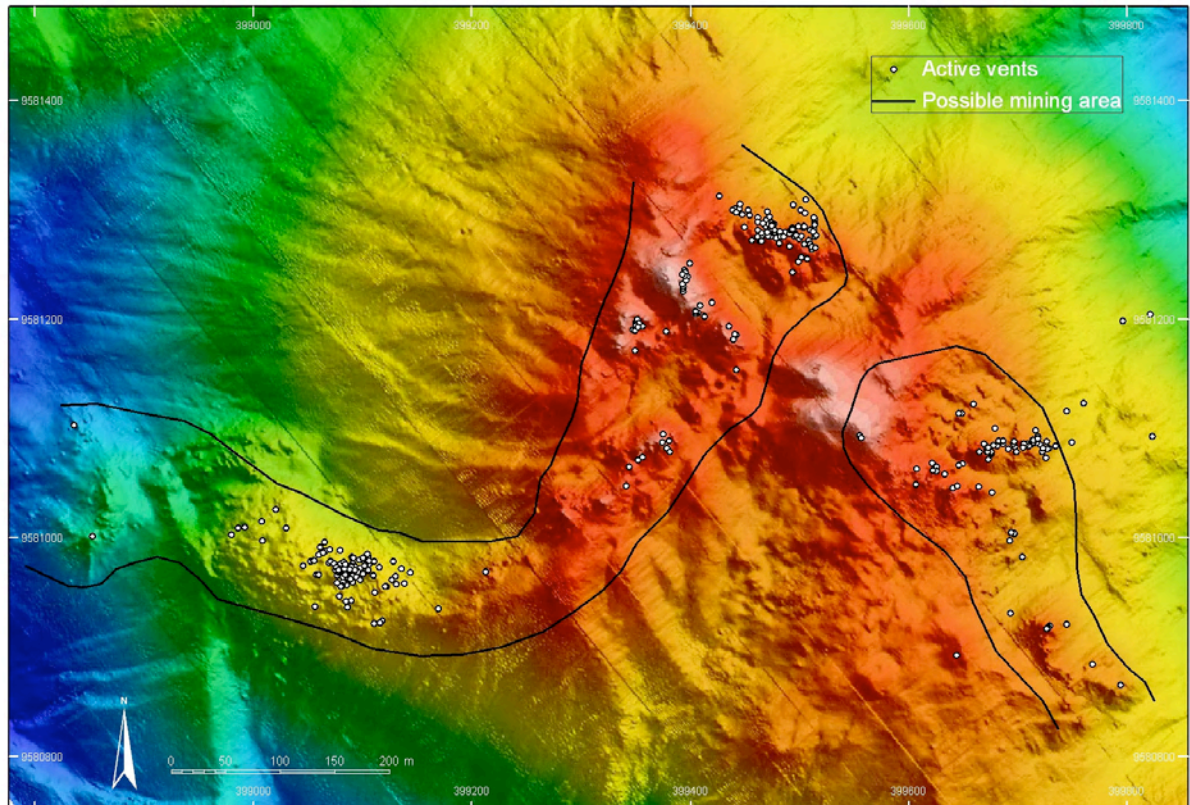
Sample:	Al (g/L)	V (g/L)	Cr (g/L)	Mn (g/L)	Fe (g/L)	Co (g/L)	N (g/L)	Cu (g/L)	Zn (g/L)	Ga (g/L)	As (g/L)	Mo (g/L)	Ag (g/L)	Cd (g/L)	Hg (g/L)	Au (g/L)	Pb (g/L)	U (g/L)
Blank/0 hr (RL)	0.676	0.401	0.104	0.093	0.323	0.060	0.007	0.233	1.11	0.002	0.324	0.481	0.01	0.026	0.20	0.720	0.011	0.192
12°C 180 min dtp 1	0.00	0.00	<RL	0.00	0.00	0.00	0.00	0.00	0.00	<RL	0.00	0.00	<RL	<RL	<RL	<RL	0.00	0.00
12°C 180 min dtp 2	3.99	<RL	<RL	144	1.42	202	17.3	401	8860	0.0000	1.37	8.40	2.65	55.2	<RL	0.750	149	2.80
12°C 180 min dtp 3	3.69	<RL	<RL	136	1.02	216	15.6	325	8860	0.110	1.30	10.5	2.88	60.2	<RL	<RL	147	2.84
24°C 180 min dtp 1	2.87	<RL	<RL	149	1.27	235	17.2	504	9360	0.100	2.02	7.30	3.27	61.1	<RL	<RL	166	2.89
24°C 180 min dtp 2	0.00	0.00	<RL	0.00	<RL	<RL	0.00	0.00	<RL	<RL	0.00	0.00	<RL	<RL	<RL	<RL	<RL	0.00
24°C 180 min dtp 3	9.23	<RL	<RL	157	2.17	226	18.8	467	9520	0.110	3.15	12.1	3.99	57.3	<RL	<RL	242	3.01
24°C 180 min dtp 4	10.3	<RL	<RL	146	2.26	233	15.4	392	8860	0.120	3.17	17.4	3.51	54.1	<RL	<RL	192	3.28
24°C 180 min dtp 5	12.3	<RL	<RL	131	1.98	193	16.6	392	8360	0.120	2.77	11.7	3.27	51.5	<RL	<RL	177	2.80

Normalised data for dissolved metals released from one gram of ore into 250 mL seawater

Sample:	Al (ng/g)	V (ng/g)	Cr (ng/g)	Mn (ng/g)	Fe (ng/g)	Co (ng/g)	N (ng/g)	Cu (ng/g)	Zn (ng/g)	Ga (ng/g)	As (ng/g)	Mo (ng/g)	Ag (ng/g)	Cd (ng/g)	Hg (g/L)	Au (ng/g)	Pb (ng/g)	U (ng/g)
12°C 180 min are	35.2	<RL	<RL	1430	12.4	2380	167	4100	91600	1.00	17.7	89.3	28.7	588	<RL	7.48	1540	28.1
24°C 180 min stdev	57.9	NA	NA	65.5	202	66.4	951	689	3630	0.100	3.30	138	3.30	320	0.00	0.00	106	1.84
24°C 180 min are	106	<RL	<RL	1440	21.4	2170	169	4240	88200	1.17	30.3	137	35.9	543	<RL	<RL	2040	30.3
24°C 180 min stdev	15.7	NA	NA	130	1.44	214	17.2	547	5710	0.0600	2.26	31.9	3.66	280	<RL	NA	340	2.42

Appendix 10

Biomass, Biodiversity and Bioaccumulation Desktop Study



NAUTILUS – SOLWARA 1 Project

Biomass, Biodiversity and Bioaccumulation

Desktop Study

June 2008



ABN	26 096 574 659
GST	The company is registered for GST
Head Office	47 Park Road Milton QLD 4064
Registered Office	Level 21 141 Queen Street Brisbane QLD 4000
Postal Address	PO Box 2050 Milton QLD 4064
Phone	61 (07) 3368 2133
Fax	61 (07) 3367 3629
Email Contact	info@hydrobiology.biz
Website	http://www.hydrobiology.biz

© Hydrobiology Pty Ltd 2007

Disclaimer: This document contains confidential information that is intended only for the use by Hydrobiology's Client. It is not for public circulation or publication or to be used by any third party without the express permission of either the Client or Hydrobiology Pty. Ltd. The concepts and information contained in this document are the property of Hydrobiology Pty Ltd. Use or copying of this document in whole or in part without the written permission of Hydrobiology Pty Ltd constitutes an infringement of copyright.

While the findings presented in this report are based on information that Hydrobiology considers reliable unless stated otherwise, the accuracy and completeness of source information cannot be guaranteed. Furthermore, the information compiled in this report addresses the specific needs of the client, so may not address the needs of third parties using this report for their own purposes. Thus, Hydrobiology and its employees accept no liability for any losses or damage for any action taken or not taken on the basis of any part of the contents of this report. Those acting on information provided in this report do so entirely at their own risk.

Nautilus – SOLWARA 1 Project

Biomass, Biodiversity and Bioaccumulation

Desktop Study

June 2008

Document Control Information

Date Printed	-				
Project Title	Solwara 1 – Desktop Study				
Project Manager	Adrian Flynn				
Job Number	ENESAR/0703				
Report Number	ENESAR_0703_v2_AF				
Document Title	Biomass, Biodiversity and Bioaccumulation Desktop Study				
Document File Name	Document Status	Originator(s)	Reviewed By	Authorised By	Date
ENESAR_0701_v1_AF	DRAFT	AF, JA	AF, JA	AF	29/11/07
Enesar_0703_Solwara 1_v2_AF.doc	DRAFT	AF	AF	AF	20/6/08
Enesar_0703_Solwara 1_v3_AF.doc	FINAL	AF	AF	AF	30/6/08

Distribution

Document File Name	Description	Issued To	Issued By
ENESAR_0701_v1_AF	DRAFT	Mike Wright	AF
Enesar_0703_Solwara 1_v2_AF.doc	DRAFT	Mike Wright	AF
Enesar_0703_Solwara 1_v3_AF.doc	FINAL	Mike Wright	AF

Nautilus – SOLWARA 1 Project

Biomass, Biodiversity and Bioaccumulation Desktop Study June 2008

CONTENTS

1	INTRODUCTION.....	1
1.1	Background.....	1
1.2	Objectives.....	4
1.2.1	Biomass and Biodiversity.....	4
1.2.2	Bioluminescence.....	4
1.2.3	Bioaccumulation.....	4
2	Methods and Data Sources.....	5
3	Water Column Structure.....	6
4	Biomass and biodiversity.....	10
4.1	Epipelagic.....	10
4.1.1	Introduction.....	10
4.1.2	Producers.....	10
4.1.3	Consumers.....	13
4.1.4	Distributions.....	17
4.2	Mesopelagic.....	21
4.2.1	Introduction.....	21
4.2.2	Producers.....	21
4.2.3	Consumers.....	22
4.2.4	Distribution.....	24
4.3	Bathypelagic.....	28
4.3.1	Introduction.....	28
4.3.2	Producers.....	28
4.3.3	Consumers.....	28
4.3.4	Distributions.....	31
5	PNG Tuna and Shark Fisheries.....	33
5.1	Introduction.....	33
5.2	Tuna.....	33
5.3	Shark.....	39
6	Data from Lihir Island.....	41
6.1	Introduction.....	41

6.2	Methods.....	41
6.2.1	Plankton	41
6.2.2	Micronekton	41
6.3	Results.....	41
6.3.1	Vertical Migration.....	41
6.3.2	Zooplankton Diversity	42
6.3.3	Micronekton	46
6.3.4	Epipelagic predators.....	49
7	Bioluminescence	50
7.1	Vision	50
7.1.1	Marine Light Environment.....	50
7.1.2	Deep-Sea Eye Design.....	50
7.2	Chemistry.....	51
7.3	Functions	52
7.3.1	Defence.....	52
7.3.2	Feeding.....	53
7.3.3	Signalling Behaviour	53
7.4	Occurrence and Distribution	54
8	Trophic Webs	57
9	Risk Pathways and assessment	64
9.1	Introduction	64
9.2	Body Burden, Bioaccumulation and Biomagnification	66
9.3	Risk Assessment.....	70
9.3.1	Summary of relevant in-situ water quality testing	70
9.3.2	Summary of physicochemical testwork.....	70
9.3.3	Summary of hydrodynamic modelling of discharge plume	71
9.4	Conclusions.....	72
10	Management and Monitoring.....	76
11	References.....	77

TABLES

Table 5-1	Species composition of PNG shark longline fishery.....	40
Table 6-1	Abundance of zooplankton taxa at Lihir Island.....	43
Table 8-1	Summary of tuna gut-contents data.....	58
Table 9-1	All potential risks of the project to pelagic, mesopelagic and bathypelagic organisms.....	64
Table 9-2	Risk assessment.....	73

FIGURES

Figure 1-1	Location of the Solwara 1 project.....	1
Figure 3-1	Temperature profiles.....	6
Figure 3-2	Dissolved oxygen profiles.....	7

Figure 3-3	Depth zones	8
Figure 4-1	Surface chlorophyll concentrations in northwest and southeast wind seasons.....	12
Figure 4-2	Broad-scale surface currents and temperature in the eastern Bismarck Sea	16
Figure 4-3	Dive profiles of bigeye tuna (top) and yellowfin tuna (bottom)	19
Figure 4-4	Hydroacoustic echogram and net catches in the mesopelagic zone.....	23
Figure 4-5	Schematic diagram of vertical migration.....	27
Figure 4-6	Location of active hydrothermal vents in the Solwara 1 project area	31
Figure 5-1	Purse seine and longline catches for Papua New Guinea tuna fishery.....	34
Figure 5-2	Distribution of total purse catch for PNG-associated fleet	35
Figure 5-3	Location of FADs in PNG waters	36
Figure 5-4	Distribution of total longline catch in PNG waters.....	37
Figure 5-5	Distribution of total longline effort in PNG waters	37
Figure 5-6	Distribution of longline effort 1979 – 1987 in PNG waters	39
Figure 5-7	Shark longline catch, 1999-2002	40
Figure 6-1	Depth distribution of zooplankton biomass at Lihir Island	42
Figure 6-2	Examples of zooplankton at Lihir Island.....	45
Figure 6-3	Selected species of micronekton from Lihir Island	47
Figure 6-4	Stomach contents of pelagic predators at Lihir Island	49
Figure 7-1	Schematic diagram of a bioluminescent reaction.....	52
Figure 8-1	Conceptual trophic web of the pelagic environment.....	63
Figure 9-1	Schematic diagram of exposure pathways and regulation in the body of a primary consumer and higher-order consumer.....	69

PLATES

Plate 1-1	Remotely-operated mining machine.....	2
Plate 4-1	Organisms identified at various depths in ROV footage at Solwara 1	26
Plate 4-2	Bathypelagic fish from the Solwara 1 project area.....	30

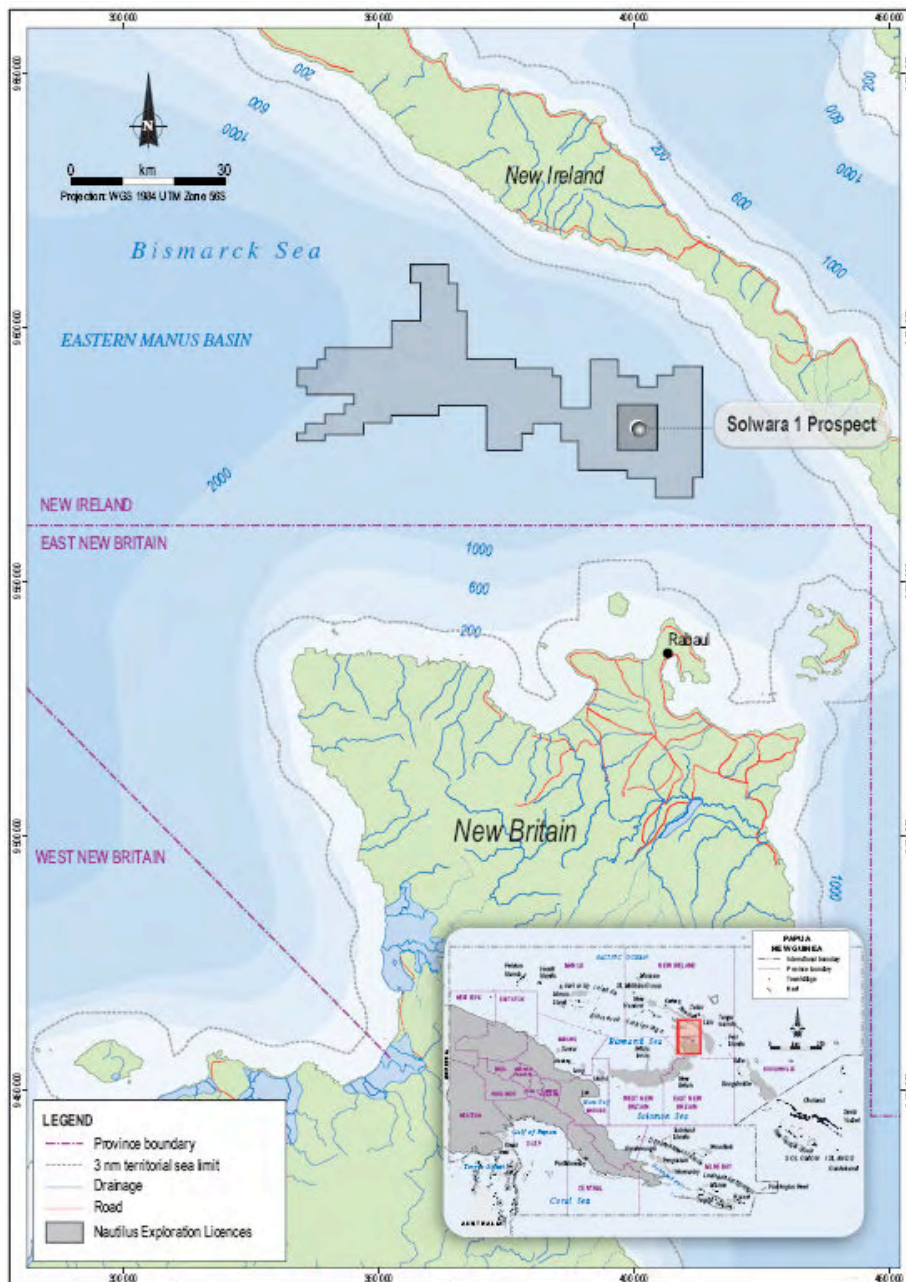
ATTACHMENTS

Attachment 1	Some of the epipelagic, mesopelagic and bathypelagic animals likely to occur in the Solwara 1 project area	85
Attachment 2	List of cetaceans and turtles likely to occur in the Solwara 1 project area.....	93

1 INTRODUCTION

1.1 Background

Nautilus Minerals Niugini (Nautilus) is proposing to develop the Solwara 1 Project to commercialise copper-, zinc-, silver- and gold-rich seafloor massive sulfide (SMS) deposits in the eastern Manus Basin, Bismarck Sea, Papua New Guinea (PNG) (Figure 1-1). The prospect is located at water depths of 1,500 to 1,700 m.



Source: Coffey Natural Systems

Figure 1-1 Location of the Solwara 1 project

This report deals with Phase 1 of the project, which is the mining of materials on the seafloor using a remotely-operated mining machine tethered to a surface support vessel (see Plate 1-1), transport of the mined material to the surface, dewatering on board a surface ship, disposal of dewatering fluid (at a depth of approximately 1,500 m) and shipping of dewatered ore to an overseas concentrator and smelter. At the time of writing, it is understood that approximately 300,000 tonnes of non-mineralised unconsolidated sediment (hereafter referred to as unconsolidated sediment) overlaying the material to be mined, is required to be extracted and deposited in a number of neighbouring sites outside the mining area. It is understood that this material will be moved without the need to bring it to the surface, by using remotely-operated machines. Phase 2 of the project involves the construction and operation of a processing plant on land.

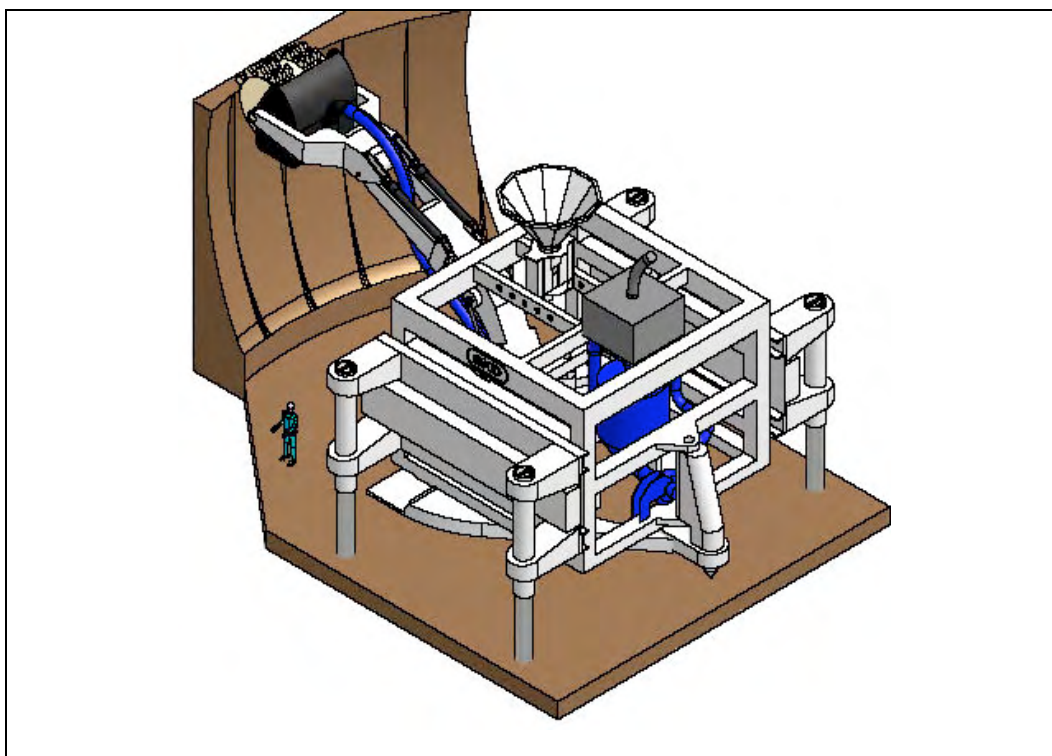


Plate 1-1 Remotely-operated mining machine

Source: Coffey Natural Systems

The key issues with respect to potential impacts of the offshore component of mining activity on marine organisms centre around the potential for the activity to directly physically impact organisms and to generate turbid and possibly metal-enriched plumes associated with the physical action of the mining machine, the movement of the unconsolidated sediment drape and a deep-water plume associated with the discharge of dewatering fluid. The specific issues related to these plumes are:

- Potential direct toxicity of metals in the plumes to deepwater organisms;
- Potential bioaccumulation of metals through various trophic levels, including vertically migrating plankton and pelagic fish;

- Optical effects of suspended sediments on organisms that depend on bioluminescence, both in the water column near the dewatering discharge and adjacent to the seafloor near mining operations;

The proponent undertook a range of modelling and testwork investigations to understand the physical and chemical behaviour of these plumes and these will be described below. The results of these investigations will be integrated with the present ecological desktop study in order to identify and assess the potential risks of the project to pelagic (epi-, meso- and bathypelagic) organisms. This review does not cover benthic fauna (organisms living on, or in, the bottom sediments) as these groups are covered in other investigations. Further description of the habitats handled in this review is given below.

The epipelagic zone, corresponding with the euphotic zone, is highly productive. It is the photosynthetic primary production in this layer that ultimately supports much of the large-bodied organisms that are the top-predators of the pelagic food chain. This includes species that are targeted for fisheries (e.g. tunas, billfish, trevallies and sharks). In the meso- and bathypelagic zones, animals are generally more sparsely distributed and, while these depths may not be targeted for fisheries, there are direct linkages with the epipelagic zone via processes such as deep-diving foraging by predators, fall-out of particulate organic matter and vertical migration.

Species in the meso- and bathypelagic zones are not well studied and these depths, along with hydrothermal vents and other recently-discovered features, represent a frontier of marine science and therefore are of inherent scientific interest.

Biological characteristics of the fauna in the deeper parts of the mesopelagic zone and in the bathypelagic zone can be generally described as follows (Nybakken and Bertness 2005, Herring 2002):

- Reproduction and Development
 - Low fecundity, large yolk-rich eggs;
 - Larger proportion of egg-brooders rather than broadcast spawners;
 - Late reproductive maturity;
 - Slow embryonic development;
- Physiology
 - Low metabolic rate;
 - Low activity level and low swimming ability;
 - High water content;
 - Low protein content;
- Ecology
 - Slow growth;
 - High longevity;
 - Slow colonisation;
 - Low population densities;
 - Low predatory mortality.

As will be described below, the unique physiology and ecology of some organisms in the meso- and bathypelagic zones dictates that unique considerations are required for potential impact mechanisms that are different from the highly mobile and transient fauna in the epipelagic zone. For example, the underlying principal of mobile fauna behaviourally avoiding adverse conditions does not necessarily hold for deep-water fauna because they may lack either the swimming capability or the metabolic reserves to undertake significant movements or to tolerate sub-optimal conditions.

1.2 Objectives

This study is divided into three, inter-related themes and the objectives of each of these themes are described below.

1.2.1 Biomass and Biodiversity

- Characterise the biomass and biodiversity (including plankton, fish, crustaceans, cephalopods, turtles, cetaceans, etc.) found in the water column via review of the literature and other relevant data available.
- Characterise the spatial and temporal presence of these species in the water column (seasonal/vertical migrations etc.) and likely trophic relationships between these animals.
- Use the outcomes, of the biomass and biodiversity characterisation and hydrodynamic and chemical modelling of the behaviour and fate of plumes formed at the seafloor and from on-board dewatering process, to assess the risks of increased water turbidity on biomass and biodiversity.

1.2.2 Bioluminescence

- Undertake a literature review to determine the likely presence of bioluminescent species.
- Use outcomes of the literature review and hydrodynamic and chemical modelling of the behaviour and fate of plumes formed at the seafloor and from on-board dewatering process, to assess risks of increased water turbidity on animals reliant on bioluminescence.

1.2.3 Bioaccumulation

- Using the data available, consider the risks and pathways of bioaccumulation of metals through the food chain and into commercial fish such as the skipjack tuna.
- Compare the potential risks found with hydrodynamic and chemical modelling to determine the likelihood of occurrence of bioaccumulation and need for further modelling.

2 METHODS AND DATA SOURCES

Literature was searched from international scientific journals and texts for information in each of the themes of this project. Data from the western and central Pacific Ocean were considered to be most relevant with respect to species occurrence records while data from the Atlantic Ocean and other seas were useful to support the understanding of ecological processes. Most attention was given to information that could be used to build a conceptual understanding of the ecological functioning of deep sea communities and the sensitivities of the environment and the organisms, and therefore, the potential threats of the Solwara 1 project on the system.

A video camera mounted on a remotely-operated vehicle (ROV) was used for various benthic investigations for the Solwara 1 project. The ROV was a Perry Slingsby ST203, 200HP workclass vehicle, configured for scientific research. This presented an opportunity to view footage taken during descent and ascent of each dive. The footage was viewed using a software package called Visual Review v7.0 at the premises of Nautilus Minerals (Brisbane). Notes were taken on the occurrence of nekton and plankton, including depth and time. Image stills were captured of each type of fauna where screen resolution was adequate. Where image stills were taken, details of the dive, time, location, and image subject were logged into Nautilus' system in an MS Access database.

Oceanographic data reported here were collected by Nautilus using a profiling CTD and graphs of oceanographic profiles were supplied by Nautilus.

Lists of expected species were compiled using various sources, including the Fishbase (2007) database, various texts (including Allen and Munday 1994) and records of bycatch from the tuna fishery as reported in PNG fisheries statistics.

3 WATER COLUMN STRUCTURE

The water column in the Solwara 1 project area is characterised by warm surface waters of approximately 29 °C and temperature near the bottom at 1,600 m water depth of about 3 °C. Figure 3-1 shows two examples of variability in the water column structure in terms of uniformity of the mixed layer and depth of thermocline.

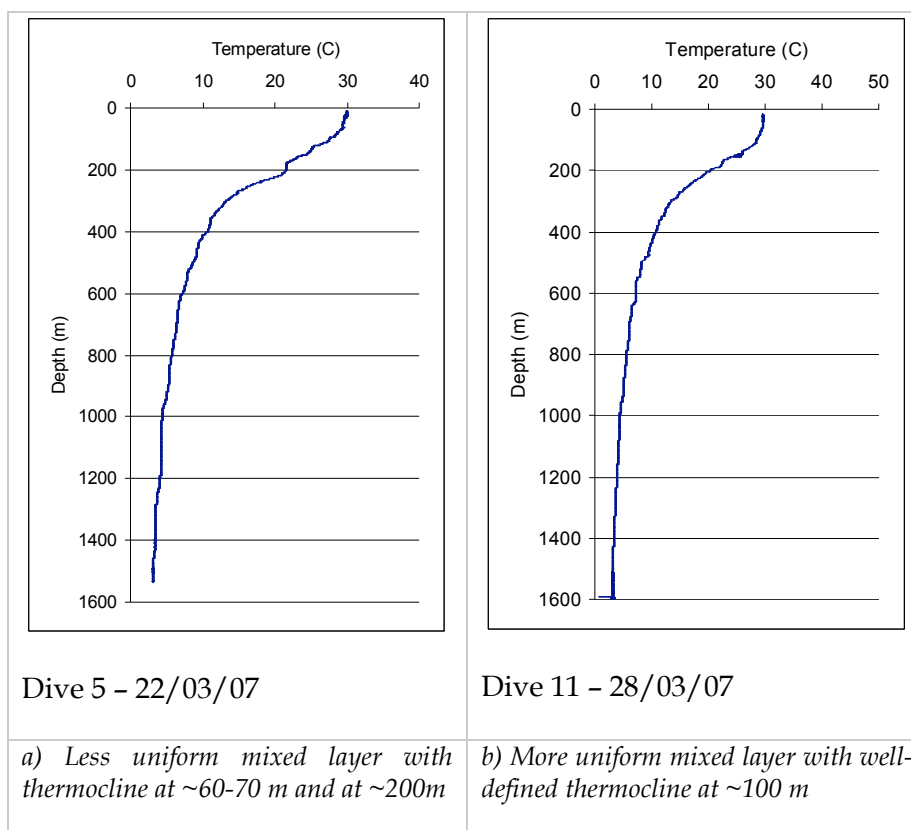


Figure 3-1 Temperature profiles

Source: Nautilus Minerals Pty Ltd

Dissolved oxygen concentrations recorded at the site also indicate some water column structure (Figure 3-2). Dissolved oxygen concentrations generally drop steadily in the first 200 m, rising again between 200 and 600 m. Interestingly, profiles from the Solwara 1 site show oxygen increases around the 400 m mark which, as will be discussed below, coincides with a concentration of consumer activity identified in ROV footage and also coincides with a commonly quoted daytime depth of a deep scatterings layer in other oceanic regions¹.

¹ A layer in the water column that has a high density of acoustic scattering sources and is readily identified by echosounders and other acoustic instruments. It is interpreted as a band of living organisms, principally micronekton and macrozooplankton.

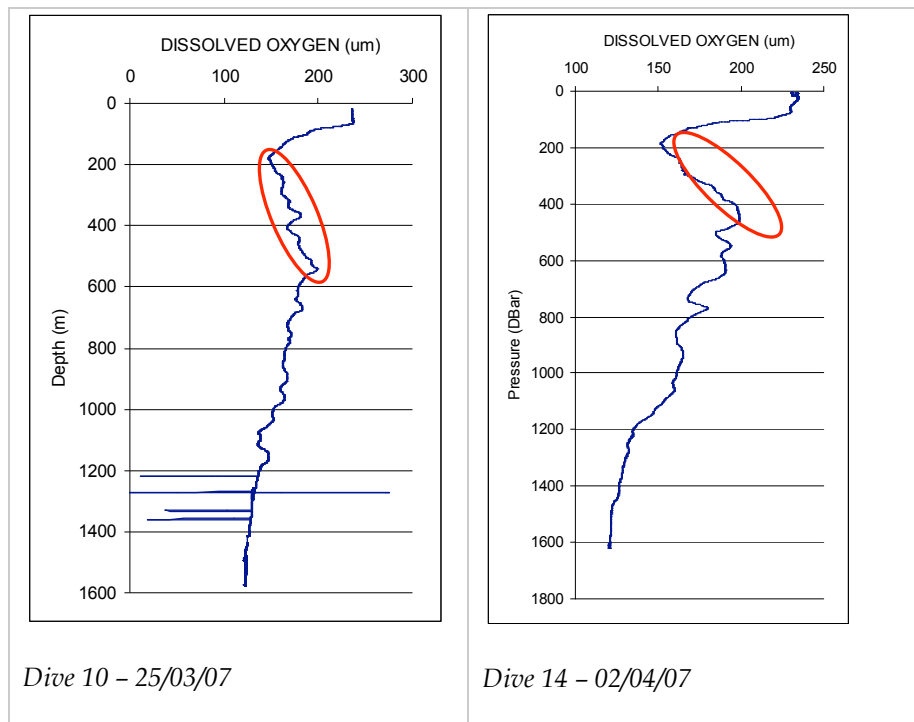


Figure 3-2 Dissolved oxygen profiles

Source: Nautilus Minerals Pty Ltd

For the purposes of this study, the water column is divided into the following layers (see Figure 3-3):

- Epipelagic zone (0-200 m);
- Mesopelagic zone (200 - 1000 m);
- Bathypelagic zone (>1000 m).

The epipelagic zone is characterised by a well-lit environment that is inhabited by plankton, large agile predatory fishes (such as tuna, billfishes and sharks) and the smaller varieties of fishes and invertebrates upon which they prey. Surface waters of the open ocean, outside the influence of riverine inputs, are generally oligotrophic (i.e., low levels of primary productivity, which is nutrient-limited).

Food webs in the epipelagic zone are classical (yet rather complex) phytoplankton-based systems, driven by photosynthesis and various microbial processes, leading to secondary production of zooplankton, larger consumers and finally to large mobile predators. While the phytoplankton-based food web is only active within the epipelagic zone, it supports life in the lower levels of the ocean as a result of downward transport through the vertical ladder of migrations and feeding, and the downward drift of particulate organic matter, known as

'marine snow'. This process will be described below. Within the epipelagic zone, the water column is structured by, for example, thermoclines, density discontinuities and nutriclines².

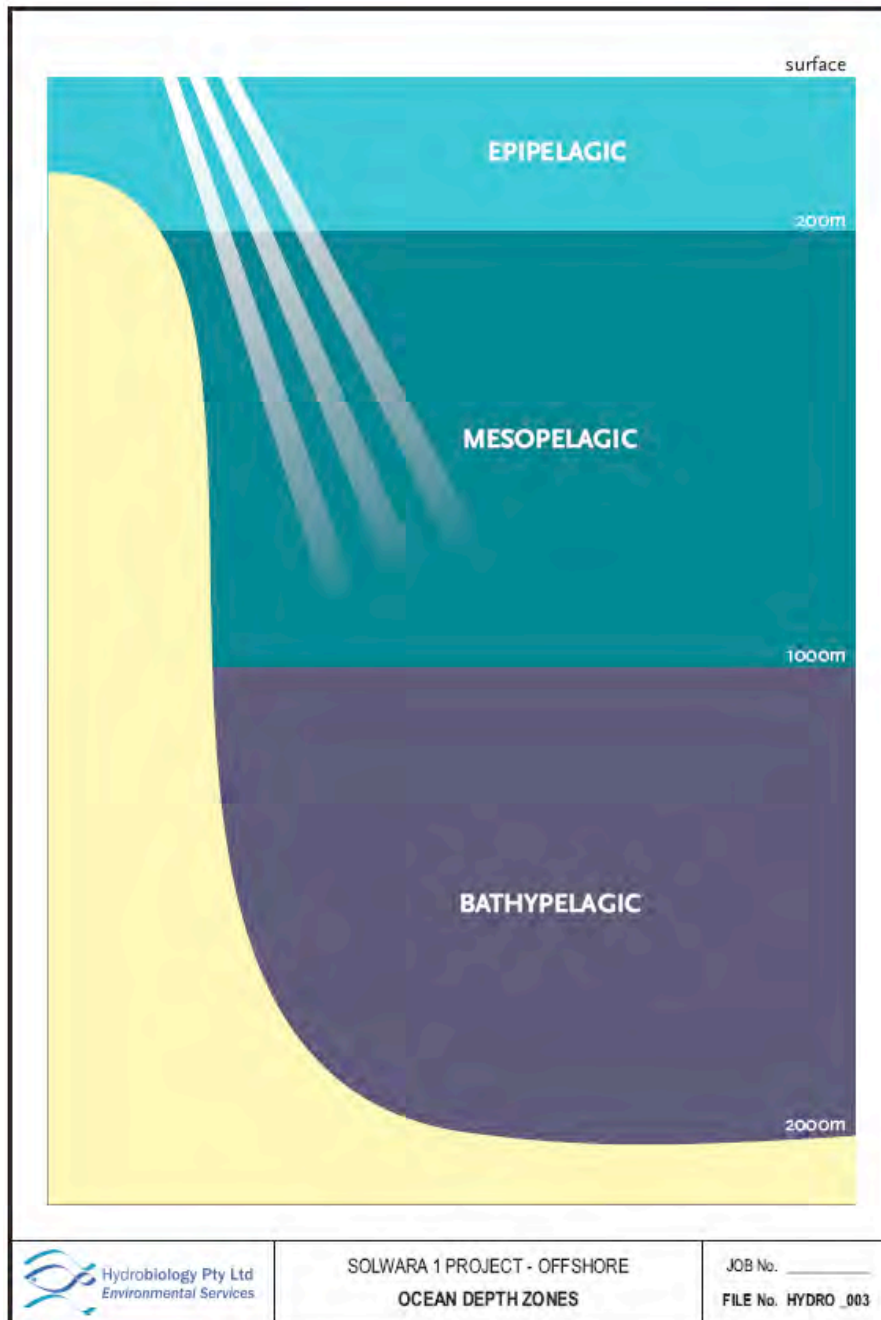


Figure 3-3 Depth zones

² Recent evidence from Australia suggests that chlorophyll-a concentration remotely sensed from the ocean surface by satellites under-estimates primary productivity and nutrient content, which previous assumed to be highest at the surface, is actually often highest at nutriclines some 60 – 150 m under the surface (Lyne and Hayes 2005). It is postulated that this is due to the upward transport and trapping of nutrient-rich waters below the thermocline.

Biomass declines exponentially with depth through the water column (Marshall 1979; Herring 2002). In the mesopelagic zone, bioluminescence becomes more common, and various colouration and body morphological adaptations exist to camouflage many fish, cephalopods and crustaceans against the weak down-welling light by counter-illumination. A very wide range of visual adaptations also occur in this zone. Within the mesopelagic zone, various oceanographic 'structures' occur, such as deep scattering layers, density discontinuities, nutriclines and an oxygen minimal layer (decrease in oxygen concentration). As will be described below, the process of diel vertical migration plays an important role in linking the mesopelagic and epipelagic environments.

The top of the bathypelagic zone represents the absolute limit of sunlight. While deeper waters typically have higher concentrations of nutrients (nitrogen, phosphorus and silicon) the conditions of low oxygen concentration, high pressure, low food availability and low temperatures severely limit the abundance and biomass of animals in this zone. Animals adapted to tolerate these conditions generally have low metabolic rates, soft skeletons and reduced protein levels, which severely limits their swimming ability. Bioluminescence plays a crucial role for organisms in this zone, and organisms are highly opportunistic feeders. The delivery of organic matter to the bathypelagic zone in the form of marine snow is slow, with sporadic events such as whale-falls providing a significant attractant to scavengers. Close to the seafloor, free-swimming animals are more abundant and some have stronger musculature (e.g. rat-tails, squalid sharks, hagfish), probably because there is a greater abundance of food sources at the sediment-water interface and because the maintenance of neutral buoyancy is not so critical (Marshall 1979; Herring 2002).

4 BIOMASS AND BIODIVERSITY

4.1 Epipelagic

4.1.1 Introduction

The epipelagic zone roughly corresponds with the euphotic zone and the surface mixed layer of the ocean. This zone extends from the sea surface to approximately 200 m water depth and generally contains the highest diversity of the pelagic zones.

4.1.2 Producers

Plankton refers to small-bodied organisms that have limited powers of locomotion, and are thus moved and distributed as the result of prevailing water movements. Plankton includes phytoplankton, photosynthetic organisms responsible for most of the primary production that occurs in the open ocean and includes a wide range of microalgae and cyanobacteria. The larger organisms which are normally captured in nets (net phytoplankton) consist mostly of diatoms and dinoflagellates, and these groups dominate net phytoplankton throughout the world (Nybakken and Bertness 2005). Productivity in tropical oceans is typically low, with nutrient limitations in surface waters placing a limitation on carbon production. Productivity of net phytoplankton has been calculated as 15-50 g C/m²/year in tropical oceans, compared to 70-120 g C/m²/year for temperate oceans (Nybakken and Bertness 2005). The smaller phytoplankton, including the nanoplankton and picoplankton, are more variable and appear to be more important in productivity in oligotrophic regions than the larger net phytoplankton (Nybakken and Bertness 2005; Partensky et al. 1999; Raven 1998). Picoplankton, including cyanobacteria, have been calculated to produce an estimated 20-80% of primary productivity in the Eastern Pacific (Li et al. 1983) and up to 60% in the Western Atlantic (Platt et al. 1983).

The physical conditions of the water column in tropical latitudes often results in communities that, while having reduced productivity, are often more species-diverse than temperate and polar regions. In the tropics, the oligotrophic (nutrient-poor) conditions and the lack of seasonal variability appear to favour smaller photosynthetic organisms that have a proportionately greater surface area to absorb nutrients (e.g. *Prochlorococcus*; Partensky et al. 1999).

The unicellular cyanobacteria genus, *Prochlorococcus* spp., part of the picoplankton, is the most abundant photosynthetic organism in the ocean. Maximum concentrations of *Prochlorococcus* have been measured at 700 000 cells ml⁻¹ in the Arabian Sea. Another genus of cyanobacteria, *Synechococcus* is a close second, generally being one order of magnitude less abundant than *Prochlorococcus* (Partensky et al. 1999). *Prochlorococcus* is ubiquitous from 40°N to 40°S in high densities, occurring in both surface waters, where presumably only reduced nitrogen is available, and at the deep chlorophyll maximum (100 – 200 m depth), where nitrates are present. In subtropical oligotrophic areas of the Atlantic and Pacific oceans, the vertical distribution of *Prochlorococcus* often exceeds the depth of the euphotic layer (Partensky et al. 1999). Its low iron requirements may be a key factor in its success in central oceanic areas, such as the equatorial Pacific, where inputs of iron are limited (Partensky et al. 1999).

In open ocean situations, *Prochlorococcus* most commonly occurs in relatively constant concentrations of 1×10^5 to 3×10^5 cells ml^{-1} , evenly distributed from the surface to the bottom of the euphotic zone, including depths with as little as 1 % of surface light irradiation. This can include the mesopelagic zone, and will be discussed in below.

In tropical areas, the net phytoplankton is most likely to consist of dinoflagellates and coccolithophores (Nybakken and Bertness 2005). Even in the stable conditions in surface waters in tropical latitudes, there can be successions of phytoplankton species composition, e.g. in the Sargasso Sea, dominant phytoplankton changes from coccolithophores and diatoms, to dinoflagellates, to coccolithophores in a successional sequence. In tropical waters, coccolithophores and dinoflagellates are generally dominant all year, although they may be interrupted by periodic diatom blooms. The causes of succession and blooms are likely to be a combination of temperature, nutrient levels, biological conditioning (e.g. producing toxins), and grazing by zooplankton. Although tropical latitudes in the open ocean are generally oligotrophic, there can be periodic equatorial upwelling, increasing surface nutrient supply, and increasing cyanobacteria and microalgae populations by up to 407 and 3.2 times, respectively (Blanchot et al. 1992).

Figure 4-1 shows surface chlorophyll-a concentration (a proxy for primary production) in Papua New Guinea over the two dominant seasons; northwest wind season (November to May) and the southeast wind season (June to October). Primary productivity in the Bismarck Sea is generally low in both seasons, with some enrichment in productivity in the area of the Solwara 1 project area during the southeast wind season. Brewer et al. (2008) identified that 'fronts' of productivity have been implicated in attracting both prey and predator species in the open ocean off eastern Australia.

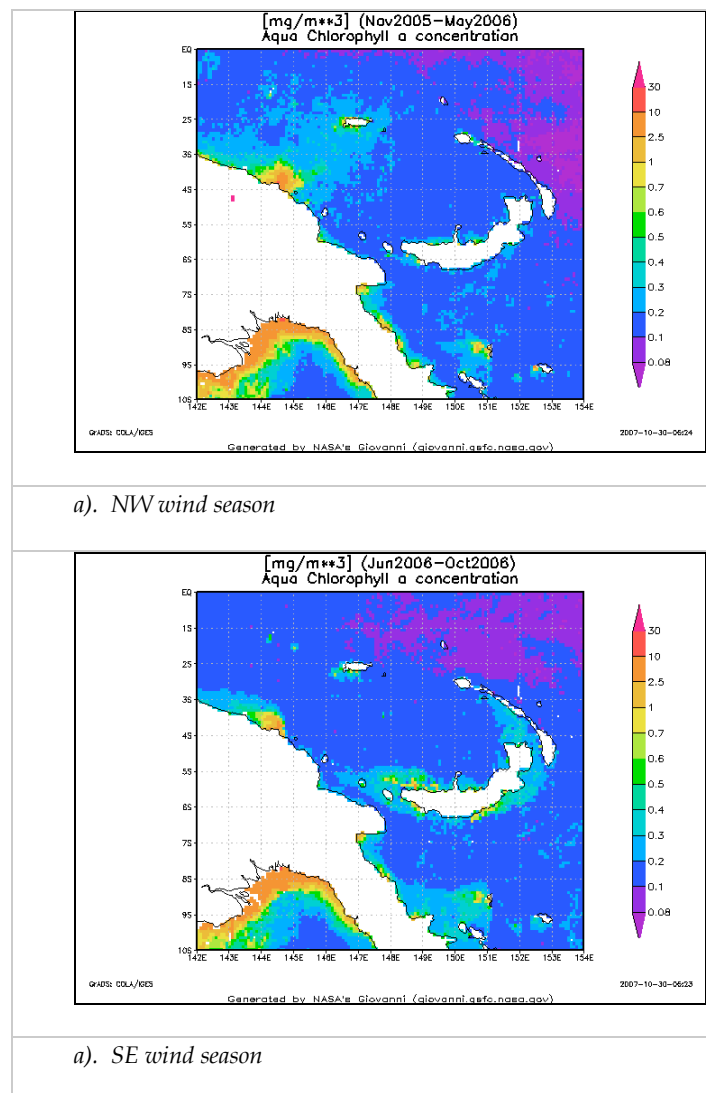


Figure 4-1 Surface chlorophyll concentrations in northwest and southeast wind seasons

The increase in chlorophyll-a during the SE wind season (Figure 4-1) may be the result of upwelling in the basin. The strait between the two islands of New Britain and New Ireland, is shallow (200 m) and likely to be well mixed and warm. When southeast winds push this water in a northwesterly direction into the Bismarck Sea, cold benthic waters may upwell at the edge of the continental shelf area, bringing nutrient rich waters to the surface and causing increased chlorophyll-a productivity in surface waters. Thus there appears to be some seasonality in productivity and plankton communities in this specific area, but it is not known how this affects the rest of the pelagic community in this particular location. Indeed, the high productivity of the tuna fishery in the Bismarck Sea (described in Section 5) is not necessarily reflected in the surface production figures.

Satellite imagery of chlorophyll-a only measures chlorophyll abundance in the upper 10 to 25 m in surface waters. However, much of the primary production may be taking place deeper in the water column at the nutricline, especially in tropical waters. This means primary production may be somewhat higher than satellite imagery suggests (Lyne and Hayes 2005). Nutriclines are typically at depths of between 50 and 140 m, and in the western Pacific at 5°S have been recorded at between 60 and 120 m (Blanchot et al. 1992). Phytoplankton within the euphotic zone tend to have a patchy vertical distribution, with chlorophyll maxima (an increase in chlorophyll concentration of 2 to 20 times) often occurring in tropical seas at about 100 - 150 m, coinciding with the nutricline (Nybakken and Bertness 2005).

Other organisms that are primary producers are the bacteria and microorganisms, although these can also be heterotrophic rather than strictly autotrophic, and therefore not strictly primary producers. Bacteria are important in taking up large amounts of dissolved organic carbon in the open ocean and converting it to particulate organic carbon, and are consumed by nanozooplankton (various small protists), which are then fed upon by larger net zooplankton, making available a significant amount of energy to planktonic food webs (Nybakken and Bertness 2005; Connell and Gillanders 2007). This process is known as the microbial loop (Lenz 1992). Bacteria are partially responsible for the regeneration of nutrients in the photic zone, fuelling the productivity of phytoplankton even in nutrient-poor waters such as the tropical open oceans.

Marine snow is an important product of the epipelagic zone that falls through the water column, delivering energy to the meso- and bathypelagic zones (Lampitt 1996; Turner, 2002). Marine snow is amorphous particulate material, aggregates of detritus, living organisms, and inorganic matter. It consists of cast-off mucous nets produced by planktonic filter feeders, e.g. pteropod molluscs and pelagic tunicates, the remains of dead gelatinous large zooplankton, such as salps and jellyfishes, and plant material. Marine snow attracts and accumulates living organisms as well as particles such as diatom frustules and faecal pellets, forming floating microcosms with populations of microorganisms (Nybakken and Bertness 2005). Marine snow aggregates contain enriched microbial communities and chemical gradients in which processes of photosynthesis, decomposition, and nutrient regeneration occur at elevated levels (Alldredge and Youngbluth 1985). Bacterial densities can be >2000-fold higher on the aggregates than in the surrounding water column (Ploug et al. 1999).

4.1.3 Consumers

There are two contrasting food-web models that are distinguished primarily using the size of the phytoplankton supporting the primary consumers:

- 1) Microplankton (including microalgae) are generally thought to be preyed upon by large crustacean grazers such as the copepods and other similar species (macrozooplankton). These large grazers are generally thought to be targeted by higher trophic level predators, including fish. However low nutrient areas of the ocean tend to have few of the 'large' phytoplankton, relative to temperate waters, where this food web model was developed (Connell and Gillanders, 2007);

- 2) Grazers of picoplankton, which dominate oligotrophic waters, include a variety of protozoa, such as ciliates and specialised heterotrophic dinoflagellates, while filter-feeders and gelatinous zooplankton such as salps and appendicularians also collect large numbers of picoplankton. This second food web model dominates the phytoplankton dynamics in Australia's oligotrophic oceanic waters, and these protozoan grazers can be numerically very abundant and dominate grazing processes in oligotrophic, open-ocean food webs (Connell and Gillanders, 2007), such as the Solwara 1 study area.

Community-wide, the respiration rate of nanoplankton generally exceeds that of net phytoplankton by a factor of 10, suggesting nanozooplankton are consuming most of the energy fixed by the picoplankton, meaning that the large phytoplankton-to-copepods view is probably less important than the nanoplankton in the open ocean (Nybakken and Bertness 2005). Copepods are the main trophic link between the phytoplankton and vertebrates (Connell and Gillander, 2007). Many tropical copepods have relatively short generation times, and because of the stable conditions of the tropical oceanic mixed layer and the continuous phytoplankton growth, copepod development is rapid and many broods are produced per year.

Other epipelagic primary consumers (consumers of primary production) include euphausiids, ostracods, chaetognaths (arrow worms), cumaceans, a few fishes, and a variety of larvae, including fishes and molluscs (Connell and Gillanders 2007). There are 45 species of euphausiids occurring in the western Pacific region (Mauchline and Murano 1977, cited in Summerhayes and Thorpe, 1996). Euphausiids tend to be pelagic and trans-oceanic in their distribution.

Plankton-feeding fishes are varied, and include small fishes (e.g. flying fish) and the largest of epipelagic animals (e.g. whale sharks and cetaceans). Most larval fish, that spend this part of their life cycle in the epipelagic region, are many are zooplanktivores.

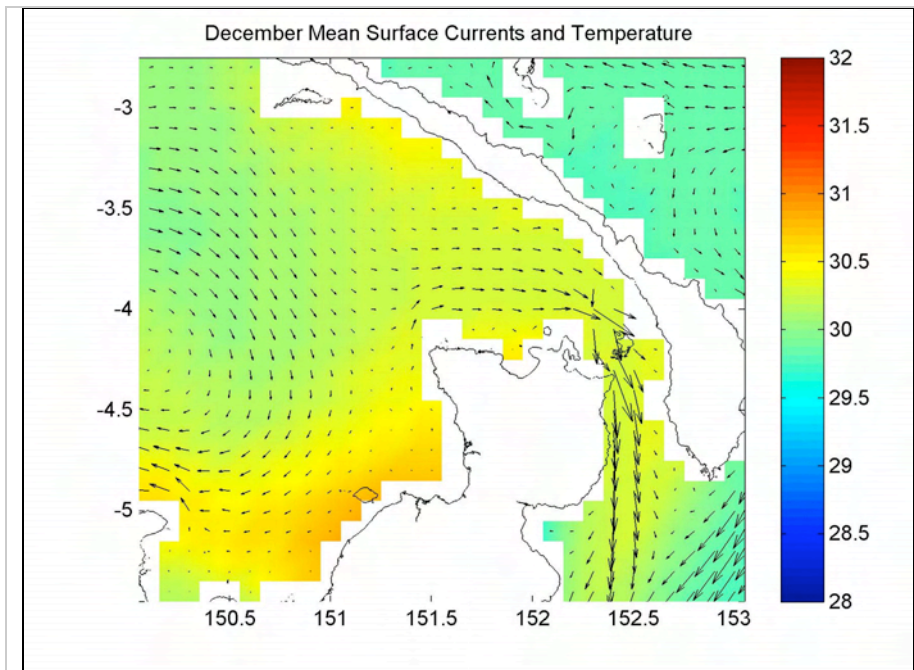
Higher-order consumers in the epipelagic zone are dominated, in terms of biomass, by transient (i.e. non site-associated) vertebrates such as fish and mammals and invertebrates such as crustaceans, squids and gelatinous zooplankton. Consumers feeding directly on primary producers are dominated by zooplankton (true planktonic animals) and micronektonic animals (animals with some swimming ability) including larvae of the larger vertebrates and invertebrates and adult life-stages of invertebrates such as crustaceans.

Consumers of particular interest in the epipelagic zone in the Bismarck Sea are the large tertiary consumers; tuna, billfish and sharks. Cetaceans and marine turtles are also of interest due to their conservation significance. A list of the most common fishes from the epipelagic zone (and deeper waters) of PNG is given in Appendix 1. A list of cetaceans and turtles known from PNG waters is given in Appendix 2. Fine-scale location data are not available for these species records, but it is expected that all of these species could potentially be present in the waters of the Bismarck Sea at some time. In fact, within the popular grey literature and eco-tourism circles, Kimbe Bay in West New Britain Province is often quoted as a 'hot-spot' for whale and dolphin sightings.

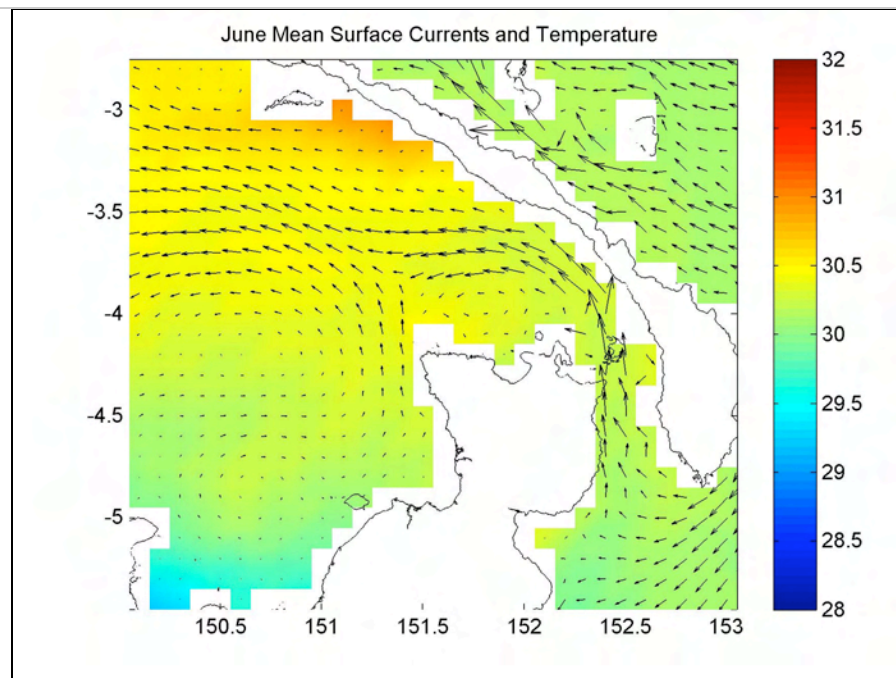
Convergence zones between epipelagic water masses with different physical characteristics, such as temperature and density, are often visible as surface drift lines which may contain phytoplankton blooms, detached seaweeds, logs, and flotsam. These structures are known to passively aggregate planktonic consumers or attract nektonic consumers. Indeed, the attractive qualities of such oceanographic or physical structures is the reason why man-made Fish Aggregation Devices (FADS) are effective and these are used in the PNG commercial seine fishery and the recreational fishery.

Oceanographic features such as upwelling, eddies, seasonal heating areas, temporary current lines and fronts also have the effect of concentrating primary productivity and aggregating primary (zooplankton) and secondary consumers (eg. schools of small fish). Pelagic predators sensing these schools are attracted to such areas and also aggregate temporarily around such oceanographic features. These food-rich patches in the epipelagic zone are often transitory, disappearing when oceanographic structures break down or when the prey resource is depleted. Therefore, large epipelagic species divide their lives between feeding at these fronts and moving quickly across large expanses of oligotrophic waters and have physiological adaptations to undertake long migrations (Block et al. 2002; Polovina et al., 2000).

Figure 4-2 shows broad-scale surface currents and temperature for the region of the eastern Bismarck Sea. At this spatial scale, temperatures are fairly uniform and there are no obvious frontal discontinuities that would suggest prey and predator aggregations. Notable current features include channelling of currents through St. Georges Channel between New Britain and New Ireland (into the Bismarck Sea in June - southeast wind season and out of the Bismarck Sea in December - northwest wind season). There also appears to be a gyre system to the west of the Solwara 1 project area, with the gyre generating clockwise surface currents in December (northwest wind season) and anti-clockwise in June (southeast wind season). Such gyre systems in tropical Australia have been demonstrated to cause aggregations of primary production and primary consumers, which then attracts predators (Brewer et al. 2008) and this may be the case for the central-western Bismarck Sea.



a). Northwest wind season



b). Southeast wind season

Source: B. King, APASA, pers. comm.

Figure 4-2 Broad-scale surface currents and temperature in the eastern Bismarck Sea

Four main species of tuna are known from the Bismarck Sea;

- Yellowfin tuna (*Thunnus albacares*);
- Skipjack tuna (*Katsuwonus pelamis*);
- Bigeye tuna (*Thunnus obesus*); and
- Albacore tuna (*Thunnus alalunga*).

These species are given particular attention in this report as they are fished commercially, recreationally and for subsistence in Papua New Guinea, and provide a case study for the potential mechanisms of trophic linkage between the epipelagic zone and deeper waters and the potential mechanisms of bioaccumulation.

4.1.4 Distributions

Horizontal Distributions

Phytoplankton species tend to be broadly distributed throughout the various oceanic gyres and regions, and none appear to be endemic to any given province (Nybakken and Bertness 2005).

All of the tunas mentioned above are wide-spread tropical and subtropical species and their movements are highly variable, being driven primarily by large-scale oceanographic factors. However, bigeye tuna (*T. obesus*) in the Coral Sea have been observed to show some degree of residency at some locations (Hampton et al. 1998). Tuna, and most other epipelagic fishes are highly transient and migrate either for food or for reproduction. The Bismarck Sea lies midway along the migratory path of each species, which predominantly originate from their spawning grounds in the Coral Sea (Hampton et al. 1998). Other transient populations originate from the surrounding Pacific islands including the Philippines. There is no evidence to suggest that tuna or other transient predators would have a particular site affinity to the waters in the Solwara 1 project area. It is more likely that these animals would range through the project area, possibly being attracted to the area if oceanographic features or, for example, light from ships, resulted in an aggregation of prey species in the area.

The migratory behaviour of tunas varies between species. Yellowfin tuna remain within a large home-range while they are <50 cm length, and at 50-65 cm they can form multi-species schools with skipjack tuna. Bigeye tuna probably have the most complex migratory behaviour of the tunas. Bigeye tuna undergo rapid growth and their habitat varies with development phase. Juveniles usually occur in equatorial zones and adults are more common in subtropical latitudes. Bigeye tuna migrations are described according to 3 size categories:

- Juvenile from 30-70 cm;
- Preadult from 70-100 cm;
- Adult >100 cm.

Juvenile bigeye tuna occur in mixed schools with yellowfin and skipjack tuna. Preadult bigeye tuna exist with similar sized yellowfin tuna schools and are also known to undergo extensive migrations. In the Atlantic, the movement of preadult bigeye tuna appears to be well-correlated to the movement of a thermal front, suggesting that these oceanographic features may be important to the distribution of the species in other seas. Little information exists for adult bigeye, although it is known that adults undertake long migrations. In the Pacific, bigeye tuna tagged in the Coral Sea off northeastern Australia have been recaptured in PNG waters and further east as far as Hawaii (Hampton et al. 1998). Interestingly, some individuals were recaptured in the release area after 6 years at liberty, suggesting some degree of residency or at least returning to a favoured area.

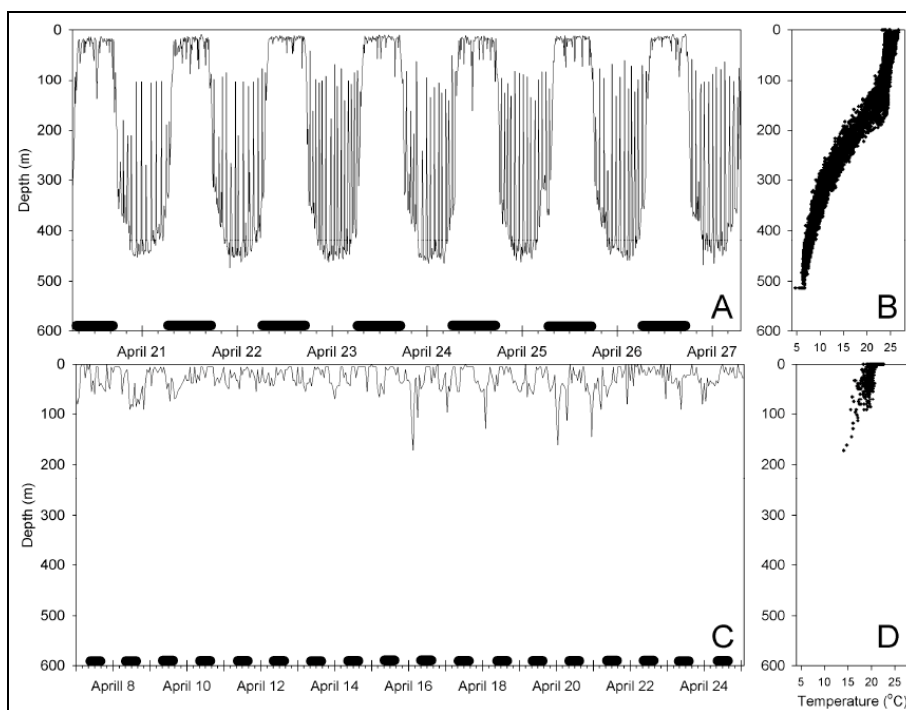
The known movements of albacore tuna support the notion that PNG stocks do not represent distinct sub-populations, but rather are part of a larger Pacific population. Albacore tuna spawn at >80 cm in length spawn in the sub-tropical waters of the south Pacific Ocean. Juveniles at 45 - 50 cm then migrate east to New Zealand coastal waters in the vicinity of the sub-tropical convergence zone in the central Pacific at 45-50 cm. From this region, albacore appear to disperse gradually to the north and towards PNG, but may make seasonal migrations between tropical and subtropical waters.

Vertical Distribution

Much of the information on vertical distribution of consumers is based on studies of trophic behaviour. As such, much of the information presented below to describe vertical distributions is included in sections 7 and 8 in a discussion on trophic webs and risk pathways for bioaccumulation

Most organisms that reside within the epipelagic zone are restricted to the surface layers as they are not adapted to the low temperature and low light conditions at depth. However, some species, while being predominantly epipelagic, have evolved certain adaptations that allow them to dive to greater depths, primarily in search of prey. Notably, these adaptations occur in some tuna and billfish species. The most important of these adaptations are the ability to keep the brain warmer than the surrounding environment, visual adaptations to hunt in low light and physiological/behavioural adaptations to tolerate accumulation of metabolic products resulting from dives into low oxygen conditions, followed by processing of those metabolic products when returning to surface waters (Bertrand et al. 2002 and summarised in Brill et al. 2005).

Bigeye tuna (*Thunnus obesus*) have distinctive depth distributions and vertical movement patterns and, of the tuna species that occur in the Bismarck Sea, have the greatest ability to forage below the thermocline, into the mesopelagic zone. Bigeye tuna have been shown to remain within the mixed layer at night, descending to over 500 m depth throughout the day (Brill et al. 2005). These deep dives are believed to be predatory excursions to target mesopelagic prey such as fishes, crustaceans and squid. Figure 4-3 shows dive profiles of bigeye tuna and yellowfin tuna from Hawaiian waters.



Note: Panel A = bigeye tuna, panel B = temperature profile for bigeye tuna dives, panel C = yellowfin tuna, panel D = temperature profile for yellowfin dives. Black bars in panels A and C represent night-time periods.
 Source: Brill et al. (2005)

Figure 4-3 Dive profiles of bigeye tuna (top) and yellowfin tuna (bottom)

At their maximum depths, bigeye tuna frequently experience prolonged exposure to ambient temperatures in the tropics that are up to 20°C colder than surface waters, and oxygen concentrations less than 1.5 ml/L (Brill et al., 2005). Tunas, and bigeye tuna in particular, conserve heat and minimise temperature changes in deep red muscle, affording some protection from external temperatures, allowing them to stay at depth and remain active for longer when compared to other similarly sized fish. Further to this, bigeye tuna have a specially adapted heating organ in muscle near their eyes which warms the brain and retinas allowing them to function in colder temperatures and improving their ability to detect fast moving prey such as squid (Collin and Partridge, 1996). Returning to warm surface waters after a dive is believed to aid in the regulation of temperature and processing of metabolic waste products (i.e. lactate) accumulated during the dives into cold, oxygen-poor waters (Dagorn et al. 2000).

Over time, longliners operating in the Bismarck Sea and other Pacific locations have identified the ability to catch larger, more valuable bigeye tuna by setting deep long-lines, down to at least 200 m depth (Beverly and Itano 2004; Hampton et al. 2006).

Skipjack tuna, yellowfin tuna and albacore tuna show some of the adaptations mentioned above for bigeye tuna and have some ability to hunt in colder, deeper waters. However, these species are generally more restricted in their vertical distributions, and are more adapted to exploiting epipelagic resources. Skipjack tuna in particular are known to occur

close to the surface, a notion that is supported by the fact that fishing for this species in the Bismarck Sea is carried out using shallow purse seine nets. Yellowfin tuna also spend most of their time in epipelagic waters but larger individuals in particular are known to occur in deeper waters. Figure 4-3 shows that yellowfin tuna in Hawaii dive to at least 150 m regularly and feeding excursions to at least 200 m have been identified for yellowfin in Australia (Lansdell and Young 2007).

Yellowfin tuna generally limit their dives to depths where water temperatures are no more than 8°C below surface layer temperatures, and ambient oxygen levels are above 3.5 ml/L (Brill et al. 2005). Further, in areas where the decrease of oxygen content with depth is not limiting, yellowfin depth distributions are set not by a specific depth or water temperature, but by the relative change in water temperature with depth (Block et al. 1997, Brill et al. 1999).

Until recently, the deepest known dive for a yellowfin tuna was 464 m (Cary and Olson 1982). This record was comprehensively broken recently when a single tagged yellowfin tuna was recorded to undertake dives to 578 m, 982 m and to 1,160 m (Dagorn et al. 2006). These dives were infrequent, with the fish spending 85% of its time shallower than 75 m, but the dives were up to 2 hours in duration and temperatures at these depths far exceeded the postulated temperature tolerance of the species. While the purpose of these dives is unknown, foraging is one obvious possibility. A yellowfin tuna was identified in ROV footage from Solwara 1 at 823 m (see Plate 4-1). Yellowfin tuna were sampled at Lihir Ireland, PNG at 362 m and 509 m (Brewer et al. 2007) (see Section 6).

The depth distribution of albacore tuna is less well known, but it is believed that the species dives deeper into the mesopelagic zone than skipjack and yellowfin tuna (Bertrand et al. 2002; Brill et al. 2005) although juvenile albacore form mixed-species schools with both skipjack and yellowfin tuna.

Squid are of considerable importance in marine pelagic food webs, and provide a key trophic link between vertically migrating micronekton and small mesopelagic fish schools (e.g. myctophid fishes (lanternfish)), to top predators in the epipelagic zone, such as tunas and billfishes (Sibert et al 2006). In addition, large gelatinous zooplankton (e.g. salps and jellyfish) that also contribute to patterns of vertical migrations can represent a significant proportion of the food resources of pelagic tuna (Lansdell and Young 2007). Again, trophic interactions will be described in more detail in Section 7 below.

Therefore, in addition to the deep foraging excursions of some epipelagic fishes providing a direct link between the epipelagic and mesopelagic zones, squid and larger gelatinous zooplankton represent another, indirect, trophic pathway linking the epipelagic and mesopelagic zones, a link that is driven by the process of vertical migration. This process has its origins in the mesopelagic zone and is described in more detail in Section 4.2.

The intolerance of zooplankton to low-oxygen conditions was long believed to limit the vertical distribution of zooplankton to oxygen-rich waters. However, recent studies in the eastern Pacific Ocean, using advanced sampling techniques that sample discrete depths, have shown that many zooplankton are distributed from the base of the thermocline into the 'oxygen minimum zone' (OMZ) (Fernández-Álamo and Färber-Lorda 2006). In the eastern

Pacific, daytime zooplankton biomass peaked within the OMZ at around 600 m water depth, with copepods found well within the OMZ (Vinogradov et al. 1991). Again in the eastern Pacific, a later study identified two maxima of zooplankton biomass, one near the thermocline (40-50 m) and another within the OMZ (600 - 1000 m) (Saltzmann and Wishner 1997a). Saltzmann and Wishner (1997b) reported that vertical distributions of copepods in the eastern Pacific (the most common zooplankton identified in the Lihir Island study) were not confined by the OMZ, with these crustaceans often migrating through the OMZ or having high biomass within this zone. Most euphausiid species in the eastern Pacific also migrate within the OMZ (Brinton 1979).

4.2 Mesopelagic

4.2.1 Introduction

The mesopelagic zone encompasses the waters between approximately 200 m and 1000 m depth and is below the seasonal thermocline, mixed layer and euphotic zone. The zone is characterised by low light and low temperatures. Typically, the mesopelagic zone has lower dissolved oxygen than the epipelagic zone. However, as described above, oceanographic structure within the mesopelagic zone and internal waves or other topographically-induced currents can result in layers of high nutrients and oxygen (see Section 4.1). In this zone, bioluminescence begins to play an important ecological role, which is described in more detail in Section 7.

In a recent study over a seamount off eastern Australia, hydroacoustic sampling and net sampling showed that, integrated over 100 m layers, total biomass peaked in the 400 - 500 m depth range at night (Young and Hobday 2004) (see Figure 4-4). This depth range coincides with a zone of particular activity identified by the ROV footage inspected at the Solwara 1 project area and at the South Su area. Figure 4-4 also illustrates that a large proportion of the mesopelagic community remained at depth during the night, indicating that not all organisms vertically migrated. It should be noted that this example originates from the Britannia Seamount, off eastern Australia, the top of which lies in about 400 m water depth, where topographically-induced currents mid-water and near-bottom have been implicated in attracting or aggregating mesopelagic biomass, thereby attracting billfish that are known to aggregate at the site.

4.2.2 Producers

The mesopelagic zone is on the lower limit of light penetration, and thus lacks much of the primary producers that occur in the euphotic epipelagic zone. The main export production entering the mesopelagic zone is the phytoplankton associated with falling marine snow, which is derived from the production that occurs in the epipelagic zone, and some cyanobacteria which can tolerate low light levels and can persist to the bottom of the epipelagic zone. An example is the ubiquitous cyanobacteria *Prochlorococcus*, are able to survive at 1 % light intensity levels (Partensky et al. 1999). Marine snow is an important food source in the meso- and bathypelagic zones (Dilling et al. 1998; Turner 2002).

4.2.3 Consumers

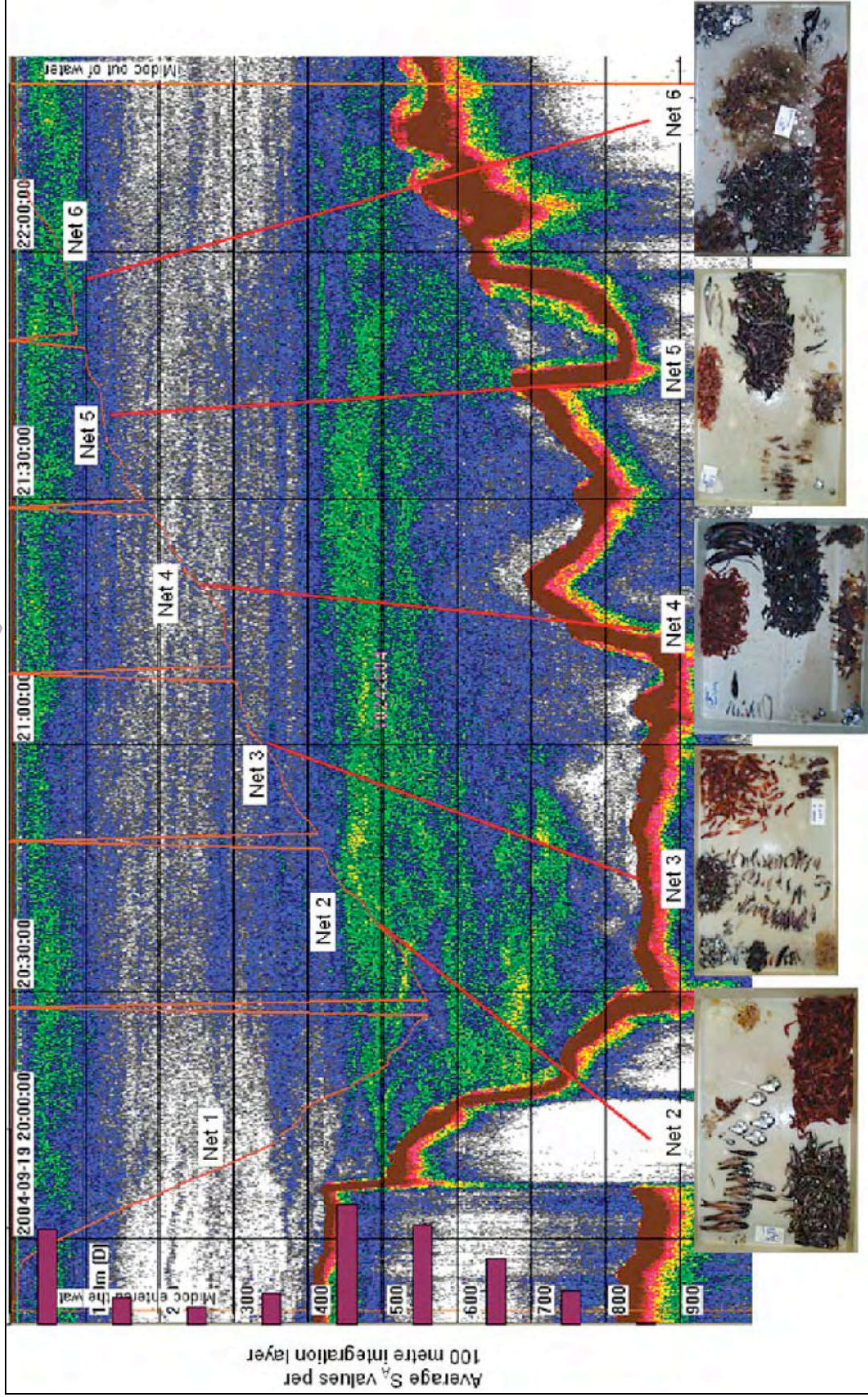
Consumer organisms in this zone comprise mainly fishes, crustaceans and molluscs, squid and other gelatinous organisms. Appendix 1 lists some of the more well-known mesopelagic species that would be expected to occur in the Bismarck Sea. Consumers in the mesopelagic zone include micronekton, a term used to describe active organisms such as small adult fishes, larvae of larger fishes, crustaceans, cephalopods and gelatinous organisms that are nektonic rather than planktonic and visible to the human eye.

The most abundant consumers in the mesopelagic zone are micronekton, with fishes, crustaceans and cephalopods the most abundant groups. Micronekton are the main component of deep scattering layers, undertaking diel vertical migration (described in section 4.2.4 below), with mesopelagic secondary consumers following these migrations. As described below, micronekton constitute a significant proportion of the diets of tuna that either dive into the mesopelagic zone to feed during the day, or encounter micronekton at dawn and dusk when vertical migration brings them into surface layers at times when predators in the epipelagic zone are still able to visually hunt (Bertrand et al 2002). Larval crabs (megalopas) and cephalopods were found to be particularly important in the diet of yellowfin tuna in eastern Australian waters (Young et al. 2001; Lansdell and Young 2007).

The fishes in this zone are active swimmers, often silver in colour, some with laterally compressed body forms and many with bioluminescence properties, and are typified by having muscular bodies, well-ossified (boned) skeletons, large hearts and kidneys and in most cases, swimbladders. Many of these fishes are zooplanktivorous and their feeding behaviour is highly sight dependent.

Myctophids (lanternfish), a bioluminescent group of fishes, dominated the biomass of the mesopelagic zone off eastern Australia (Young and Hobday 2004, see Figure 4-4) and were common in the mesopelagic zone off Lihir Island, Papua New Guinea (Brewer et al. 2007, see Section 6). In the mesopelagic net hauls marked on Figure 4-4, Young and Hobday (2004) reported consistently higher biomass of fishes, squid, crustaceans and gelatinous organisms during the night compared to daytime hauls, a fact that may be due in part to the reduced avoidance of sampling gear during the night. Myctophids displayed a clear pattern of changes in the biomass maximum from bottom layers during the day to the surface during the night, indicating vertical migration. Gelatinous organisms also showed evidence of vertical migration, with a marked increase in biomass at the surface at night (Young and Hobday 2004). Gelatinous zooplankton were observed from mesopelagic tows at Lihir Island (see Section 6) and these organisms have been found to be present in the diets of tuna in Australia and other Pacific locations (Bertrand et al. 2002; Young et al. 2001).

Larval stages of crustaceans and fishes occur in the mesopelagic zone and these were observed in the ROV dive footage from the South Su site neighbouring the Solwara 1 project area. On one occasion a dense patch of what appeared to be crab zoeas, was observed from approximately 200 to 300 m depth at during the day.



Source: Young and Hobday (2004). Purple bars on y-axis indicate integrated backscatter-strength (biomass) values.

Figure 4-4 Hydroacoustic echogram and net catches in the mesopelagic zone

4.2.4 Distribution

Horizontal

The main factors influencing the distribution of species in this zone are oceanographic structure, currents and primary productivity regime. Water masses of the mesopelagic zone, particularly the deeper portions of the zone, are relatively uniform at the scale of ocean basins, presenting a relatively uniform physical environment over very large areas. However, the upper portion of the mesopelagic zone interacts with the lower portion of the epipelagic zone and is exposed to oceanographic features such as internal waves that can result in features such as oxygen gradients, nutriclines, turbulence and other structure, which may provide some horizontal variability to the mesopelagic zone (see Section 4.1.2).

Mid-water and near-bottom currents, upwelling or eddies induced by benthic features, such as seamounts or rapid depth changes, has been implicated in the attraction or aggregation of mesopelagic organisms off the eastern Australian coast (Brewer et al. 2008). On the relatively featureless seafloor at the Solwara 1 project area, the influence of currents is expected to be minor and the distribution of food is likely to be the main limiting factor within the mesopelagic environment. However, oceanographic measurements made at the Solwara 1 site have identified some interesting features in the mesopelagic zone. Relatively high currents were observed in surface waters, overlaying a region of relatively low current speeds, overlaying another deeper zone of relatively high current speeds at depths between 140 m and 250 m at various times (B. King, pers. comm.). This observation is consistent with the presence of long-amplitude internal waves that could be established as a result of deep water masses interacting with the eastern side of the Bismarck Sea (western side of New Ireland) or topographically-induced mixing as a result of water movement through St. Georges Passage, that pushes water through a shallow, narrow passage possible inducing some upwelling. Such oceanographic processes may explain, for example, the dissolved oxygen profiles measured at the site (see Section 3) because such processes can disturb vertical structures in the water column and entrain oxygen and nutrients into deeper layers. Such processes may also have relevance to the distribution of mesopelagic communities because these water movements may passively aggregate mesopelagic plankton or attract mesopelagic nekton to areas of high turbulence or productivity.

In addition, oceanographic instruments deployed at the Solwara 1 site have detected particulate matter originating from below the ocean surface, falling through the water column at velocities that are faster than typical for falling particulate organic matter (POM, otherwise known as 'marine snow'). One hypothesis put forward to explain this observation is that the instruments are detecting material originating from black smokers being transported through the water column, trapped at depth and falling down through the water column (B. King, pers. comm.). If present, these kinds of processes may also be controlling the horizontal distribution of mesopelagic organisms in the project area, although has not been demonstrated in other studies. Midwater trawling above vent sites has not identified significant differences in micronekton populations from trawls at similar depths at non-vent site (P. Herring, pers. comm.).

POM is the main consistent input of nutrition to the mesopelagic zone and would be expected to be a driver of distribution and abundance of mesopelagic organisms. As will be described further in Section 8 on trophic webs, delivery of organic 'fall-out' to the mesopelagic zone is controlled by a number of processes centred in the epipelagic zone. Marine snow consists of detritus, faeces and carcasses of dead animals, typically colonised by bacteria (Radchenko 2007). As will be discussed in Section 7 (Bioluminescence), these

described further in Section 8 on trophic webs, delivery of organic 'fall-out' to the mesopelagic zone is controlled by a number of processes centred in the epipelagic zone. Marine snow consists of detritus, faeces and carcasses of dead animals, typically colonised by bacteria (Radchenko 2007). As will be discussed in Section 7 (Bioluminescence), these bacteria are often bioluminescent and play an important role in bioluminescent processes in the meso- and bathypelagic zones.

Vertical

The vertical distribution of cyanobacteria (producers) in the mesopelagic zone can be relatively uniform. However, a very sharp maximum concentration of cells, on the order of 10^5 cells ml^{-1} , near the bottom of the euphotic zone is often observed for plankton (Partensky et al. 1999).

The process of falling particulate organic matter represents a continuous and gradual flow of nutrition to the mesopelagic zone while the process of vertical migration is a direct link whereby organisms of the mesopelagic zone come into contact with the epipelagic zone. The process of vertical migration creates an avenue whereby production originating in the epipelagic zone is consumed by vertically migrating planktivores feeding in the productive surface waters at night and then this organic matter is transported into the deeper layers of the ocean during the day, where mesopelagic secondary consumers (e.g. lanternfish and squid) feed on these primary consumers (see Figure 4-5).

A large proportion of organisms in the mesopelagic zone undertake diel vertical migrations, thus becoming exposed to visual predators in the epipelagic zone during twilight hours, and sinking to greater depths during the day to escape visual epipelagic predators (although, as described below, some mesopelagic organisms are exposed to deep-diving epipelagic predators during the day). Most fish species rely on swim bladders for their buoyancy whereas most crustaceans rely on osmotic and ionic regulation (Salvanes and Kristoffersen 2001; Schmidt-Nielsen 1995). Vertical migration of groups of organisms can be staggered, with some species of fish, for example, migrating later in the evening and more slowly (Radchenko 2007; Frank and Widder 1997). A portion of the mesopelagic fauna does not vertically migrate, remaining in deep water at all times, as appears to be the case in Figure 4-4.

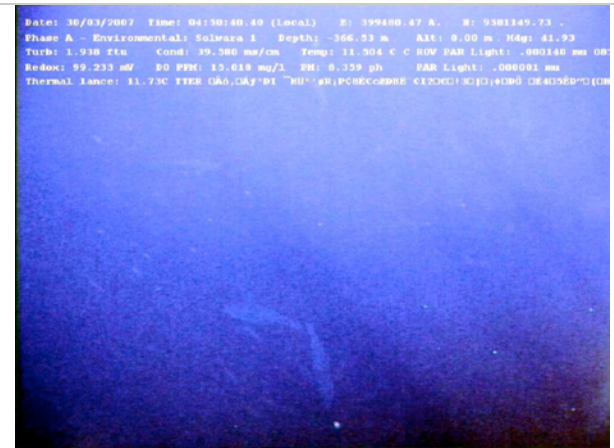
As mentioned above, within the mesopelagic zone at the Solwara 1 project area, the 400 – 500 m depth interval represent a significant vertical feature in terms of the abundance of pelagic organisms and this ~400 m feature appears to also be evident in other parts of the world. At these depths, particularly in early morning dives, significant activity of gelatinous organisms, squid and tuna was identified in the ROV footage (Plate 4-1).



a). Skipjack tuna at 172 m



b). Tuna school at 306 m



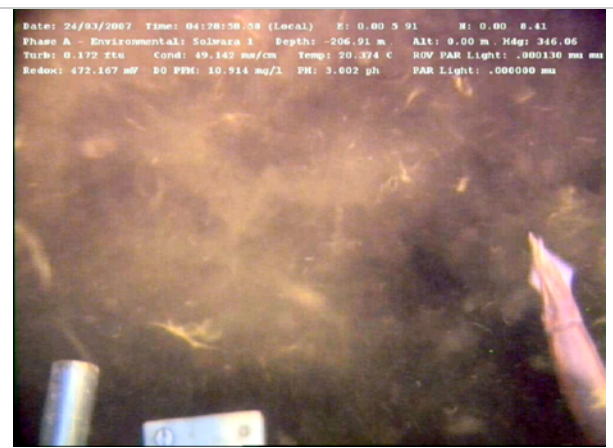
c). Tuna school at 366 m



d). Yellowfin tuna at 823 m



e). Siphonophore at 390 m



f). Squid and crustaceans at 206 m

Plate 4-1 Organisms identified at various depths in ROV footage at Solwara 1

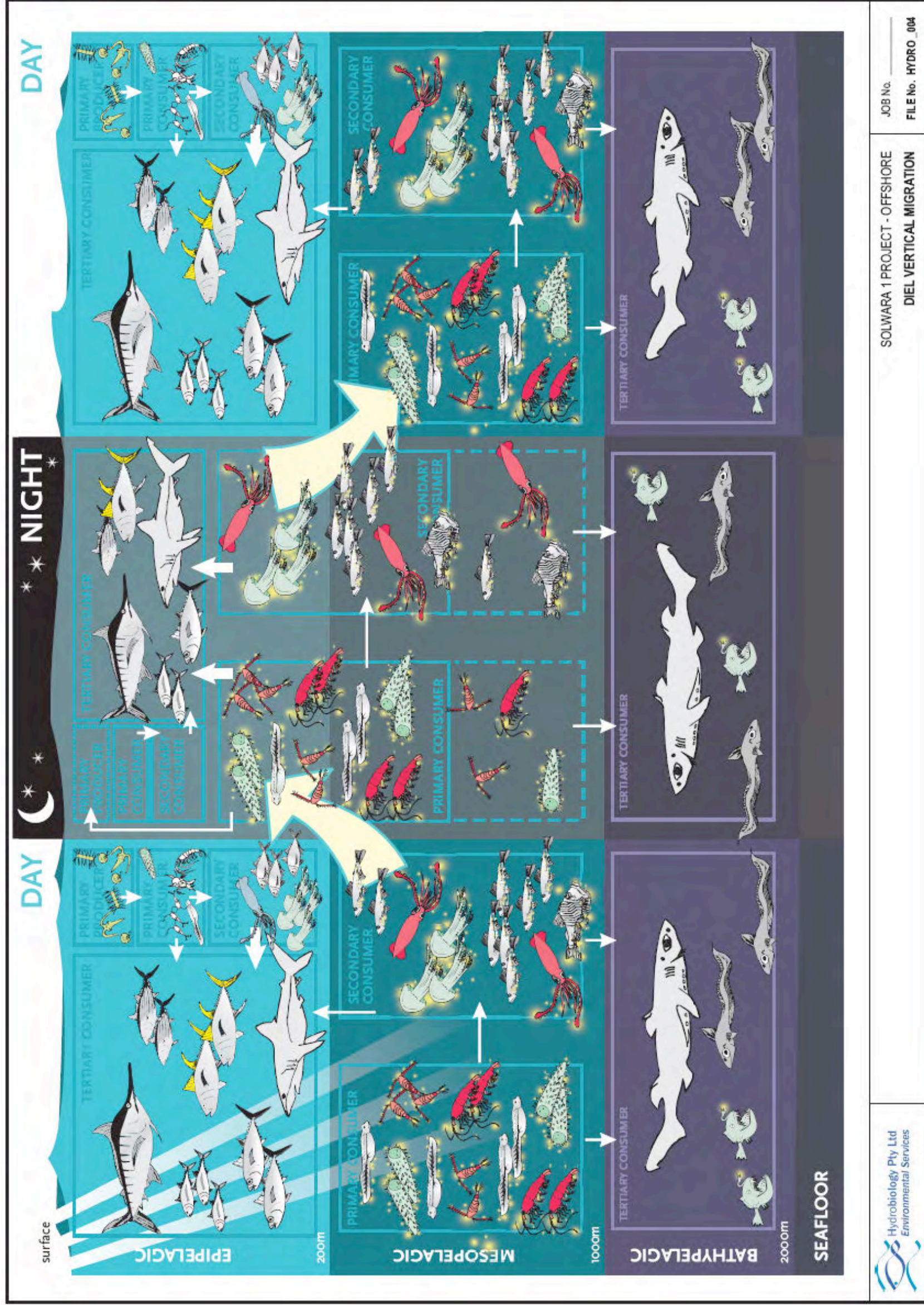


Figure 4-5 Schematic diagram of vertical migration

4.3 Bathypelagic

4.3.1 Introduction

The bathypelagic zone encompasses the water body >1000 m under the ocean surface. The environmental parameters that characterise the zone include the complete absence of light, uniform low temperature, low dissolved oxygen (DO), low nutrients and high pressure (see Section 3). The bathypelagic zone represents that largest habitat on the planet, but is the least studied environment. Literature and data are available for localities such as Norway and the Gulf of Mexico that are traditional centres of deep-sea research. The water masses of the world's oceans are relatively uniform at depths below 1000 m (Brewer et al. 2008, for Australian example) and so some extrapolation between oceans is possible, with caution.

4.3.2 Producers

Due to the absence of light in the bathypelagic zone, there are no photosynthetic organisms in this zone. The only primary production occurring in the deep sea is from chemosynthetic bacteria in certain areas, e.g. hydrothermal vents. All organisms living in the deep sea are thus dependent on food that ultimately is produced in the photic zones, and subsequently transported into the deep sea, making the deep sea unique among world ecosystems, in having no indigenous primary productivity (Nybakken and Bertness 2005; Polunin et al. 2001; Turner 2002).

The major source of nutrition for the bathypelagic zone is sinking marine snow (Wishner 1980; Polunin et al. 2001), and the downward flux of particles is generally considered even more important to energy cycling than pathways relating to vertically migrating zooplankton (Turner 2002).

Whale falls, and falls of other large animals at their death are another source of energy input to the deep sea. Falls of large animals are colonised by a succession of consumers which attract other scavengers (Gage and Tyler 1991).

Generally, conditions in the bathypelagic zone are unaffected by seasonal change, with physical water column conditions being relatively stable compared to surface waters that experience periodic and variable inputs of nutrients and currents. However, the delivery of marine snow and other pelagic fall-out to the bathypelagic zone can be seasonal, directly relating to conditions in the epipelagic (Turner 2002; Billett et al. 1983).

4.3.3 Consumers

The most abundant organisms in the bathypelagic zone are the microneckton, comprising larval stages and adults of various groups, dominated by crustaceans. Fish in the bathypelagic zone vary considerably in their swimming abilities, with some species essentially living a planktonic existence, with only limited movements in a vertical or horizontal direction. Indeed, as will be discussed in Section 9, it is this very limited mobility that separates this fauna from impact assessments in the epipelagic or mesopelagic zones where behavioural avoidance of unfavourable conditions is more likely. However, there are some active bathypelagic fishes that are active, such as families Macrouridae (rattails) and

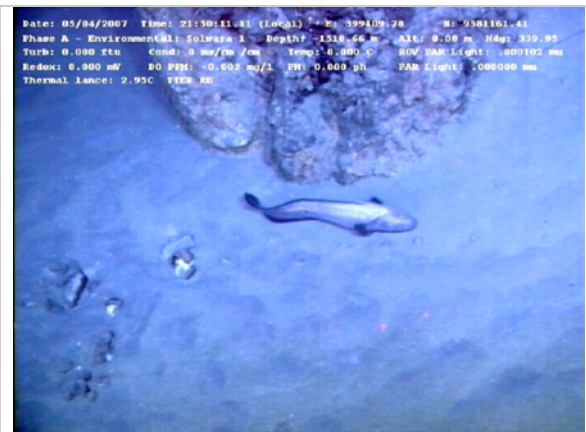
Morridae (cods). Plate 4-2 shows some of these types of bathypelagic fish species identified from ROV footage at the Solwara 1 project area. These species are, strictly speaking, demersal as they are associated with that habitat a short distance from the seafloor.

Species found at this depth are generally adapted for a low swimming activity in an environment that places energetic and metabolic restriction on organisms due to low, temperature, oxygen concentrations and nutritional input. The bathypelagic zone has been found to support lower abundance and biomass, of crustaceans at least, than the mesopelagic zone (Burghart et al. 2007 for Gulf of Mexico example).

The bathypelagic environment contains endemic species resident in the near-bottom environment, as well as infaunal species emerging into the water column. The top-level predators in these systems tend to be demersal fish associations (Mauchline and Gordon 1991).

The most common fish types include bristlemouths, hatchetfish, lanternfish and deep-sea angler fish. Fishes (and other organisms) in the bathypelagic zone are typically small-bodied. Bathypelagic fish have less developed gills and muscles and smaller eyes than those fish which reside higher in the water column and have a higher water content which is an adaptation to life in the extremely high pressures of the deep-sea (Cocker 1978; Herring 2002). The metabolic rate of fish, cephalopods and crustaceans also tends to decrease with depth, which is believed to be an evolutionary response to the overriding environmental factors such as the oxygen minimum layer and not in response to the biomass of possible food items (Childress 1995; Bulman and Koslow 1992).

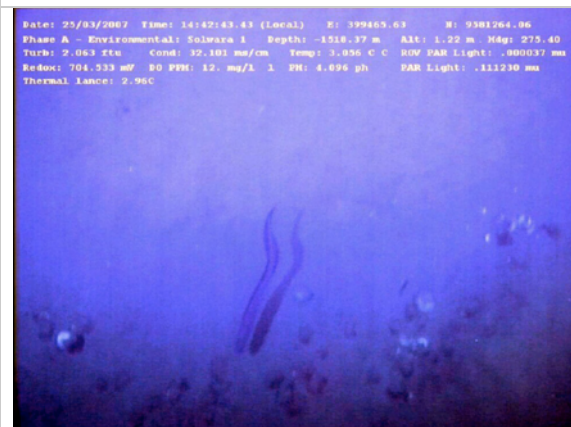
Many bathypelagic species are opportunistic feeders and certainly the fishes in this zone exhibit a range of adaptations that allow them to eat a greater variety of the prey. Many have massive gaping jaws lined with rows of sharp teeth, and highly elastic stomachs that can accommodate prey larger than themselves. Bioluminescence plays a major role in feeding, predator evasion, and communication in the bathypelagic zone (Herring 2002; see Section 7 Bioluminescence). Olfactory adaptations are also important in the ecological functioning of the bathypelagic zone. Female anglerfish, for example, are believed to release pheromones in order to attract the smaller male fish. When they find the female, males attach themselves by biting and gripping the female. In some species the male's jaw then fuses with the female tissue, the two circulatory systems and the male circulatory system degenerates, becoming subject entirely to the hormonal regime of the host. Other deep sea fish are hermaphroditic, ensuring that any encounter between the same species will provide both eggs and sperm.



a). Moriid cod at ~1,500 m



b). Zoarcid at ~1,500 m



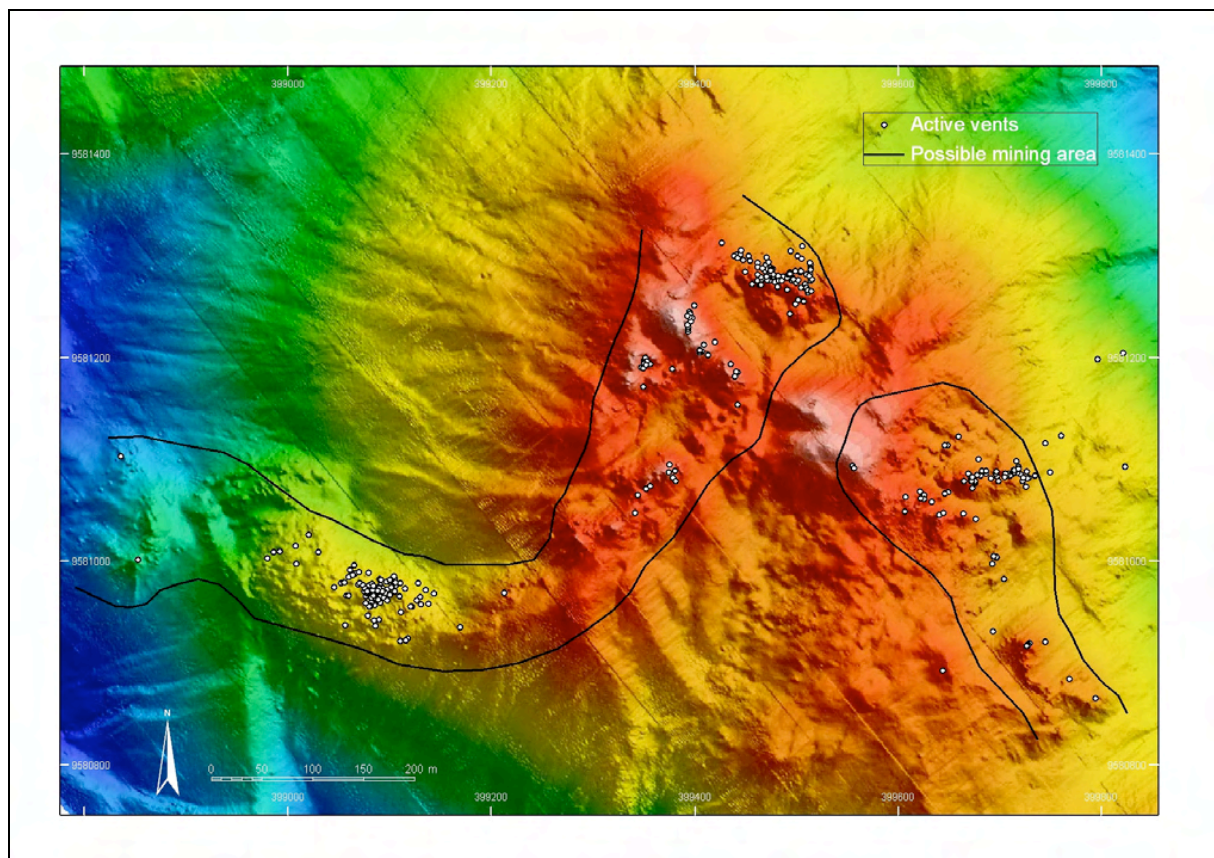
c). Eel at ~1,500m

Plate 4-2 Bathypelagic fish from the Solwara 1 project area

4.3.4 Distributions

Horizontal

While the bathypelagic zone is typically a homogenous environment, biomass does show considerable patchiness in the deep sea, and this is believed to be driven by variability in the distribution of organic input, mainly in the form of falling particulate matter and terrigenous input via rivers that discharge into submarine canyons (Gage and Tyler 1991). The influence of hydrothermal vents in the Solwara 1 project area (see Figure 4-6) may also have an influence on the distribution of bathypelagic organisms, although the mechanism for this is unknown. Hydrothermal vents are centres of biodiversity for vent-associated benthic fauna and the plumes associated with these vents provide an avenue for the dispersal of larvae of vent fauna, suggesting that the plumes are not inherently toxic. The effect of discharges of hydrothermal vents on bathypelagic organisms is not known, although there is no evidence to suggest that they have any significant impact on bathypelagic fauna.



Source: Nautilus Minerals

Figure 4-6 Location of active hydrothermal vents in the Solwara 1 project area

Vertical

Recent studies in the Gulf of Mexico have found that the faunal assemblages of the bathypelagic zone (defined as >1000 m) overlap somewhat with those of the mesopelagic zone, but also that a high proportion of bathypelagic crustaceans in particular (which comprise most of the biomass), migrate within the bathypelagic zone only (Burghart et al. 2007). Bathypelagic fishes also generally remain within the deeper layers of the ocean, upward range probably being limited by physical oceanographic factors such as density and pressure, although vertical distribution of these fishes is not well known. Vertical migrations may be within the bathypelagic zone or into the mesopelagic zone for feeding.

5 PNG TUNA AND SHARK FISHERIES

5.1 Introduction

In oceanic waters, PNG's commercial fisheries consist of a tuna purse seine netting fishery, a tuna longline fishery, a tuna handline fishery and a shark longline fishery. The purse seine fishery is made of six domestic vessels (which process all catch in PNG's canneries), 33 locally-based foreign vessels (14 of which are associated directly with PNG canneries) and some 186 foreign vessels that are licensed to fish in PNG waters (that process their catch overseas) (Kumoru and Koren 2007). PNG domestic vessels and locally-based foreign vessels are referred to as "PNG-associated" in the discussion below.

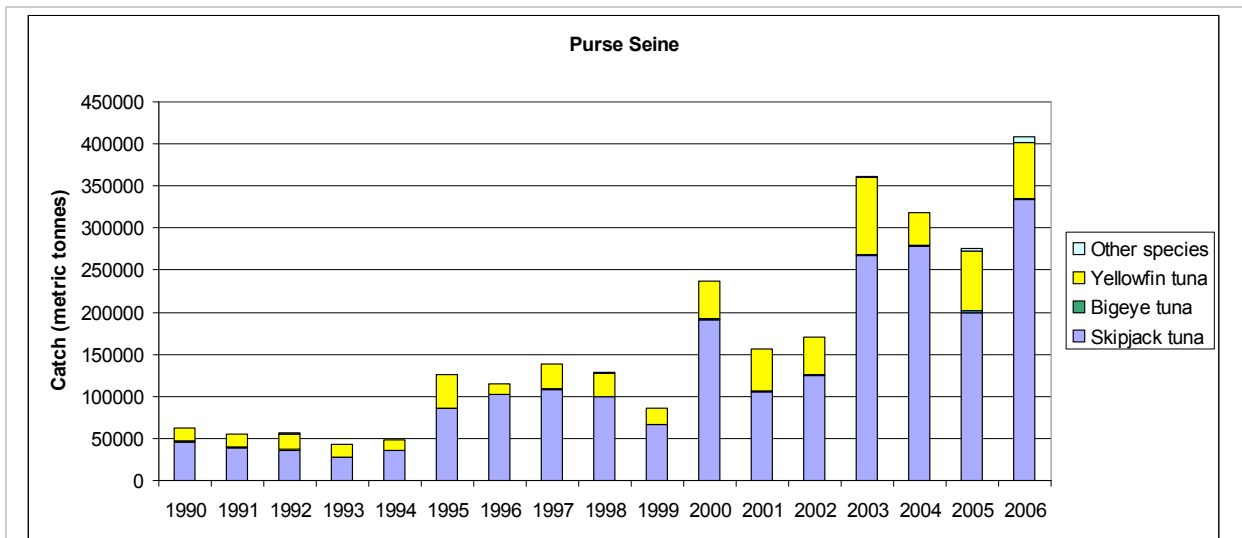
PNG's tuna and shark longline fisheries are entirely domestic. While the PNG's Tuna Fishery Management Plan allows for 100 tuna longline vessels, over the past four years, the number of tuna longline vessels has been about 42, with only 26 to 27 of these actually being active in the last 3 years. The number of shark longline vessels is at the maximum number allowable under the management plan of nine (Kumoru and Koren 2007).

The handline fishery is a small fishery in PNG, with 10 Philippine vessels active in PNG waters over the last two years.

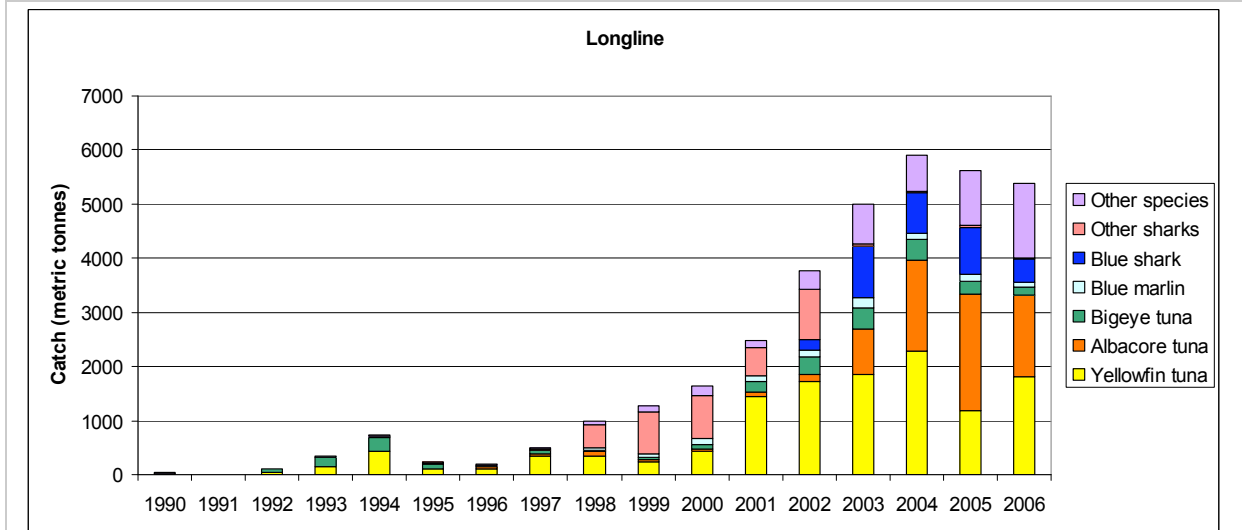
Tuna canneries are located in Madang (RD Tuna), Wewak (South Seas Tuna), Lae (Frescomer) and another cannery is proposed for Lae (Frabelle) (Kumoru and Koren 2007)..

5.2 Tuna

Figure 5-1 shows a summary of the total commercial catch in PNG waters for purse seines and longlines. Purse seine catches are dominated by skipjack tuna with some yellowfin tuna and small numbers of other species, far exceeding the catches from longlines. Longline catches are dominated by yellowfin tuna, with albacore tuna contributing significantly to the catch from 2003 to 2006. The catch of bigeye tuna has been consistently lower than the other species and peaked over the 2002 to 2004 period. Sharks constitute a large part of the tuna fishery 'by-catch'.



a). PNG commercial purse seine catch, 1990-2006

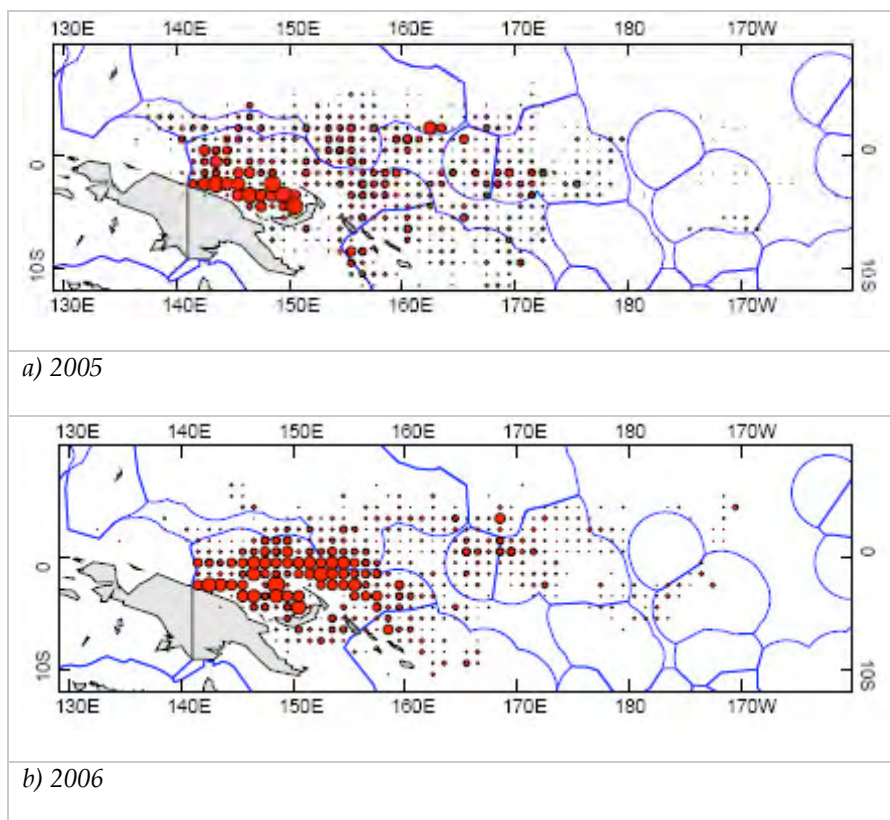


b). PNG commercial longline catch, 1990-2006

Figure 5-1 Purse seine and longline catches for Papua New Guinea tuna fishery

Source: NFA statistics (NFA website)

The geographic distribution of purse seine tuna catch for the two most recent years of data is shown in Figure 5-2. Highest catches are reported from the northern margin of the Bismarck Sea and through the central Bismarck Sea. The southeast corner of the Bismarck Sea, where the Solwara 1 project is located, does not appear to be a productive area for purse seiners (this is reflected in maps of purse seine effort, not reproduced here, but reported in Kumoru and Koren (2007). Between 2001 and 2006, purse seine catches were strongly dominated by skipjack tuna (71.3%), followed by yellowfin (27.9%) and bigeye tuna (0.45%).



Source: Kumoru and Koren (2007).

Figure 5-2 Distribution of total purse catch for PNG-associated fleet

The vast majority of purse seining effort (and therefore catch) is associated with Fish Aggregating Devices (FADs). FADs are installed to attract baitfish and tuna and the PNG purse seine fishery is strongly associated with these devices. The location of FADs in the Bismarck Sea, as of June 2006, is shown in Figure 5-3. There appear to be no FADs in the immediate vicinity of the Solwara 1 project area.

The red square (dashed line) in Figure 5-3 is an area known as Mogardo Square, an area that has been recently designated as prohibited for FAD deployment. At the time of writing, there is a proposal to close Mogardo Square to foreign purse seine fleets, leaving the area open to PNG fleets only.

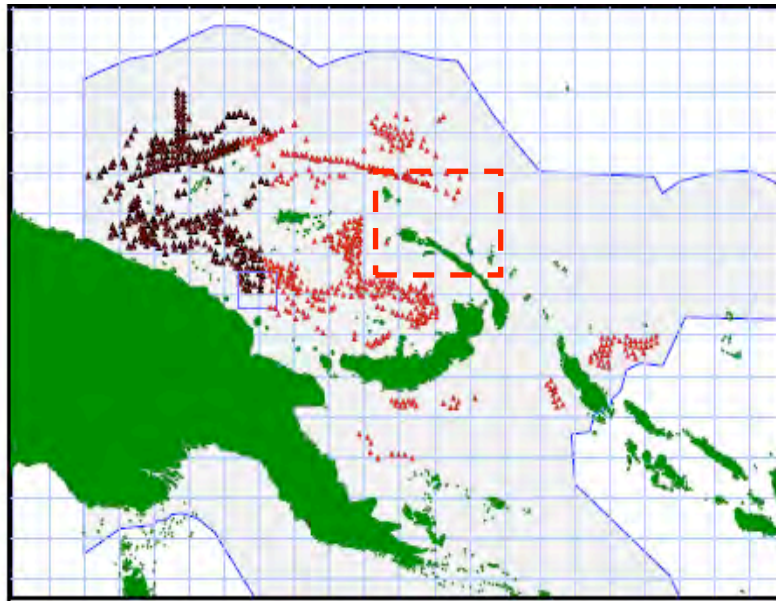


Figure 5-3 Location of FADs in PNG waters

Source: National Fisheries Authority PNG, pers. comm. Note: Dashed red square = Mogardo Square.

Longline vessels are based primarily in Port Moresby because their catches typically consist of larger fish that are exported to Japan by air, rather than processed at canneries. As such, access to international airports is important and limits that range of the longliners. New cold storage and ice facilities being developed in Lae (Kumuru and Koren 2007), which commenced in 2006, may change this situation.

Longline fishing is focussed in the Coral Sea, with catches being dominated by yellowfin tuna and albacore tuna (Figure 5-4). Some of the patterns in species catches are dictated by selective targeting of species. Albacore tuna, for example, achieved increase market acceptance and higher prices in Japan in 2005 and this was reflected in higher catches. There is generally much lower longline effort in the Bismarck Sea compared to purse seining (see Figure 5-5).

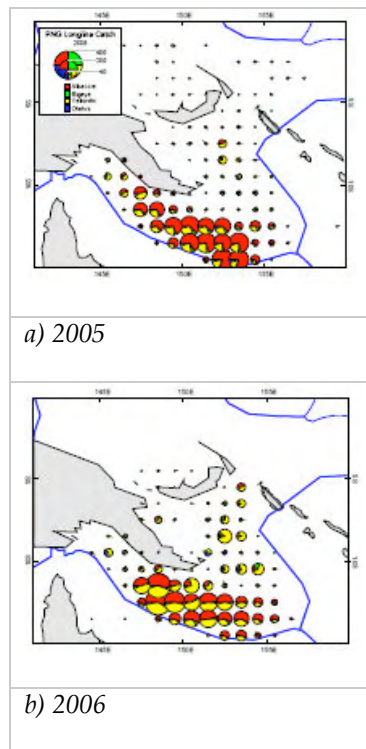


Figure 5-4 Distribution of total longline catch in PNG waters

Source: Kumoru and Koren (2007).

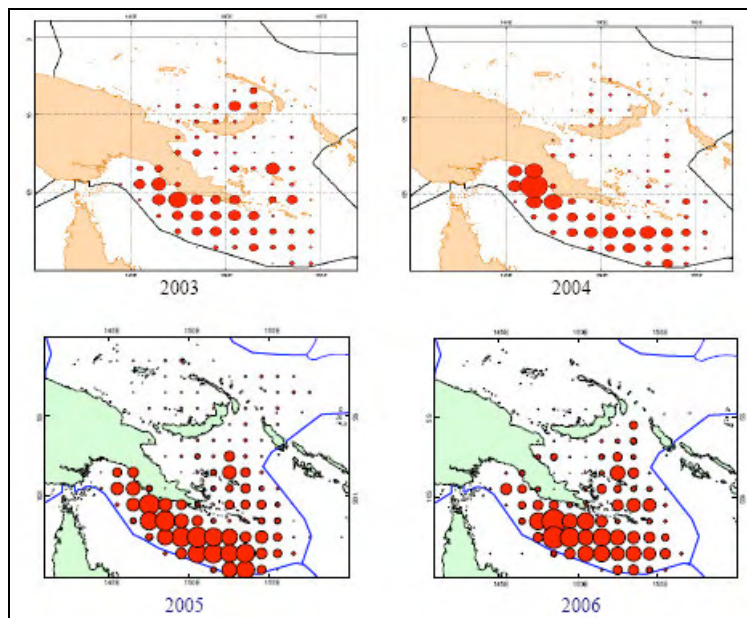


Figure 5-5 Distribution of total longline effort in PNG waters

Source: Kumoru and Koren (2007).

In the past, there has been considerably more longlining effort in the Bismarck Sea, primarily by Japanese longliners. Figure 5-6 shows the distribution of longlining effort from 1979 to 1987, showing high effort in the Bismarck Sea. Even during this high effort period, there was very little effort focussed in the southeastern corner of the Bismarck Sea, where the Solwara 1 project is located. Catches were known to be productive during this time and PNG National Fisheries Authority tuna specialists have suggested that the Bismarck Sea is very productive but logistical constraints of exporting product prohibits targeted fishing there (Kumoru, L. pers. comm.).

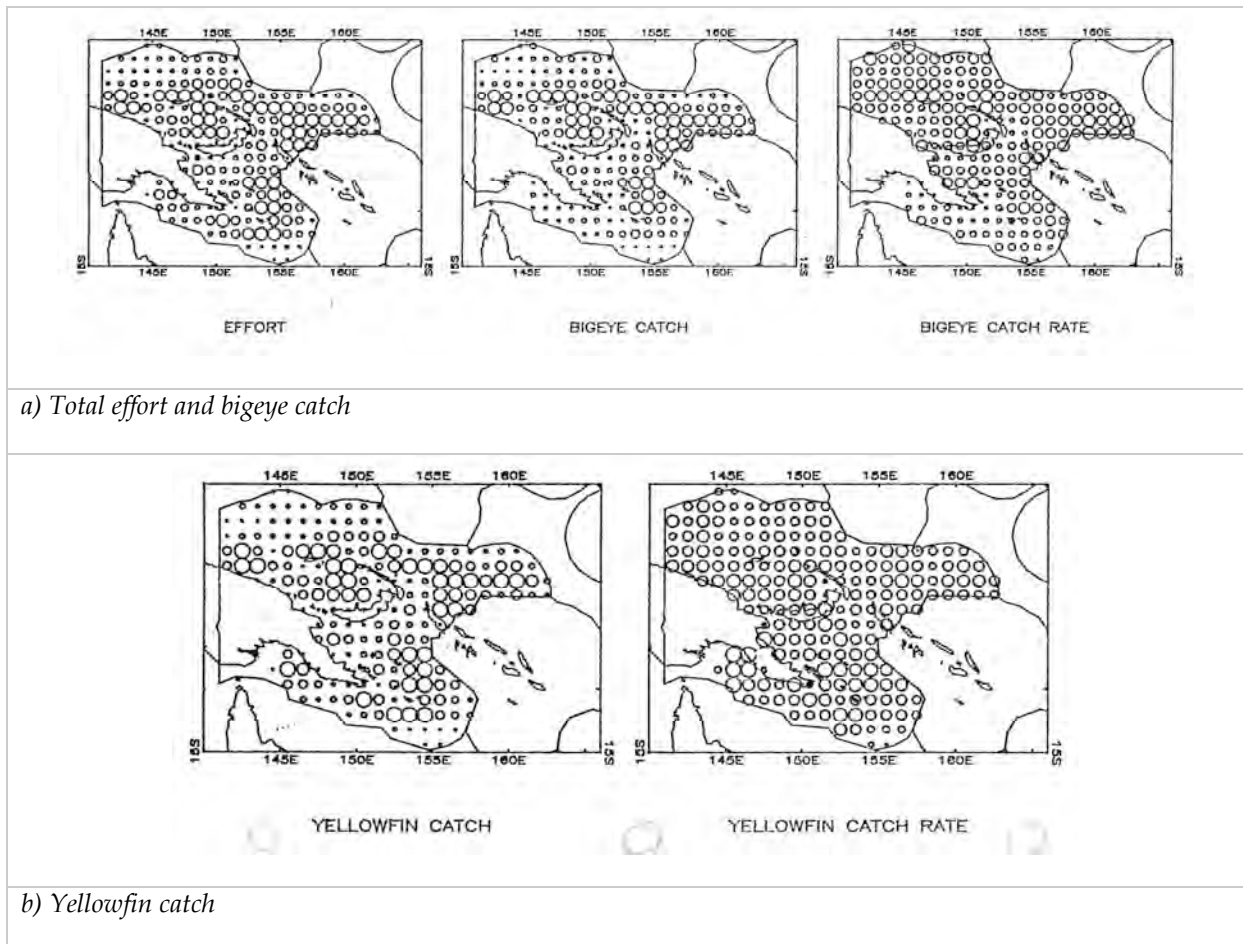


Figure 5-6 Distribution of longline effort 1979 – 1987 in PNG waters

Source: SPC (1988)

5.3 Shark

The shark longline fishery is focussed in the Gulf of Papua, Huon Gulf area, Milne Bay area and the northern margin of the Bismarck Sea. While catches in the central Bismarck Sea are lower than other areas, there does appear to be some activity in the area adjacent to Rabaul (Figure 5-7). Within the Bismarck Sea, the silky shark represents the majority of the shark longline fishery catch in the area (Kumoru, 2003). The shark longline fishery targets shallower water than the tuna longline fishery. Sharks comprise about 80% of the total catch in the shark longline fishery, with tuna and billfish comprising most of the 'by-catch'.

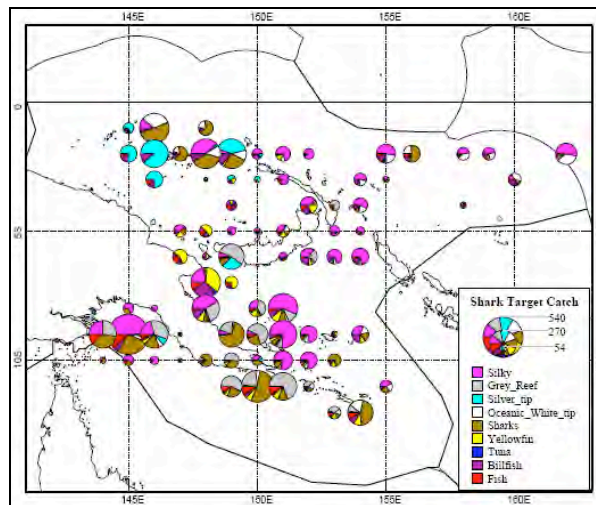


Figure 5-7 Shark longline catch, 1999-2002

Source: Kumoru (2003) – SPC observer data

The silky shark (*Carcharhinus falciformis*) is the most abundant species in catches from the Bismarck Sea and the other species represented in the PNG fishery are listed in Table 5-1. The silky shark, along with most other pelagic shark species, is able to roam through the mesopelagic in search of prey, reaching depths greater than 500m (Kumoru, 2003). It is usually associated with schools of tuna (and consequently are the main by-catch species of the tuna long-line fishery (Kumoru, 2003) and would thus be expected to mirror their movements.

Table 5-1 Species composition of PNG shark longline fishery

Common Name	Species Name	% by No.	% by Weight
Silky shark	<i>Carcharhinus falciformis</i>	49.3	47.4
Oceanic whitetip shark	<i>Carcharhinus longimanus</i>	9.1	10.9
Grey reef shark	<i>Carcharhinus amblyrhynchos</i>	11.2	9.0
Blacktip shark	<i>Carcharhinus melanopterus</i>	8.7	3.6
Silvertip shark	<i>Carcharhinus albimarginatus</i>	6.2	4.8
Hammerhead shark	Family Sphyrnidae	4.8	7.9
Blue shark	<i>Prionace glauca</i>	2.2	2.8
Other		8.5	13.6

Source: Kumoru (2003) – SPC observer data

6 DATA FROM LIHIR ISLAND

6.1 Introduction

CSIRO Marine and Atmospheric Research (CMAR) undertook a pelagic and mesopelagic sampling at Lihir Island (New Ireland Province, PNG), on behalf of Lihir Gold Limited (LGL), between October and December 2006. A variety of sampling devices were used to provide data on plankton, micronekton, benthic infauna, epifauna and animal tissues. The data for the pelagic environment is of interest to the Solwara 1 study as it provides by far the most relevant site-specific data in Papua New Guinea. CMAR and LGL have made these data available to Hydrobiology for this review.

6.2 Methods

6.2.1 Plankton

A total of 210 plankton samples were collected off Lihir Island using a Mid-water Opening-Closing (MIDOC) net with a 1 m x 1 m mouth opening and fitted with 150 µm mesh net. Depth-stratified sampling was undertaken to investigate vertical migration. Organisms collected were preserved and identified in the laboratory.

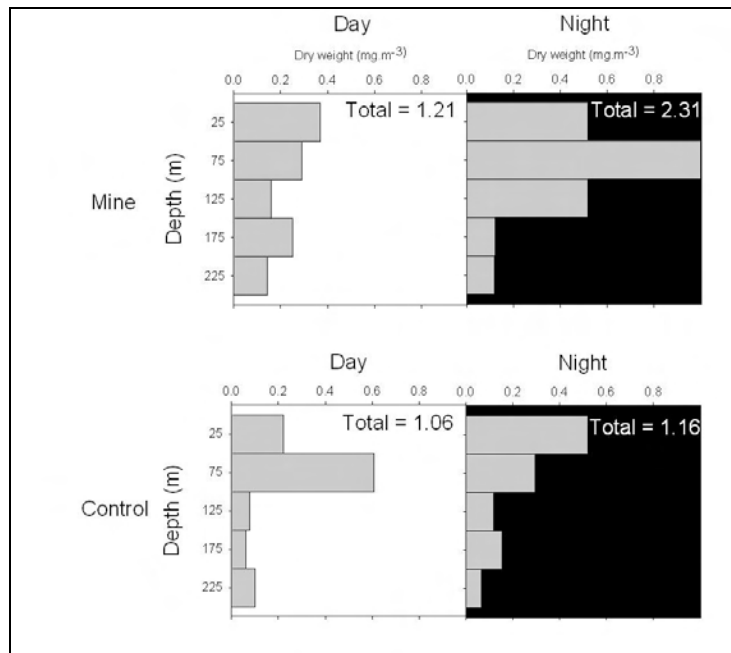
6.2.2 Micronekton

A total of 42 micronekton trawls were made during the day and night using an Isaacs-Kidd Midwater Trawl (IKMT). The trawl had a mouth opening of 5.06 m² (2.25 m x 2.25 m) and the net was about 8 m long, with mesh size of 10 mm in the body, and 2 mm in the cod-end. The IKMT is a fixed opening net that fishes from the moment of deployment, unlike the plankton (MIDOC) net that samples discreet depth strata. The greatest depth sampled was around 550 m, at the control site on the opposite side of the island to the mine. The fishing depth of the net was recorded by a transducer attached immediately above the net with depth readings relayed to a laptop equipped with a custom LabVIEW application on board. Animals collected were preserved for identification and enumeration in the lab.

6.3 Results

6.3.1 Vertical Migration

Analysis of depth-stratified day/night zooplankton sampling showed a strong vertical migration signal. The maximum depth of the origin of vertical migration is not well defined due to the limitations in the maximum depth sampling, but zooplankton moved from at least 225 m depth to 25-75 m depth



Source: Brewer et al. (2007)

Figure 6-1 Depth distribution of zooplankton biomass at Lihir Island

6.3.2 Zooplankton Diversity

Zooplankton diversity was very high (59 taxa identified from just 4 samples) and was dominated by crustaceans, in particular calanoid, cyclopoid and harpacticoid copepods (Table 6-1).

Table 6-1 Abundance of zooplankton taxa at Lihir Island

Taxa	Group	Abundance*
Calanoid copepod juveniles	Crustacea, Copepoda	280
Clausocalanus/Paracalanus spp. calanoid copepods	Crustacea, Copepoda	83
Oncaea spp.	Crustacea, Copepoda	101
Veliger larvae	Mollusc	83
Cyclopoid juveniles	Crustacea, Copepoda	52
Unidentified calanoid copepods	Crustacea, Copepoda	42
Chaetognatha	Arrow worm	30
Lucicutia flavicornis	Crustacea, Copepoda	18
Coryceidae	Crustacea, Copepoda	18
Eucalanus spp.	Crustacea, Copepoda	16
Ostracod	Crustacea	15
Rhincalanus spp.	Crustacea, Copepoda	12
Euterpina spp.	Crustacea, Copepoda	16
Appendicularia	Tunicate	11
Decapod larvae	Crustacea, Decapoda	11
Zoea larvae	Crustacea, Decapoda	10
Oithona spp.	Crustacea, Copepoda	9
Acartia spp.	Crustacea, Copepoda	9
Pleuromamma spp.	Crustacea, Copepoda	8
Furcilia larvae	Crustacea, Euphausiacea	8
Siphonophore	Hydrozoan	8
Calanopia elliptica	Crustacea, Copepoda	7
Temora discaudata	Crustacea, Copepoda	7
Euphausid larvae	Crustacea, Euphausiacea	7
Calocalanus spp.	Crustacea, Copepoda	6
Microsetella spp.	Crustacea, Copepoda	6
Candacia spp.	Crustacea, Copepoda	6
Euphausid	Crustacea	5
Polychaeta	Worm	5
Hyperiid amphipod	Crustacea	5
Sapphirina spp.	Crustacea, Copepoda	5
Salp	Tunicate	5
Polychaeta larvae	Worm	4
Calyptopis larvae	Crustacea, Euphausiacea	4
Euchaeta spp.	Crustacea	3
Scolecithricella/Scolecithrix spp.	Crustacea, Copepoda	3
Macrosetella gracilis	Crustacea, Copepoda	3
Harpacticoid juvenile	Crustacea, Copepoda	3
Macrosetella spp.	Crustacea, Copepoda	3
Lamellibranch larvae	Mollusc	3
Copilia spp.	Crustacea, Copepoda	3
Scolecithrix spp.	Crustacea, Copepoda	2
Penaeid protozoa larvae	Crustacea, Decapoda	2
Barnacle nauplius	Mollusc	2
Pteropod	Mollusc (gastropod)	2
Copepod nauplius	Crustacea, Copepoda	1
Megalopa larvae	Crustacea, Decapoda	1

Cyphonautes larvae	Bryozoan	1
Lucifer spp.	Crustacea, Decapoda	1
Porcellanidae zoea larvae	Crustacea, Decapoda	1
Pontellina plumata	Crustacea, Copepoda	1
Scottocalanus spp.	Crustacea, Copepoda	1
Fish larvae	Fish	1
Harpacticoid juvenile	Crustacea, Copepoda	1
Tortanus spp.	Crustacea, Copepoda	1
Isopod	Crustacea	1
Centropages spp.	Crustacea, Copepoda	1

Source: Brewer et al. (2007). *Abundance measure from 4 samples that were processed and therefore data available at the time of writing.

Figure 6-2 shows examples of some common zooplankton recorded from Lihir Island during the 2006 study.







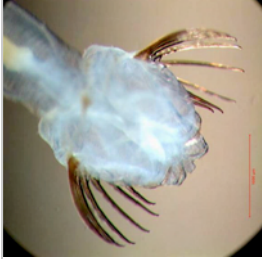



			
<i>Euphausiid</i>	<i>Colonial salp</i>	<i>Amphipod</i>	<i>Copepod</i>
			
<i>Palaemonid prawn</i>	<i>Mollusc</i>	<i>Arrow worm</i>	<i>Siphonophore</i>
			
<i>Copepod</i>	<i>Crustacean nauplius larva</i>		

Figure 6-2 Examples of zooplankton at Lihir Island

Source: Brewer et al. (2007)

6.3.3 Micronekton

Micronekton sampling recorded the presence of a range of fishes, crustaceans (dominated by decapod shrimps), salps and other gelatinous micronekton. Large caridean shrimps included the families Oplophoridae, Pandalidae, Pasiphaeidae and Palaemonidae. Penaeid prawns in the micronekton community included Sergestidae, Aristaeidae, Benthesicymidae and Solenoceridae. Other groups included Euphausiidae, Sergestidae, stomatopods, crab megalopa, porcellanids, amphipods, isopods, gastropods and Pyrosoma.

Many of the micronekton species recorded were bioluminescent and examples of common species are shown in Figure 6-3.

		
<p>Micronekton haul from 250 to 10 m. Late afternoon. Note gelatinous zooplankton</p>	<p>Micronekton haul from 500 to 250 m. Approximately midnight. Note red-coloured decapod crustaceans dominate</p>	<p><i>Diaphus</i> spp. (lanternfish – bioluminescent)</p>
		
<p>Possibly <i>Ectreposeastes imus</i> (Deepsea scorpionfish)</p>	<p>Bristlemouth (note bioluminescent patches on ventral surface)</p>	<p><i>Palaemonid</i> prawn</p>

Figure 6-3 Selected species of micronekton from Lihir Island

Source: Brewer et al. (2007)

	<p><i>Oplophoridae shrimp</i></p>
	<p><i>Pandallidae shrimp</i></p>
	<p><i>Sergestidae shrimp</i></p>

Figure 5-3 cont.

6.3.4 Epipelagic predators

Sampling of pelagic predators at Lihir Island recorded the presence of yellowfin tuna (*Thunnus albacares*) at depths of 362 and 509 m. A suite of predatory species were targeted for analysis of dietary composition. The species targeted were:

- Mackerel tuna (*Euthynnus affinis*);
- Frigate mackerel (*Auxis thazard*);
- Skipjack tuna (*Katsuwonus pelamis*);
- Flat-tail longtom (*Platybelone platyura*);
- Sailfish (*Istiophorus platypterus*);
- Rainbow runner (*Elagatis bipinnulata*);
- Spanish mackerel (*Scomberomorus commerson*);
- Great barracuda (*Sphyræna barracuda*);
- Dolphinfish (*Coryphaena hippurus*);

The results of stomach contents analysis of these predatory species combined are shown in Figure 6-4.

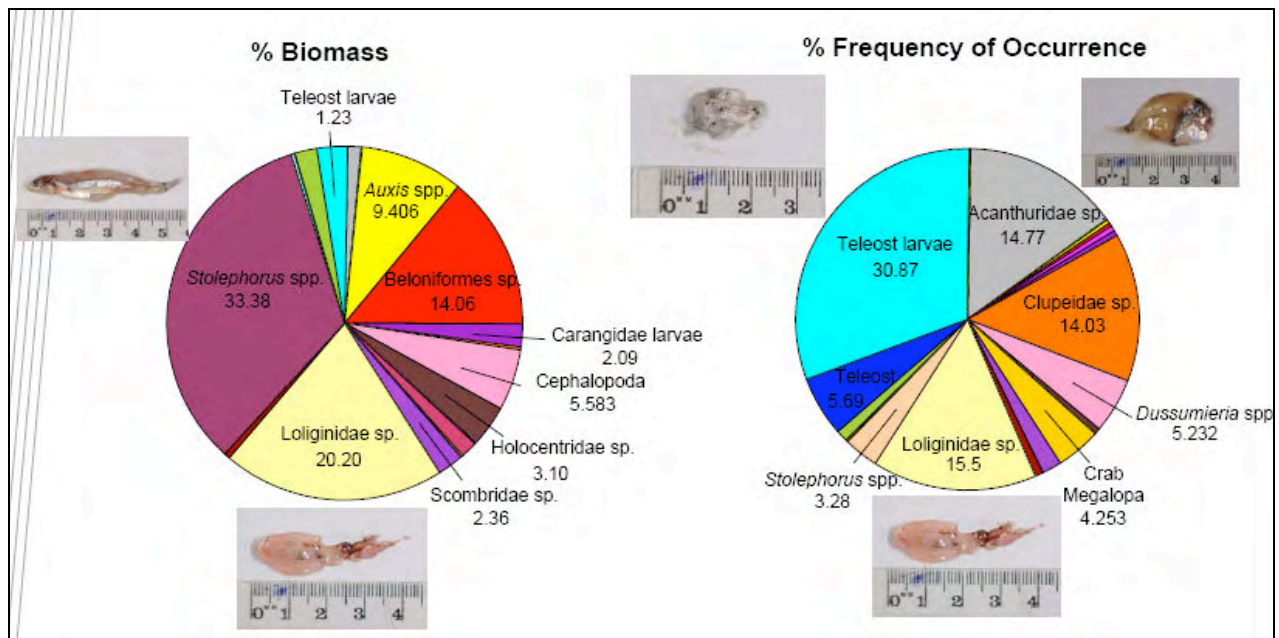


Figure 6-4 Stomach contents of pelagic predators at Lihir Island

Source: Brewer et al. (2007)

7 BIOLUMINESCENCE

7.1 Vision

Bioluminescence plays an important role in the life histories of many mesopelagic and bathypelagic organisms. Bioluminescence and vision in these animals is constrained by the marine light environment and by the eye design of each species (Warrant and Locket 2004). This section describes both these dominating influences.

7.1.1 Marine Light Environment

The two main natural sources of light in the sea are from celestial bodies (sun, moon, stars) and bioluminescence produced by aquatic organisms. The optical properties of water govern the transmission of light through the water column such that the prominence and intensity from both natural sources changes with depth, from the sun-lit shallows of the euphotic zone (~0-200 m; Section 4.1) to a scene dominated by point-source bioluminescent flashes in the bathypelagic zone (below 1000 m; Section 4.3).

Blue light (~475 nm) is transmitted best through clear ocean water, whilst the orange-red part (beyond 550 nm) of the daylight spectrum is almost entirely absorbed within the first 100 m. Whereas animals living in the euphotic zone experience light more characteristic of the terrestrial environment, animals living in the mesopelagic (200 – 1000 m) experience a relatively constant colour and exponential decrease of light intensity with depth. Almost no daylight reaches past 1000 m that can be perceived by deep-sea animals (Warrant and Locket 2004). For example, a shrimp eye (aperture 1 mm²) would receive approximately 100 photons blue light per day at 2000 m (Herring 2002) compared to 2.5×10^{19} photons m⁻² s⁻¹ at the surface (Warrant and Locket 2004). It is this reduction of light from the surface layers down to the bathypelagic that has had the greatest influence on the evolution of vision and eye design in the sea.

7.1.2 Deep-Sea Eye Design

Before discussing eye design it is important to understand the actual light sources and the frequency of these sources in the marine environment. In the well-lit upper levels, the higher light intensity allows three-dimensional vision for feeding, predator evasion and mating. In the dark lower-levels, eye design is adapted to sensing point-source bioluminescence and/or a flat two-dimensional plane (i.e. the seafloor). Bioluminescent signals are usually point-source flashes, although some organisms may distribute luminescent flashes around their bodies (e.g. tunicate *Pyrosoma atlanticum*), produce intricate bioluminescent displays (jellyfish) or expel bioluminescent clouds (crustaceans and cephalopods). The duration of these flashes can vary from hundreds of milliseconds to several seconds (Warrant and Locket 2004) and early measurement of the actual frequency of flashes has been recorded at 160 flashes per minute at 100 m and 90 flashes per minute at 900 m, decreasing to 3 flashes per minute below 2000 m (Clarke and Hubbard 1959). It is now recognised that these flashes were stimulated by the turbulence surrounding the recording bathyphotometer and observers in completely neutrally buoyant submersibles rarely see any unstimulated flashes (P. Herring, pers. com.). Bioluminescent flashes, as described above, may have spectral, kinetic or spatial differences, but are generally blue and contain 10^7 and 10^{13} photons, some

10 times above the typical background light level in the epipelagic zone (Clarke and Hubbard 1959).

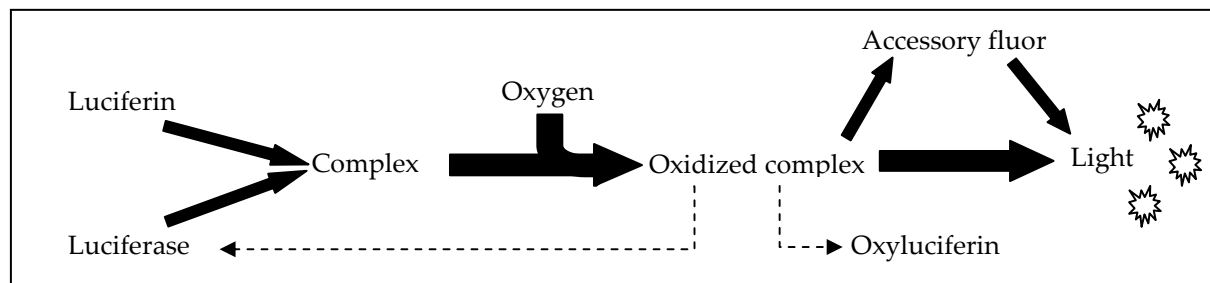
There are four main types of aquatic eye design; camera (Land and Nilsson 2002), concave-mirror, compound apposition and compound superposition. All terrestrial and aquatic vertebrates, as well as gastropod and cephalopod molluscs, certain annelid worms and crustaceans (e.g. copepods) have camera-type eyes (Warrant and Locket 2004). Camera eyes receive light through a surface layer called the cornea (in air) refracts the light through the pupil towards the lens. In water, the cornea has little refractive effect. The lens focuses the light on the retina at the back of the eye. Photoreceptors within the retina are stimulated by incoming light and send visual information to the brain's visual centre via the optic nerve which elicits certain responsive behaviours. In bivalve scallops and crustaceans of the ostracod genus *Gigantocypris*, light passes through the retina and is then reflected and focussed back onto the retina by a concave mirror lining at the back of the eye (Warrant and Locket 2004). Image contrast is reduced in this eye type because the light has already passed through the retina before being refocused by the concave mirror, however, relative to other eye designs, the concave mirror is excellent for light capture (Warrant and Locket 2004). The compound eye is the most widespread eye design in the animal kingdom, possessed by arthropods, including insects and most crustaceans, and amongst certain clams and polychaetes. Compound eyes are found in two forms, apposition and superposition. Both forms of compound eyes are composed of several thousand optical units called ommatidia, each consisting of a cornea and a crystalline cone (lens pair) which focuses light onto an underlying photoreceptor bundle (rhabdom). Superposition eyes differ from apposition eyes because the lens pair is separated by a wide, optically transparent space called the 'clear zone' which allows light to be focussed from several ommatidia onto a single rhabdom, in some cases as many as 2000 ommatidia can collect light for one rhabdom (Land and Nilsson 2002; Warrant and Locket 2004). Apposition eyes are common in epipelagic crustaceans, where the high ambient light levels provide scope for good image resolution. Conversely, in the deep-sea environment, light levels are low and the optical emphasis is on sensitivity and superposition eyes. The eyes and vision of deep-sea animals thus match the way the light environment changes with depth. Mesopelagic euphausiid and sergestid shrimp make vertical migrations in the ocean water column and it is assumed that these shrimp use their eyes as optical depth gauges, maintaining an environment with constant light intensity in which they are less visible to predators but are still able to find food as they swim through different depths (Warrant and Locket 2004; Widder and Frank 2001).

Benthopelagic animals, that have a close association with the sea floor, tend to have smaller eyes than mesopelagic fauna, possibly because the sea bed is comparatively food-deficient and therefore deep-sea fauna do not rely as heavily on visual cues for food detection.

7.2 Chemistry

Bioluminescence is the production and emission of light by a living organism resulting from chemiluminescent reactions. It is generated by the chemical 'excitation' of a small, fluorescent organic molecule called luciferin. This 'excitation' is essentially the raising of luciferin to a higher energy state through oxidization in the presence of the enzyme luciferase (Figure 7-1). Light energy is then released when the excited luciferin decays and

returns to a stable ground state. Alternatively, the energy may be passed onto an accessory fluorescent molecule which emits light at a different wavelength.



Source: Herring (2002)

Figure 7-1 Schematic diagram of a bioluminescent reaction

There are many chemically different types of luciferin, however one type, the imidazolopyrazine known as coelenterazine, appears to be more prevalent in marine species, occurring in seven phyla and approximately fifty genera including many squid, myctophid fish and decapod shrimps (Herring 2002; Campbell and Herring 1990; Thomson et al. 1997).

7.3 Functions

7.3.1 Defence

Most deep-sea bioluminescence functions as a defence mechanism (Herring 2002). Certain organisms emit flashes or squirts of light that can serve to distract or inhibit a visual predator long enough to enable escape (Herring 2002). For structurally fragile animals that are either sessile (e.g. sea-pens) or slow-moving (e.g. salps, jellyfish) bioluminescence can also serve to startle and thereby prevent collisions with larger animals (Morin 1974). Larger animals, including cnidarians, ctenophores and dragonfishes (e.g. *Astronesthes*) also produce defensive flashes (Herring 2002). As these organisms are potentially vulnerable to predation, they utilise bioluminescent flashes at or near to their extremities thereby giving the impression that they are a large predator (Herring 2002). Some animals exaggerate this effect by rhythmically flashing at the extremities of elongated limbs e.g. the amphipod *Scina* (Herring 2002). Rhythmic flashing also occurs in deep-sea animals following disturbance including medusa (*Atolla*), siphonophores (*Agalma*), ctenophores (*Beroe*), colonial sea-pens (*Pennatula*), brittle-stars (*Ophiacantha*) and holothurians (*Pannychia*) which may disorientate and possibly temporarily stun a predator (Herring 2002).

Some fauna may also shed luminescent appendages which act as independently flashing decoys which distract would-be predators (Herring 2002). As described above (see 5.2 Occurrence and Distribution), bioluminescent secretions, released as clouds similar to squid ink can also be used as a distractive predator response. Further to the expelled bioluminescent material response, some copepods may also propel the material away from themselves, by flicking or kicking (e.g. *Gaussia*). One genus, *Disseta*, also has a time delay on the bioluminescent droplets which may distract approaching predator (Herring 2002).

While the above uses are designed to be conspicuous, bioluminescence can also be employed to camouflage an individual. The method of bioluminescent camouflage is commonly called counter-illumination. The ventral surface of organisms (e.g. decapods shrimps *Oplophorus* and *Sergestes*, squid *Abralia* and *Histioteuthis*, hatchetfish, lanternfish, sharks *Isistius* and *Etmopterus*) which utilise counter-illumination usually have a series of photophores on them which act to blend in with the downwelling light, so that predators looking towards the surface cannot see them as a silhouette (Herring 2002). This form of camouflage can be modified according to the light intensity at any given depth or time, such that animals are able to vertically migrate and remain hidden. Some animals may also match light intensity at different depths with different photophores which emit light of different spectral maxima e.g. the squid *Abralia* (Young and Mencher 1980).

7.3.2 Feeding

Bioluminescence also functions to aide feeding by illuminating or attracting prey (Herring 2002). The loosejaw fish, *Malacosteus* sp., has a blue-emitting, postorbital photophore which is used to illuminate prey, and because blue light has the maximum effective range in seawater it is able to utilise this feeding strategy at greater depths. *Malacosteus* sp. also has a red-emitting, suborbital photophore which can be used to detect red organisms such as deep-sea shrimp. Some organisms attract their prey with bioluminescent lures, for example, the female anglerfish *Linophryne* has a bacteria-derived luminescent lure on the head and a branched barbel hanging from the lower jaw which contains bioluminescent organs. Such chin barbels are also found on long black dragonfishes (*Eustomias*). Squid such as *Chiroteuthis* and *Octopoteuthis* have luminescent arm tips used to lure prey. Photophores for prey attraction are also present in the mouths of certain fish (e.g. *Steroptyx*, *Chauliodus*, *Pseudoscopelus*).

An indirect aide to feeding is effected by certain bacteria. The bacterial species *Photobacterium fischeri*, has a unique mechanism which allows it to control luciferase synthesis depending on the population density (a phenomenon known as 'quorum sensing'). Each individual releases what is called an autoinducer into the water. This triggers bioluminescence once a certain concentration is reached (Nealson 1977; Eberhard et al 1981). The autoinducer effect ensures that there are a sufficient number of bacteria to produce clearly visible light. This can occur when bacteria accumulate on decomposing matter and marine snow which consequently gives off light, thereby attracting opportunist feeders (Bailey et al. in press) whilst also benefiting the bacteria themselves as they are ingested into the nutrient rich environment of the host's gut (Herring 2002).

7.3.3 Signalling Behaviour

Bioluminescent signalling behaviour amongst the deep-sea fauna is probably less-frequent when compared with nocturnal near-surface fauna such as the flashlight fish *Photoblepharon* (Herring 2002). Of the limited amount known, the aforementioned red emitting photophore of *Malacosteus* may also be used for intraspecific communication (Herring and Cope 2005). *Malacosteus* has visual pigments that allow it to detect red and blue, whilst most organisms can only detect blue light. This allows one *Malacosteus* fish to signal to another without risking predation.

With no existing in-situ observations of luminescent sexual signalling amongst deep-sea organisms, it is only assumed to occur from the variations in photophore arrangement between the males and females of certain animals (Herring 2007). Mesopelagic lanternfishes have different sized photophores which are positioned differently around the body depending on the sex. The lanternfish *Diaphus*, for example, has two forward-facing photophores which are larger in the males and many lanternfish generally have sexually dimorphic photophores on the caudal peduncle (rear of the body just before the tail fin).

7.4 Occurrence and Distribution

The simplest luminescent marine organisms are bacteria. Approximately half a dozen luminescent bacterial species, split between the genera *Photobacterium*, *Vibrio* and *Shewanella*, have been cultured from seawater samples (Reichelt and Baumann 1973). These species have been noted for their distinct temperature sensitivities, for example *Vibrio fischeri* occur within warmer surface waters and *Photobacterium phosphoreum* tend to be found in greater concentrations in colder, deeper waters (Hastings and Nealson 1977). Bioluminescent bacteria are also found in symbiotic relationships with specific host fish which must have similar temperature preferences in order for the bacteria to survive. Symbiont specificity occurs in shallow, warm-water between pony fishes (Leiognathidae) and *Photobacterium leiognathi* (Reichelt and Nealson 1977), and in deep, cold-water between rattails (Macrouridae) and *Photobacterium phosphoreum* (Nealson *et al* 1981)

Many fishes have specialised light organs which develop as protrusions from different parts of the gut and encapsulate luminescent, symbiotic bacteria (Herring 2002). Midwater (mesopelagic) examples include the barreleye fishes (Opisthoproctidae). Rattails (Macrouridae) which also have bacterial bioluminescent organs (Marshall and Cohen 1973) were observed in the ROV footage at approximately 1500 m.

In shallow waters, the family Anomapolidae (flashlight fishes) encompasses five genera of tropical reef fishes that have large suborbital light organs (Haygood and Distel 1993). The deep-sea anglerfishes (Ceratioidei) have bacterial light organs at the end of a lure, a modified fin ray. Some squid have light organs unconnected to the gut and seated on the inc sac. The Hawaiian bobtail squid, *Euprymna scolopes*, contains no bacteria at hatching but is able to acquire bacteria from the surrounding environment using special ciliated lobes situated at the entrance to the light organ duct (Herring 2002; McFall-Ngai 1994). Another group of organisms whose light organs contain structures that are probably contain bacteria are pyrosomes, holoplanktonic colonial tunicates which are found at depths up to 1000 m (Bowlby *et al* 1990). Unlike those of fish and squid, the pair of bacterial-light organs in a pyrosome are not open to the surrounding water, but appear to be intracellular. Little is known of the mechanism by which they control light emissions. (Mackie and Bone 1978).

In order to utilise these symbiotic bacteria, animals must maintain a constant environment within the light organ otherwise the bacterial luminescence would be extinguished. The host also needs to be able to control the light output for its own purposes and a variety of mechanisms are employed (Herring 1982, 1985). The light organ requirement and the energy expenditure associated with harbouring luminescent bacteria may explain why most marine organisms do not use bacteria but contain their own luciferin, usually in the form of coelenterazine. In a few species, luciferin can be obtained through diet, as in the case of the

giant deep-sea mysid *Gnathophausia* (Herring 1985; Frank *et al* 1984) and the midshipman fish *Porichthys notatus* (Mesinger and Case 1991). The majority of bioluminescent organisms contain their own luciferin stored within a variable number of light organs called photophores, e.g. deep-sea squid *Taningia danae* (Kubodera *et al* 2007) and lanternfish. The latter was observed at depths of 200 to 300 m in the ROV footage from the Solwara 1 dives. Bioluminescent material can also be secreted by some animals (e.g. crustaceans such as the pelagic shrimp (*Oplophorus*), deep-sea jellyfish (*Periphylla periphylla*), ctenophores, worms and molluscs) (see Section 7.3.1 Defence; Herring and Widder 2004; Herring 2002; Herring 1985).

Relatively little is known about the vertical profile of bioluminescence through the water column. BathypHOTometer profiles have been undertaken for over 50 years and record the *potential* bioluminescence by continuous measurements made in a turbulent chamber as the probes moves vertically in the water. Video profiles have also recorded the impacts of bioluminescent animals on a mesh moving horizontally (Widder and Johnsen 2000) or vertically through the water column. Studies of the latter type have been conducted in the Atlantic Ocean, off Cape Verde (Priede *et al.* 2006) and in Sognefjord, Norway (Bailey *et al.* in press) using specialist camera and profiling devices which have been able to record the abundance and distribution of luminous organisms. In Sognefjord, bioluminescence was observed at all depths but was most abundant between 300 and 750 m depth. Concurrent sampling at different depths showed that the organisms most likely to account for this luminescence were metridiid copepods, of which certain species (*Gaussia princeps*) are known to occur below 400 m in other oceans (Bowlby and Case 1991), emitting bursts of light by releasing luminous material from specialised glands (see 5.3.1 Defence). In addition, aggregations of large, spherical particulate matter, up to 5 mm in diameter and reaching 5000 mm³ l⁻¹, an order of magnitude more concentrated than the rest of the water column (Allredge *et al.* 2002; Bailey *et al.* in press) are known to exist at density discontinuities, together with aggregations of luminescent bacterial colonies. Thin layers of luminescent animals occur at density discontinuities or other internal water column structures that may trap luminescent organisms at depth (Widder *et al.* 1999).

Interestingly, the 400 m depth layer has been reported to sometimes be a focal area of bioluminescent activity (Bailey *et al.* in press; Widder *et al.* 1999). Four hundred metres represents the approximate depth at which megafaunal activity was most apparent within the Nautilus ROV footage, namely squid, comb jellyfish and tuna. The 400 m depth layer was also identified as an area of potentially some internal wave action at the Solwara 1 site, which was one possible explanation of the high dissolved oxygen concentration measured around this depth.

A summary of the above information on bioluminescence and trophic interactions, combined into a model for an ecological process through the water column is as follows; as particulate organic matter (POM) falls through the water column it may reach this depth having aggregated into larger particles and having been colonised by luminescent bacteria which attaches and consumes POM (Bailey *et al.* in press). Consequently, the POM then reaches a size suitable for zooplankton consumption (e.g. copepods), primarily in the mesopelagic zone (e.g. copepods) and also provides a visual cue for opportunistic feeders due to the presence of luminescent bacteria. In turn, these smaller zooplankton (themselves

bioluminescent), attract micronekton which attracts larger consumers, eventually leading to tertiary (often epipelagic) consumers.

Observations of bioluminescent light at depth have been recorded at all depths by observers in bathysphere, bathyscapes and manned submersibles who have turned out the lights, and recorded at depths in excess of 6000 m (Widder 1999). Records have also been obtained within deep-scattering layers comprised of planktonic, bioluminescent organisms (Widder et al. 1992). The occurrence of these deep-scattering layers at 400 m (Clarke and Backus 1956), the same depth as the aforementioned particle aggregations (and the highest zone of nekton activity identified in the ROV footage at Solwara 1), is reportedly linked to the light intensity at these depths (Clarke and Backus, 1956; Clarke and Wertheim, 1956). Echo sounder records have revealed that deep-scattering layers commonly occur at depths of 400 to 600 m during the daytime but also as deep as 1,000 m (Clarke and Backus, 1956). Net and plankton hauls at these depths have also revealed that the organisms within these layers are comprised of vertically migrating crustacea and fish which feed on the plankton (Young and Hobday 2004) and this was certainly the case at Lihir Island. In turn, these vertically migrating organisms are fed on by secondary consumers such as small shoaling fish (e.g. *Caesionidae*) and squid which are predated by tertiary consumers such as tuna. These secondary and tertiary consumers were observed in the Nautilus ROV footage from the Solwara 1 site and at Lihir Island, suggesting that this process, probably involving bioluminescent interactions, with particular relevance to the biomass the 400 m depth mark, is probably occurring in the Solwara project area.

8 TROPHIC WEBS

This desktop study has placed particular emphasis on the depth distributions of various species and their trophic interactions because these two factors play a key role in determining the interaction between the epipelagic zone and the deeper layers and the potential for exposure to mid-water dewatering plumes and near-bottom plumes. Specifically, the interaction between tuna and the meso- and bathypelagic zones was most important because tuna are a), the main tertiary consumers (top predators) in the pelagic system, b), fished commercially in the Bismarck Sea and support a significant economy in fishing and processing and c), are fished for subsistence in the Bismarck Sea.

Table 8-1 summarises some of the more recent literature on the composition of tuna gut contents in the Pacific Ocean. The information obtained from this desk study was used to construct a conceptual model for the trophic webs of the epi-, meso- and bathypelagic environments, again, with a focus on the linkages between these zones (see Figure 8-1).

Table 8-1 Summary of tuna gut-contents data

Species	Locality	Stomach Contents		Abundance/Proportions	Prey Depth Range	Reference
		Family	Common Name			
Yellowfin tuna (<i>Thunnus albacares</i>)	East Coast Australia - Seamounts	Argonautidae	Pelagic octopus	~2.8% by weight	?	Lansdell and Young (2007)
		Octopoteuthidae	Squid	~1.2% by weight	?	
		Octopodidae	Octopus	~4.5% by weight	?	
		Ommastrephidae	Squid, dominated by <i>Ornithoteuthis volatilis</i> and <i>Notodarus gouldii</i>	~71% by weight	to ~700m	
		Ancistrocheiridae	Squid	~10.6% by weight	to ~1000m	
		Enoploteuthidae	Squid	~0.3% by weight	to ~1000m – bioluminescing	
		Brachioteuthidae	Squid	~0.3% by weight	to ~800m	
		Chiroteuthidae	Squid	~0.03% by weight	“deep-sea”	
		Loliginidae	Squid	~6.3% by weight	“shallow-water”	
		Septiolidae	Bobtail squid	~0.3% by weight	?	
Yellowfin tuna (<i>Thunnus albacares</i>), bigeye tuna (<i>Thunnus obesus</i>), and albacore tuna (<i>Thunnus alalunga</i>)	French Polynesia	Spirulidae	Squid	<0.01% by weight	550-1000m (day time), 100-300m (night time)	Bertrand et al. (2002)
		Onychoteuthidae	Squid	~1.9% by weight	?	
		Cranchiidae	Glass squid	~0.1% by weight	“deep sea”	
		Fish		38% by number	-	
		Cephalopods		22% by number	-	
		Crustaceans		36% by number	-	
		Gelatinous organisms		4% by number	-	

Table 8-1 cont.

Yellowfin tuna <i>Thunnus albacares</i> , bigeye tuna (<i>Thunnus obesus</i>), and albacore tuna (<i>Thunnus alalunga</i>)	French Polynesia	Myctophids	Lanternfish	~7.5% by weight	Bertrand et al. (2002)
		Piscivorous fish	Fishes feeding on myctophids (mesopelagic fish)	~25.4% by weight	
		Reef fish		~1.7% by weight	
		Epi-pelagic zooplankton feeders	Including hatchetfish (deep-sea bioluminescing), spinyfins, dories, tinselfish (deep-sea), fang-tooth (deep-sea)	~5.5% by weight	
		Meso-pelagic zooplankton feeders	Including bristlemouths (to 1000m), perch	~0.02% by weight	
		Other fish		~14.9% by weight	
		Meso-pelagic cephalopods	Including drifffish, pomfrets, chiasmodontids (deep-sea)	~25.2% by weight	
		Deeper meso-pelagic cephalopods		~14.9% by weight	
		Holoplanktonic crustacean		~2.7% by weight	
		Meroplanktonic crustacean	Including euphausiids, amphipods, isopods	~1.1% by weight	
		Gelatinous zooplankton	Crustacean megalopoda	~0.92% by weight	
			Including tunicates, gastropods, pteropods		

Table 8-1 cont.

Yellowfin tuna (<i>Thunnus albacares</i>)	French Polynesia				"feed mainly in the upper 100 m"	Bertrand et al. (2002)
Bigeye tuna (<i>Thunnus obesus</i>)	French Polynesia				"feed more on mesopelagic fish and cephalopods to >550 m"	Bertrand et al. (2002)
Albacore tuna (<i>Thunnus alalunga</i>)	French Polynesia				"high proportion of cephalopods and crustaceans in diet, vertical behaviour largely unknown"	Bertrand et al. (2002)
Yellowfin tuna (<i>Thunnus albacares</i>)	East Coast Australia (NSW)	Crustacean	<i>Principally crab megalopoda (larvae)</i>	~72.1% by number and ~6.2% by weight	Vertically migrating to at least 400m	Young et al. (2001)
		Cephalopod	Principally squid	~19.6% by number and 14.2% by weight	Vertically migrating to at least 400m	
		Fish	Principally mackerel	~6.9% by number and 79.3% by weight		
		Other			Principally epi-pelagic species in this study	

Table 8-1 cont.

Yellowfin tuna (<i>Thunnus albacares</i>)	Western and Central Pacific		Overall stomach contents: Pelagic crustaceans Megalopod stages of crustaceans Shrimps Heteropoda molluscs	40% 20% 17% 31%	Vertically migrating Vertically migrating Vertically migrating Vertically migrating	Allain (2002/2005)
		Larger prey: Alepisaurus Scombridae Sternoptichidae	Lancetfish Mackerels Hatchetfish Squids	22% 15% 15% 44%	Meso/bathypelagic Pelagic fishes Meso/bathypelagic, bioluminescing	
Bigeye tuna (<i>Thunnus obesus</i>)	Western and Central Pacific	Overall stomach contents: Fish Myctophids Alepisaurus Sternoptichidae Molluscs Crustaceans	Lanternfish Lancetfish Hatchetfish	72.3% 67% 51% 39% 38.6% 5.6%	Meso/bathypelagic, vertically migrating, bioluminescing Meso/bathypelagic Meso/bathypelagic, bioluminescing Vertically migrating Vertically migrating	Allain (2002)
Skipjack tuna (<i>Katsuwonus pelamis</i>)	Western and Central Pacific	Overall stomach contents: Fish		95%	“Consumes primarily pelagic prey”	Allain (2002)

Table 8-1 cont.

Skipjack tuna (<i>Katsuwonus pelamis</i>)	Western and Central Pacific				<p>"Primarily epipelagic prey" "Dives to depth of up to 250m" "Probably feeds primarily during the day"</p>	Allain (2005)
Albacore tuna (<i>Thunnus alalunga</i>)	Western and Central Pacific	<p>Mesopelagics Bathypelagics Epipelagics Reef-associated</p>	<p>47% of total 12% of total 8% of total 5% of total</p>	<p>"Primarily juvenile fish and squid"</p>	Allain (2005)	
Yellowfin tuna (<i>Thunnus albacares</i>)	Western and Central Pacific	<p>Mesopelagics Bathypelagics Epipelagics Reef-associated</p>	<p>8% of total 5% of total 40% of total 10% of total</p>	<p>"Typically between surface and 200 m, diving up to 500 m"</p>	Allain (2005)	
Bigeye tuna (<i>Thunnus obesus</i>)	Western and Central Pacific	<p>Mesopelagics Bathypelagics Epipelagics</p>	<p>36% of total 16% of total 5% of total</p>	<p>"Primarily juvenile fish and squid" "Feeds between surface and 150 m during the day, diving up to 500 – 900 m at night"</p>	Allain (2005)	
Yellowfin tuna (<i>Thunnus albacares</i>)	Hawaii			<p>"Juveniles do not dive as deep as large fish" "Ontogenetic change in diets at 45-50cm FL" "Small fish feed primarily on planktonic organisms in the surface mixed layer, while larger fish feed primarily on teleosts and vertically migrating meso-pelagic shrimp (to at least 700m)"</p>	Graham et al (2007)	

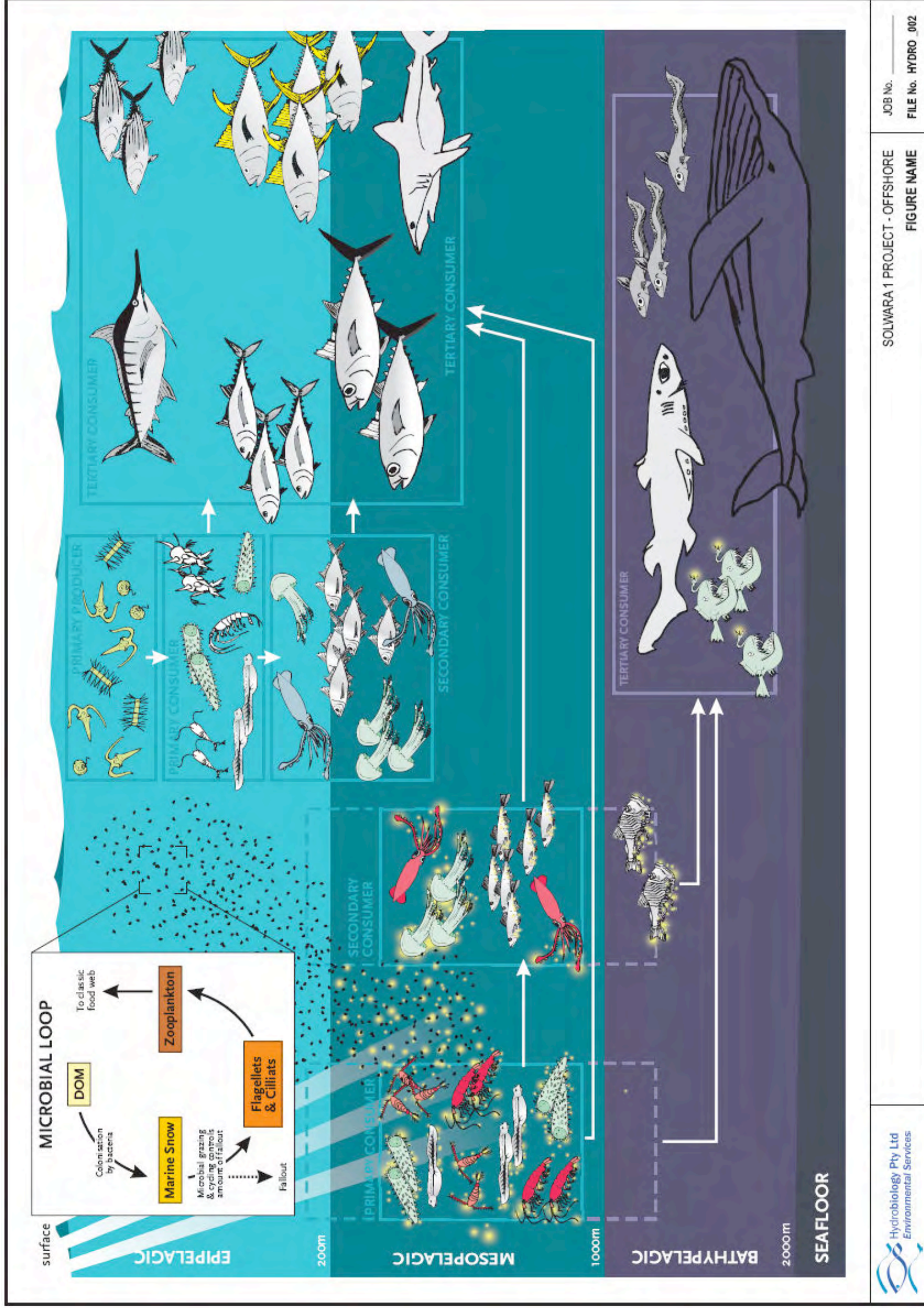


Figure 8-1 Conceptual trophic web of the pelagic environment

9 RISK PATHWAYS AND ASSESSMENT

9.1 Introduction

The main ecological risks related to this project are shown in Table 9-1.

Table 9-1 All potential risks of the project to pelagic, mesopelagic and bathypelagic organisms

Risk	Pathway	Worst-case Consequence / Effect
Potential risk of adverse physical impact to endemic species or species of scientific interest	<p>1. Direct</p> <p>a). Physical interaction of organisms with:</p> <ul style="list-style-type: none"> • discharge of turbid/metal-enriched dewatering fluid. • Machinery/ noise from the mining activity <p>b). Physical interaction of organisms with discharge of turbid/metal-enriched plume generated by the mining machine or re-location of unconsolidated sediment.</p> <p>2. Indirect</p> <p>Effects on processes or trophic web that places organisms at indirect risk</p>	<p>Loss of biodiversity/biomass from an area around the Solwara 1 project</p> <p>Loss of potentially endemic species, or species of scientific interest from an area around the Solwara 1 project</p>
Potential risk of exposure of epi-, meso- and bathypelagic organisms to metal-enriched waters/sediments	<p>1. Direct</p> <p>Physical interaction of (dissolved) metals with organisms body integuments</p> <p>2. Indirect</p> <p>Physical interaction of (dissolved and particulate) metals with food sources that are consumed by organisms</p>	<p>Bioaccumulation of metals in the body of an organism if exposure exceeds organism's ability to excrete/regulate metals, causing chronic sub-lethal effects such as organ stress, decreased survival or fecundity of the organism</p> <p>Acute lethal effects if prolonged exposure to intolerable levels</p>
Potential risk of organisms exposed to metal-enriched water/sediments in the meso- and bathypelagic zone being consumed by epipelagic organisms, leading to bioaccumulation and biomagnification in tunas and other predators which are then consumed by people	<p>Indirect</p> <p>a). Foraging excursions by epipelagic predators into the mesopelagic zone encountering prey exposed to metals</p> <p>b). Meso/bathypelagic organisms entering the epipelagic food web during vertical migrations</p>	<p>Bioaccumulation of metals in prey organisms leading to bioaccumulation or biomagnification in predators, leading to effects to ecosystem functioning and real or perceived risks to human health and fisheries</p>

With respect to the assessment of these potential risks, the key findings of this desktop study are as follows:

- Organisms in the epipelagic environment of the study area are widely distributed throughout the Pacific Ocean. Populations of epipelagic organisms in the Bismarck Sea probably mix throughout the western and central Pacific Ocean. For some groups of organisms, populations in the Bismarck Sea may represent distinct sub-populations of Pacific stock;
- There is less confidence as to the endemism of organisms in the mesopelagic zone. However, literature and ROV footage would suggest that most of the populations of the mesopelagic zone are widespread, due in part to the relatively high spatial uniformity of deep water masses (less water structure horizontally than vertically at these depths);
- There is very low confidence as to the endemism of organisms in the bathypelagic zone at the Solwara 1 site. There were very few organisms identified in ROV footage, but those that were identified were from families very widely distributed. Literature from other Pacific locations also indicates that most bathypelagic organisms are widespread. Again, at depths over 1000 m, there is little differentiation between tropical and temperate latitudes and there is little horizontal structure in water masses;
- Tuna are the main tertiary consumers (top predators) in the pelagic environment of the Bismarck Sea;
- At least four species of tuna occur in the Bismarck Sea; yellowfin, bigeye, skipjack and albacore and these are fished commercially in PNG. While the Solwara 1 project area does not appear to be located in a high commercial fishing activity area (and therefore the potential for physical obstruction of fishing is minimal), the tunas, billfish and sharks of interest in the fishery likely range throughout the Bismarck Sea and therefore have the potential to come into contact with the project.
- Skipjack tuna forage primarily within the epipelagic environment;
- The diet of yellowfin tuna includes significant proportions of mesopelagic organisms, namely fishes, crustaceans (including micronekton) and cephalopods. These prey are consumed either during daytime dives into the mesopelagic zone (which are recorded to ~250 – 400 m commonly and to greater depths infrequently – yellowfin tuna have been recorded at 500 m at Lihir Island and over 800 m depth at the Solwara 1 site) or during dusk and when vertically migration meso- and bathypelagic prey are shallower waters and light is sufficient for visual predators;

- The diet of bigeye tuna consists primarily of meso- and bathypelagic organisms, namely fishes, crustaceans, molluscs and cephalopods. The depth range of bigeye tuna is demonstrated to be the greatest of the tuna species, with regular and frequent daytime dives to at least 500 m depth. Bigeye tuna may also encounter these prey at dawn and dusk when vertically migration meso- and bathypelagic prey are shallower and light is sufficient for visual predators;
- The diet of albacore tuna are less well understood, but the species is known to dive to around 500 m, with diet consisting mainly of meso- and bathypelagic crustaceans and cephalopods;
- Squid are known to feature prominently in the diet of tuna, particularly yellowfin tuna and squid were observed, sometimes in high concentrations in the ROV footage from the Solwara 1 site. The 400 m depth mark at the Solwara 1 site was a zone of particularly high activity observed from the ROV footage. Especially in the early hours of the morning (~4 am), squid and tuna were observed in high concentrations at 400 m depth;
- Bioluminescence is critical for a range of ecological processes, and plays an important role in the trophic web. Inter- and intraspecific bioluminescent interactions could be adversely affected by increased turbidity. The mechanism for this would likely to be a reduction in the range at which animals could visually recognise prey, predators or mates;
- Bioluminescence is likely to be linked to deep scattering layers, again with the 400 m to 500 m depth layer being a focal point at the Solwara 1 site.

9.2 Body Burden, Bioaccumulation and Biomagnification

The process of bioaccumulation is not a straightforward relationship between metals in water and an animal's tissue. Complex processes relating to variable exposure pathways, trophic biomagnification (which only occurs for some metals), regulation, detoxification and storage of metals within the animal, all interact before an animal is at risk of bioaccumulation. Figure 9-1 illustrates some of the most important of these controlling factors for a prey species (crustacean) and a predator (tuna). The relative thicknesses of arrows in Figure 9-1 represent the relative importance of the pathway or process involved.

For many organisms, trophic pathways actually constitute a relatively minor exposure pathway, compared to the direct-exposure of soft body integuments (e.g. gills) to dissolved metals in water. The importance of trophic exposure routes can be higher for some organisms such as certain macroinvertebrates and crustaceans that are known to physically manipulate food particles, stripping nutritious organic matter from the outside surface of a particle, which would also contain the majority of metals if they were adhered to the particle.

As shown in Figure 9-1, there are numerous points at which an animal can regulate metals before they become problematic. Indeed, some metals are classed as 'essential metals' and are required by the animal for survival. Crustaceans, for example, have a circulatory system based on haemocyanin (instead of haemoglobin), a protein that is high in copper.

There are two potential mechanisms of concern with respect to the exposure of tuna to metals:

- i). Direct exposure to metals in the dissolved-phase, leading to bioaccumulation and/or toxicity;
- ii). Trophic pathway exposure to dissolved or particulate metals, leading to bioaccumulation and/or toxicity and/or biomagnification.

The metals of most concern for direct exposure and exposure through trophic pathways, possibly leading to *bioaccumulation*, are:

- Copper;
- Silver;
- Cadmium;
- Nickel (to a lesser extent).

Of these, copper and arsenic were reported to be liberated in relatively high concentrations in CSIRO elutriate tests. These metals are generally not commonly known to *biomagnify*. In other words, they may enter an organism through body integuments or through feeding and, once in the organism, these metals may produce acute toxic effects at high concentrations or, at lower concentrations, may be excreted or regulated. With continued low-level exposure, the metal may *bioaccumulate* inside the organism if the rate of uptake exceeds the ability for excretion. This bioaccumulation may lead to longer-term chronic (non-acute) effects, but there is a low likelihood *biomagnification* through the food chain for these metals.

The trophic pathway of most significance would probably relate to the exposure of vertically-migrating zooplankton or micronekton to metals through the discharge plume and the consumption of these organisms by tuna. While there remains the potential for some trophic interactions, the trophic linkages between tuna and organisms inhabiting the depths of the plume are likely to be weak. Tuna have been demonstrated to make deep foraging dive to approximately 1000 m and feed on vertically migrating organisms that migrate upwards from about 1000 m water depth. Thus the trophic exposure to depths greater than 1000 m is unlikely.

The metals of most potential concern for *biomagnification* are:

- Selenium;
- Mercury; and possibly
- Arsenic.

These metals are known to *biomagnify* through the food chain in some circumstances. These metals were not measured in the elutriate tests and so the risk of adverse impacts associated with these metals is unknown. However, the 'trapping' of the discharge plume below

approximately 1,300 m water depth (the bathypelagic zone), rapid dilution and the relatively low biomass occurring at these depths would suggest that the potential risk of *biomagnification* of these metals is low.

The overall outcome of the CSIRO jarosite modelling study (CSIRO 1994) was that, after some 19 years of surface-dumping, metals that were tracers for jarosite (mainly Zn and Cd) were not found to be bioaccumulating in marine organisms, including tuna. While there are key differences between the jarosite study and the scenario of deepwater discharge of dewatering material for the Solwara 1 study, this the finding suggests that, even for surface-dumping, the 'contact' between tuna and discharge was low. This contact is expected to be even lower in the case of Solwara 1.

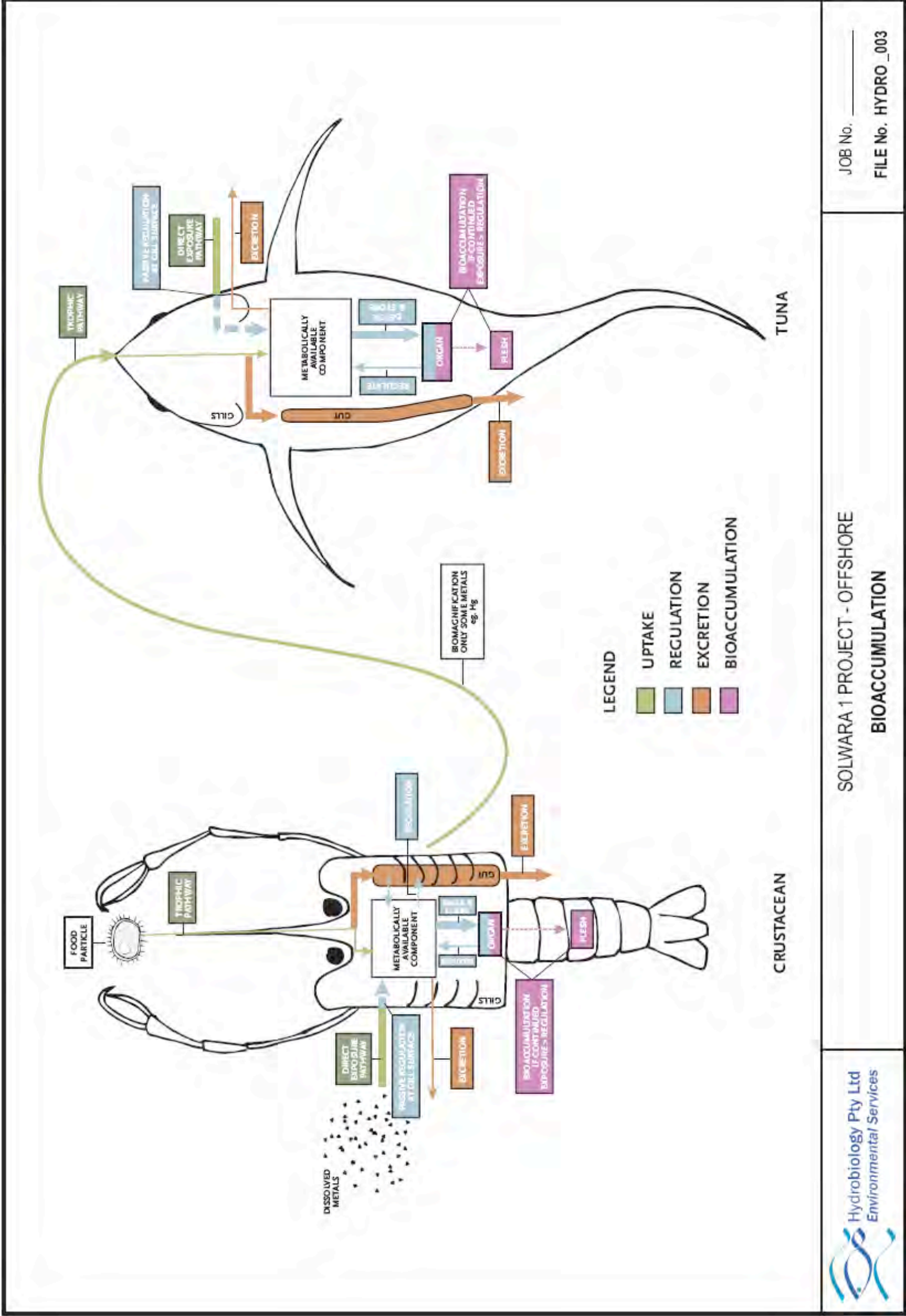


Figure 9-1 Schematic diagram of exposure pathways and regulation in the body of a primary consumer and higher-order consumer

9.3 Risk Assessment

This risk assessment has taken into consideration the findings of this report, results from in-situ water quality testing, results of physicochemical testwork undertaken by CSIRO (2007) and results of hydrodynamic modelling undertaken by APASA (2008). The water chemistry and testwork provided insights into the potential metals of concern and the concentrations likely to be liberated. The hydrodynamic modelling provided insights into movement and dilution of material liberated at the mining machine and disposed after dewatering.

In addition, a previous heavy metals trophic modelling study, related to the surface dumping of jarosite, carried out for southern bluefin tuna off Tasmania (CSIRO 1994) was reviewed and key findings of that study were considered in this risk assessment. Obviously, the environment, species, dumping method and material being dumped differ from the project under consideration here. However, the trophic modelling was useful in understanding factors such as the interaction between metals and various parts of the tuna food chain.

9.3.1 Summary of relevant in-situ water quality testing

Coffey Natural Systems undertook a water quality sampling program that aimed to sample bottom-waters during a test of a deep-sea mining cutter (Enesar 2006). A summary of the key water quality findings that are relevant to this risk assessment is as follows:

- Turbidity increased during cutting, but seemed to dilute or move away quickly. After a short period time after cutting, high turbidity was no longer measured.
- Total suspended solids concentration increased marginally during cutting. Again, high TSS did not persist, either diluting or moving away quickly after cutting.
- Dissolved Metals: Mean Zn concentrations during cutting were higher than pre-cutting. Possible contamination of sample by metal cutter machine identified.
- Total Metals: Mean Al, As, Cu, Fe, Pb and Zn were higher during cutting than pre-cutting. As, Pb and Zn concentrations fell away rapidly after cutting, while Al, Cu, and Fe concentrations remained elevated for longer.
- Ammonia concentration increased during cutting and remained elevated for a short time after cutting.

9.3.2 Summary of physicochemical testwork

This section summarises the findings of toxicological testwork carried out by CSIRO (2007) and elutriate testing by Parry (2008) that are relevant to this risk assessment.

- There was considerable variability in results depending on whether 'active' or 'inactive' sediments were sampled;

- Laboratory elutriate tests using chimney material recorded relatively high releases for As, Cu, Mn and Zn and relatively low releases for Ag, Cd, Ni and Pb;
- Se and Hg were not measured – these are the only metals that may exist at environmentally relevant concentrations in the discharges that could *biomagnify* in the receiving ecosystems;
- Based on elutriate tests alone, dilutions up to 4000 times may be required to meet ANZECC/ARMCANZ 99% ecosystem protection water quality trigger values;
- Total suspended solids concentration and re-suspension time had the greatest effects on dissolved metal concentration in elutriate waters, suggesting that the longer the sediments were suspended, the more likely they were to liberate metals;
- Toxicity tests performed on undiluted elutriate waters measured toxic effects to both algae and copepods;
- From the toxicity test results, it was estimated that dilutions of up to 700 times would be required to remove toxicity;
- Sampling next to the seafloor cutting/mining machine did not measure significantly elevated concentrations of metals or other contaminants from the simulating mining process compared with background, with the possible exception of Zn;
- Upon contact with oxygenated seawater (~6°C), elutriate tests showed that the ore, previously not exposed to oxygen, liberated Co, Cu, Cd, Mn, Pb and Zn.
- The concentrations of these metals were above ANZECC/ARMCANZ 99% ecosystem protection water quality trigger values. Dilutions of approximately 300-500 times were estimated to meet ANZECC/ARMCANZ 99% trigger values.

9.3.3 Summary of hydrodynamic modelling of discharge plume

This section summarises the findings of hydrodynamic modelling carried out by APASA (2008) that are relevant to this risk assessment.

- The returned water discharge will be a vertical, upward-pointing discharge placed some 25 m above the seafloor, at a depth of approximately 1,500 m;
- Modelling of the discharge plume has estimated that the plume thickness will be approximately 80 to 120 m thick, occupying a band from about 1,390 to 1,510 m water depth;
- The discharge plume was modelled to extend from 1.0 to 1.4 km from the discharge, in the horizontal plane, the direction of which is dictated by tidal flow;
- Modelling indicated that a 1:180 dilution of the discharge plume is reached within 50 m of the discharge, which represents the end of the 'jet' phase of the discharge.

- Modelling of the 1:300 and 1:5000 (10-times more dilutions than required to meet ANZECC/ARMCANZ 99% trigger values (CSIRO 2007)) dilution factors showed that these dilutions occur over an area of 0.004 km² and 6.78 km² respectively. These dilution areas were modelled to appear in 'patches' within the more diluted plume throughout the dispersal field, rather than as a consistent 'stream'.

9.4 Conclusions

With these findings in place, the risks identified in Table 9-1 can now be assessed (Table 9-2). The placement of the return water discharge at approximately 1,500 m water depth, an engineering solution that was devised part-way through this study, places the discharge below the depths believed to be directly inhabited by tuna, thus precluding the direct exposure of tuna to the return water discharge plume.

Obviously, the assumptions underpinning this assessment relate to the accuracy of the plume modelling and toxicological tests. The major assumption relating to the behaviour of any turbid plumes related to the removal and re-deposition of the unconsolidated sediment is that these plumes would behave in a similar fashion to the return water discharges, that is, plumes would be trapped at depth, have a limited horizontal and vertical dispersal and not rise into upper water layers.

A ranking of the confidence in the assessment is included in Table 9-2. It should be appreciated that, while there is a certain degree of confidence in the assessments made for the epipelagic and mesopelagic environment (particularly considering that the plume modelling has indicated that plumes will be trapped at depth), there are considerable uncertainties as to the tolerances and responses of fauna in the bathypelagic zone. It is generally accepted that fauna in this zone are generally widely distributed, the ability for organisms to tolerate poor water quality is unknown, as is the ability for organisms to sense and behaviourally avoid intolerable conditions (a behaviour that commonly holds true for mobile fauna). Bathypelagic species in particular, and deep sea demersal species to a lesser extent, are generally believed to have a very low metabolic rate, living on scarce nutrient inputs and thus do not have musculature or metabolic reserves to undergo significant swimming activities.

It is important to note that an active subsea volcano, known as North Su, is located a short distance from the Solwara 1 site (approximately 1 km to the northwest). The nature of discharge from the venting of the North Su subsea volcano is unknown, but it is reasonable to assume that it would be highly turbid and metal-enriched. The presence of this existing volcanic discharge suggests that organisms in the vicinity are tolerant of the discharge or, perhaps more likely, the discharge may be limiting the abundance of mobile bathypelagic organisms in the area as they may behaviourally avoid unfavourable conditions associated with the plume. It is assumed that the volcanic discharge from North Su would create a plume that is trapped at depth, in a similar fashion to that modelled for the return water discharge and so, the aforementioned tolerance or avoidance probably relates only to bathypelagic organisms. Mesopelagic and pelagic organisms in the area are not likely to be unaffected by the natural volcanic discharge. Further, there is active venting from the Solwara 1 site, also potentially limiting the distribution of mobile bathypelagic organisms.

Table 9-2 Risk assessment

Potential Risk	Pathway	Potential Consequence	Mitigating Factors	Predicted Risk
Adverse impact to endemic species or species of scientific interest	Direct Physical interaction of organisms with discharge of turbid/metal-enriched return water discharge.	High	Discharge trapped at depth in a narrow band. Water quality criteria met within a relatively small area. Low likelihood of endemic species in the bathypelagic environment.	Low
	Direct Physical interaction of organisms with machinery / noise from the mining activity.	High	Very low likelihood of endemic species in the epipelagic environment that could interact with surface facilities. Mobile fauna predicted to behaviourally avoid intolerable conditions. Small area of potential direct impact.	Very Low
	Direct Physical interaction of organisms with discharge of turbid/metal-enriched plume generated by the mining machine or re-location of unconsolidated sediment.	High	Plumes likely to be trapped at depth. Water quality criteria likely to be met within a relatively small area. Low likelihood of endemic species in the bathypelagic environment.	Low
	Indirect Effects on processes or trophic web.	High	Low likelihood of endemic species in epi-, meso- and bathypelagic. Minimal linkages between bathypelagic and upper layers.	Low

Risk	Pathway	Potential Consequence	Mitigating Factors	Predicted Risk
Exposure of epi-, mesopelagic organisms to metal-enriched waters/sediments	<p>Direct Interaction of (dissolved) metals with organism.</p>	Medium	<p>Discharge at 1,500 m. Plumes trapped at depth. Water quality criteria met within a relatively small area. Mobile organisms assumed to sense and avoid intolerable conditions. Any interactions likely to be short, interspersed with longer periods of non-exposure.</p>	Very Low
	<p>Indirect Interaction of (dissolved and particulate) metals with food sources.</p>	Low	<p>Discharge at 1,500 m. Plumes trapped at depth.</p>	Low
Exposure bathypelagic organisms to metal-enriched waters/sediments	<p>Direct Interaction of (dissolved) metals with organism.</p>	High	<p>Mobile organisms assumed to sense and avoid intolerable conditions. Existing volcanic venting from Solwara 1 and North Su potentially suppressing distribution and abundance of mobile bathypelagic organisms in the area. Any interactions likely to be short, interspersed with longer periods of non-exposure. Water quality criteria met within a relatively small area.</p>	Low
	<p>Indirect Interaction of (dissolved and particulate) metals with food sources.</p>	Medium	<p>Mobile organisms assumed to sense and avoid intolerable conditions. Volcanic venting from Solwara 1 and North Su potentially suppressing distribution and abundance of mobile bathypelagic organisms in the area.</p>	Low



<p>Potential risk of bioaccumulation and biomagnification in tunas and other predators, leading to a human health risk or perceived risk to fishery</p>	<p>Indirect Interaction of (dissolved and particulate) metals with food sources.</p>	<p>Very High</p>	<p>Discharge at 1,500 m. Plumes trapped at depth. Minimal interaction between these depths and epipelagic zone. Any interactions likely to be short, interspersed with longer periods of non-exposure. Water quality criteria met within a relatively small area.</p>	<p>Low</p>
---	---	------------------	---	------------

10 MANAGEMENT AND MONITORING

As described in Section 9, the major assumptions of the risk assessment are that the modelled physical and chemical behaviour of plumes and discharges will be realised in practice. Considering that these assumptions underpin the impact assessment for the epipelagic, mesopelagic and bathypelagic environment, it is recommended that these assumptions are tested and monitoring during the project inception phase and at suitable intervals throughout operation. Techniques involving water quality probes (moored in an array or mounted on project ROVs) could be employed to check the assumptions of the modelling.

As shown in Table 9-2, the risks are mostly assessed to be low. The direct and indirect risk to tuna is expected to be low. The depth of the discharge and the modeled extent of plumes is beyond the epipelagic and mesopelagic range of tuna and their trophic interactions. Additionally, in another major study of exposure of tuna to metals, even when tuna are potentially in contact with metals, there was found to be negligible effect (CSIRO 1994). While the risks to tuna fisheries are assessed to be low, there may be a residual perception among some stakeholders of some threat to tuna fisheries value, 'food quality' or risk of bioaccumulation and thus may deserve some management and monitoring effort.

A monitoring program could be established to monitor the risk of bioaccumulation and biomagnification in tuna. An opportunity exists to monitor bioaccumulation risk in tuna and prey organisms from commercial fishing vessels operating in the Bismark Sea, either by placing sampling personnel on board a vessel, by obtaining samples at a cannery (if there is sufficient reliability in catch location data or vessel position monitoring systems). An opportunity also exists to established linkages with the PNG National Fisheries Authority training college in Kavieng. Annual biomonitoring of metals concentration in tuna collected in the vicinity of the project is expected to be sufficient. For this to be of any value, baseline data would be required. Naturally, care would need to be taken to protect against the implication of the Solwara 1 project in potential background basin-wide bioaccumulation issues that are not related to the project.

11 REFERENCES

- Adam, M.S., Merrett, N.R., Anderson, R.C. (1998). An annotated checklist of the deep demersal fishes of the Maldivian Islands. *Ichthyological Bulletin*, 67:1-32.
- Allen, G.R. and Munday, P.L. (1994). Kimbe Bay rapid ecological assessment: the coral reefs of Kimbe Bay (West New Britain, Papua New Guinea), Volume 3: Fish diversity of Kimbe Bay. The Nature Conservancy, South Pacific program Office, Auckland, New Zealand. 107 p
- Allain, V. (2002). Food web study in the tuna ecosystem of the Western and Central Pacific Ocean. SCTB15 Working Paper, BBRD-7. 15th Meeting of the Standing Committee on Tuna and Billfish. Oceanic Fisheries Programme, Secretariat of the Pacific Community, Noumea, New Caledonia.
- Allain, V. (2005). Diet of four tuna species of the Western and Central Pacific Ocean. SPC Fisheries Newsletter #114 - July/September 2005.
- Aldredge, A.L. and Youngbluth, M.J. (1985). The significance of macroscopic aggregates (marine snow) as sites for heterotrophic bacterial production in the mesopelagic zone of the Subtropical Atlantic. *Deep-Sea Research*, 32 (12A): 1445-1456.
- APASA (2008). Modelling the dispersion of the returned water discharge plume from the Solwara 1 seafloor mining project, Manus Basin, Papua New Guinea. Report by Asia-Pacific ASA for Coffey Natural Systems.
- Bailey, D.M., Picheral, M., Jamieson, A.J., Gorsky, G., Gødo, O.R., Bagley, P.M. (in press). Distribution of bioluminescence and plankton in a deep Norwegian fjord measured using an ISIT camera and the Digital Underwater Video Profiler. *Journal of Marine Science*. Document accessed on the world wide web at http://www.obs-vlfr.fr/LOV/ZooPart/UVP/article.php3?id_article=18 (last accessed on 12 November 2007)
- Bertrand, A., Bard, F.-X. and Josse, E. (2002). Tuna food habits related to the micronekton distribution in French Polynesia. *Marine Biology* 140: 1023-1037.
- Beverly, S., Robinson, E. and Itano, D. (2004). Trial setting of deep longline techniques to reduce bycatch and increase targeting of deep-swimming tunas. 17th Meeting of the Standing Committee on Tuna and Billfish. SCTB 17 Working Paper FTWG -- WP-7a. Majuro, Marshall Islands. 9th - 18th August 2004.
- Billett, D.S.M., Lampitt, R.S., Rice, A.L. and Mantoura, R.F.C. (1983). Seasonal sedimentation of phytoplankton to the deep-sea benthos. *Nature*, (302), 520-522.
- Blanchot, J., Rodier, M. and Bouteiller, A. L. (1992). Effect of El Niño southern oscillation on the distribution and abundance of phytoplankton in the western Pacific tropical Ocean along 165°E. *Journal of Plankton Research*, 14: 137-156.
- Block, B.A., Dewar, H., Blackwell, S.B., Williams, T.D., Prince, E.D., Farwell, C.J., Boustany, A., Teo, S.L.H., Seitz, A., Walli, A., Fudge, D. (2001). Migratory Movements, Depth Preferences, and Thermal Biology of Atlantic Bluefin Tuna. *Science*, 293: 1310-1314.

Bowlby, M.R. and Case, J.F. (1991). Flash kinetics and spatial patterns of bioluminescence in the copepod *Gaussia princeps*. *Marine Biology*, 110, 329-336.

Bowlby, M.R., Widder, E.A. and Case, J.F. (1990). Patterns of Stimulated Bioluminescence in Two Pyrosomes (Tunicata: Pyrosomatidae). *Biological Bulletin* 179: 340-350.

Brewer, D., Cannard, T., Fry, G., Griffiths, S., Heales, D., Lansdell, M., Moeseneder, C., Richardson, A., Rothlisberg, P. and Smith, G. (2007). Field trip report: Assessment of mine waste disposal on the marine, benthic-pelagic communities at Lihir Island, Papua New Guinea. A report prepared by CSIRO Marine Research for Lihir Gold Limited.

Brewer, D., Flynn, A., Skewes, T., Alawo, J., Shelley, J., Pearson, B. and Corfield, J. (2008). Ecosystems of the East Marine Region. A report to the Department of Environment and Water Resources. CSIRO Marine Research.

Brill, R.W., Bigelow, K.A., Musyl, M.K., Fritsches, K.A., Warrant, E.J. (2005). Bigeye tuna (*Thunnus obesus*) behaviour and physiology and their relevance to stock assessments and fishery biology. *Collect. Vol. Sci. Pap. ICCAT*, 57(2): 142-161

Brinton, E. (1979). Parameters relating to the distribution of planktonic organisms, especially euphausiids in the eastern tropical Pacific. *Progress in Oceanography*, 8: 125-189.

Bulman, C.M. and Koslow, J. A. (1992). Diet and food consumption of a deep-sea fish, orange roughy *Hoplostethus atlanticus* (Pisces:Trachichthyidae), off southeastern Australia. *Marine Ecology Progress Series*, 19-115-129.

Burghart, S.E., Hopkins, T.L. and Torres, J.J. (2007). The bathypelagic Decapoda, Lophogastrida and Mysida of the eastern Gulf of Mexico. *Marine Biology*, 152: 315-327.

Campbell, A.K. and Herring, P.J. 1990 Imidazolopyrazine bioluminescence in copepods and other marine organisms. *Marine Biology*, 104, 219-225

Carey, F.G. and Olson, R.J. (1982). Sonic tracking experiments with tunas. *Collect. Vol. Sci. Pap. ICCAT* 17: 458-466.

Childress, J.J. (1995). Are there physiological and biochemical adaptations of metabolism in deep-sea animals? *Trends in Ecology and Evolution*, 10, 30-36.

Clarke, G.L. and Backus, R.H. (1956). Measurements of light penetration in relation to vertical migration and records of luminescence of deep-sea animals. *Deep-Sea Research*, 4, 1-14.

Clarke, G.L., and Hubbard, C.J. (1959). Quantitative Records of the Luminescent Flashing of Oceanic Animals at Great Depths. *Limnology and Oceanography*, 4(2), 163-180.

Clarke, G.L. and Wertheim, G.K. (1956). Measurements of illumination at great depths and at night in the Atlantic Ocean by means of a new bathyphotometer. *Deep-Sea Research*, 3, 189-205.

Cocker, J.E. (1978). Adaptations of deep sea fishes. *Environmental Biology of Fishes*, **3**(4), 389-399.

Cohen, D.M. (1964). Bioluminescence in the Gulf of Mexico Anacanthine Fish *Steindachneria argentea*. *Copeia*, 1964(2), 406-409.

Collin, S.P. and Partridge, J.C. (1996). Retinal specialisations in deep-sea teleosts. *Journal of Fish Biology* **49**(a): 157-174.

Connell, S.D. and Gillanders, B.M. (2007). *Marine Ecology*. Oxford University Press, Oxford, England.

CSIRO (1994). Research on jarosite dumping at sea: A program of research on jarosite dumping at sea by Pasminco Metals-EZ: Physical dispersal of jarosite and surveys of marine biota heavy metal levels 1991-1994. Volumes 1, 4 and 5. CSIRO Marine Research, Tasmania.

CSIRO (2007). Water and sediment characterisation and toxicity assessment for the Solwara 1 project. A report to Coffey Natural Systems for Nautilus Minerals Pty Ltd.

Dagorn, L., Bach, P. and Josse, E. (2000). Movement patterns of large bigeye tuna (*Thunnus obesus*) in the open ocean, determined using ultrasonic telemetry. *Marine Biology*, **136**(2): 361-371.

Dagorn, L., Holland, K.N., Hallier, J.-P., Taquet, M., Moreno, G., Sancho, G., Itano, D.G., Aumeeruddy, R., Girard, C., Million, J. and Fonteneau, A. (2006). Deep diving behaviour observed in yellowfin tuna (*Thunnus albacares*). *Aquatic Living Resources*, **19**: 85-88.

Dilling, L., Wilson, J., Steinberg, D. and Alldredge, A. (1998). Feeding by the Euphausiid, *Euphausia pacifica* and the Copepod *Calanus pacificus* on marine snow. *Marine Ecology Progress Series*, **170**, 189-201.

Eberhard, A., Burlingame, A.L., Eberhard, C., Kenyon, G.L., Nealson, K.H. and Oppenheimer, N.J. (1981). Structural Identification of Autoinducer of *Photobacterium fischeri* Luciferase. *Biochemistry*, **20**, 2444-2449.

Enesar (2006). Water quality monitoring report. Report by Enesar Consulting Pty Ltd for Nautilus Minerals Inc. CR 853_7_v3.

Fernández-Álamo, M.A. and Färber-Lorda, J. (2006). Zooplankton and the oceanography of the eastern tropical Pacific: A review. *Progress in Oceanography*, **69**: 318-359.

Frank, T.M. and Widder, E.A. (1997). The correlation of downwelling irradiance and staggered vertical migration patterns of zooplankton in Wilkinson Basin, Gulf of Maine. *Journal of Plankton Research*, **19**, 1975-1991.

Frank, T.M., Widder, E.A., Latz, M.I., and Case, J.F. (1984). Dietary maintenance of bioluminescence in a deep-sea mysid. *Journal of Experimental Biology*, **109**, 385-389.

Fritsches, K. and Warrant, E. (2001). New Discoveries in Visual Performance of Pelagic Fishes. Pelagic Fisheries Research Program, pp. 1-16.

Froese, R. and Pauly D., (eds) (2007). FishBase. World Wide Web electronic publication. www.fishbase.org, version (last accessed in October 2007).

Gage, J.D. and Tyler, P.A. (1991). Deep-Sea Biology: A Natural History of Organisms at the Deep-Sea Floor. Cambridge University Press, Cambridge, England.

Greene, C.H., Wiebe, P.H. and Burczynski, J. (1989). Analyzing Zooplankton Size Distributions Using High-Frequency Sound. *Limnology and Oceanography*, 34(1), 129-139.

Hampton, J., Bigelow, K. and Labell, M. (1998). A summary of current information on the biology, fisheries and stock assessment of bigeye tuna (*Thunnus obesus*) in the Pacific Ocean, with recommendations for data requirements and future research. Oceanic Fisheries Programme, Technical Report No. 36. Secretariat of the Pacific Community, New Caledonia.

Hampton, J., Langley, A. and Kleiber, P. (2006). Stock assessment of bigeye tuna in the western and central Pacific Ocean, including an assessment of management options. Second meeting of the WCPFC-Scientific Committee, 7th -18th August 2006, Manila, Philippines. WCPFC-SC2-2006/SA WP-2.

Hastings, J.W. and Nealson, K.H. (1977). Bacterial bioluminescence. *Annual Reviews of Microbiology*, 31: 549-595.

Haygood, M.G. and Distel, D.L. (1993). Bioluminescent symbionts of flashlight fishes and deep-sea anglerfishes form unique lineages related to the genus *Vibrio*. *Nature*, 363, 154-156.

Herring, P.J. (1982). Aspects of the bioluminescence of fishes. *Oceanography and Marine Biology, Annual Review*, 20: 415-470.

Herring, P.J. (1985). Bioluminescence in Crustacea. *Journal of Experimental Biology*, 5(4), 557-573.

Herring, P.J. (2002). *The Biology of the Deep Ocean*. Oxford University Press, Oxford, England.

Herring, P.J. (2007) Sex with the lights on? A review of bioluminescent sexual dimorphism in the sea (review article). *Journal of the Marine Biological Association of the United Kingdom*, 87(4), 829-842.

Herring, P.J. and Cope, C. (2005). Red bioluminescence in fishes: on the suborbital photophores of *Malacosteus*, *Pachystomias* and *Aristostomias*. *Marine Biology*, 148, 383-394.

Herring, P.J., & Widder, E.A. (2004). Bioluminescence of deep-sea coronate medusae (Cnidaria: Scyphozoa). *Marine Biology*, 146, 39-51.

Kubodera, T., Koyama, Y., and Mori, K. (2007). Observations of wild hunting behaviour and bioluminescent of a deep-sea eight-armed squid, *Taningia danae*. Proceedings of the Royal Society, Series B, 274, 1029-1034.

Kumoru, L. (2003). The Shark Longline Fishery in Papua New Guinea. Papua New Guinea National Fisheries Authority, Port Moresby, Papua New Guinea. A paper prepared for the Billfish and By-catch Research Group, at the 176th Meeting of the Standing Committee on Tuna and Billfish, Mooloolaba, Australia, 9th - 16th July 2003.

Kumoru, L. and Koren, L. (2007). Tuna Fisheries Report - Papua New Guinea. Report prepared by the Papua New Guinea National Fisheries Authority for the 3rd Science Committee Meeting of the Western and Central Pacific Fisheries Commission, Honolulu, Hawaii, 2007. Annual Report, Part 1. WCPFC-SC3_AR Part 1/WP-23.

Lampitt, R.S. (1996). Snow falls in the open ocean. In *Oceanography: an illustrated guide* (eds Summerhayes, C.P. and Thorpe, S.A.), pp 96-112. Manson Publishing, London, England.

Land, M.F. and Nilsson, D.-E. (2001). *Animal Eyes*. Oxford University Press, Oxford, England.

Lansdell, M. and Young, J. (2007). Pelagic cephalopods from eastern Australia: species composition, horizontal and vertical distribution determined from the diets of pelagic fishes. *Reviews in Fish Biology and Fisheries*, 17: 125-138.

Lenz, J. (1992). Microbial loop, microbial food web and classical food chains: their significance in pelagic marine ecosystems. *Archiv fur Hydrobiologie*, (37), 265-278.

Li, W.K.W., Subba Rao, D.V., Harrison, W.G., Smith, J.C., Cullen, J.J., Irwin, B. and Platt, T. (1983). Autotrophic Picoplankton in the Tropical Ocean. *Science*, 219, 4582, 292-295.

Lyne, V. and Hayes, D. (2005). Pelagic regionalisation: National marine bioregionalisation integration project. A report to the National Oceans Office. Department of Environment and Heritage and CSIRO Marine Research, Australia, 2005.

Mackie, G.O. and Bone, Q. (1978). Luminescence and associated effector activity in *Pyrosoma* (Tunicata: Pyrosomida) Proceedings of the Royal Society of London Series B, 202, 483-495.

Marshall, N.B. (1979). *Developments in Deep-Sea Biology*. Blandford, Poole, England.

Marshall, N.B. and Cohen, D.M. (1973). Order Anacanthini (Gadiformes). Characters and syniopsis of Families. *Memoirs of the Sears Foundation for Marine research*, I (6):479-495.

Mauchline, J., Gordon, J.D.M. (1991). Oceanic pelagic prey of benthopelagic fish in the benthic boundary layer of a marginal oceanic region. *Marine Ecology Progress Series*, 74: 109-115.

McFall-Ngai, M.J. (1994). Animal-bacteria interactions in the early life history of marine invertebrates: the *Euprymna scolopes* / *Vibrio fischeri* symbiosis. *American Zoologist*, 34, 554-561.

- Messinger, A.F. and Case, J.F. (1991). Bioluminescence Maintenance in Juvenile *Porichthys notatus*. *Biological Bulletin*, 181, 181-188.
- Morin, J.G. (1974). Coelenterate bioluminescence. In *Coelenterate biology: reviews and new perspectives*. (eds Muscatine, L. and Lenhoff, H.M.) pp. 397-438. Academic Press, New York, USA.
- Nealson, K.H. (1977). Autoinduction of bacterial luciferase: occurrence, mechanism and significance. *Archives of Microbiology*, 112: 73-79.
- Nealson, K., Cohn, D., Leisman, G., and Tebo, B. (1981). Co-evolution of luminous bacteria and their eukaryotic hosts. *Annals of the New York Academy of Sciences*, 361, 76-91.
- Nishiguchi, M. K. (2000). Temperature Affects Species Distribution in Symbiotic Populations of *Vibrio* spp. *Applied and Environmental Microbiology*, 66(8), 3550-3555.
- Nybakken, J.W. and Bertness, M.G. (2005). *Marine Biology: an ecological approach*. (6th edn). Addison-Wesley, Boston, Massachusetts, USA.
- Parry, D.L. (2008). Elutriate testing, Solwara 1 Project. Phase 1 Report: Effect of holding time. Report prepared by Tropical Futures: Mineral Program, Charles Darwin University for Coffey Natural Systems Pty Ltd.
- Partensky, F., Blanchot, J. and Vaultot, D. (1999). Differential distribution and ecology of *Prochlorococcus* and *Synechococcus* in oceanic waters: A review. In *Marine Cyanobacteria*. (eds Charpy, L. and Larkum, A.W.D.). *Bulletin de l'Institut Oceanographique*. NS19, 457-475.
- Platt, T., Subba Rao, T.V. and Irwin, B. (1983). Photosynthesis of picoplankton in the oligotrophic ocean. *Nature*, 300, 702-704.
- Ploug, H., Azam, F. and Jorgensen, B.B. (1999). Photosynthesis, respiration, and carbon turnover in sinking marine snow from surface waters of Southern California Bight: Implications for the carbon cycle in the ocean. *Marine Ecology Progress Series*, 179, 1-11.
- Polovina, J.J., Kobayashi, D.R., Parker, D.M., Seki, M.P. and Balazs, G.H. (2000). Turtles on the edge: Movement of loggerhead turtles (*Caretta caretta*) along oceanic fronts spanning logline fishing grounds in the central North Pacific, 1997-1998. *Fisheries Oceanography*, 9, 71-82.
- Polunin, N.V.C., Morales-Nin, B., Pawsey, W.E., Cartes, J.E., Pinnegar, J.K., Moranta, J. (2001). Feeding relationships in Mediterranean bathyal assemblages elucidated by carbon and nitrogen stable-isotope data. *Marine Ecology Progress Series*, 220, 13-23.
- Priede, I. G., Bagley, P. M., Way, S., Herring, P. J., & Partridge, J. C. (2006). Bioluminescence in the deep-sea: Free-fall lander observations in the Atlantic Ocean off Cape Verde. *Deep-Sea Research Part 1*, 53, 1272-1283.

- Radchenko, V.I (2007). Mesopelagic Fish Community Supplies 'Biological Pump'. The Raffles Bulletin of Zoology (14): 265-271
- Raven, J.A. (1998). Small is beautiful: the picophytoplankton. *Functional Ecology*, (12), 503-513.
- Reichelt, J.L., and Baumann, P. (1973). Taxonomy of the Marine, Luminous Bacteria. *Archives of Microbiology*, 94, 283-330.
- Reichelt, J.L., and Neelson, K. (1977). The Specificity of Symbiosis: Pony Fish and Luminescent Bacteria. *Archives of Microbiology*, 112, 157-161.
- Saltzman, J. and Wishner, K.F. (1997a). Zooplankton ecology in the eastern tropical Pacific oxygen minimum zone above a seamount: 1. General trends. *Deep-Sea Research, I* (44): 907-930.
- Saltzman, J. and Wishner, K.F. (1997b). Zooplankton ecology in the eastern tropical Pacific oxygen minimum zone above a seamount: 1. Vertical distribution of copepods. *Deep-Sea Research, I* (44): 931-954.
- Salvanes, G. V. and Kristofersen, J. B. (2001). Mesopelagic Fishes. *Encyclopedia of Ocean Sciences* 3, pp. 1711-1717
- Schmidt-Nielsen, K. (1995). *Animal physiology, adaptation and environment* (5th edn). Cambridge University Press, Cambridge.
- Sibert, J., Hampton, J., Kleiber, P. and Maunder, M. (2006). Biomass, size, and trophic status of top predators in the Pacific Ocean. *Science*, 314: 1772-1776.
- SPC (1988). Papua New Guinea Country Report No. 1. Tuna and billfish assessment programme. South Pacific Commission, Noumea, New Caledonia.
- Thomson, C.M., Herring, P.J. and Campbell, A.K. (1997). The Widespread Occurrence and Tissue Distribution of the Imidazolopyrazine Luciferins. *Journal of Bioluminescence and Chemiluminescence*, 12, 87-91.
- Turner, J.T. (2002). Zooplankton fecal pellets, marine snow and sinking phytoplankton blooms. *Aquatic Microbial Ecology*, 27, 57-102.
- Vinogradov, M.E., Shushkina, E.A., Gorbunov, A.Y., Shashkov, N.L. (1991). Vertical distribution of the macro- and mesoplankton in the region of the Cost Rica Dome. *Oceanology*, 31: 559-565.
- Warrant, E. J. and Locket, N. A. (2004). Vision in the deep sea. *Biological Reviews*, 79, 671-712.
- Widder, E.A. and Johnsen, S. (2000). 3D spatial point patterns of bioluminescent plankton: a map of the minefield. *Journal of Plankton research*, 22:409-420.

Widder, E.A. and Frank, T.M. (2001). The speed of an isolume: a shrimp's eye view. 138, 669-677.

Widder, E.A., Greene, C.H. and Youngbluth, M.J. (1992). Bioluminescence of sound-scattering layers in the Gulf of Maine. *Journal of Plankton Research*, 14: 1607-1624.

Widder, E.A., Johnsen, S., Bernstein, S.A., Case, J.F. and Neilson, D.J. (1999). Thin layers of bioluminescent copepods found at density discontinuities in the water column. *Marine Biology*, 134, 429-437.

Wishner, K.E. (1980). Aspects of the community ecology of deep-sea, benthopelagic plankton, with special attention to gymnopleid copepods. *Marine Biology*, 60, 179-187.

Young, J.W., Bradford, R., Lamb, T.D., Clementson, L.A., Kloser, R. and Galea, H. (2001). Yellowfin tuna (*Thunnus albacares*) aggregations along the shelf break off south-eastern Australia: links between inshore and offshore processes. *Marine and Freshwater Research*, 52: 463-474.

Young, J. and Hobday, A. (2004). Pelagic habitat and community comparisons in the fishing grounds of the tuna and billfish fishery off eastern Australia. CSIRO Marine Research, Cruise Report SS09/2004.

Young, R.E. and Mencher, F.M. (1980). Bioluminescence in mesopelagic squid: diel color change during counterillumination. *Science*, 191, 1286-1288.



ATTACHMENT 1

**Some of the epipelagic, mesopelagic and bathypelagic animals
likely to occur in the Solwara 1 project area**

* Identified at Lihir Island

** Identified Maldives deep-sea research (Adam et al. 1998).

*** Identified in Solwara 1 ROV footage

Scientific Name	Common Name	Zone	Depth Range
Rhincodontidae			
Rhincodon			
typus	whale shark	Epipelagic	0-700
Carcharhinidae			
Carcharhinus			
albimarginatus	Silvertip shark	Epipelagic	0-800
amblyrhynchos	Grey Reef Shark	Epipelagic	0-280
falciformis	Silky Shark	Epi/Mesopelagic	0-600
longimanus	Oceanic Whitetip Shark	Epipelagic	0-150
Galeocerdo			
cuvier	Tiger Shark	Epipelagic	0-350
Hemigaleidae			
Triaenodon			
obesus	Whitetip Reef Shark	Epipelagic	0-330
Sphyrna			
lewini	Scalloped Hammerhead	Epipelagic	0-512
mokarran	Great hammerhead shark	Epipelagic	0-300
Scombridae			
Acanthocybium			
solandri	Wahoo	Epipelagic	0-12
Auxis			
thazard	Frigate Tuna	Epipelagic	0-50
Euthynnus			
affinis	Mackerel tuna	Epipelagic	0-200
Grammatorcynus			
bilineatus	Double-lined Mackerel	Epipelagic	15-???
Gymnosarda			
unicolor	Dogtooth tuna	Epipelagic	10-100
Katsuwonus			
pelamis	Skipjack tuna	Epipelagic	0-260
Rastrelliger			
kanagurta	Indian mackerel	Epipelagic	20-90



Scomber			
australasicus	Blue mackerel	Epipelagic	87-200
Scomberomorus			
commerson	Narrow-barred Spanish mackerel	Epipelagic	10-70
queenslandicus	Queensland school mackerel	Epipelagic	0-100
Thunnus			
albacares	Yellowfin tuna	Epi/Mesopelagic	0-250
alalunga	Albacore tuna	Epi/Mesopelagic	0-500
obesus	Bigeye tuna	Epi/Mesopelagic	0->500
Sphyraenidae			
Sphyraena			
barracuda	Great barracuda	Epipelagic	0-100
flavicauda	Yellowtail barracuda	Epipelagic	2-25
forsteri	Bigeye barracuda	Epipelagic	6-300
jello	Pickhandle barracuda	Epipelagic	20-200
qenie	Backfin barracuda	Epipelagic	???
Mugilidae			
Mugil			
cephalus	Flathead mullet	Epipelagic	0-120
Balistidae			
Canthidermis			
maculatus	Oceanic triggerfish	Epipelagic	0-50
Kyphosidae			
Kyphosus			
cinerascens	Drummer	Epipelagic	0-100
Carangidae			
Carangoides			
fulvoguttatus	Turrum	Epipelagic	0-100
orthogrammus	Island trevally	Epipelagic	0-168
plagiotaenia	Barcheck trevally	Epipelagic	0-200
Caranx			
ignobilis	Giant trevally	Epipelagic	0-100
melampyus	Bluefin trevally	Epipelagic	0-120
papuensis	Brassy trevally	Epipelagic	0-120
sexfasciatus	Bigeye trevally	Epipelagic	0-146
tille	Tille trevally	Epipelagic	30-120
Decapterus			
macarellus	Mackerel scad	Epipelagic	0-200
macrosoma	Shortfin scad	Epipelagic	20-170



Elagatis			
bipinnulata	Rainbow runner	Epipelagic	0-150
Gnathanodon			
speciosus	Golden trevally	Epipelagic	0-100
Selar			
boops	Oxeye scad	Epi/Mesopelagic	35-500
crumenophthalmus	Bigeye scad	Epipelagic	0-170
Seriola			
rivoliana	Almaco jack	Epipelagic	5-160
Coryphaenidae			
Coryphaena			
hippurus	Common dolphinfish	Epipelagic	0-85
Lutjanidae		Epipelagic	
Aprion			
virescens	Green jobfish	Epipelagic	0-180
Lutjanus			
argentimaculatus	Mangrove red snapper	Epipelagic	10-120
bohar		Epipelagic	
kasmira	Common bluestripe snapper	Epipelagic	3-265
rivulatus	Blubberlip snapper	Epipelagic	50-100
sebae	Emperor red snapper	Epipelagic	5-180
Macolor			
macularis	Midnight snapper	Epipelagic	3-90
niger	Black and white snapper	Epipelagic	2-90
Paracaesio			
kusakarii	Saddle-back snapper	Epipelagic	100-310
Pristipomoides			
typus	Sharptooth jobfish	Epipelagic	40-120
zonatus	Oblique-banded snapper	Epipelagic	70-300
Gonostomatidae***			
Cyclothone			
acclinidens	Benttooth bristlemouth	Mesopelagic	50-1900
alba	Bristlemouth	Mesopelagic	25-4938
braueri	Garrick	Mesopelagic	10-2000
microdon	Veiled anglemouth	Meso/Bathypelagic	200-5300
pallida	Tan bristlemouth	Meso/Bathypelagic	16-4663



pseudopallida	Slender bristlemouth	Meso/Bathypelagic	33-4938
Diplophos			
taenia	Pacific portholefish	Mesopelagic	0-800
Gonostoma			
atlanticum	Atlantic fangjaw	Mesopelagic	0-800
bathyphilum	Spark anglemouth	Mesopelagic	700-3000
elongatum	Elongated bristlemouth	Mesopelagic	25-3385
Ichthyococcus			
ovatus	Lightfish	Mesopelagic	0-2000
Polymetme			
corythaeola**		Mesopelagic	165-800
Valenciennellus			
tripunctulatus	Constellation fish	Mesopelagic	100-700
Vinciguerria			
nimbaria	Oceanic lightfish	Meso/Bathypelagic	20-5000
Myctophidae			
Benthoosema			
suborbitale	Smallfin lanternfish	Mesopelagic	50-2500
Bolinichthys			
indicus	Lanternfish	Mesopelagic	25-900
supralateralis	???	Mesopelagic	40-850
Centrobranchus			
andreae	Andre's lanternfish	Mesopelagic	???
nigroocellatus	Roundnose lanternfish	Mesopelagic	0-700
Ceratoscopelus			
townsendi	Dogtooth lampfish	Mesopelagic	0-1500



Diaphus			
effulgens	Headlight fish	Mesopelagic	40-700
elucens	Transparent lantern fish	Mesopelagic	0-1500
fragilis	Fragile lantern fish	Mesopelagic	15-1313
garmani	???	Meso/Bathypelagic	0-2091
lucidus	???	Mesopelagic	40-750
luetkeni	???	Mesopelagic	40-750
metopoclampus	Spothead lantern fish	Mesopelagic	90-1085
mollis	???	Mesopelagic	50-600
problematicus	???	Mesopelagic	40-820
rafinesquei	White-spotted lantern fish	Mesopelagic	40-1080
splendidus	???	Meso/Bathypelagic	40-3872
termophilus	Taaning's lantern fish	Mesopelagic	40-850
Diogenichthys			
atlanticus	Longfin lanternfish	Mesopelagic	18-1050
laternatus	Diogenes lanternfish	Meso/Bathypelagic	0-2091
Electrona			
rissoi	Chubby flashlightfish	Mesopelagic	90-820
Gonichthys			
cocoi	???	Mesopelagic	0-1000
Hygophum			
reinhardtii	Reinhardt's lantern fish	Mesopelagic	0-1050
Lampadena			
luminosa	???	Mesopelagic	50-850
speculigera	Mirror lanternfish	Mesopelagic	60-950
uophaos			
Lampanyctus			
alatus	???	Mesopelagic	40-1500
festivus	???	Mesopelagic	40-1000
nobilis	Noble lampfish	Mesopelagic	100-1000
Myctophum			
asperum	Prickly lanternfish	Mesopelagic	0-750
aurolaternatum	Golden lanternfish	Mesopelagic	???
nitidulum	Pearly lanternfish	Mesopelagic	0-950
selenops	Wisner's lantern fish	Mesopelagic	40-500
spinosum	Spiny lantern fish	Mesopelagic	???



Notolychnus			
valdiviae	Topside lampfish	Mesopelagic	25-700
Symbolophorus			
evermanni	Evermann's lantern fish	Mesopelagic	0-???
Taaningichthys			
bathophilus	???	Mesopelagic	400-1550
Macrouridae***		Bathypelagic	At least 1600
Setarchidae			
Ectreposebastes imus*	Deepsea scorpionfish	Meso/Bathypelagic	150-2000
Stomiidae	Barbled dragonfishes	Meso/Bathypelagic	To at least 3000
Melanocetidae	Anglerfishes	Bathypelagic	To at least 6000
Oneirodidae	Anglerfishes	Bathypelagic	To at least 1000
Ceratiidae	Anglerfishes	Bathypelagic	To at least 1000
Searsiidae	Tubeshoulders	Bathypelagic	To at least 1000
Alepocephalidae	Slickheads	Bathypelagic	To at least 1000
Melamphaeidae	Bigscales	Bathypelagic	To at least 1000
Anguilliforms	Snipe eels, gulper eels, cutthroat	Bathypelagic	To at least 1000
Halosauridae			
Aldrovandia			
affinis **	Halosaur	Meso/Bathypelagic	730-2560
phalacra **	Halosaur	Meso/Bathypelagic	500-2300
Halosaurus			
carinicauda **	Halosaur	Meso/Bathypelagic	835-1609
Ipnopidae			
Bathypterois			
guentheri**	Tripodfish	Bathypelagic	800-1300
atricolor**	Tripodfish	Bathypelagic	800-1300
Neoscopelidae			
Neoscopelus			
microchir **	Black chin	Mesopelagic	250-700
Sternoptychidae			
Argyropelecus			
aculeatus	Lovely hatchetfish	Mesopelagic	100-600
affinis	Pacific hatchet fish	Mesopelagic	1-3872
gigas	Hatchetfish	Mesopelagic	300-650
hemigymnus	Half-naked hatchetfish	Mesopelagic	0-1500
sladeni	Sladen's hatchet fish	Mesopelagic	0-2926
Danaphos			



oculatus	Bottlelights	Mesopelagic	183-914
Sternoptyx			
diaphana	Diaphanous hatchet fish	Mesopelagic	400-3676
pseudobscura	Highlight hatchetfish	Mesopelagic	760-1500



ATTACHMENT 2

List of cetaceans and turtles likely to occur in the Solwara 1 project area



Cetaceans

Common Name	Scientific Name	Notes
Pygmy sperm whale	<i>Kogia breviceps</i>	LR/lc
Dwarf sperm whale	<i>Kogia sima</i>	LR/lc
Blainville's beaked whale	<i>Mesoplodon densirostris</i>	DD
Ginkgo-toothed whale	<i>Mesoplodon ginkgodens</i>	DD
Rough-toothed dolphin	<i>Steno bredanensis</i>	DD
Indo-Pacific hump-backed dolphin	<i>Sousa chinensis</i>	DD
Spotted dolphin	<i>Stenella attenuate</i>	LR/cd
Spinner dolphin	<i>Stenella longirostris</i>	LR/cd
Fraser's dolphin	<i>Lagenodelphis hosei</i>	DD
Risso's dolphin	<i>Grampus griseus</i>	DD
Melon-headed whale	<i>Peponocephala electra</i>	LR/lc
Pygmy killer whale	<i>Feresa attenuata</i>	DD
Killer whale	<i>Orcinus orca</i>	LR/cd
False killer whale	<i>Pseudorca crassidens</i>	LR/lc
Bottlenose dolphin	<i>Tursiops truncatus</i>	DD
Indo-Pacific bottlenose dolphin	<i>Tursiops aduncus</i>	
Densebeak whale	<i>Mesoplodon desirostris</i>	DD Tentative ID by Vissner (2003)
Shortfinned pilot whale	<i>Globicephala macrorhynchus</i>	LR/cd Specialised squid predator
Sperm whale	<i>Physeter macrocephalus</i>	VU A1bd
Minke whale	<i>Balaenoptera acutorostrata</i>	LR/nt
Humpback whale	<i>Megaptera novaeangliae</i>	VUA1ad

Turtles

Common Name	Scientific Name	Notes
Loggerhead turtle	<i>Caretta caretta</i>	EN A1abd (out of date, 1994)
Green turtle	<i>Chelonia mydas</i>	EN A2bd
Leatherback turtle	<i>Dermochelys coriacea</i>	CR A1abd
Hawksbill turtle	<i>Erytmochelys imbricata</i>	CR A1bd (out of date, 1996)
Olive ridley	<i>Lepidochelys olivacea</i>	EN A1bd (out of date, 1996)
Flatback turtle	<i>Natador depressus</i>	DD (out of date, 1996)

References

Hitipeuw, C., Dutton, P.H., Benson, S., Thebu, J., Bakarbessy, J. (2007) Population Status and Interesting Movement of Leatherback Turtles, *Dermochelys coriacea*, Nesting on the Northwest Coast of Papua, Indonesia. *Chelonian Conservation and Biology*, 6(1):28-36.

Miller, J.D., Dobbs, K.A., Limpus, C.J., Mattocks, N., Landry, A.M. (1998) Long-distance migrations by the hawksbill turtle, *Eretmochelys imbricata*, from north-eastern Australia. *Wildlife Research*, 25(1):89-95.

Kwan, D. (date unknown). The Artisanal Sea Turtle Fishery in Daru, Papua New Guinea. Torres Strait Baseline Conference Study: Biological Environment. Townsville, James Cook University.

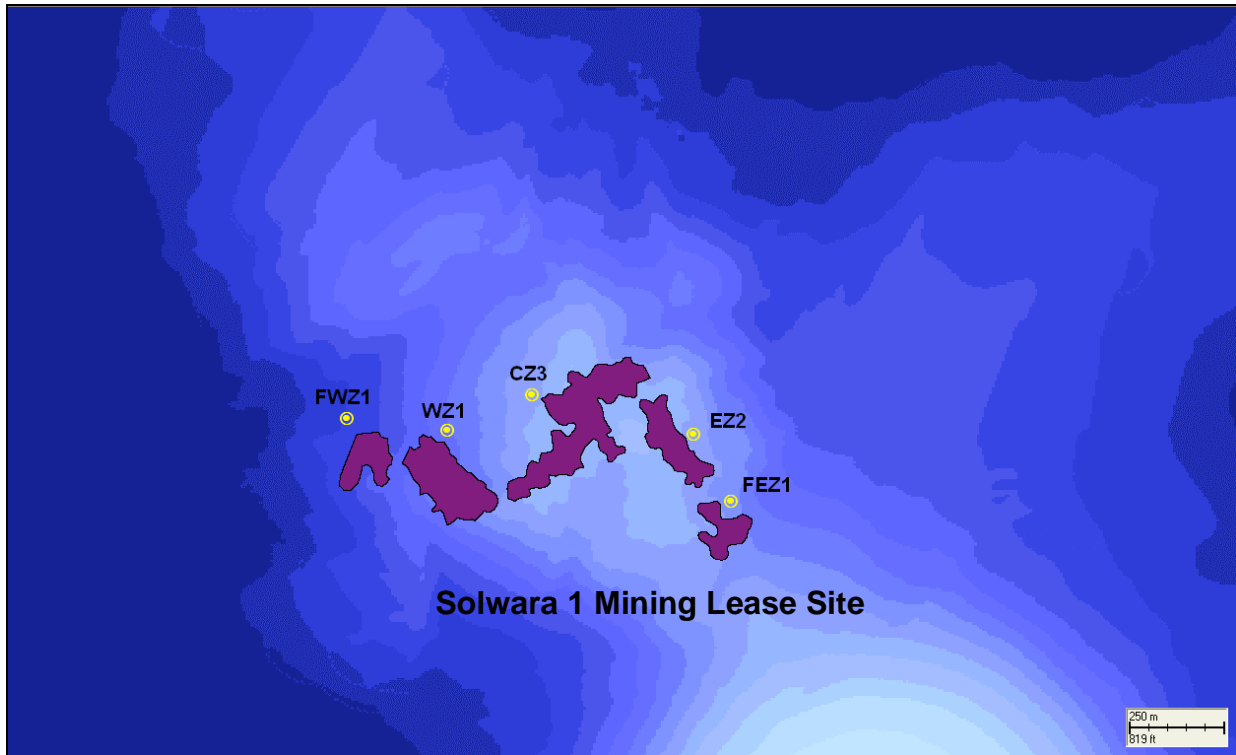
IOSEA (2007). Indian Ocean South East Asian Marine Turtle Memorandum of Understanding Fact Sheet. Document posted on the worldwide web at <http://www.ioseaturtles.org>, accessed 5 November 2007.

Spring, C.S. (1982). Status of marine turtle populations in Papua New Guinea. In: Bjorndal, K. A., (ed.), *Biology and Conservation of Sea Turtles*. Page(s) 281-289. Washington D. C., Smithsonian Institute Press.

Appendix 11

Modelling the Dispersion and Settlement of Sediment Removal Operation Prior to Mining at the Solwara 1 Mining Lease, Papua New Guinea

MODELLING THE DISPERSION AND SETTLEMENT OF THE SEDIMENT REMOVAL OPERATION PRIOR TO MINING AT THE SOLWARA 1 MINING LEASE, PAPUA NEW GUINEA



Prepared for: Coffey Natural Systems

August 2008

Prepared by:



Gold Coast: Suite 3A, Lvl 1, 142 Bundall Rd
Bundall, Qld 4217 Ph: +61 7 5574 1112
Perth: Unit 2B, Shafto Lane, 872 Hay St
Perth WA 6000 Ph: +61 8 9226 2911
ABN 79 097 553 734

Document control form

Document draft	Originated by	Edit & review	Authorised for release by	Date
Draft 1 for internal review	Nathan Benfer	Dr Brian King	Dr Brian King	28/08/2008
Draft for client review		Dr Brian King	Dr Brian King	29/08/2008
Final Report	Nathan Benfer	Dr Brian King	Dr Brian King	31/08/2008

APASA Project Manager: Dr Brian King
 Document Title: Solwara Pre-Mining Operations (Final).doc
 APASA Project Number: S008

DISCLAIMER: This document contains confidential information that is intended only for use by the client and is not for public circulation or publication or for the use of any third party without the approval of Asia-Pacific ASA Pty Ltd (ABN 79 097 553 734) trading as Asia-Pacific Applied Science Associates.

While this report is based on source information Asia-Pacific ASA Pty Ltd considers reliable, its accuracy and completeness cannot be guaranteed. Therefore, Asia-Pacific ASA Pty Ltd and its directors and employees accept no liability for the result of any action taken or not taken on the basis of information in this report, or for any negligent misstatements, errors, or omissions. This report is compiled with consideration for the specified client's objectives, situation, or needs. Those acting upon such information without first consulting Asia-Pacific ASA Pty Ltd do so entirely at their own risk. We strongly recommend that any person who wishes to act upon this report first consult an Asia-Pacific ASA Pty Ltd advisor.

TABLE OF CONTENTS

1	EXECUTIVE SUMMARY	3
2	MODELLING METHODOLOGY AND DATA	4
2.1	Current Data.....	4
2.2	Bathymetry	5
2.3	The SSFATE Model	6
2.4	Sediment Data	6
2.5	Tip Head Placement Operation	8
3	RESULTS AND DISCUSSION.....	10
4	REFERENCES	18

1 EXECUTIVE SUMMARY

This report quantifies the dispersion and settlement patterns associated with the placement of sediment during the pre-mining removal operations on the seafloor at the Solwara 1 mining lease in the Manus Basin, Papua New Guinea. The Solwara 1 prospect is located at 1,500-1,700 m water depth approximately 50 km north of Rabaul in the eastern extent of the Manus Basin, Bismarck Sea.

The modelling system known as SSFATE (**S**uspended **S**ediment **F**ATE) from Applied Science Associates (ASA) was used to quantify the sediment load on the seafloor resulting from the full pre-mining surface sediment removal and placement operation. The SSFATE system required input data such as the current meter data, sediment size distribution data and the complete schedule of the operation and discharge as well as the discharge quantities for 5 discharge sites. Using this data, the SSFATE system simulated the ROV removal of unconsolidated sediments and the Seafloor Mining Tool (SMT) removal of hard rock competent waste prior to mining.

Due to the fast falling velocity of the coarse sands/gravel, SSFATE calculated that this material would be concentrated at the Tip Head Sites; thus only clays, silts and fine sands were capable of travelling beyond the 5 discharge tip head sites under the weak current conditions at these depths. Indeed, a small proportion of these clays, silts and fine sands were predicted to settle back onto the mining site (< 376mm), due to the ambient currents and vertical turbulence.

The SSFATE simulation of this operation quantified the depositional thicknesses of the discharge from the ROV and SMT excavated pre-mining material surrounding the Solwara 1 mining lease site after this operation is completed in full. Bottom thicknesses, quantified by the simulations, varied from 0.18 mm to small areas adjacent to the tip heads site slightly exceeding 500 mm or 0.5m.

The furthest extent of influence from the tip head discharge sites was less than 1 km (972m) from the nearest tip head sites, where depositional thickness was limited to 0.18 mm. The complete coverage from sediment settlement exceeding 0.18 mm was 2.343 km². Some deposition was noted to fall outside this area, but at a thickness that was less than the measured natural sedimentation rate for the site (being approximately 0.18 mm over a 20 month period).

2 MODELLING METHODOLOGY AND DATA

2.1 Current Data

The Modelling used ADCP current data (provided by the client) dated from 20/8/2006 to 25/8/2007. This ADCP was a 300kHz ADCP deployed on top of the Solwara 1 mound (at 1,500 m depth) looking upwards. This current data was analysed and entered into the modelling system. The analysis of this year long current data at 6m above the mound is summarized in Figure 2.1 (as a current rose). Figure 2.1 shows that the currents are relatively weak at these depths. Figure 2.1 also shows that flow directions are typically north-northeast and westsouthwest, which corresponds to the tidal axis at these depths. The median current speed just above the mound is only 7 cm/s, the maximum speed recorded at this depth was 35 cm/s, however only 5% of the current speeds exceeded 15 cm/s.

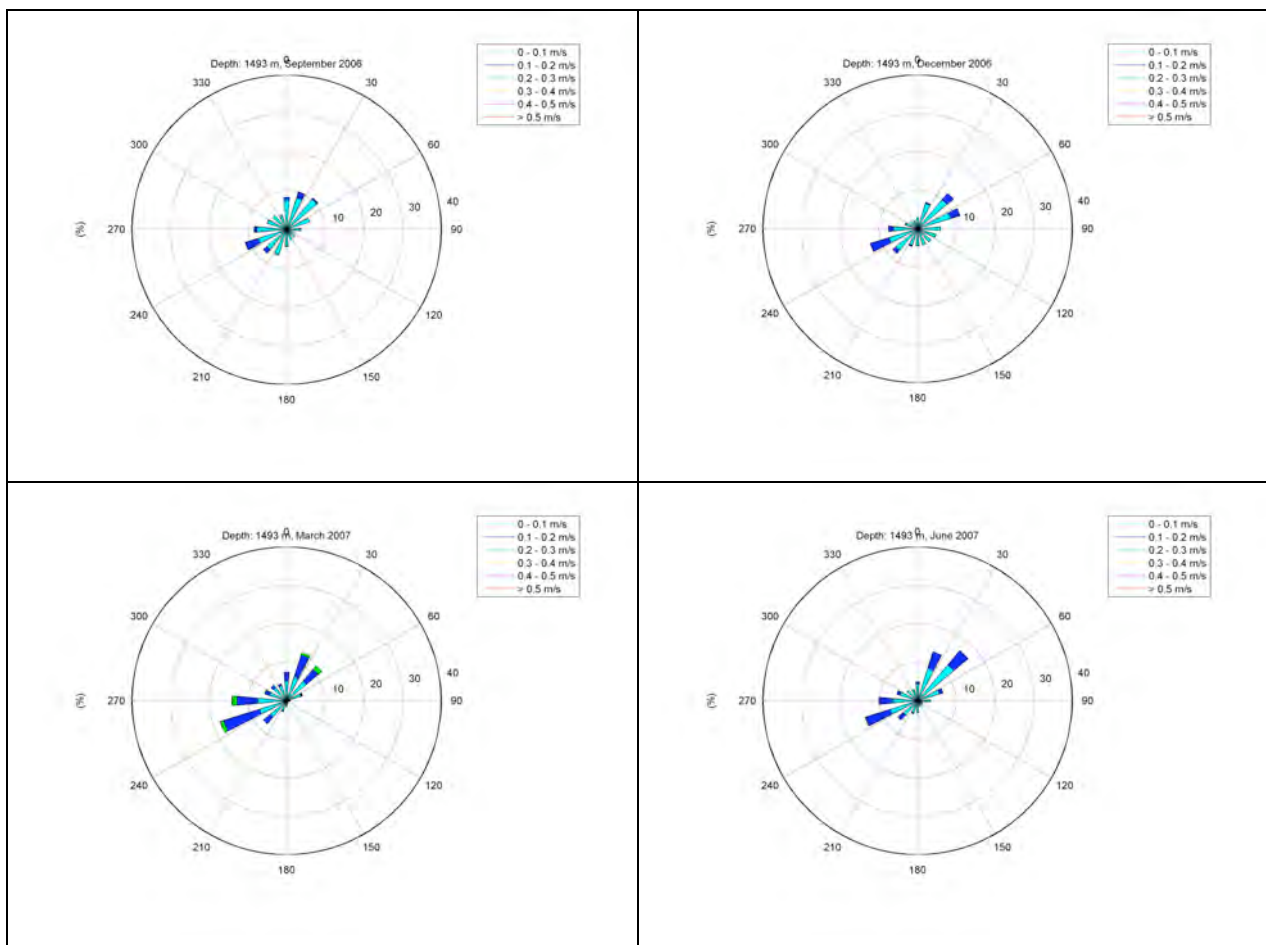


Figure 2.1. Data from the ADCP at 6 m above the seabed presented as a summary current rose plot. Directions in this plot reflect the direction that the current flows to.

2.2 Bathymetry

High resolution digital bathymetry of the Solwara 1 prospect site was provided by the client. Additional digital bathymetry of the Manus Basin region was sourced by APASA for modelling purposes. In Figure 2.2 the bathymetry profile for the study area is provided with the mining activities centered on 152° 5.7' E 3° 47.34' S which is approximately 1,500 m deep.

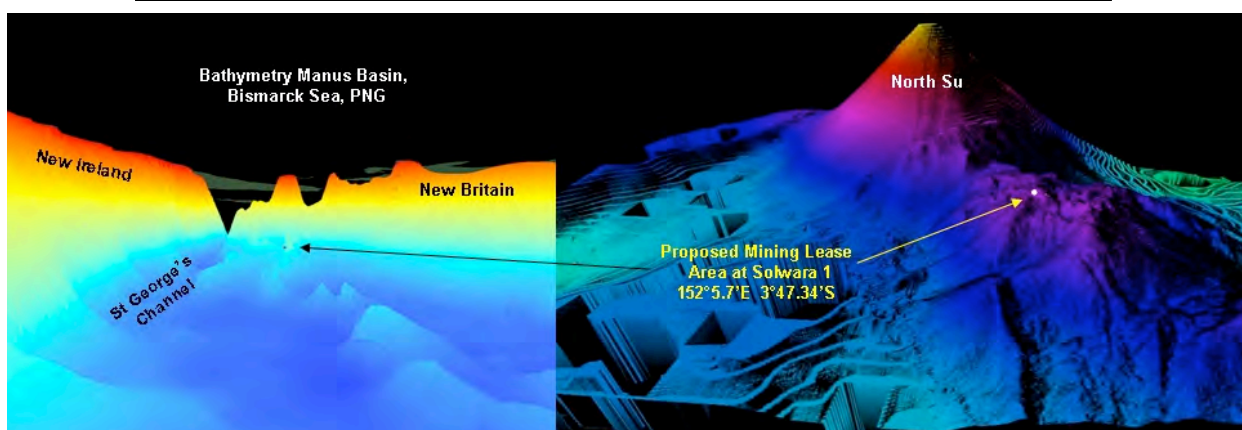


Figure 2.2. Location Map showing the Solwara 1 mining lease site (top) and the bathymetric profile of the Eastern Bismarck Sea (bottom left) and the specific mining lease location (bottom right). Red peaks (bottom left) show the above sea level features of New Ireland, Duke of York Island and New Britain. The large active subsea volcano North Su can be seen as a conical peak behind the mining location (bottom right).

2.3 The SSFATE Model

Sediment dispersion modeling of unconsolidated surface sediments and hard rock competent waste removal and discharge was carried out using the SSFATE model (see Swanson et al. 2007). SSFATE is a Lagrangian particle tracking model designed for determining the fate of sediment in the water column. Thousands of computer generated particles are assigned a mass for the amount of material it represents and each is transported individually based on the sediment type it represents. After the transport calculation stage of the model, the results are applied to a detailed bathymetric dataset and concentration grid using a Gaussian distribution of the mass over area. This gives the effect that the particles move as a plume and not as a clump of mass. Horizontal transport of material is due to advection by currents and diffusion. Current velocity fields are imported into the model from a separate hydrodynamic model and/or field data. Vertical transport is based on particle settling rates and turbulent mixing which the model parameterises with vertical diffusion coefficients. Particle settling velocities are calculated using Stokes' law and through the complex processes of flocculation due to cohesiveness.

Deposition is based on a probability which is a function of bottom stress and concentration. Matter that is deposited can be resuspended if the critical bottom stress is exceeded. The model employs two different resuspension algorithms. The first applies to material deposited in the last tidal cycle (12 hours) and is from Lin et al. (2003). It accounts for the fact that newly deposited material will not be consolidated and will therefore resuspend with less effort than consolidated bottom material. The second algorithm is the Van Rijn method (Van Rijn, 1989) and applies to all other material that has been deposited prior to the start of the last tidal cycle. Swanson et al. (2007) summarise justifications and tests for these schemes.

The characterization of different dredge types is represented by the initial vertical distribution of released material as well as the sediment grain size distribution. For example the majority of sediment release from a trailer suction dredge is due to overflow of fine material. Therefore the initial vertical distribution of material is set to release near the surface and the grain size distribution is biased towards the finer material.

2.4 Sediment Data

Nautilus took samples of the sediment for analysis which was used to provide the SSFATE model with realistic data on the sediment's characteristics. Of particular importance for the modelling study was the grain size associated with the unconsolidated surface sediments (removed using an ROV) and the hard rock competent waste clearing (removed using the purpose built Seafloor Mining Tool or SMT).

The School of Geology at James Cook University of North Queensland carried out the grain size analysis from samples of the unconsolidated surface sediments at the Solwara-1 site. The results from all samples were examined and the worst-case distribution was selected based on the maximum composition of fine material. The results from this grain size analysis of this worst-case sample were then provided to APASA for input into the SSFATE model to represent the placement from the ROV operation to remove this unconsolidated surface sediments prior to mining. This data is shown Figure 2.3. In summary the sediment was 25% clay, 38% fine silt, 15% coarse silt, 10% fine sand and 12% coarse sand or greater. This data was used by the SSFATE system to calculate the fall velocities of each sediment class through the water column after discharge.

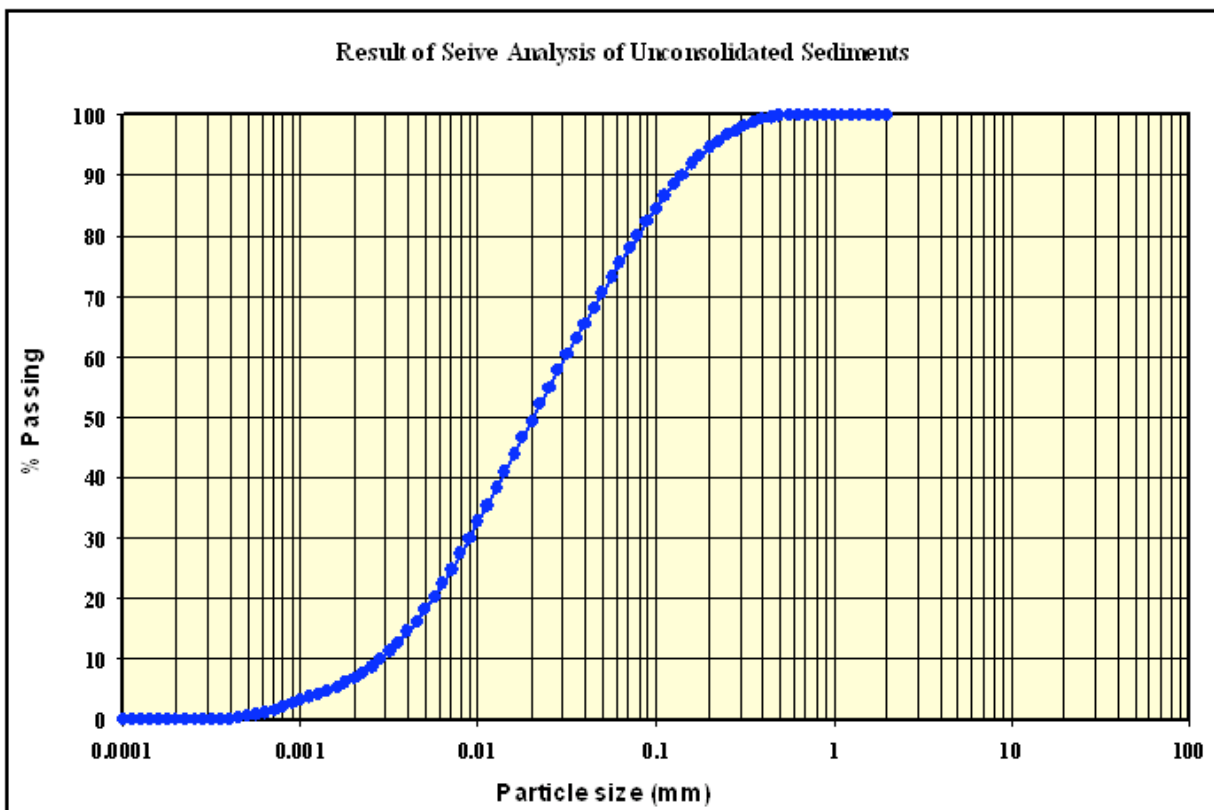


Figure 2.3. Particle size distribution (microns) graph from the 'worst-case' sample from the unconsolidated sediments at the Solwara-1 site.

Earth Mechanics Institute of the Colorado School of Mines carried out the analysis on the cuttings from a linear cutting test using the SMT. The results were examined and the worst-case distribution was selected based on the maximum composition of fine material. The results from this detailed sieve analysis of this worst-case sample were then provided to APASA for input into the SSFATE model. This data is shown Figure 2.4. In summary the sediment was only 2% clay, 2% fine silt, 2% coarse silt, 2% fine sand and 92% coarse sand or greater. This data was used by the SSFATE system to calculate the fall velocities of each sediment class through the water column.

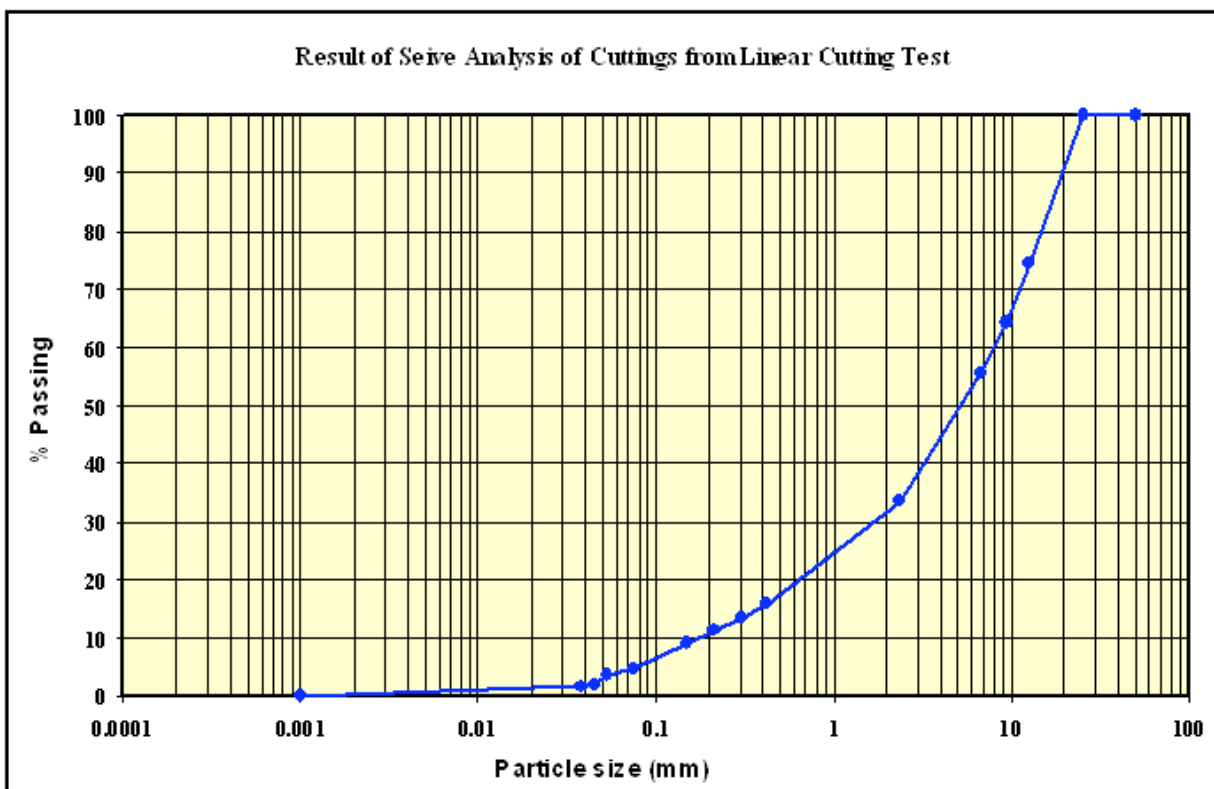


Figure 2.4. Particle size distribution (mm) graph from the 'worst-case' sample from the linear cuttings test of the SMT.

2.5 Tip Head Placement Operation

Prior to mining, the surface unconsolidated sediments (US) will be removed from each mining cut site and placed at designated tip head areas (as shown in Figure 2.5) based on their proximity to the removal operation. An ROV will undertake the US removal and replacement via a 4 inch diameter pipe at an average rate of 250 m³/h of a 4% US slurry with seawater (= 10 m³/h US). Any hard rock competent waste (if present) will then be removed via the SMT and discharged in a similar manner via the nearest tip head.

A detailed scheduled of this ROV and SMT removal operation was provided to APASA for inclusion into the SSFATE model, including timing and quantities of material that will be involved. This data was entered into the SSFATE model to simulate the entire process and tip head placement at the five sites (FWZ1, WZ1, CZ3, EZ2, FEZ1 as shown in Figure 2.5) for the entire operation.

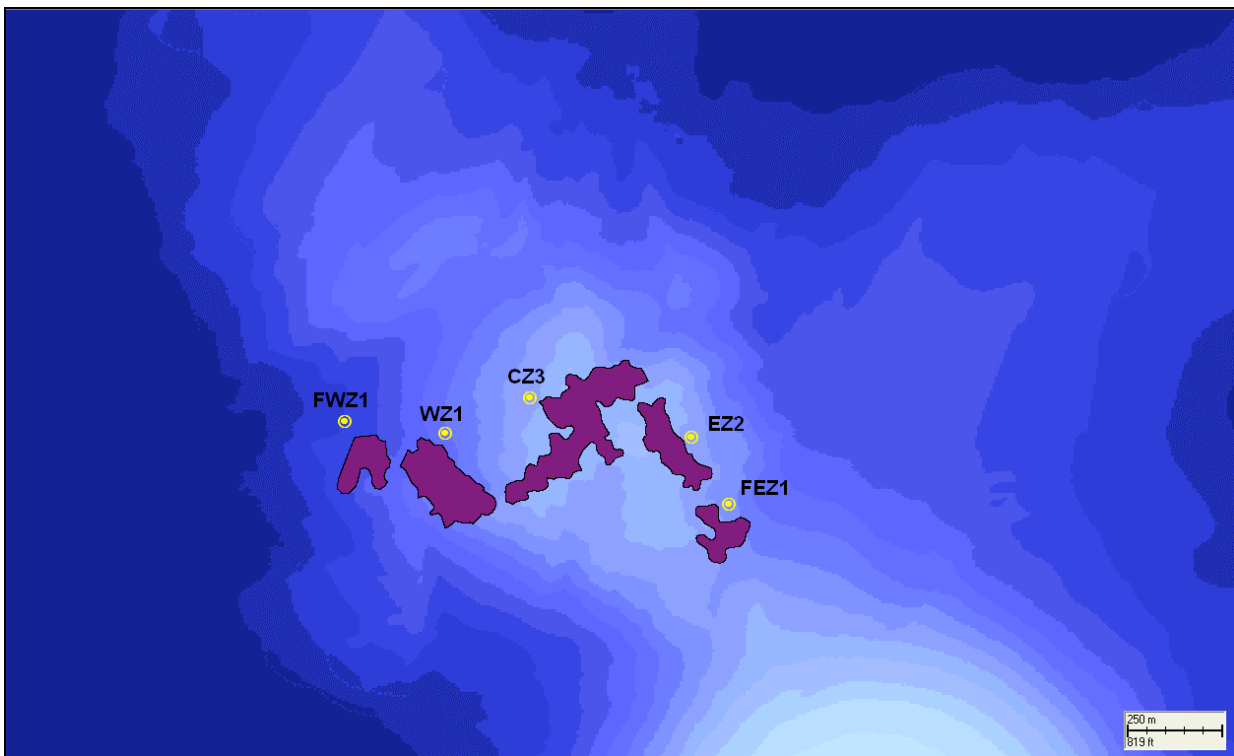


Figure 2.5. Location Map showing the Solwara 1 mining area, the bathymetric profile of location and the five tip head sites, FWZ1, WZ1, CZ3, EZ2, FEZ1.

3 RESULTS AND DISCUSSION

The calculation of the complete pre-mining removal and placement operation (comprising the surface unconsolidated sediments and some hard rock competent waste) using the ROV and the Seafloor Mining Tool (SMT) was undertaken with the SSFATE model described herein. This operation will be carried out, intermittently, as required over a 20 month period.

The SSFATE simulations demonstrated that due to the fast falling velocity of the coarse sands and heavier materials, these larger particles would fall down-slope, but near the tip head sites. In contrast, the finer particles, the clays and silts would spread more widely since their lower fall velocities enabled them to be carried by the tidal currents before settling.

Figure 3.1 shows the depositional thicknesses of the placement from the ROV and SMT excavated pre-mining material surrounding the Solwara 1 mining lease site after this operation is completed in full. Bottom thicknesses, shown in Figure 3.1, varied from 0.18 mm to small areas adjacent to the tip heads site slightly exceeding 500 mm or 0.5m. Some deposition was noted to fall outside the areas shown in Figure 3.1, but at a thickness that was less than the measured natural sedimentation rate for the site (being 0.18 mm over a 20 month period).

The model results also detailed the composition of the benthic loading in the area as shown in Figure 3.2 for the mining sites and Figure 3.3 for the area in general. Figure 3.2 shows the particle size distributions for sediment that returned to the mining zone, while Figures 3.3a to Figure 3.3e show the extent of the individual sediment size classes. The coarse sands were found to settle very close to the tip head sites, given the larger settling velocities of these particles. These sands are predicted to mound near the tip head site by SSFATE. This is to be expected, although the SSFATE model does not account for post settlement slumping or any instability associated with these higher sediment peaks. It is possible that these mounds may collapse and spread the coarser sands down the slope of the Solwara-1 mound. In contrast, the significant quantities of clays and silts within the unconsolidated sediments have very low settling velocities and hence are subjected to the ambient currents. While the SSFATE model accounts for the bathymetric profile of the site as shown in Figure 3.1 and Figure 3.3, a small proportion of these clays, silts and some fine sands are predicted to settle back on the mining site (maximum thickness on mining area < 376mm) due to the ambient currents and vertical turbulence. Indeed, the benthic loading predicted within the mining boundaries, shown in Figure 3.2 and Figure 3.3, is comprised of these clays, silts and fine sands from the unconsolidated sediments.

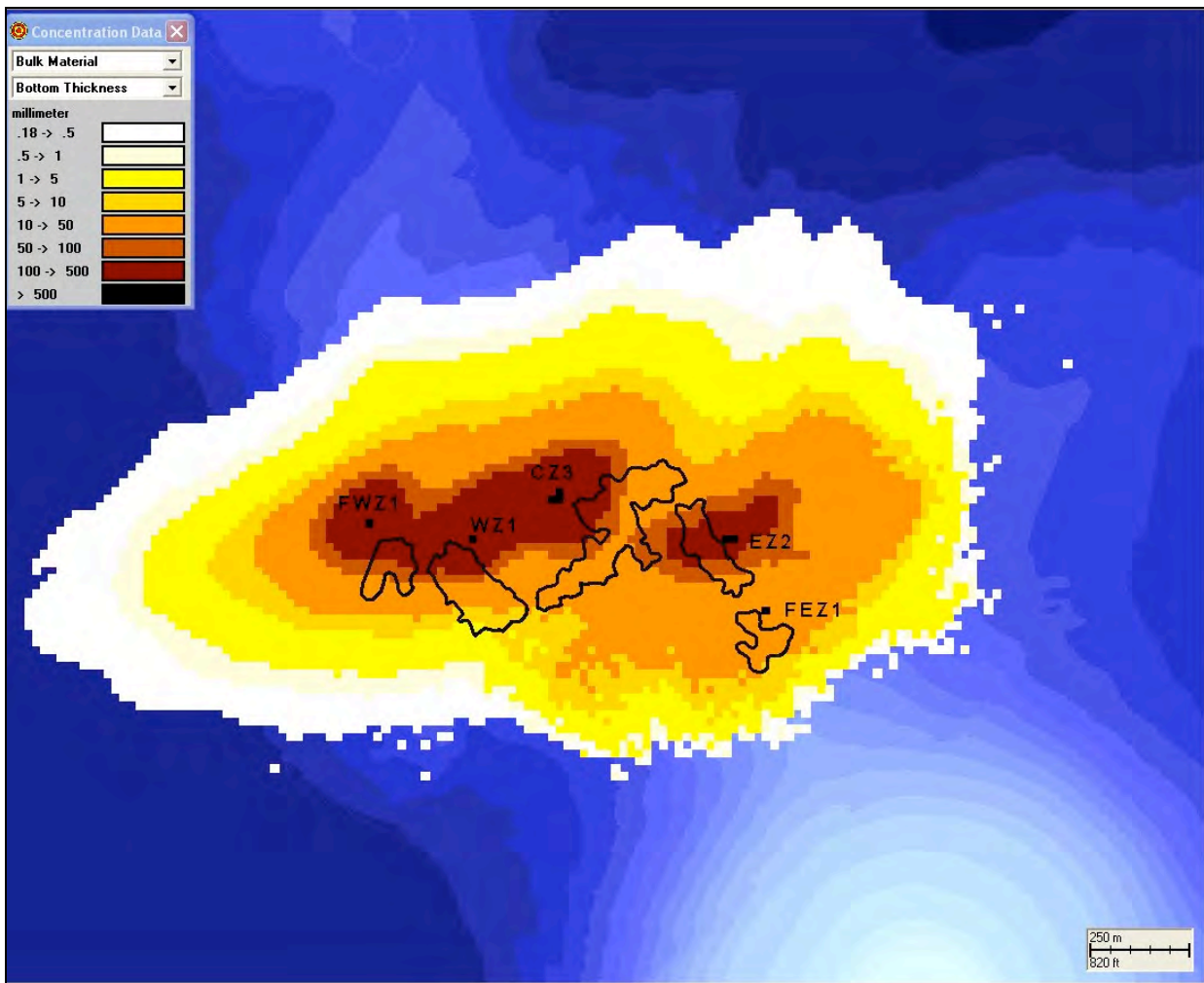


Figure 3.1. Sediment bottom thickness surrounding the Solwara 1 mining lease area after simulating the full removal operation. Also shown are the location of the Tip head discharge sites and the outline of the mining zone.

Table 3.1 gives a summary of the area covered by each thickness range, their maximum extents and the total area covered. The furthest extent of influence from the mining operation was less than 1 km from the nearest tip head site, where depositional thickness was limited to 0.18 mm which, after a 20 month period, is equal to the natural background sedimentation rate for the region.

Table 3.1. Summary of areas covered by each bottom thickness range.

Bottom Thickness Range (mm)	Area Covered (km ²)	Maximum Distance from A Tiphead (km)
0.18 – 0.5	2.343	0.972
0.5 – 1.0	1.798	0.710
1 – 5	1.568	0.660
5 – 10	1.047	0.615
10 – 50	0.801	0.565
50 – 100	0.278	0.264
100 - 500	0.166	0.166
> 500	0.003	0.036

* Note. Area and distance calculations are cumulative

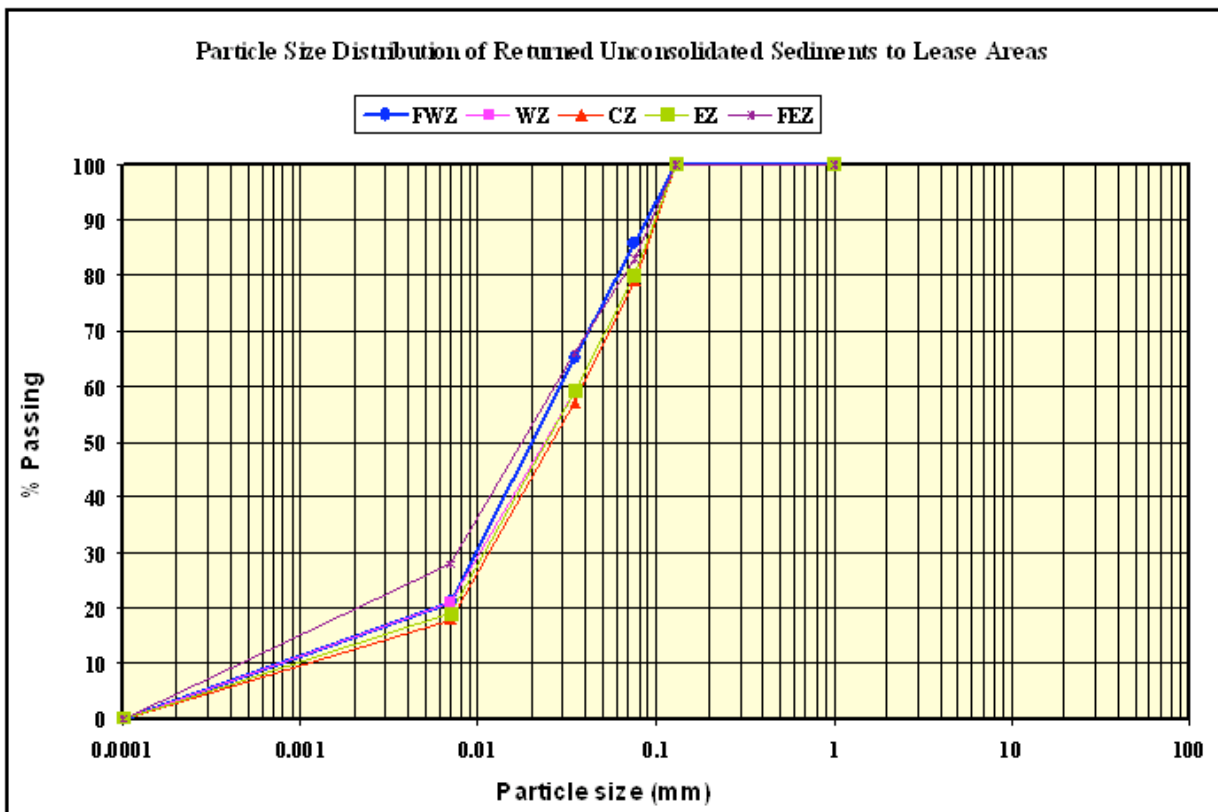


Figure 3.2. Particle size distribution (microns) graph for the unconsolidated sediments that return to settle back in the Solwara-1 lease areas.

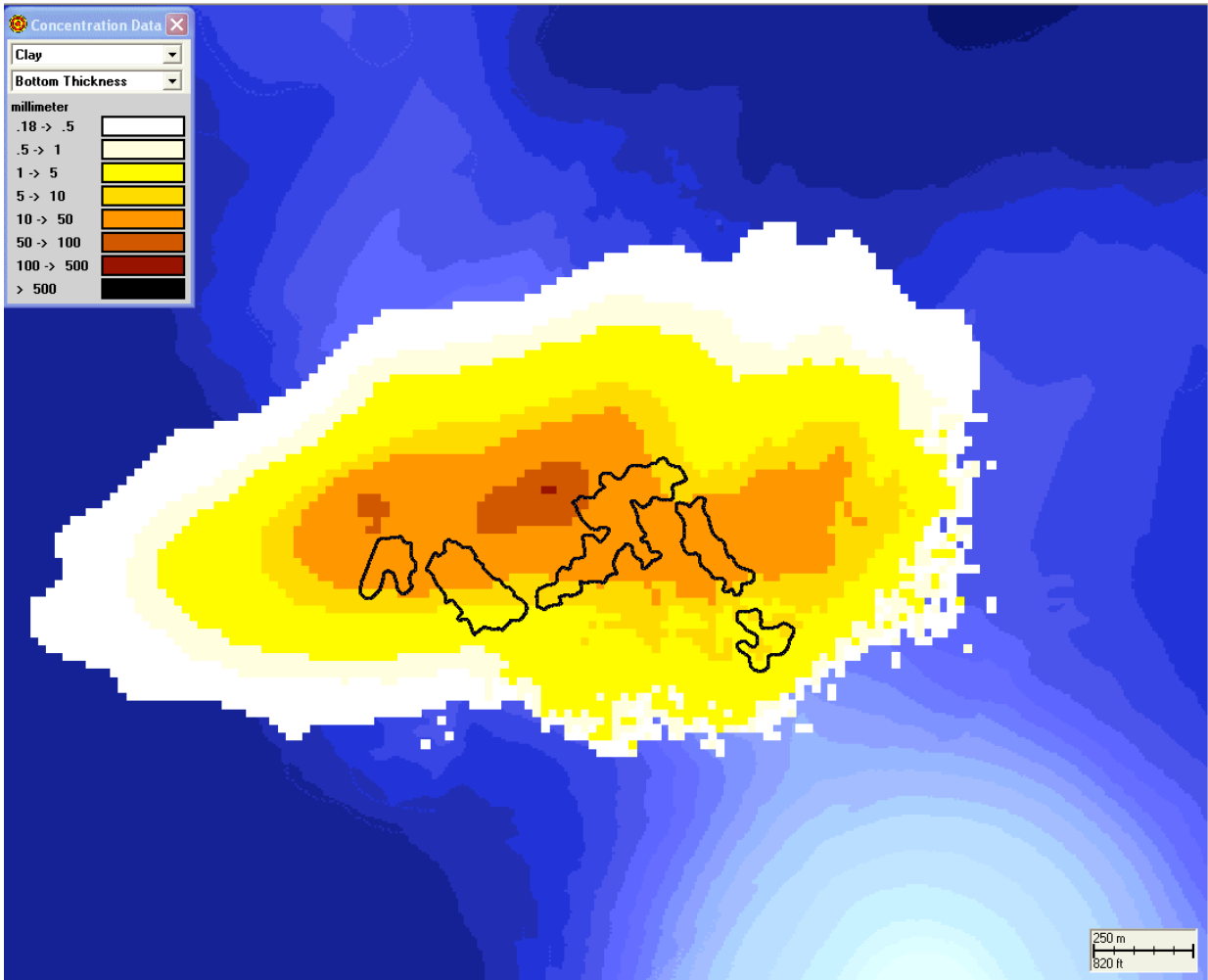


Figure 3.3a. Sediment bottom thickness for clay particles surrounding the Solwara 1 mining lease area after simulating the full removal and placement operation.

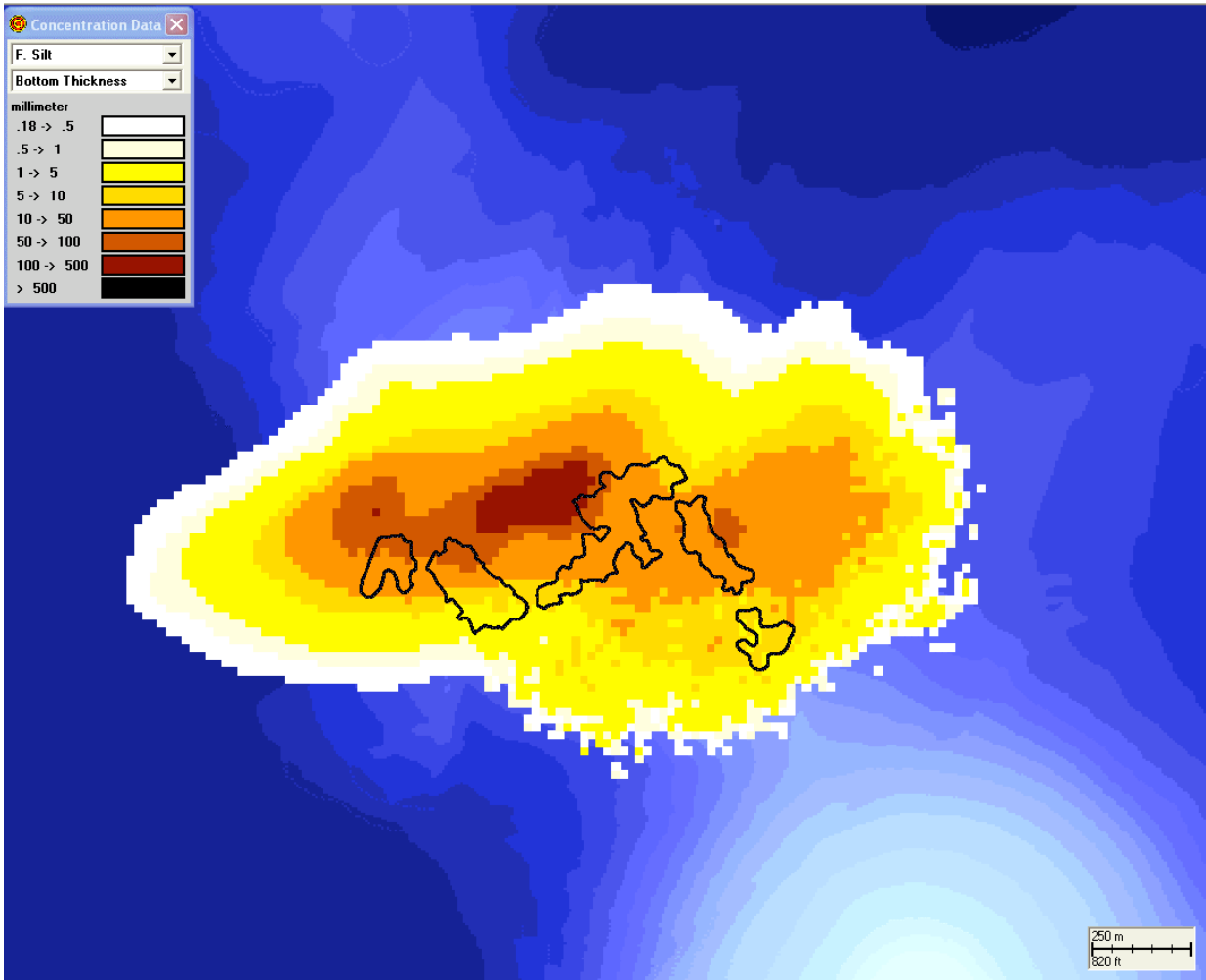


Figure 3.3b. Sediment bottom thickness for fine silt particles surrounding the Solwara 1 mining lease area after simulating the full removal and placement operation.

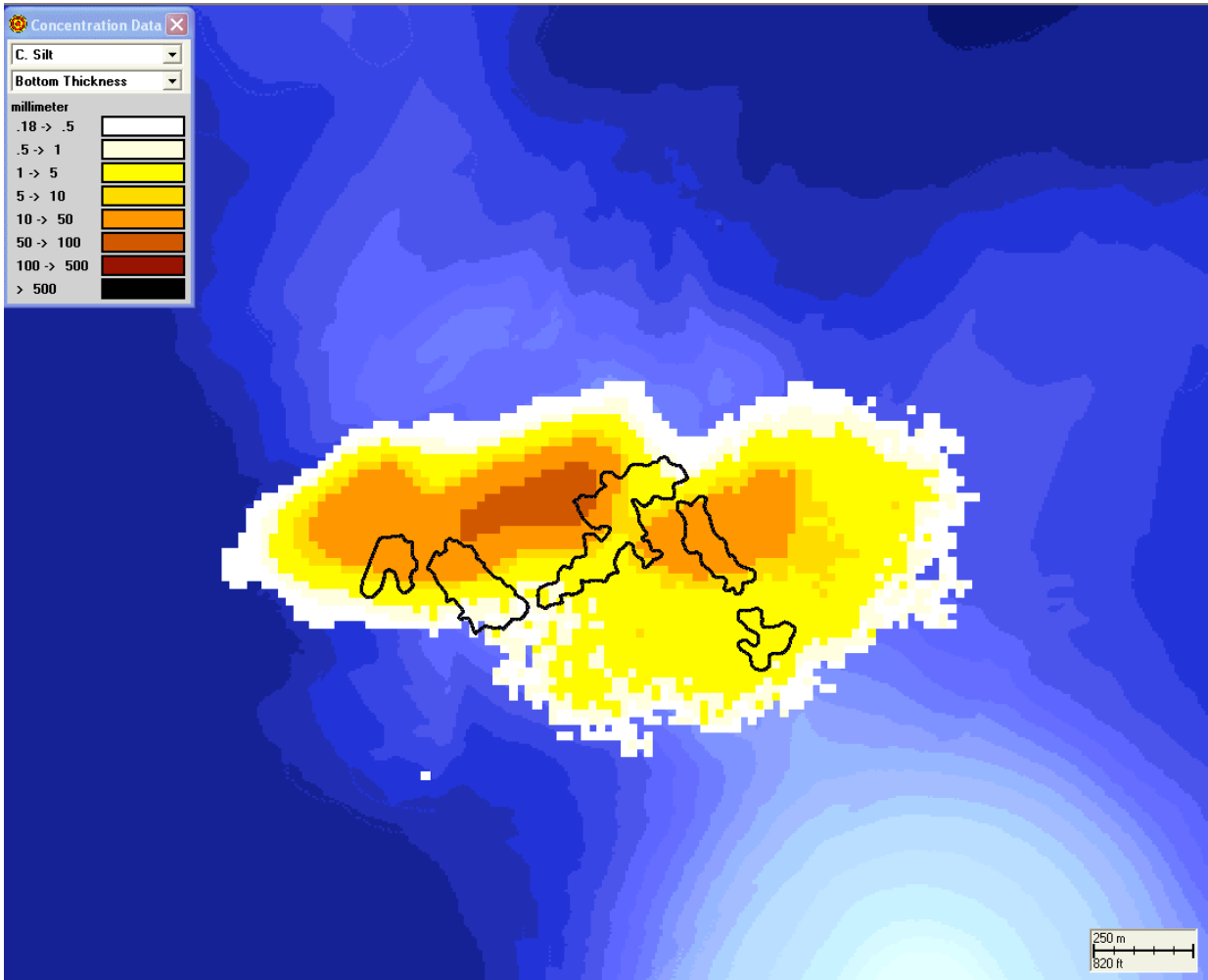


Figure 3.3c. Sediment bottom thickness for coarse silt particles surrounding the Solwara 1 mining lease area after simulating the full removal and placement operation.

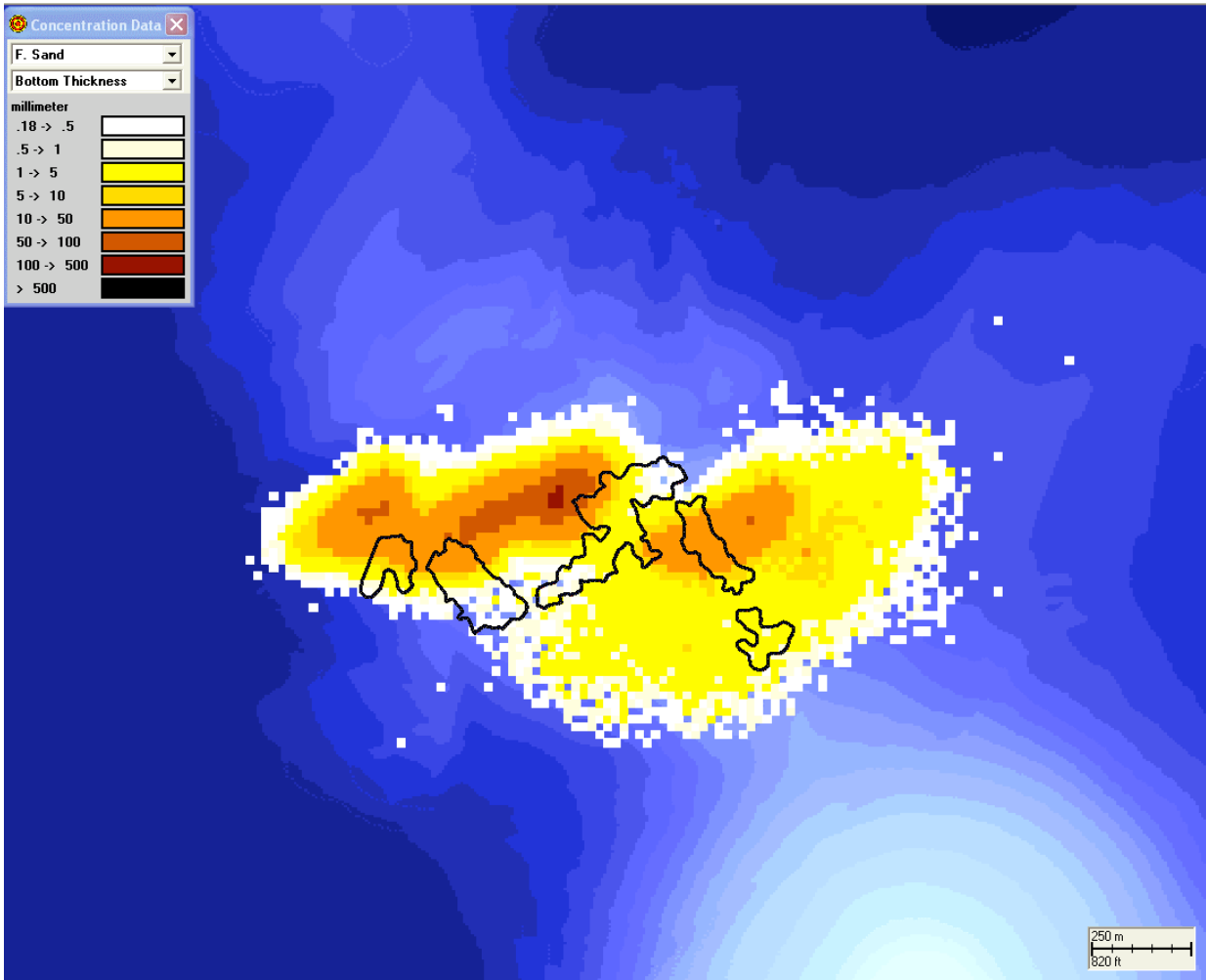


Figure 3.3d. Sediment bottom thickness for fine sand particles surrounding the Solwara 1 mining lease area after simulating the full removal and placement operation.

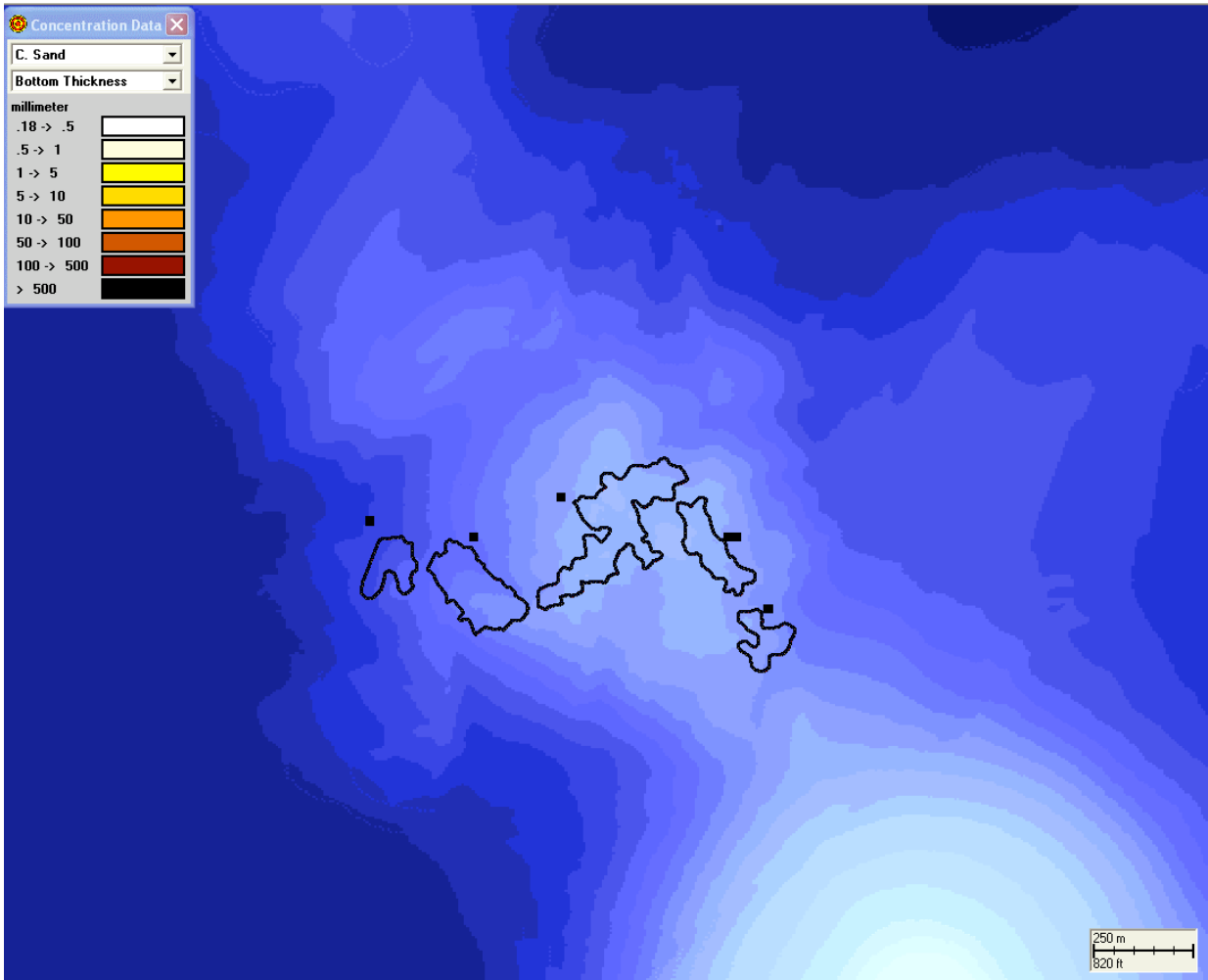


Figure 3.3e. Sediment bottom thickness for coarse sand particles or greater surrounding the Solwara 1 mining lease area after simulating the full removal and placement operation.

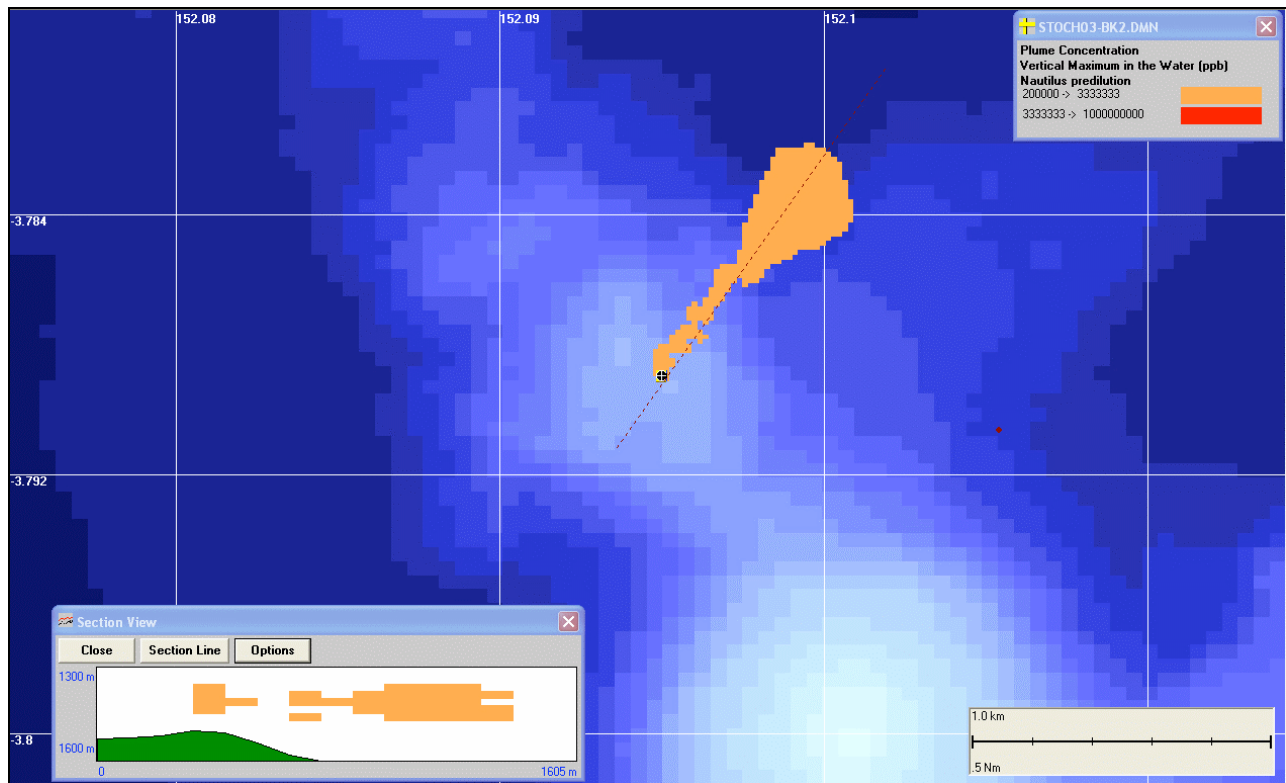
4 REFERENCES

- Swanson J.C., Isaji T., Galagan C., 2007, Modeling the Ultimate Transport and Fate of Dredge-Induced Suspended Sediment Transport and Deposition. Proceedings of Wodcon 2007, Lake Buena Vista, Florida.
- Van Rijn L.C., 1989, Sediment Transport by Currents and Waves, Rep. H461, Delft Hydraul. Lab., Delft, Netherlands

Appendix 12

**Modelling the Dispersion of the Returned Water Discharge Plume from the
Solwara 1 Seabed Mining Project, Manus Basin, Papua New Guinea**

MODELLING THE DISPERSION OF THE RETURN WATER DISCHARGE PLUME FROM THE SOLWARA 1 SEAFLOOR MINING PROJECT, MANUS BASIN, PAPUA NEW GUINEA



Produced for:

Coffey Natural Systems

August 2008

Produced by:

Document control form

Document draft	Originated by	Edit & review	Authorised for release by	Date
Draft 1 for internal review	Trevor Gilbert	Dr Brian King	Dr Brian King	March 2008
Draft for client review	Trevor Gilbert	Dr Brian King	Dr Brian King	20 th May 2008
Draft for client review	Trevor Gilbert	Dr Brian King	Dr Brian King	20 th June 2008
Draft for client review	Nathan Benfer	Dr Brian King	Dr Brian King	27 th August 2008
Final Report	Nathan Benfer	Dr Brian King Greg Terrens	Dr Brian King	2 nd September 2008

APASA Project Manager: Dr Brian King

Document Title: Solwara Plume Modelling (Final).doc

APASA Project Number: S007

DISCLAIMER: This document contains confidential information that is intended only for use by the client and is not for public circulation or publication or for the use of any third party without the approval of Asia-Pacific ASA Pty Ltd (ABN 79 097 553 734) trading as Asia-Pacific Applied Science Associates.

While this report is based on source information Asia-Pacific ASA Pty Ltd considers reliable, its accuracy and completeness cannot be guaranteed. Therefore, Asia-Pacific ASA Pty Ltd and its directors and employees accept no liability for the result of any action taken or not taken on the basis of information in this report, or for any negligent misstatements, errors, or omissions. This report is compiled with consideration for the specified client's objectives, situation, or needs. Those acting upon such information without first consulting Asia-Pacific ASA Pty Ltd do so entirely at their own risk. We strongly recommend that any person who wishes to act upon this report first consult an Asia-Pacific ASA Pty Ltd advisor.

TABLE OF CONTENTS

1	EXECUTIVE SUMMARY	3
2	MODELLING METHODOLOGY AND DATA	5
2.1	Single Release Modelling	5
2.2	Stochastic Modelling	6
2.3	Deep Sea Temperature and Current Data	7
2.4	Bathymetry	9
2.5	Outfall Configuration and Assumptions.....	10
3	RESULTS AND DISCUSSION.....	12
3.1	Dilution Thresholds.....	12
3.2	Plume dynamics	12
3.3	Affected areas and extents.....	15
3.4	Plume Thickness	16
3.5	Sedimentation Thickness	17
4	CONCLUSIONS.....	17
5	REFERENCES	22

1 EXECUTIVE SUMMARY

The following report used advanced computer modelling to quantify the plume discharge operation and its subsequent dispersion and fate, as part of the subsurface discharge of return water from the deep sea mining project of the Solwara 1 prospect, Manus Basin, Papua New Guinea. The Solwara 1 prospect is located at 1,500-1,700 m water depth approximately 50 km north of Rabaul in the eastern extent of the Manus Basin, Bismarck Sea.

Several probable scenarios were modelled using the Applied Science Associates, Ltd (ASA) chemical discharge model system, CHEMMAP, which related to the return water discharge being a vertical discharge, via a dual discharge pipe from a mining support vessel to the mining site at a point 20 to 30 m above the seafloor (seafloor approximately 1,500m below surface). The scenarios modelled were an upwards exiting discharge stream at two extremes of the potential discharge temperatures being 5.8 °C and 11.4 °C. This range of discharge temperatures is due to the 20% (approximate) additional surface waters being added to the discharge stream and other operational/seasonal variances. The addition of the surface water also aids in the pre-dilution of the return water prior to discharge reducing the subsurface mixing zones size.

Stochastic modelling was carried out for 100 samples using random commencement time periods over a calendar year from late August 2006 to late August 2007 (a period for which current meter data was available). The model was performed on each discharge scenarios for the nominated discharge rate on a continuous basis over an 8 day period.

A number of dilution rates were used in this study to determine the area affected from each discharge scenarios i.e. vertical upwards discharge of 4,005 gallons/minute (0.253 m³/s or 909.6 m³/hr) from a pipe 25 m above the seabed with 2 different discharge temperatures (given seasonal variations). Key dilution ratios used in the modelling (options for mixing zone boundaries) were 1/300, 1/600 and 1/5,000. These key dilution ratios were used in the discussion and presentation of results.

The model results presented here demonstrated that the mixing of the discharged plume is slightly enhanced when the return water temperature is at the higher end of its potential range in comparison to when the return water is at the lower end of its temperature range. This is expected, since the buoyancy of the warmer plume will be greater after discharge, hence enabling it to rise higher through the water column, entraining more ambient water as it ascends.

Given the range of tidal and basin wide currents operating within the Manus Basin, the model results demonstrated that the plume will only exceed the 1/5,000 dilution threshold more than 50% of the time over an area of 0.81 km² at no more than 0.9 km from the discharge site regardless of the temperature of the discharge plume. The model results also showed that the extent of the plume at concentrations exceeding a 1/5,000 dilution is unlikely to extend more than 5.0 km at any time during the discharge operation regardless of the temperature. The model also demonstrated that the 1/300 dilution threshold is achieved rapidly, due to the addition of surface water ensuring a degree of pre-dilution before discharge. The buoyancy effects of these additional warmer surface waters also ensured that the 1/300 dilution threshold is achieved, on average, within 60 m of the discharge point. The 1/600 dilution threshold is achieved, on average, within 85 m of the discharge point.

Utilising the stochastic model and individual worse case scenarios for both temperature extremes of the discharge water, the estimated maximum sub-sea plume thickness within the water column is no more than 175 metres for these plume temperature extremes. The plume extends beyond these depths over time, but not at concentrations exceeding the thresholds described herein. Hence, given that the temperature of the discharge plume will fluctuate, the modelling conducted herein quantified that the plume will extend, at times, from 1,300 m deep to 1,475m deep at concentrations exceeding the thresholds.

Finally, the return water contains fine particulate (< 8 micron) ore. Additional model runs were conducted to quantify the sedimentation of this fine ore over the full mining operation (20 months) particularly since this fine material will settle very slowly. Given that the background daily sedimentation rate for the area has been measured at 0.0965 mg/cm²/day, which equals to approximately 590 g/m² for the 20 months of mining operation (or 0.180 mm) assuming average density of 3,300 kg/m³). The model results demonstrated that the peak bottom thickness from the settling fines is less than 0.1 mm for the same 20 month period. Indeed, the model predicted that sedimentation level between 0.05 mm and 0.1 mm was possible, but extremely patchy. Between these patches, sedimentation levels were below the model resolution here and an order of magnitude less than the natural background sedimentation for the region.

2 MODELLING METHODOLOGY AND DATA

2.1 *Single Release Modelling*

To quantify potential mixing zones for the return water discharge into ambient waters, this study made use of advanced computer simulation software known as CHEMMAP to quantify the mixing, transport and dispersion of the plume water taking account of the release characteristics (discharge rate, discharge temperature, pipe configuration) and the movement and physical conditions within the receiving environment.

CHEMMAP has been developed over two decades for the assessment of physical fate, biological impacts, natural resource damages and ecological risks. The algorithms and assumptions of the chemical spill/discharge model have been described previously (French et al. 1996, French McCay and Isaji, 2004; French McCay et al 2004). The fates model processes and database are briefly summarized below.

The chemical fates model estimates the distribution of chemical (as mass and concentrations) on the water surface, on shorelines, in the water column and in the sediments. The model is three-dimensional, separately tracking surface floating chemical, entrained droplets or suspended particles of pure chemical, chemical adsorbed to suspended particulates, and dissolved chemical. Processes that are simulated are spreading (floating liquids), transport, dispersion, evaporation-volatilization, entrainment (liquids), dissolution, partitioning, sedimentation, and degradation.

The model uses physical-chemical properties to predict the fate of a discharge or chemical spill, including density, vapor pressure, water solubility, environmental degradation rates, adsorbed/dissolved partitioning coefficients (K_{ow} , K_{ow}), viscosity, and surface tension. The discharged mass is initialized at the location and depth of the release, in a state dependant upon the physical-chemical properties of the material. The discharge is modelled using the Lagrangian approach, where multiple sublots, called spilletts, of the entire mass (or volume) discharged are tracked as they move in three-dimensional space over time (by addition of the transport vectors due to currents and buoyancy). The currents are those provided by the ADCP data collected by Nautilus at the discharge location. Stoke's Law is used to compute the vertical velocity of the chemical particles or suspended sediment with adsorbed chemical. If rise or settling velocity overcomes turbulent mixing, the particles are assumed to float or settle to the bottom. Settled particles may later resuspend (assumed to occur above 20 cm/sec current speed). Turbulent

dispersion is modelled using a random walk scheme (Bear and Verruijt, 1987), with the magnitudes scaled by horizontal and vertical diffusion coefficients (Okubo, 1971). The mixing parameters were conservative estimates of deep water conditions.

2.2 Stochastic Modelling

Originally CHEMMAP was designed to simulate specific spill incidents and/or ongoing discharges for evaluating impacts and damages (French et al. 1996). More recently, the model has been set up in a probabilistic stochastic configuration, allowing evaluation of risks of consequences and statistical computations (French McCay and Isaji, 2004). While a few chemical spill models exist that can simulate transport and physical fate of single events (Lunel, 1991; Shen et al., 1995; Rusin et al., 1996), CHEMMAP is unique in being able to evaluate biological impacts, in its stochastic implementation, and in its interconnection with hydrodynamic models, geographical information systems, and its graphical user interface. In the stochastic mode, CHEMMAP can be used to predict the fate of multiple or continuous releases that occur under a random selection of prevailing conditions (also known as stochastic modelling). The stochastic model performs a large number of sample simulations for a given release site, randomly varying the sample time frame, so that the transport, concentration and dilution of each particle representing the plume mass and concentration are subject to a different set of prevailing current conditions and water properties. During each simulation, the model records the grid cells that were contacted by the plume, as well as the amount of time that had elapsed prior to the contact or exposure.

Once the stochastic modelling is complete, the results are compiled from each of the sample trajectories to provide a statistical weighting to the likelihood of exposure of grid cells. Stochastic results can be summarised as:

1. The probability, frequency or risk that a grid cell may be exposed to the plume; and
2. The maximum expected (averaged) concentrations of the plume in each grid cell.

The stochastic modelling approach provides an objective measure of the possible outcomes of a release, as well as the means of quantifying the likelihood of a given outcome. The most commonly occurring conditions would be selected most often while conditions that are more unusual can also be represented.

Stochastic modelling was carried out for 100 samples using random commencement time periods over a calendar year from late August 2006 to late August 2007. The model was performed on each discharge scenario for a continuous discharge including the additional surface waters used for predilution, over an 8 day period. Deep sea water currents and some bathymetry data were provided by the client and used in this modelling.

2.3 Deep Sea Temperature and Current Data

Modelling was performed using the ADCP-A current data (provided by the client) dated from 20/8/2006 to 25/8/2007. This ADCP-A was a 300kHz ADCP deployed on top of the Solwara 1 mound (at 1,500 m depth) looking upwards.

This current data was analysed and entered into the modelling system. The analysis of this year long current data at 6m above the mound is summarized in Figure 2.1 (as a current rose) and corresponds to the approximate location of the operation. Figure 2.1 shows that the currents are relatively weak at these depths. Figure 2.1 also shows that flow directions are typically north-northeast and westsouthwest, which corresponds to the tidal axis at these depths. The median current speed just above the mound is only 7 cm/s (0.07 m/s), the maximum speed recorded at this depth was 35 cm/s, however only 5% of the current speeds exceeded 15 cm/s.

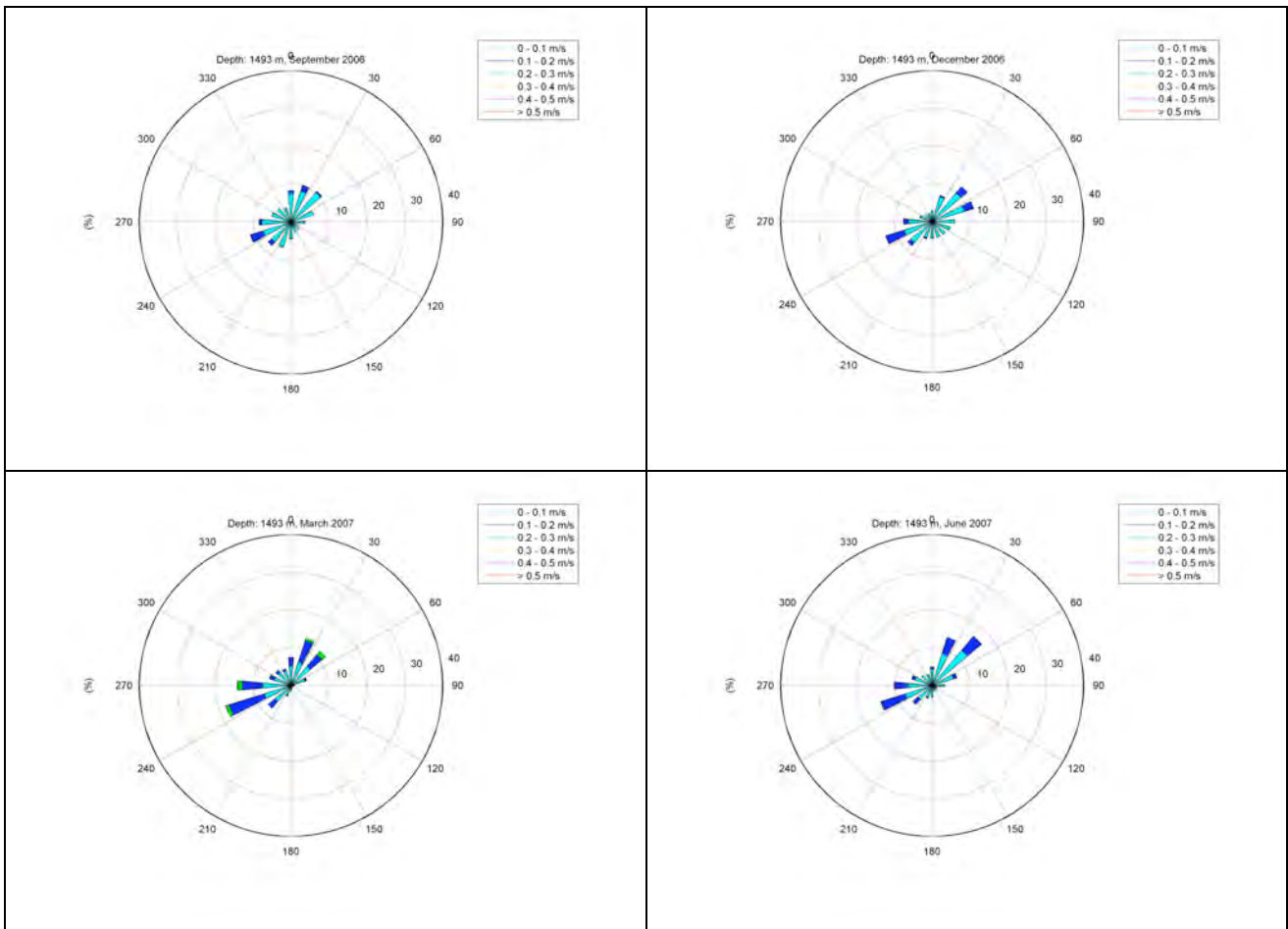


Figure 2.1. Data from the ADCP at 6 m above the seabed presented as a summary current rose plot. Directions in this plot reflect the direction that the current flows to.

Figure 2.2 shows the temperature profile at the Solwara 1 prospect site during December 2005. From this figure, it is noted that the surface temperatures were greater than 30°C while temperatures at the bottom were approximately 3°C. The data in Figure 2.2 demonstrates that the water column in the Bismarck Sea is stable and layered since temperature decreases as depth below the water surface increases. Note also that the top of thermocline starts around 200 m.

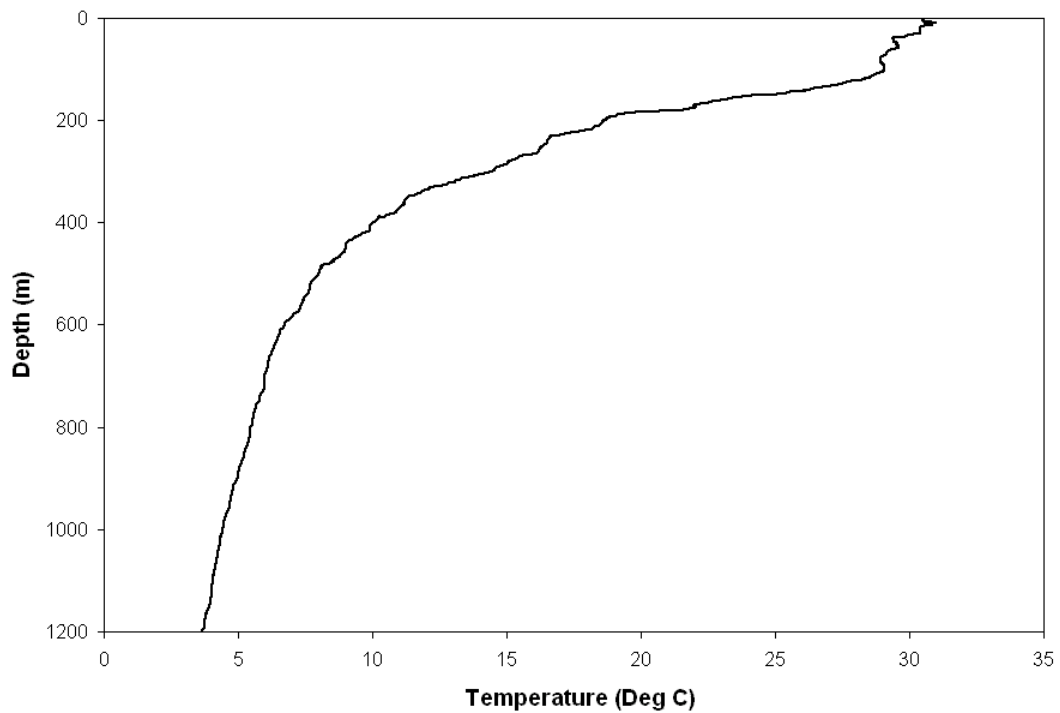


Figure 2.2. Temperature profile at the Solwara 1 prospect site during December 2005.

2.4 Bathymetry

High resolution digital bathymetry of the Solwara 1 prospect site was provided by the client. Additional digital bathymetry of the Manus Basin region was sourced by APASA for modelling purposes. In Figure 2.3 the bathymetry profile for the study area is provided with the identification of the discharge location at 152° 5.7' E 3° 47.34' S which is approximately 1,500 m deep. This bathymetry data was imported into the CHEMMAP system onto a bathymetric grid using 500 x 500 grid cells, each at 60m x 60m resolution.

2.5 Outfall Configuration and Assumptions

This study focussed on quantifying the dilution of the discharge plume under worst-case conditions and assumptions. This approach (worst-case input data for the modelling) then quantifies the worst-case extents of dilution. In practice, the results of mixing are expected to be better than those presented herein. The outfall pipe extends from the surface to approximately 20-30 m above the mound at the Solwara 1 lease site. At the bottom, the pipe will be split into two discharge pipes, both pointing vertically upwards. The temperature of the discharge will range from 5.8 °C to 11.4 °C. The two pipes will be located diagonally opposite at the lower end of the pump module frame, approximately 7.5m apart. It is anticipated that each pipe will be approx. 6 & 5/8" (170mm) internal diameter (I.D.).

Nominal discharge rate will be of the order of 2002.5 gpm through each pipe (i.e., a total discharge of 4005 gallons/minute) being 5 parts production water and 1 part surface water.

The following parameters were assumed as input to the model.

- Discharge rate of 2002.5 gpm through each of two pipes
- Discharge salinity is the same as the receiving water salinity
- Discharge water temperature range is 5.8 °C to 11.4 °C
- Receiving water temperature is 3 °C
- Discharge pipe diameter is 170 mm internal diameter
- Discharge pipe facing directly upwards at 1,475m below sea level
- Starting concentration of discharge plume after pre-dilution is set to 833,333,333 PPB (part per billion or 83.3% return production water).

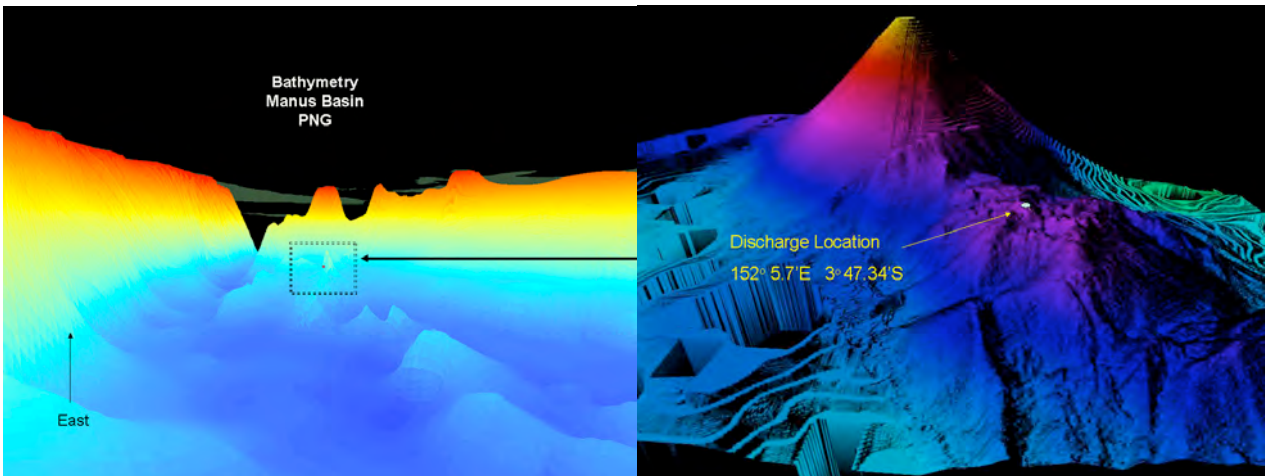


Figure 2.3. Location Map showing the Solwara 1 discharge site (top) and the bathymetric profile of the Eastern Bismarck Sea (bottom left) and the specific discharge location (bottom right). The peak behind the discharge location (bottom left) is Duke of York Island. The large active submarine volcano North Su can be seen as a conical peak behind the discharge location (bottom right).

3 RESULTS AND DISCUSSION

3.1 *Dilution Thresholds*

Two dilution thresholds were used in this study to determine the plume extent from each discharge option (scenarios).

Key dilution ratios used in the modelling were 1/300, 1/600 and 1/5,000. These key dilution ratios were used in the discussion and presentation of modelling results. The discharge water undergoes pre-dilution with ambient seawater at the surface by increasing the discharge from 758 m³/h to 909.6 m³/h, hence the model is set to an initial concentration of 833,333,333 PPB of production water. Therefore the target dilution ratios equate to plume concentrations as follows:

- Pre-dilution is 833,333,333 PPB or 83.33% of the discharge stream
- 1/300 dilution is 3,333,333 PPB
- 1/600 dilution is 1,666,667 PPB
- 1/5,000 dilution is 200,000 PPB

The plume was modelled using a non-reactive tracer within the CHEMMAP system.

3.2 *Plume dynamics*

The discharge configurations tested using the modelling were two extremes in discharge temperature and 5 parts returning production water and 1 part surface seawater. The orientation of the end pipes are designed to face vertically upwards to maximize the initial mixing of the discharge due to the turbulence associated with a large discharge stream. If the pipes were facing downwards, this initial mixing zone would be limited by the close proximity of the bottom to the outfall site. Two scenarios were conducted, one representing the potentially cooler discharge stream, 5.8°C and the potentially warmer discharge stream, 11.4°C For each scenario, 100 simulations were conducted (using the CHEMMAP stochastic model) for both temperatures for comparison purposes. From the 200 in total simulations conducted, some were selected and examined in detail to determine the dynamics of the plume created by the two extremes in discharge temperature as follows.

For these scenarios, the dual discharge pipes were constructed to face upwards. If the discharge rate was at a maximum under these circumstances, then 4005 gpm (or 0.253 m³/s) of discharge water would be directed upwards away from the seabed through two openings. The 5.8°C plume would rise through the water column reaching a height of approximately 90 m above its starting point, that is, 115 m above the seafloor (1,385 m below the surface). In contrast, the warmer 11.4°C plume would rise through the water column reaching a height of approximately 120 m above its starting point, that is, 145 m above the seafloor (1,355 m below the surface). At these heights above the seafloor, the plume loses its jet momentum and buoyancy, since it has mixed sufficiently due to the turbulence created by the jet, that is, its temperature and density are now the same as the ambient water. The buoyancy differences are negligible after the jet phase and the plume centreline dilution ratio (that is, minimum dilution ratio) is at least 1:180 at this point, that is, 1 part discharge to 180 parts ambient receiving water. Beyond this initial rapid dilution, the plume dynamics are now influenced by the tidal currents and basin wide circulation of the Bismarck Sea. This phase of the mixing dynamics is known as far field mixing and is the slowest of the mixing process of a discharge plume.

Figure 3.1 shows a plan and cross-sectional view (between 1,300 m and 1,600 m depth) of the plume in the far field at opposite phases of the tidal cycle. In the cross-sectional view in Figure 3.1 the bottom topography is shown as green. Note that the full plume is shown in Figure 3.1 and that the concentrations of plume water within the ambient waters are coloured as follows:

- Plume concentrations are RED if dilutions are less than 1:300
- Plume concentrations are ORANGE if between 1:300 dilution and 1:5,000 dilution.

Figure 3.1 demonstrates that the plume is extremely patchy, since the discharge occurs in a tidally varying current field for the 11.4°C scenario. That is, when currents are weak during the turning of the tide, plume water builds up around the discharge point. In contrast, when currents are strong, the plume is advected away from the discharge site quickly enough to prevent any buildup, thus reducing plume concentrations within the ambient waters. The example plume extent in Figure 3.1 is about 0.96 km beyond the discharge site in the horizontal. The plume extent in the vertical is only about 120 m in Figure 3.1 (between 1,350 m and 1,470 m below the surface) and remains within its ambient temperature layer.

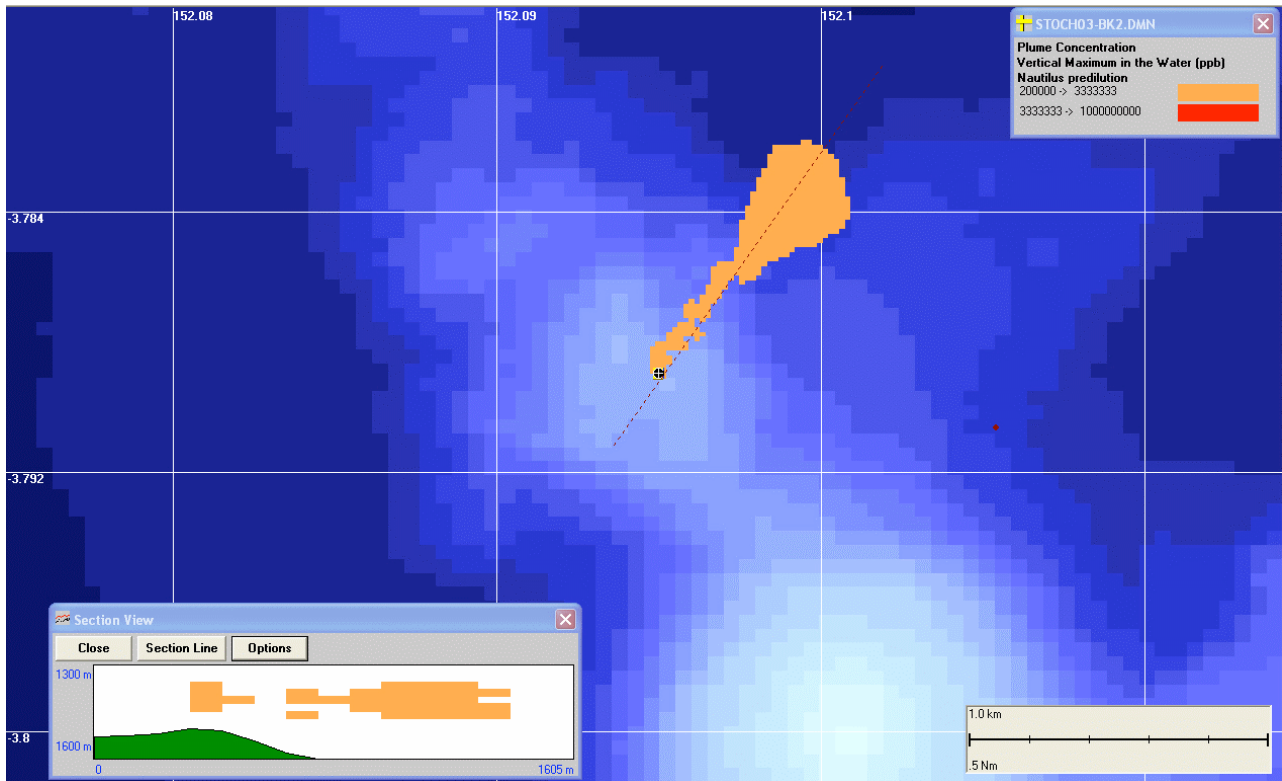


Figure 3.1. Snapshot in time of a ‘worst-case’ plume demonstrating the patchy nature of plumes under the conditions prevailing within the depths of the Bismarck Sea for the 11.4°C scenario. Note insert shows cross-section of the plume between 1,300 m and 1,600 m water depth.

3.3 Affected areas and extents

In Table 3.1, from the stochastic modelling, a comparison of the expected maximum plume concentration for the selected dilution ratios for the discharge given the two potential temperature extremes and the affected areas (square kilometres) and maximum extents (kilometres) from the discharge point are provided. The term “expected maximum concentration” is the mean expected maximum concentration at each grid cell location (the mean value of the maximum from the 100 sample simulations per scenario). In Table 3.1 it can be determined that, on average, plume concentrations exceeding 1/300 dilution was below the grid resolution of 60m x 60m for both discharge temperature extremes. Indeed, a 1/600 dilution is just measurable at this resolution given an average maximum extent of 0.085 km and area being 0.0144 km².

Table 3.1 Comparison of Expected Maximum Plume Concentrations*

Plume Concentration PPB	Plume Concentration Dilution factor	Area (km²) & Extent (km) of each division. Discharge at 5.8°C	Area (km²) & Extent (km) of each division. Discharge at 11.4°C
200000 - 3333333	1/300 -1/5,000	0.47 km ² & 0.60 km	0.30 km ² & 0.49 km
3333333-1000000000	1/300 -1	< 0.0036 km ² & 0.060 km	< 0.0036 km ² & 0.060 km

** Note. Area and extent calculations are cumulative*

In Figure 3.2 the expected maximum concentration (over a 60m x 60m grid cell area) for the lower temperature discharge, 5.8°C is shown. The colour coding represents the selected dilution ratios from Table 3.1. In Figure 3.3 the expected maximum concentration for the higher temperature discharge, 11.4°C, is shown. From Figures 3.2 and 3.3, it can be seen that the discharge temperature creates some variability in the plume extent.

Stochastic modelling also provides a measure of probability for each cell with the model grid. The term “probability of exceeding threshold” is the probability (as percent of samples) that the threshold for the chosen threshold is exceeded at any time at each grid cell location. In Table 3.3 a comparison of the probability of plume concentrations for each cell exceeding the 200,000 PPB (1/5,000 dilution) is provided. Table 3.3 shows that the plume will only exceed the 1/5,000 dilution threshold more than 50% of the time over an area of 0.81 km² at no more than 0.9 km from the discharge site regardless of the temperature of the discharge plume. Table 3.3 also shows that the extent of the plume at concentrations exceeding a 1/5,000 dilution is unlikely to extend more than

5.0 km at any time during the discharge operation regardless of the temperature.

Table 3.3 Comparison of Plume Concentrations Probability (Percent).

Probability of exceeding 1/5,000 threshold (%)	Area (km ²) and extent (km) of each probability band.	
	Discharge at 5.8°C	Discharge at 11.4°C
0-10	11.6 km ² & 4.2 km	9.71 km ² & 5.0 km
10-20	3.78 km ² & 2.5 km	2.49 km ² & 1.9 km
20-30	2.33 km ² & 1.7 km	1.50 km ² & 1.2 km
30-40	1.61 km ² & 1.2 km	1.05 km ² & 0.95 km
40-50	1.11 km ² & 1.0 km	0.76 km ² & 0.81 km
50-60	0.81 km ² & 0.90 km	0.58 km ² & 0.67 km
60-70	0.60 km ² & 0.70 km	0.43 km ² & 0.58 km
70-80	0.42 km ² & 0.60 km	0.29 km ² & 0.44 km
80-100	0.27 km ² & 0.41 km	0.19 km ² & 0.36 km

** Note. Area and extent calculations are cumulative*

In Figure 3.4 a comparison of the probability of exceeding the 1/5,000 concentration threshold is provided showing the “foot-print” for the two extreme of the probable discharge temperatures. The higher probability envelopes (50%-100%) near the proposed release site are affected by the alignment and strength of the tidal currents at this site (southwest/northeast). The lower probability envelopes (0%-50%) in Figure 3.4 show the more variable basin wide circulation characteristics of the Manus Basin.

3.4 Plume Thickness

The 200 individual stochastic model outputs were examined to determine the current and release time/date conditions for the worse case concentrations and greatest movement from the release location. Individual single models were run for 10 time releases and results of plume movement examined in cross section i.e. 3D. Utilising the stochastic model and individual worse case scenarios for both temperature extremes of the discharge water, the estimated maximum sub-sea plume thickness within the water column is no more than 175 metres for these plume temperature extremes. The plume extends beyond these depths over time, but not at concentrations exceeding the thresholds described herein. Hence, given that the temperature of the discharge plume will fluctuate, the modelling conducted herein quantified that the plume will extend, at times, from 1,300 m deep to 1,475m deep at concentrations exceeding the thresholds.

3.5 Sedimentation Thickness

The 1:5,000 dilution ratio is based on the presence of fine particulate (< 8 micron) ore which is still contained within the return production water at concentrations of 5,940 mg/L. Hence a 1:5,000 dilution of this suspended sediment equates to 1.2 mg/L threshold of total suspended solids. However, even though the modelling conducted here demonstrated that the concentrations of this fine material falls rapidly below this threshold after discharge in the water column, this sediment will slowly continue to fall to the seafloor over time and beyond the extents of the plume. In order to understand and quantify the sedimentation of this fine ore over time, additional model runs were conducted to quantify the sedimentation of this ore over the full mining operation (20 months) particularly since this fine material will settle very slowly.

Note that the background daily sedimentation rate for the area has been measured at 0.0965 mg/cm²/day, which equals to approximately 590 g/m² for the 20 months of mining operation (or 0.180 mm) assuming average density of 3,300 kg/m³. From Figure 3.5, it can be seen that the peak bottom thickness from the settling fines is less than 0.1 mm for the same 20 month period. Indeed, the model predicted that sedimentation level between 0.05 mm and 0.1 mm were possible, but extremely patchy. Between these patches, sedimentation levels were below the model resolution here and a few orders of magnitude less than the natural background sedimentation for the region.

4 CONCLUSIONS

In conclusion, from the CHEMMAP single release modelling, and stochastic modelling of the plume concentrations (200 individual sample simulations) for each of the two discharge options using expected maximum concentrations and percent probabilities, the mixing is slightly enhanced when the return water temperature is at the higher end of its potential range in a comparison to when the return water is at the lower end of its temperature range. This is expected, since the buoyancy of the warmer plume will be greater after discharge, hence enabling it to rise higher through the water column, entraining more ambient water as it ascends.

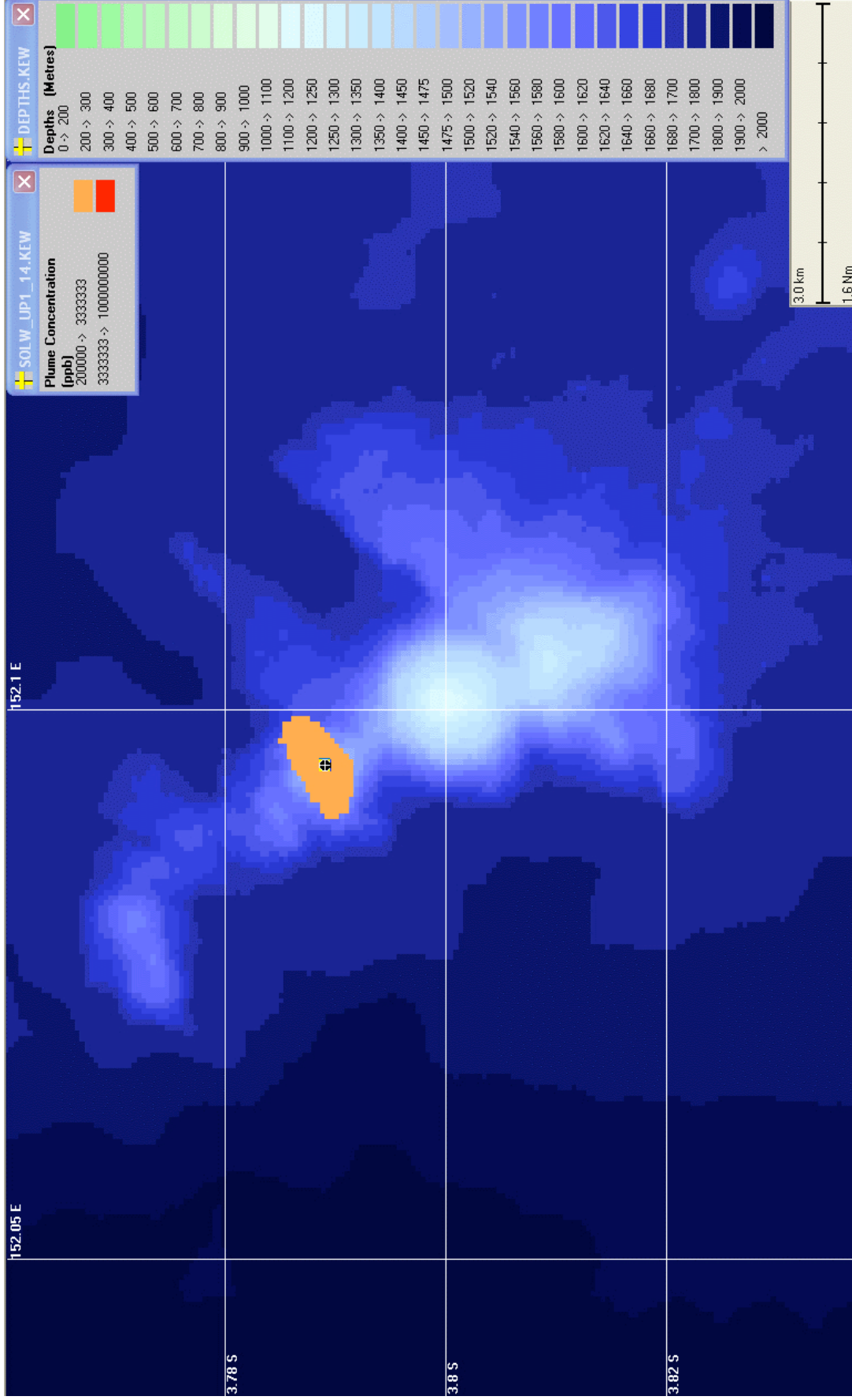


Figure 3.2. The expected (or averaged) maximum concentrations from the return water plume which exceeded the defined thresholds after one year of discharges when discharge temperature is 5.8°C.

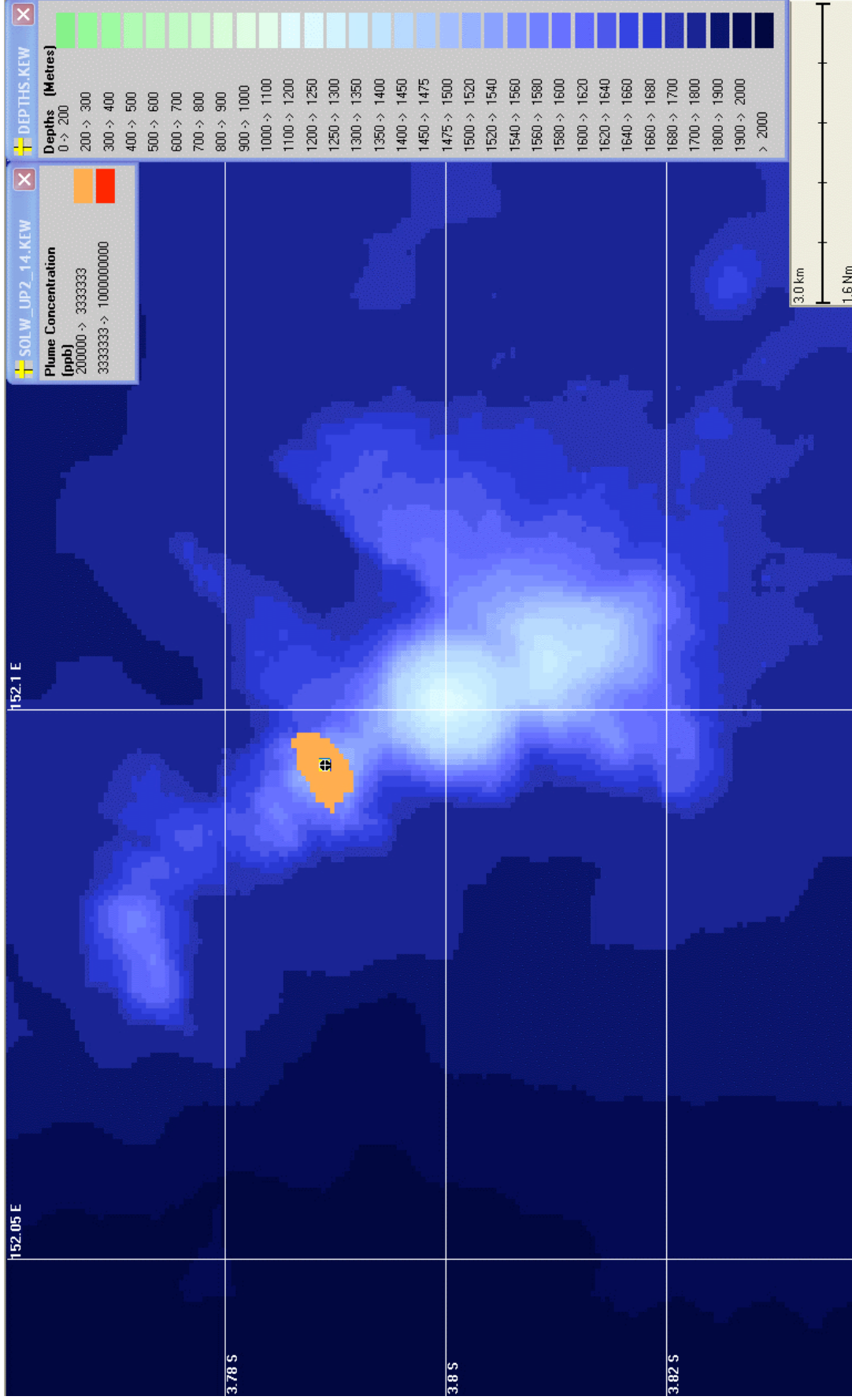
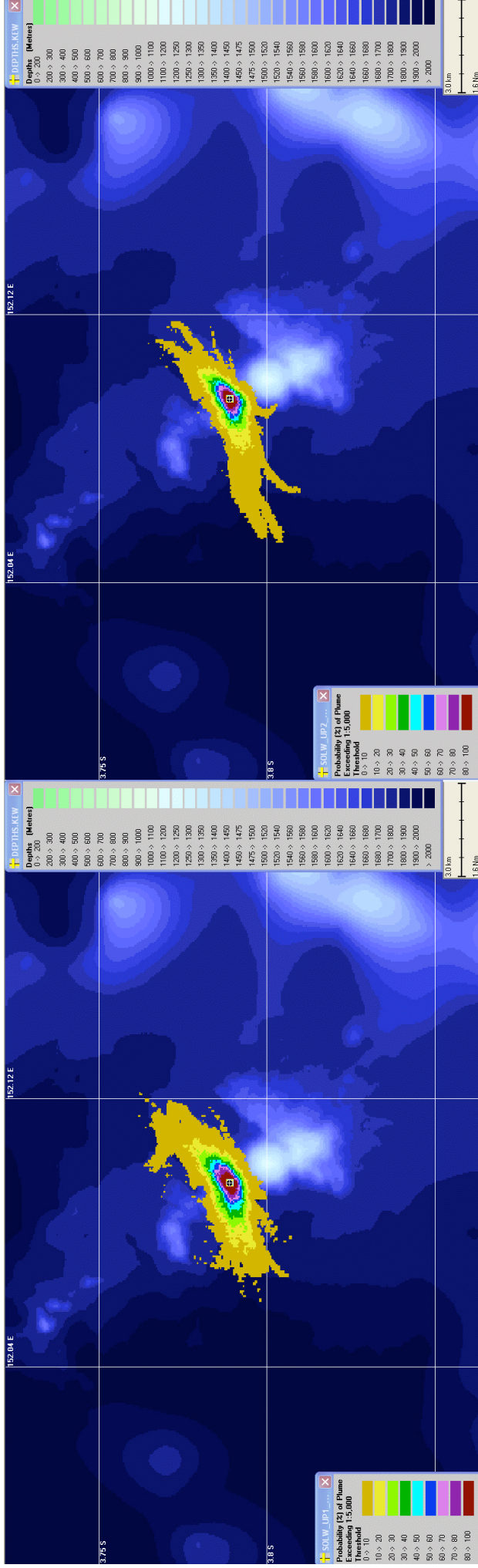


Figure 3.3. The expected (or averaged) maximum concentrations from the return water plume which exceeded the defined thresholds after one year of discharges when discharge temperature is 11.4°C

Figure 3.4
 A zoomed in comparison of the probability of exceeding 1/5,000 threshold concentration at any time over a one year period

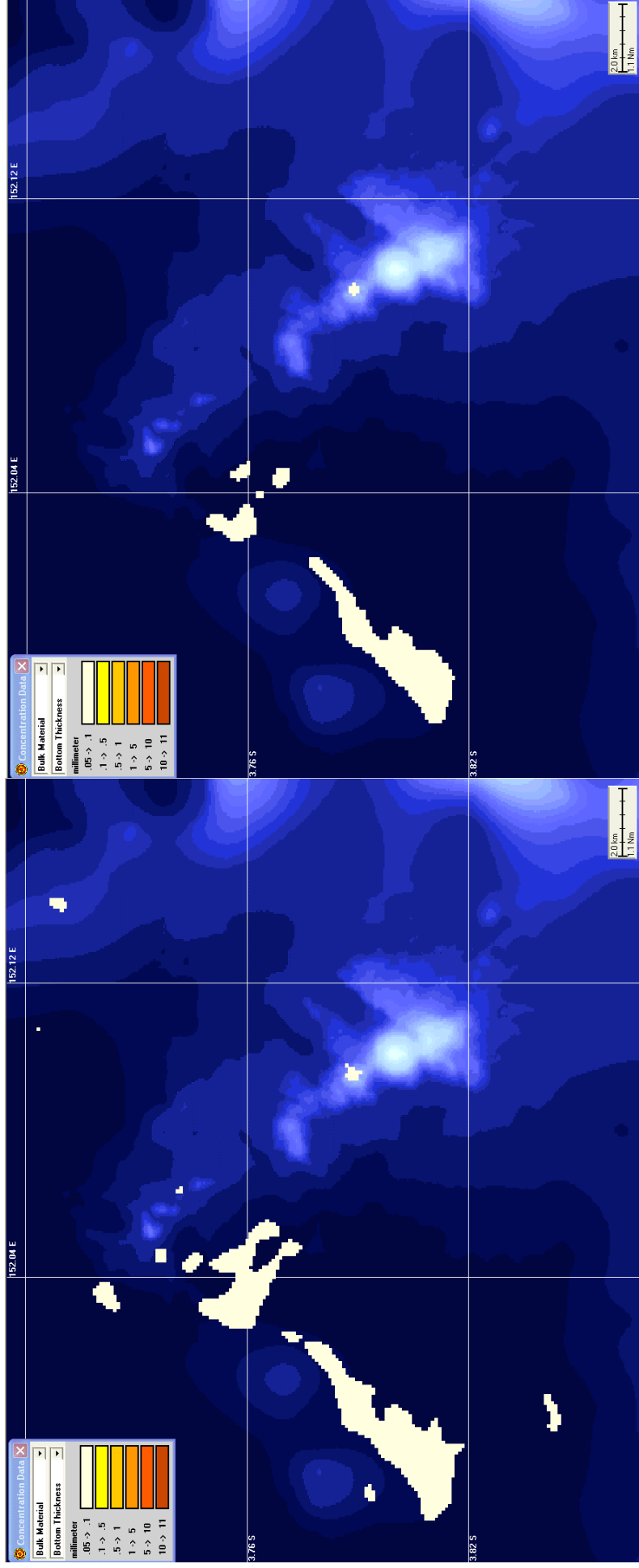


Discharge Temperature at 5.8°C

Discharge Temperature at 11.4°C

Figure 3.5

Bottom sedimentation patterns from the accumulating fine sediment fall-out from the return water plume after 20 months of mining operation. Both figures show some evidence of sediment beyond the plume extent, but patchy and well below the background sedimentation rate for the region.



Discharge Temperature at 5.8°C

Discharge Temperature at 11.4°C

5 REFERENCES

Bear, J. and Verruijt, A. 1987. Modeling groundwater flow and pollution with computer programs for sample cases. Kluwer Academic Publishers.

Bonn Agreement, 1999. Chemical spills at sea – Case studies (Agenda item 3). 11th Meeting of the Contracting Parties, Brest, France, 29 September – 1 October 1999.

Bonn Agreement, 2000. Bonn Agreement Counter Pollution Manual, Volume 2-Strategy/Policy of Pollution Combating, European Classification System.

CambridgeSoft Corporation (2000). ChemFinder Database and Internet Searching. ChemFinder.Com. <http://chemfinder.com>

Center for Disease Control and Prevention, National Institute for Occupational Safety and Health (NIOSH), 2004. International Chemical Safety Cards and International Program on Chemical Safety Projects, U.S. National Version. Available: <http://www.cdc.gov/niosh/npg/npg.html>

The Centre for Environment Fisheries and Aquaculture Science (CEFAS), 2001. Toxicity Database. Available: <http://www.cefas.co.uk/basic/toxdata.htm>

CERC, 1984. Shore protection manual, Vol. I. Coastal Engineering Research Center, Department of the Army, Waterways Experiment Station, U.S. Army Corps of Engineers, Vicksburg, MS.

"Chemical Hazardous Response Information System" (CHRIS) U.S. Coast Guard

Csanady, G.T., 1973. Turbulent diffusion in the environment. D. Reidel Publishing Company, Dordrecht, Holland, 74p.

DiToro, D.M., Zarba, C.S., Hansen, D.J., Berry, W.J., Swartz, R.C., Cowan, C.E., Pavlou, S.P., Allen, H.E., Thomas, N.A., Paquin, P.R., 1991. Annual Review: Technical basis for establishing sediment quality criteria for nonionic organic chemicals using equilibrium partitioning. Environmental Toxicology and Chemistry 10: 1541-1583.

EnvironTIPS, Environment Canada, 1985

European Chemical Bureau (ECB), 2002. European Chemical Bureau Newsletter 12 October 2002. Available: <http://ihcp.jrc.it/DOCUMENTATION/ECB/newsletter200210.pdf>

European Chemical Bureau (ECB), 2004. Risk Assessment Reports. Available: <http://ecb.jrc.it/existing-chemicals/>

French, D., Reed, M., Jayko, K., Feng, S., Rines, H., Pavignano, S., Isaji, T., Puckett, S., Keller, A., French III, F. W., Gifford, D., McCue, J., Brown, G., MacDonald, E., Quirk, J., Natzke, S., Bishop, R., Welsh, M., Phillips, M., Ingram, B.S., 1996. The CERCLA Type A Natural Resource Damage Assessment Model for Coastal and Marine Environments (NRDAM/CME), Technical Documentation, Vol. I -VI, Final Report, submitted to the Office of Environmental Policy and Compliance, U.S. Dept. of the Interior, Washington, D.C., Contract No. 14-0001-91-C-11. April, 1996.

French, D., Schuttenberg, H., Isaji, T., 1999. Probabilities of oil exceeding thresholds of concern: examples from an evaluation for Florida Power and Light. In: Proceedings of the 22nd Arctic and Marine Oil Spill Program (AMOP) Technical Seminar, Environmental Protection Service, Environment Canada, pp.243-270.

French McCay, D.P., 2002. Development and application of an oil toxicity and exposure model, OilToxEx. *Environmental Toxicology and Chemistry* 21(10) 2080-2094.

French McCay, D.P. and Isaji, T., 2004. Evaluation of the consequences of chemical spills using modeling: chemicals used in deepwater oil and gas operations. *Environmental Modelling & Software* 19(7-8): 629-644.

French McCay, D., N. Whittier, M. Ward, and C. Santos, 2004. Spill hazard evaluation for chemicals shipped in bulk using modeling. *Environmental Modelling & Software* 19: in press

Gifford, F.A., 1961. Use of routine meteorological observations for estimating atmospheric dispersion. *Nuclear Safety* 2:47

Ippen, 1966. *Estuary and Coastline Hydrodynamics*. Engineering Scientific Monographs, MacGraw-Hill Book Co., New York, 611p.

Lunel, T. 1991. Chemical spill model based on modeling turbulent mixing at sea. In: Proceedings of the Eighth Technical Seminar on Chemical Spills, Vancouver, BC, Canada, Environmental Protection Service, Environment Canada, pp.47-60.

Lyman, C.J., Reehl, W.F., Rosenblatt, D.H., 1982. *Handbook of Chemical Property Estimation Methods*. McGraw-Hill Book Co., New York.

Mackay, D., Matsugu, R.S., 1973. Evaporation rates of liquid hydrocarbon spills on land and water. *The Canadian Journal of Chemical Engineering* 51: 434-439.

Mackay, D., Shiu, W.Y., Ma, K.C., 1992a. *Illustrated Handbook of Physical-Chemical Properties and Environmental Fate for Organic Chemicals, Vol. I, Monoaromatic Hydrocarbons, Chlorobenzenes, and PCBs*. Lewis Publishers, Chelsea, Michigan, 668p.

Mackay, D., Shiu, W.Y., Ma, K.C., 1992b. *Illustrated Handbook of Physical-Chemical Properties and Environmental Fate for Organic Chemicals, Vol. II, Polynuclear Aromatic Hydrocarbons, Polychlorinated Dioxins, and Dibenzofurans*. Lewis Publishers, Chelsea, Michigan, 566p.

Mackay, D., Shiu, W.Y., Ma, K.C., 1992c. *Illustrated Handbook of Physical-Chemical Properties and Environmental Fate for Organic Chemicals, Vol. III, Volatile Organic Chemicals*. Lewis Publishers, Chelsea, Michigan, 885p.

Mackay, D., Shiu, W.Y., Ma, K.C., 1992d. *Illustrated Handbook of Physical-Chemical Properties and Environmental Fate for Organic Chemicals. Volume IV Oxygen, Nitrogen, and Sulfur Containing Compounds*. Lewis Publishers, Chelsea, Michigan, 930p.

"Oil and Hazardous Materials Technical Assistance Data System" (OHMTADS) NIH/EPA, 1983

Okubo, A., 1971. Oceanic diffusion diagrams. *Deep-Sea Research* 8:789-802.

Proudman Oceanographic Laboratory, 1999. Coastal Observatory Project, Ocean-Shelf Model. Birkenhead, United Kingdom.

Rusin J., Lunel T. and Davies L., 1996. Validation of the Eurospill chemical spill model. In: Proceedings of the 19th Arctic and Marine Oil Spill Program Technical Seminar, Calgary, Alberta, Canada, Environmental Protection Service, Environment Canada, pp. 1437-1478.

Shen, H.T., Yapa, P.D., and Zhang, B. (1995) `A simulation model for chemical spills in the upper St. Lawrence River,. J. Great Lakes Research 21(4) 652-664.

Sloss, P. September 2001. "National Geophysical Data Center(NGDC) CD-ROM, ETOPO2

Strumm, W. and J.J. Morgan, 1996. Aquatic Chemistry. Chemical Equilibria and Rates in Natural Waters. Third Edition. John Wiley & Sons, Inc. NY.

Syracuse Research Center, 2000. Interactive LogKow (KowWin) Demo. <http://esc.syrres.com/interkow/kowdemo.htm>

Thorpe S.A., 1984. On the determination of K in the near surface ocean from acoustic measurements of bubbles. Journal of American Meteorological Society 1984:861-863.

USEPA AND NOAA, 1995. Areal Locations of Hazardous Atmospheres., (ALOHA), Washington D.C., National Safety Council, 1995.

USEPA (U.S. Environmental Protection Agency), 2002. ECOTOX User Guide: ECOTOXicology Database System. Version 2.0. Available: <http://www.epa.gov/ecotox/>

U.S. Secretary of Commerce, 2000. NIST Standard Reference Database Number 69 – February 2000 Release. NIST Chemistry WebBook. <http://webbook.nist.gov/chemistry>

Youssef, M., Spaulding, M.L., 1993. Drift current under the action of wind and waves. In: Proceedings of the 16th Arctic and Marine Oil Spill Program Technical Seminar, Calgary, Alberta, Canada, Environmental Protection Service, Environment Canada, pp.587-615.

Appendix 13

**Prediction of Underwater Noise Associated with a Proposed Deep-Sea Mining
Operation in the Bismarck Sea**

Curtin

UNIVERSITY OF TECHNOLOGY

Centre for Marine Science and Technology

**Prediction of underwater noise associated with a
proposed deep-sea mining operation in the Bismarck Sea**

By:

Alec Duncan, Robert McCauley, and Chandra Salgado-Kent

Prepared for:

Coffey Natural Systems

PROJECT CMST 769
REPORT 2008-30

July 2008

Abstract

This report presents the results of numerical modelling of the production and underwater propagation of thruster cavitation noise from a surface vessel carrying out a subsea mining operation. Modelling indicates that received levels will drop rapidly with distance from the vessel out to a horizontal distance of approximately 2 km, after which they will decay more slowly in accordance with cylindrical spreading.

The noise is likely to be audible to marine animals at ranges in excess of 600 km in directions unimpeded by land or shallow water depths (to the west in this case), however levels will be insufficient to produce physiological effects such as temporary threshold shifts at any range, except perhaps in the immediate vicinity of the vessel (within tens of metres). To put this audibility range in context it is important to note that long range sound propagation in the ocean is common for both natural and man-made sounds. For example, low frequency sounds produced by the nearby North Su subsea volcano are likely to be audible for thousands of kilometres, and other seismic events such as earthquakes can produce sounds that are well above ambient noise levels at ranges of thousands to tens of thousands of kilometres. In the case of man-made sources, sounds produced by airgun arrays during seismic surveys have been recorded by the authors at ranges of several thousand kilometres.

Marine mammals are likely to avoid the vessel at ranges of approximately 15 km, and may suffer signal masking effects at similar ranges. However, some animals may also be attracted to the vessel, and the avoidance range is likely to reduce over time as animals habituate to the vessel's presence.

An analysis of the production and propagation of noise from the subsea mining machine and the potential impacts of these noise levels on marine mammals has not been carried out due to a lack of information about the machine's likely source characteristics. The noise produced by this device needs to be considered in the context of the operation being carried out approximately 1 km from an active subsea volcano, which is itself likely to be a major source of low frequency underwater sound.

Table of Contents

1	Introduction	5
2	Methods	7
2.1	Source modelling	7
2.2	Propagation modelling	9
2.3	Received level calculations	13
3	Results	14
4	Discussion	19
4.1	Received level modelling	19
4.2	Potential impacts on marine mammals	22
5	Conclusions	27
	References	29

List of Figures

Figure 1. Geographical location of the proposed mining operation (red square).....	6
Figure 2. Third octave source spectra. Red - measured spectrum of the <i>Pacific Ariki</i> , blue - extrapolated spectrum for mining vessel.	9
Figure 3. Source location for the subsea mining operation showing detailed bathymetry. The dotted magenta lines show the bathymetry profiles used for the propagation model runs.....	11
Figure 4. Bathymetry profiles used for propagation modelling for source location P1.....	12
Figure 5. Comparison between acoustic reflection coefficients for a basalt seabed (blue), the equivalent fluid seabed (red), and the sandy silt seabed (green). Acoustic properties of the materials are given in Table 2.	12
Figure 6. Water column sound speed profile used for propagation modelling.	13
Figure 7. Plots of predicted received level vs. range and depth for azimuths from 0° to 135°. Top four plots are for seabed model A., bottom four plots are for seabed model B.	15
Figure 8. Plots of predicted received level vs. range and depth for azimuths from 180° to 315°. Top four plots are for seabed model A., bottom four plots are for seabed model B.	16
Figure 9. Zoomed view of plots of predicted receive level vs. range and depth for the eight different azimuths (seabed model A).....	17
Figure 10. Scatter plot of received levels as a function of range for all depths and azimuths. Blue 'x' are for seabed model A, red '+' are for seabed model B. Solid line is for spherical spreading with a source level of 196.4 dB re 1 μ Pa @ 1m. Broken line is cylindrical spreading with a best-fit source level of 172 dB re 1 μ Pa @ 1m.	18
Figure 11. Predicted maximum level at any depth as a function of range and azimuth. Top plot is for seabed model A. Bottom plot is for seabed model B.	19
Figure 12. Extrapolated transmission loss vs. range assuming cylindrical spreading without (blue) and with (red) absorption.	21
Figure 13. Distribution of received pygmy blue whale call components heard in the Perth Canyon in 2000.	27

List of Tables

Table 1. Characteristics of the <i>Pacific Ariki</i> and the vessel under consideration for the mining operation.	8
Table 2. Seabed acoustic data used in propagation modelling.....	11
Table 3. Range beyond which all received levels are expected to be below the specified threshold. Spherical spreading results are based on a point source with a source level of 196.4 dB re 1 μ Pa @ 1m.	14

1 Introduction

This report presents the results of numerical modelling of underwater sound levels from a proposed deep-sea mining operation in the Bismarck Sea (see Figure 1), and a discussion of the likely impacts of these levels on any marine mammals in the area.

Although there would be a variety of sound sources involved in such an operation, the most significant are likely to be the cavitation noise produced by the thrusters on the surface vessel, and noise produced by the subsea mining machine as it grinds the rock face. Cavitation noise is well understood and therefore predictable with a reasonable degree of confidence, and forms the focus of this report.

Conversely, the subsea mining machine is a unique device being constructed specifically for this operation. It is likely to produce an acoustic spectrum with prominent peaks in a harmonic series based on the frequency corresponding to the rate at which cutting teeth strike the rock face. However, the likely acoustic source level, and the rate of decay of the spectrum with frequency are unknown, and the uniqueness of the device means that any estimates of these parameters will have such large uncertainties that they are of no practical use. Consequently, the likely effects of noise produced by the machine have not been quantified.

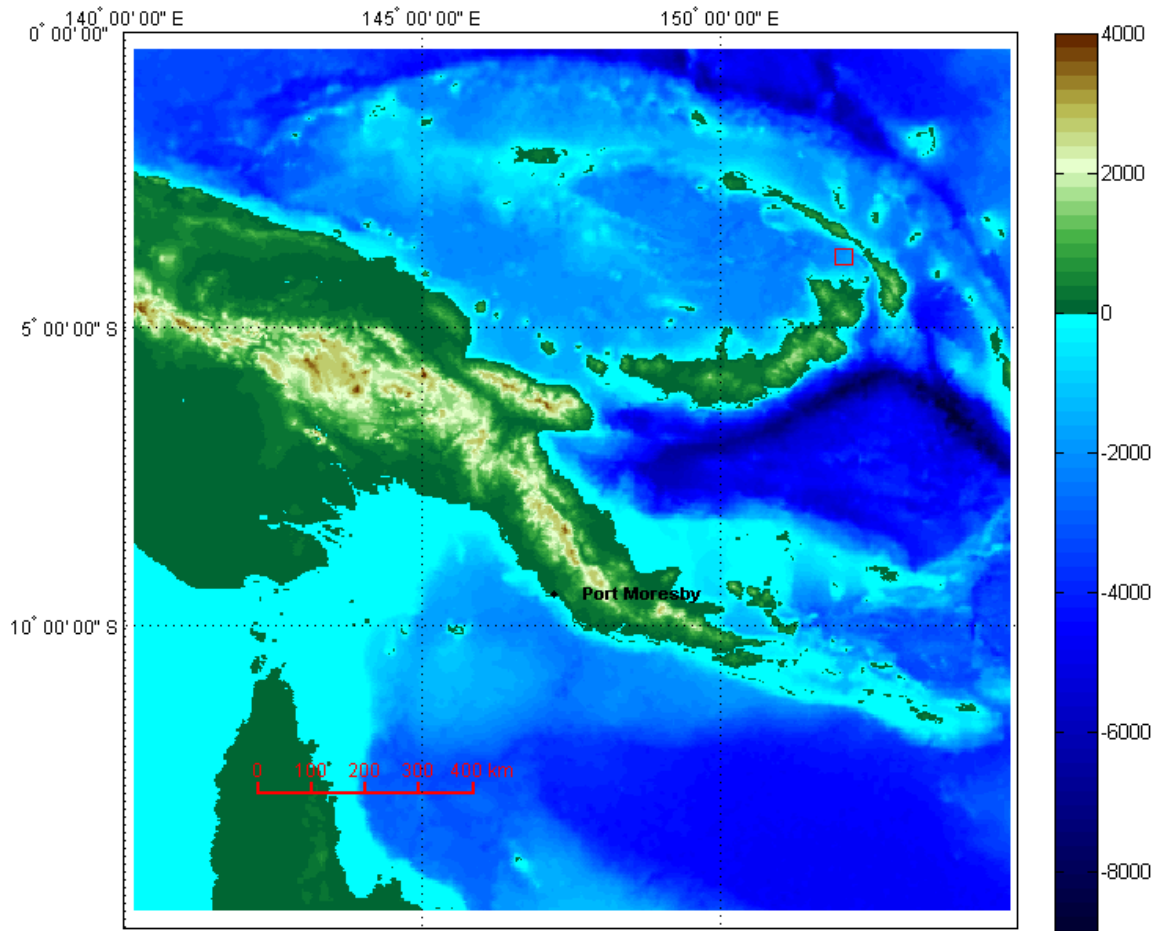


Figure 1. Geographical location of the proposed mining operation (red square).

2 Methods

2.1 Source modelling

Cavitation in water occurs when the pressure in a particular location drops below the saturated water vapour pressure. Bubbles of water vapour then form - the water effectively boils, but due to a lowering of pressure, rather than the increase in water vapour pressure with temperature. When these bubbles move into a region of higher pressure they implode violently, producing a sharp, impulsive sound.

For a propeller, there is a low pressure region on the forward face of each blade which can (and usually does) result in the continuous formation of cavitation bubbles, which subsequently move into a region of higher pressure and implode. The combined effect of the implosion of many cavitation bubbles is high intensity, broadband noise, usually modulated at the propeller blade rate (the shaft rotation rate multiplied by the number of blades).

Because of its importance for passive sonar detection of ships and submarines, cavitation noise has been extensively studied (see eg. Ross, 1987), however this has been in the context of ships travelling at speed, rather than ships holding station on DP. The source model used in this report is therefore based on measurements made by one of the authors of underwater sound levels produced by a rig tender (*Pacific Ariki*) on DP (McCauley 1998). The characteristics of the *Pacific Ariki* are given in Table 1, and the measured, third octave source spectrum is shown in Figure 2. The *Pacific Ariki* is a much smaller vessel than the proposed mining vessel (see Table 1). Levels have therefore been extrapolated to those to be expected for a larger vessel by assuming that a constant proportion of the mechanical power is converted to acoustic power. This relationship has been found to hold reasonably well for surface vessels operating at their normal cruising speed (Ross 1987). The source level corrections given in Table 1 are therefore given by:

$$Correction = 10 \log_{10} \left(\frac{P_{vessel}}{P_{Ariki}} \right) \text{ (dB)}$$

where P_{vessel} is the total installed thruster power on the vessel, and P_{Ariki} is the total installed thruster power on *Pacific Ariki*. The resulting source spectrum is shown in

Figure 2. The corresponding broadband source level was calculated to be 196.4 dB re 1 μ Pa @ 1 m (this is the sum of the mean square pressure contributions from each of the 1/3 octave bands shown in Figure 2).

This *Pacific Ariki* spectrum is based on measurements made in a single direction relative to the vessel, so no source directionality data is available. However, given the nature of cavitation noise, and the fact that the thrusters are located at different positions on the vessel, and in many cases can be rotated in azimuth, it is reasonable to assume that it is omnidirectional.

Based on the expected vessel draft, the source was assumed to be at a depth of 7 m below the water surface.

Table 1. Characteristics of the *Pacific Ariki* and the vessel under consideration for the mining operation.

Vessel	Pacific Ariki	Proposed mining vessel
Length Over All	64 m	150 m
Operating draft	6.6 m	7 m
Tonnage	2,600 (displacement)	14,000
Propulsion power	4 x 1500 kW = 6,000 kW	22,800
Retractable thrusters	1 x 600 kW	5 x 3800 kW + 1 x 2000 kW = 21000 kW
Tunnel thrusters	2 x 600 kW = 1200 kW	
Total thruster power	1,800 kW	21,000 kW
Total thruster power relative to Pacific Ariki	1	11.7
Source level dB correction	0 dB	10.7 dB

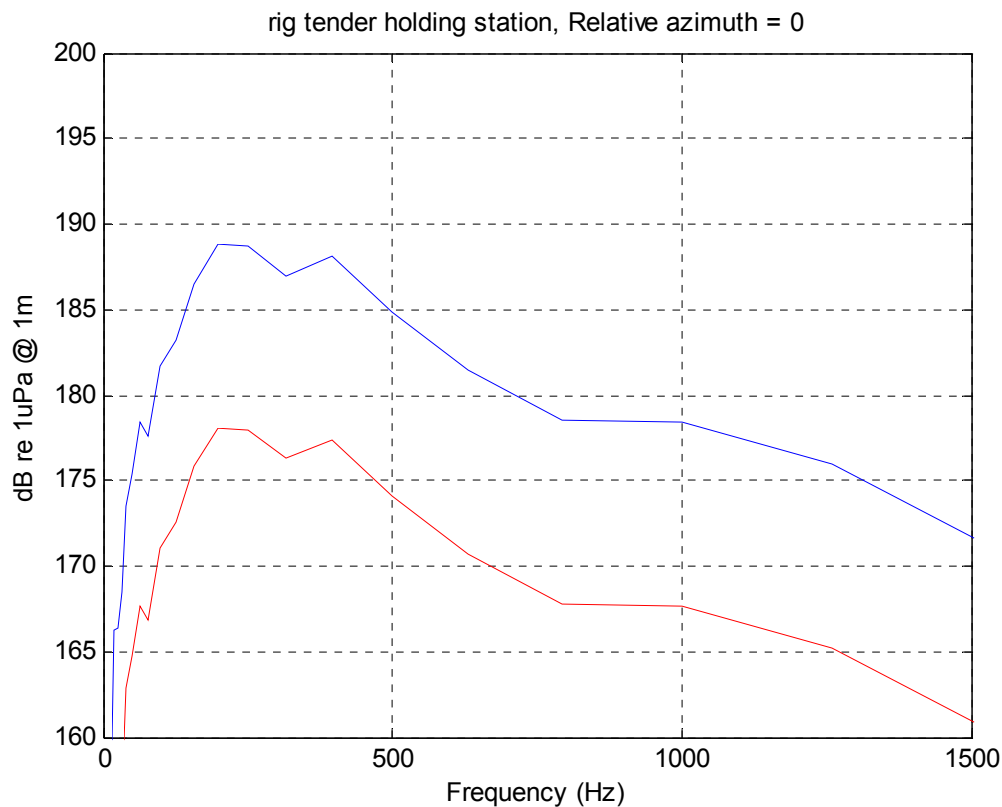


Figure 2. Third octave source spectra. Red - measured spectrum of the *Pacific Ariki*, blue - extrapolated spectrum for mining vessel.

2.2 Propagation modelling

The location of the proposed mining operation (see Figure 3) is a seamount formed by volcanic activity. Geological information for the area indicates that the seabed is primarily a hard massive sulphide material with some basalt, but that at depths greater than 1650 m this is "covered by an apron of dark gray volcanic sandy silts and silty sands" (Coffey Natural Systems, personal communication, July 2008). For comparison purposes propagation modelling was carried out using two seabed models: A. a basalt seabed at all water depths, and B. a basalt seabed for depths less than 1650 m, and a sandy silt seabed for greater depths. A basalt seabed is highly reflective to sound, so model A represents the worst-case situation.

Geoacoustic parameters appropriate for these materials are given in Table 2 (based on Jensen et. al. 2000). Propagation model runs were carried out using bathymetry profiles

corresponding to the eight directions indicated in Figure 3. These profiles are plotted in Figure 4.

Attempts to run the elastic parabolic equation model, RAMS, using these bathymetry profiles and a basalt seabed model were unsuccessful, with the model becoming unstable at higher frequencies. An equivalent fluid model was therefore devised, with parameters chosen to provide as close a match as possible to the reflection coefficient for basalt over the grazing angle range 0° to 70° , which enabled the more stable fluid parabolic equation model RAMGeo, written by Mike Collins from the US Naval Research Laboratory, to be used for propagation modelling.

The geoacoustic parameters of the equivalent fluid are also given in Table 2, and a comparison between reflection coefficients for the basalt seabed and the equivalent fluid seabed is shown in Figure 5. There is very good agreement between the two seabed models for all grazing angles less than 70° , but the fluid model underestimates the reflection coefficient at steeper angles. This will lead to a slight underestimation of noise levels in the lower half of the water column at very short range (< 1 km).

The sound speed profile used for the modelling was obtained from the nearest grid point of the World Ocean Atlas (2005) and is shown in Figure 6.

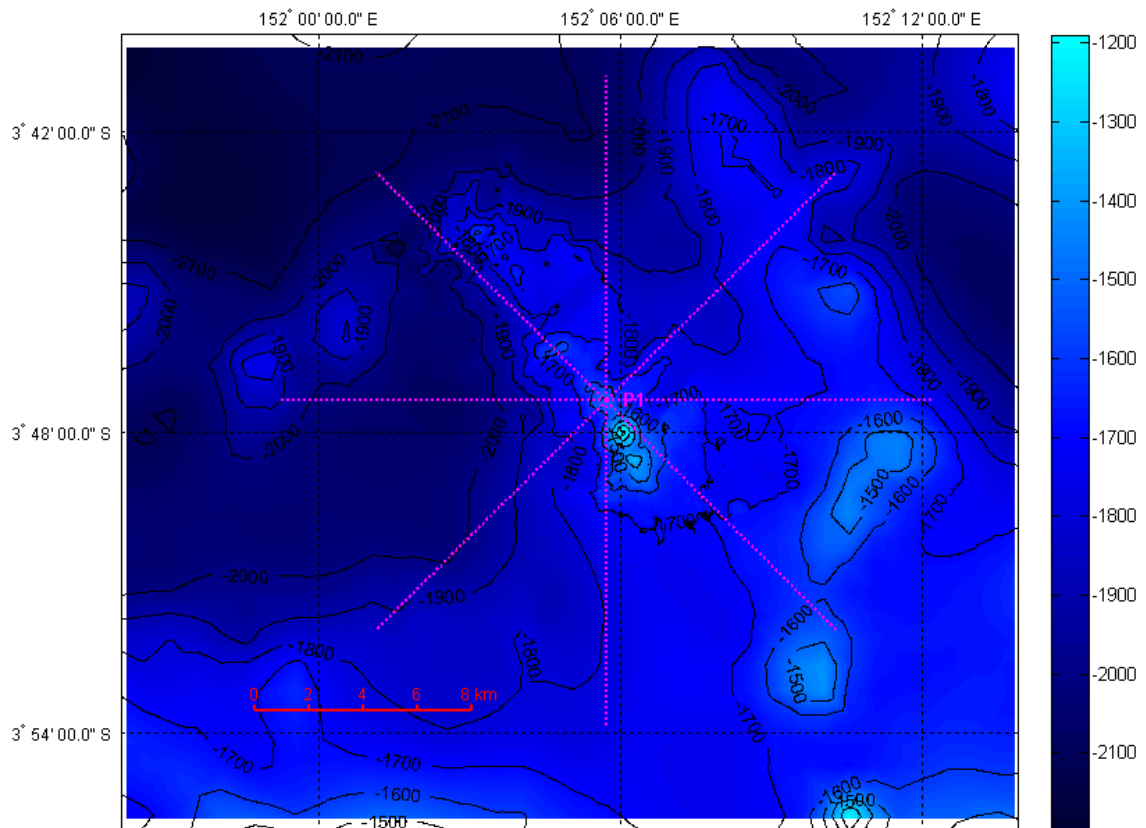


Figure 3. Source location for the subsea mining operation showing detailed bathymetry. The dotted magenta lines show the bathymetry profiles used for the propagation model runs.

Table 2. Seabed acoustic data used in propagation modelling.

Material	Density (kg.m ⁻³)	Compressional wave speed (m/s)	Compressional wave attenuation (dB per wavelength)	Shear wave speed (m/s)	Shear wave attenuation (dB per wavelength)
Basalt	2700	5250	0.1	2500	0.2
Equivalent fluid seabed	2700	2330	1.15	0	0
Sandy silt	1800	1650	0.9	0	0

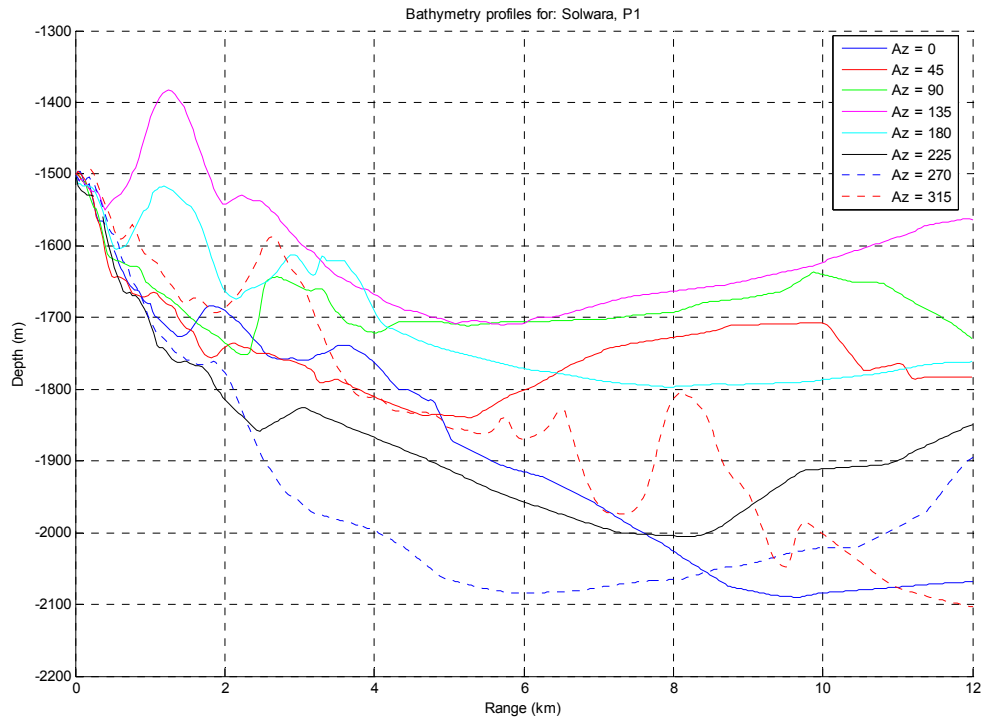


Figure 4. Bathymetry profiles used for propagation modelling for source location P1.

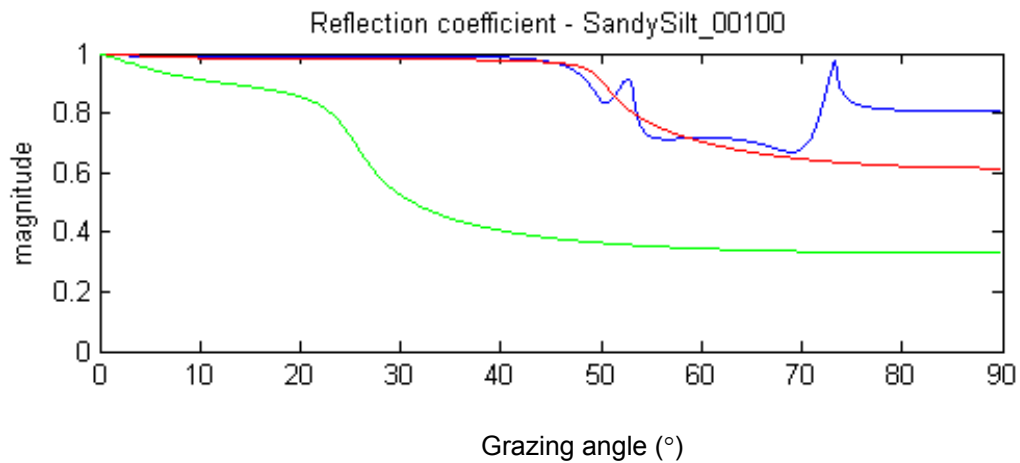


Figure 5. Comparison between acoustic reflection coefficients for a basalt seabed (blue), the equivalent fluid seabed (red), and the sandy silt seabed (green). Acoustic properties of the materials are given in Table 2.

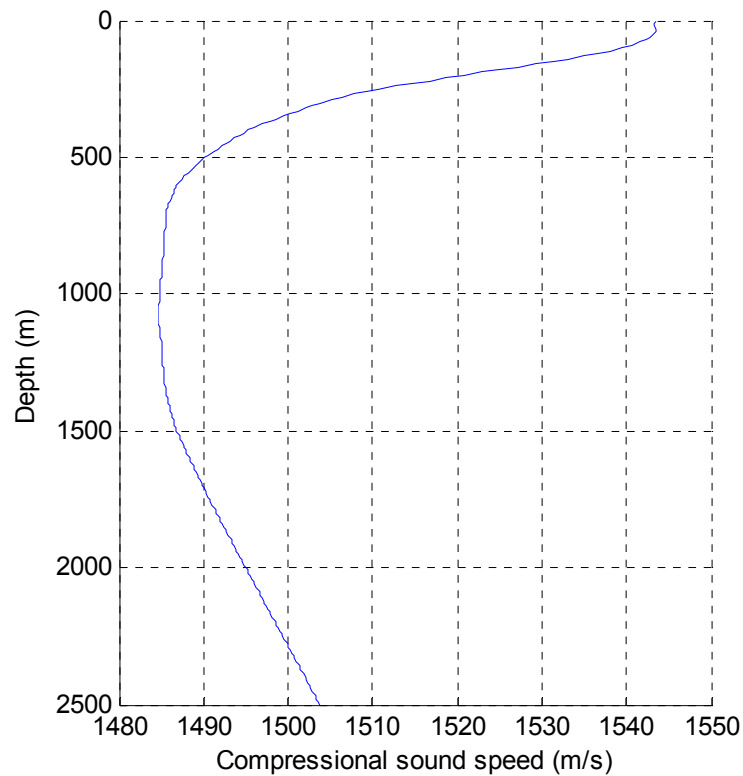


Figure 6. Water column sound speed profile used for propagation modelling.

2.3 Received level calculations

Received levels were calculated for each bathymetry track as follows:

- The propagation model was run to obtain transmission loss as a function of range and depth for frequencies spaced at 1/3 octave intervals from 8 Hz to 1 kHz.
- The source level at each of these frequencies was obtained by integrating the source spectrum over a 1/3 octave frequency band centred on the desired frequency.
- The source level and transmission loss were then combined to compute the received level as a function of range and depth for a grid of points covering the length of the propagation track (12 km) to a depth of 2000 m. Range and depth increments were both 50 m.

3 Results

Plots of the received level as a function of range and depth out to the maximum modelled range of 12 km are given in Figure 7 and Figure 8. Zoomed versions of the same plots for seabed model A, covering horizontal ranges of 0 to 3 km, are shown in Figure 9, and a scatter plot of received level vs. range for all azimuths is shown in Figure 10. Plots of maximum received level at any depth as a function of azimuth are given in Figure 11.

In addition, Table 3 summarises the maximum ranges for specific received level thresholds being exceeded, and compares the modelling results to spherical spreading. Note that the spherical spreading results are based on the assumption of a point source, whereas in practice the source will be distributed in space, and the 180 dB re 1 μ Pa level may not be exceeded anywhere.

Table 3. Range beyond which all received levels are expected to be below the specified threshold. Spherical spreading results are based on a point source with a source level of 196.4 dB re 1 μ Pa @ 1m.

Threshold	180 dB re 1 μ Pa	170 dB re 1 μ Pa	160 dB re 1 μ Pa	150 dB re 1 μ Pa	140 dB re 1 μ Pa
Range assuming spherical spreading	6.6 m	21 m	66 m	209 m	661 m
Range from modelling	-	-	70 m	350 m	1100 m

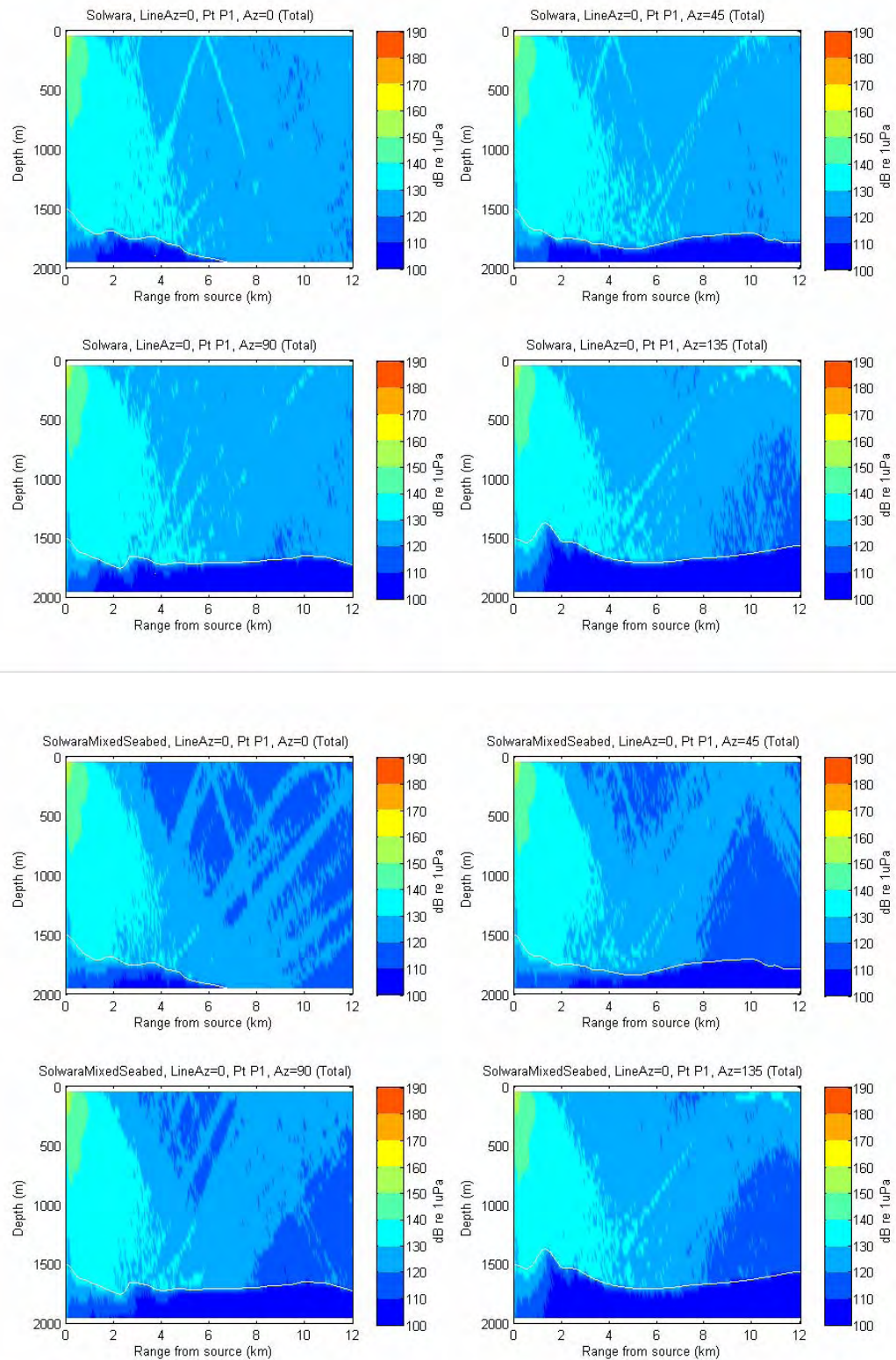


Figure 7. Plots of predicted received level vs. range and depth for azimuths from 0° to 135° . Top four plots are for seabed model A., bottom four plots are for seabed model B.

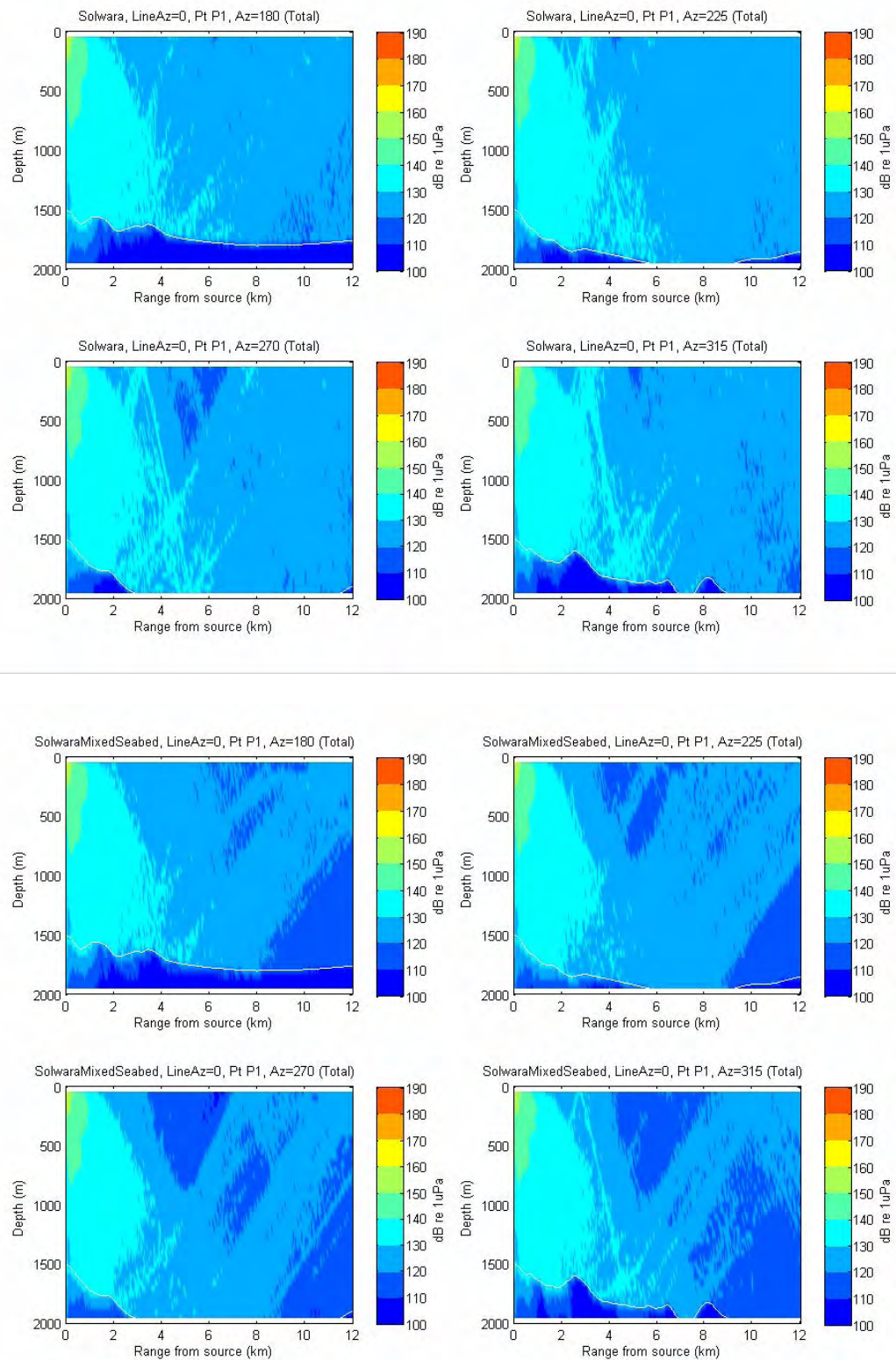


Figure 8. Plots of predicted received level vs. range and depth for azimuths from 180° to 315° . Top four plots are for seabed model A., bottom four plots are for seabed model B.

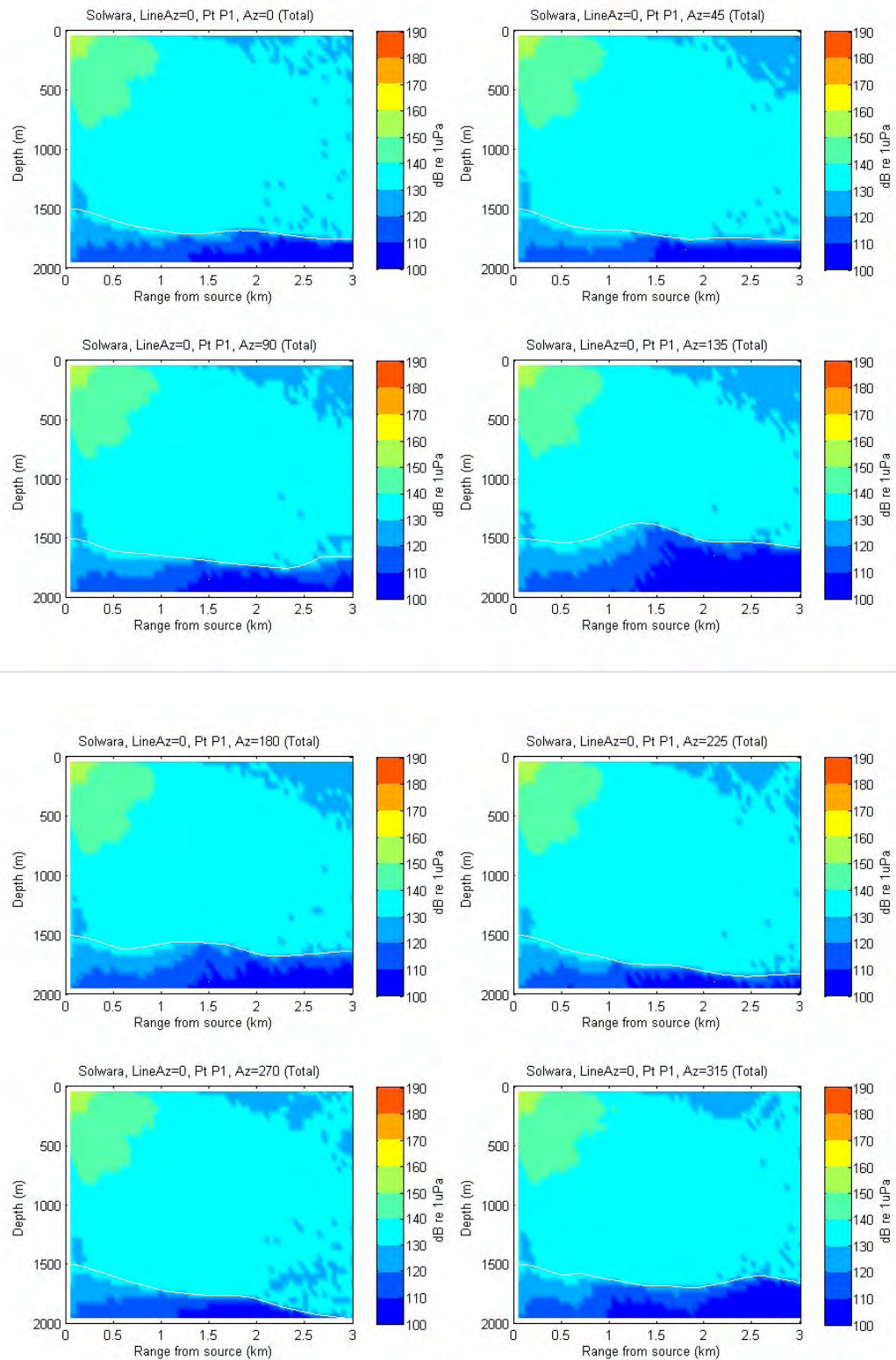


Figure 9. Zoomed view of plots of predicted receive level vs. range and depth for the eight different azimuths (seabed model A).

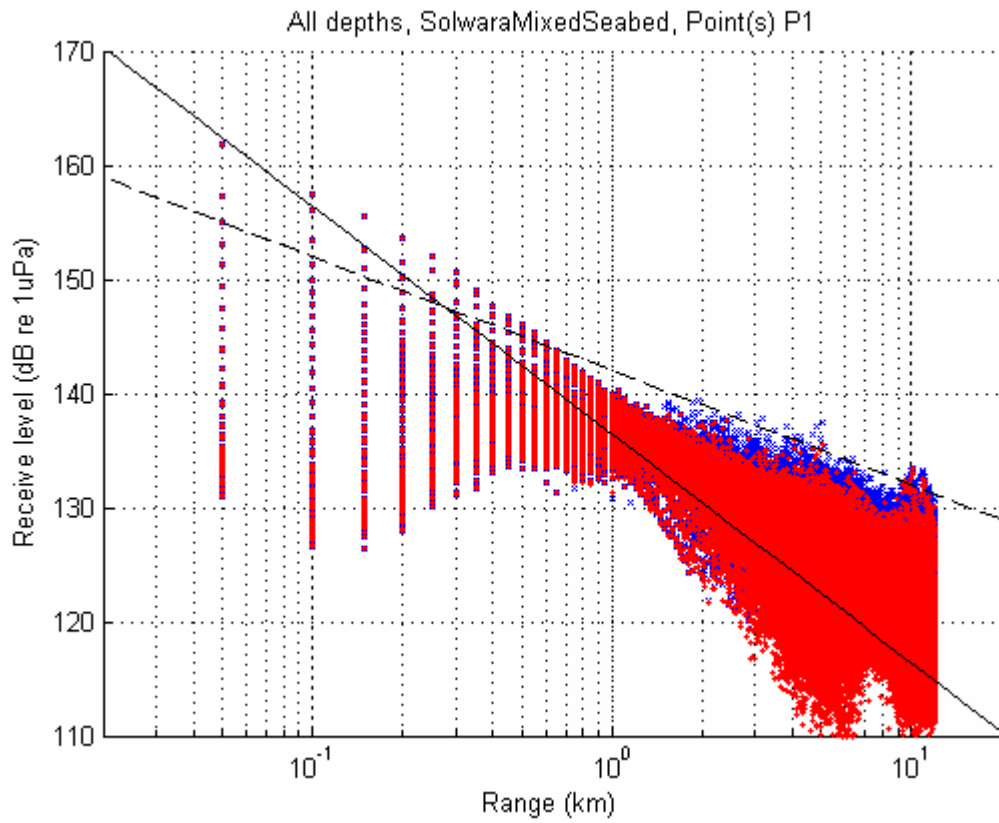


Figure 10. Scatter plot of received levels as a function of range for all depths and azimuths. Blue 'x' are for seabed model A, red '+' are for seabed model B. Solid line is for spherical spreading with a source level of 196.4 dB re 1 μ Pa @ 1m. Broken line is cylindrical spreading with a best-fit source level of 172 dB re 1 μ Pa @ 1m.

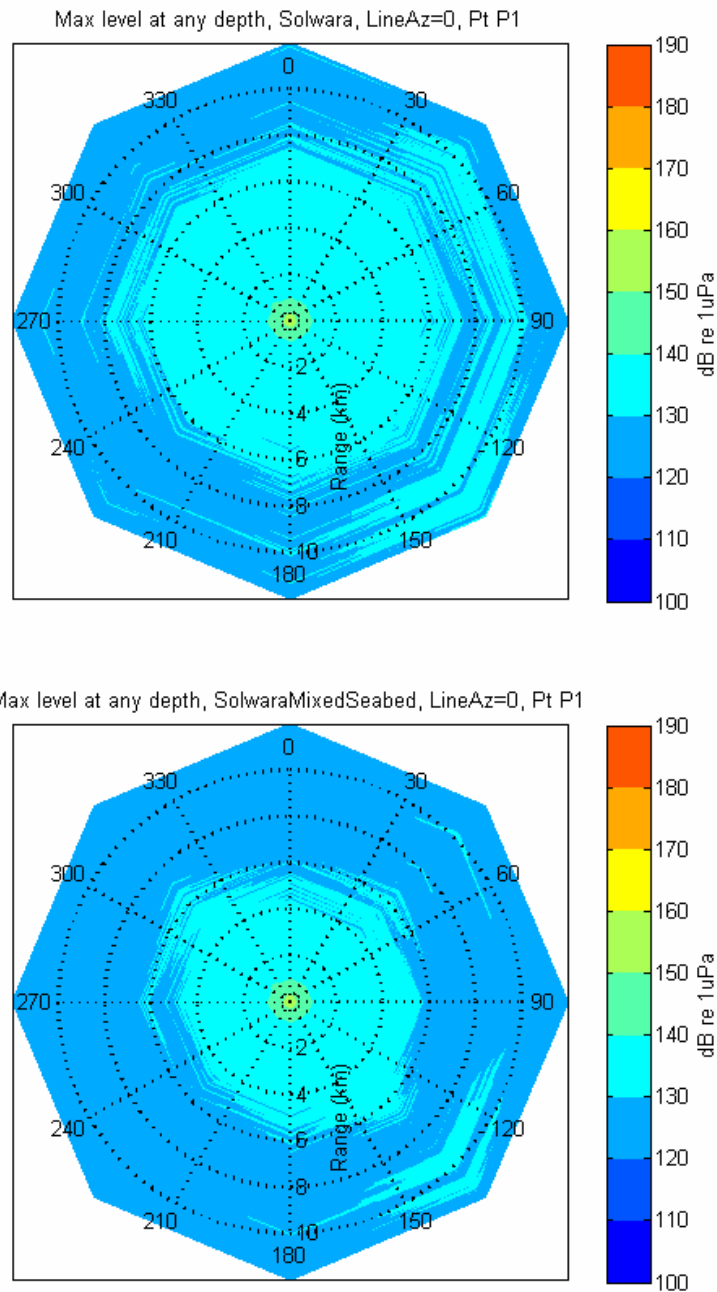


Figure 11. Predicted maximum level at any depth as a function of range and azimuth. Top plot is for seabed model A. Bottom plot is for seabed model B.

4 Discussion

4.1 Received level modelling

The following features of the propagation modelling results are noteworthy:

- Noise levels attenuate rapidly with range out to about 2 km, after which they drop off more slowly. This is due to the increasingly important contribution of seabed reflected sound at longer ranges.
- Results for different azimuths are similar, indicating that the overall seabed topography has a relatively minor effect. However, some bathymetry profiles result in distinct focussing effects, resulting in localised increases in received sound levels.
- At very short range the reduction in sound level with increasing range corresponds to spherical spreading (see Table 3 and Figure 10), but this approximation becomes successively worse as the range increases and the contributions of the seabed and sea surface reflections become more important.
- At ranges beyond 2 km the rate of reduction of maximum received level corresponds well to cylindrical spreading (see Figure 10). This is to be expected given that the sea surface and basalt seabed are almost perfect reflectors at small grazing angles, and even the sandy silt seabed has a high reflection coefficient at these angles (see Figure 5). In addition, the sound speed profile in Figure 6 will result in sound being refracted away from the boundaries, towards the depth of the sound speed minimum at around 1000 m, further reducing boundary losses. Seawater absorption losses are very small at these frequencies and ranges, so the only significant loss mechanism is spreading in the horizontal plane. It would therefore be reasonable to use the following formula, based on cylindrical spreading and a best-fit effective source level, to predict the maximum received level at longer ranges:

$$RL = 172 - 10 \log_{10}(r) \quad (1)$$

where RL is the received level (dB re 1 μ Pa), and r is the horizontal range in metres. Note that this formula is only valid for ranges greater than 2 km and small enough that absorption isn't a significant factor. Absorption increases strongly with increasing frequency and therefore acts as a low-pass filter. For a reasonably narrow band source spectrum like the one considered here its effects can be included approximately by modifying (1) as follows:

$$RL = 172 - 10 \log_{10}(r) - ar \quad (2)$$

where a is the absorption coefficient at the centre frequency in dB/m. A formula

for computing a is given in Fisher and Simmons (1977), and yields a value of 7.3×10^{-6} dB/m at 250 Hz. Figure 12 shows that in this case absorption is likely to become significant at ranges in excess of 100 km.

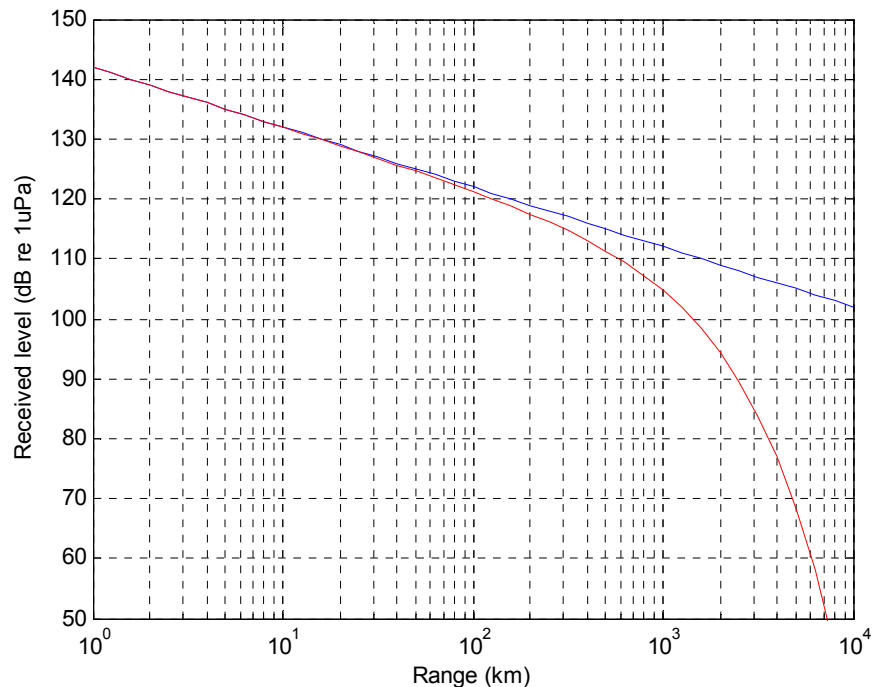


Figure 12. Extrapolated transmission loss vs. range assuming cylindrical spreading without (blue) and with (red) absorption.

- There is only a minor difference between results obtained using the two different seabed models. This appears to be because the interaction of the sound with the relatively steep basalt downhill slopes results in the rays being flattened so that by the time they hit the softer seabed a lot of the energy is at grazing angles less than the critical angle (~ 20 degrees) and is therefore strongly reflected. The most noticeable difference between the results for the two seabed models can be seen in the range-depth plots of Figure 7 and Figure 8. It is apparent that in the case of the basalt seabed (model A), there is energy travelling at steep angles that fills in the 'holes' in the model B received level plots. Conversely, the softer sediment in model B rapidly attenuates this energy.

4.2 Potential impacts on marine mammals

Modelling of the likely underwater noise produced by the mining vessel holding position indicates:

- That the vessel will be audible at ranges > 600 km. This is based on Equation (2), which assumes cylindrical spreading, and an absorption coefficient of 7.3×10^{-6} dB/m, which is the applicable value for 250 Hz. The definition of audible used here is that the received level due to vessel noise is greater than a background broadband noise level at the upper end of a 'normal' range of 95-110 dB re $1 \mu\text{Pa}$. This is not an exact calculation because it doesn't take into account the frequency dependent effects of absorption, which will result in the received signal spectrum being progressively biased towards lower frequencies as the range increases. Whether Equation (2), continues to apply over such long ranges depends primarily on the water depth over the propagation path, as boundary interactions, and hence attenuation will increase rapidly once the sound reaches continental shelf depths of a few hundred metres. From the geography of the area shown in Figure 1 it is apparent that unimpeded propagation to this range would only be possible in an arc from south-west to north-west of the mining site.
- That the range at which a broadband noise level of 140 dB re $1 \mu\text{Pa}$ was estimated to be reached was 1100 m.
- That the range at which a broadband noise level of 150 dB re $1 \mu\text{Pa}$ was estimated to be reached was 350 m
- That the range at which a broadband noise level of 160 dB re $1 \mu\text{Pa}$ was estimated to be reached was approximately 70 m. Note that the modelling exercise, by necessity, considers the source to be a point in space. In reality this is not the case, the source is spatially distributed across the vessel dimensions plus some portion of the bubble plume around the vessel. Hence the higher levels experienced (ie. > 160 dB re $1 \mu\text{Pa}$) can conservatively be considered as occurring approximately within 70 m of the vessel extent.

It is believed that broadband noise levels above approximately 180 dB re $1 \mu\text{Pa}$ are required to produce detectable physiological effects such as temporary hearing threshold shifts (variety of workers, summarised in Richardson et. al. 1995), although some more

recent studies have indicated that continuous signals with levels as low as 160 dB re 1 μ Pa may produce measurable effects in some species (National Research Council, 2005). Given that predicted broadband noise levels are < 180 dB re 1 μ Pa even at close range, and drop to 160 dB re 1 μ Pa within 70 m of the vessel, then it is very unlikely that the mining vessel will cause significant physiological effects to marine mammals unless they are immediately adjacent to the vessel. This leaves potential environmental effects as:

- Attraction to the source
- Avoidance from the source at some range
- Masking of signals of interest
- Possible increase in noise induced stress for animals which linger in the area.

The frequency content of cavitation noise is broad band, that is it has energy spread over a remarkably wide range of frequencies. Highest noise levels will likely occur in the 10 Hz to several kHz range but there will be significant energy in the higher frequencies, up into many tens of kHz. This will make the mining vessel audible to a wide range of marine fauna, including toothed whales which hear best in higher frequencies (optimal range for species likely to be in the area is 20-80 kHz) and great whales (optimal hearing sensitivity < 1 kHz).

The mining vessel will be a static or slowly moving source. The possible avoidance effects, which involve an animal deviating to avoid vessel collision, may therefore be reduced. Sources which are continual and do not move favour marine animals readily acclimating to them.

Attraction

It is possible that the mining vessel will attract some marine animals. There have been recent experiments which have shown that many late stage larval fish are attracted to relatively non-specific broadcast sounds emulating reef systems (Simpson et. al. 2005). It may be possible that similar attraction of larval fishes to the vicinity of the mining vessel may occur.

It may also be possible that the fixed mining noise will attract whales. The noise will be detectable typically at hundreds of km depending on the prevailing background sea noise

conditions (noting that for a signal to be discernible amongst the background noise it needs to be a few dB above the ambient conditions). It would not be inconceivable that some whales are attracted to the vessel noise out of "curiosity" or that through time the vessel becomes considered by resident animals as "landmarks".

Avoidance and behavioural effects

The estimated noise levels calculated indicate that when the mining vessel is working an approaching marine animal may detect the facility at hundreds of km. If the wind picks up then the range where the vessel is clearly audible will drop. Although the vessel may be audible at potentially long ranges its noise will not be greatly above background noise conditions. As the animal approaches the vessel the underwater noise will become more intense and perceived by an animal as louder. But, it would not be until the animal is within perhaps 1-2 km of the vessel that the signal could be considered to be 'loud', as indicated by the 140 dB re 1 μ Pa level.

Richardson et. al. (1995) have summarised many workers findings on the response of great whales to noise. Several features emerge from this summary:

- there is definitive evidence of behavioural responses of great whales to various noise sources;
- the type of response is variable, and ranges from none to active avoidance of a source;
- there is evidence that at the species level whales respond differently to a given noise depending on their gender, behavioural state and habits at that particular time;
- there is evidence that the response of a species to man-made noise may change through time due to familiarisation or sensitisation of whales to the noise source.

Richardson et. al. (1995) summarises several workers observations to, and experimental playbacks of, petroleum drilling and associated industrial noise to mostly gray and bowhead whales. Their summary states "*that stationary industrial activities producing continuous noise result in less dramatic reactions by cetaceans than do moving sound sources, particularly ships*". They noted that some cetaceans approached industrial noise

sources to close range, and that the radius of avoidance of these sources was considerably less than the radius at which the source was audible. Richardson et. al. (1995) present summary tables of the broadband levels at which avoidance occurred in various observations and experimental trials, and present the level at which 10% of migrating gray whales avoided a semi-submersible drilling rig at 114 dB re 1 μ Pa, 50% avoidance at 117 dB re 1 μ Pa and 90% avoidance at > 128 dB re 1 μ Pa. For spring-migrating bowhead whales passing drilling operations they estimated strong behavioural changes at levels near 124 dB re 1 μ Pa and typical closest approach to levels of 131 dB re 1 μ Pa. Using the 130 dB re 1 μ Pa value as an estimate of avoidance ranges for the mining vessel under its DP operating state gives a 90% avoidance range from the vessel of 15 km.

Perhaps the best long term study of whale response to vessel approaches is that of Watkins (1986). He reports on more than 25 years of observations made of whales and vessels in the vicinity of Cape Cod, on the eastern US seaboard. Watkins (1986) reported that over the years the response of minke and finback whales to nearby vessels changed from frequent positive responses to uninterested reactions, the response of northern right whales did not change and humpbacks changed from mixed, often negative encounters, to generally positive responses. Given the long time frame of the mining operations it is probable that resident marine fauna will eventually acclimate to its nearby presence.

Watkins (1986) stressed that the most vigorous whale responses came from noise sources that changed suddenly, rapidly increased (such as an approaching vessel) or were unexpected. He also noted that whales that were preoccupied with some activity were less responsive than whales that were inactive. Richardson et. al. (1995) reiterates this in his summary of baleen whale responses to vessels, stating that when vessels approach whales slowly and non-aggressively, the whale response is similar, whereas rapidly changing vessel noise often resulted in strong avoidance responses from nearby whales. McCauley et. al. (1996) estimated the underwater noise level received at humpback whales involved in whale watching encounters and simultaneously measured their behavioural reactions. The most vigorous responses consistently came from vessels which either produced the most erratic noise levels with many sharp increases in level, or which had deliberately approached whales too closely (tens of metres).

The noise of the mining vessel in DP mode, while relatively intense, has the redeeming feature of being produced by a stable platform which either does not move, only moves

slowly, or moves independently of any nearby whales (i.e. no deliberate approaches). The noise is also predicted to be reasonably constant in nature - that is there would normally be few sharp changes in noise level with time. Watkins (1986) and McCauley et. al. (1996) have shown that rapidly approaching or rapidly increasing noise may constitute a threat to whales and that vessel noises which are erratic and involve many sharp changes in levels over short time scales are more likely to cause adverse behavioural reactions.

Hence it is probable that under normal activities nearby marine mega fauna will be aware of the mining vessel from hundreds of km, and may approach it to approximately 15 km. Given the continual and constant nature of the noise it is probable that some resident animals may quickly habituate, and the noise will not produce any startle or alarm types of response. Animals resident in the area are also likely to approach the vessel more closely as they habituate to its presence.

Masking of signals of interest

When a signal (marine animal call) cannot be detected by a listener because of the presence of noise (potentially the mining vessel noise) then the noise is said to mask the signal. The masking of signals is a complex function that involves understanding how an animal hears in the presence of noise, and understanding the character and level of the masking noise and the signal of interest. Most vertebrates are particularly good at filtering out noise so as to detect weak signals of interest. Although little is known about the hearing capabilities of whales, their extensive use of sound and the high and variable levels of natural background noise in the sea suggest that they have highly adapted capabilities for detecting signals in noise. For masking to occur the most important factors are the relative locations of the sender, receiver and masking noise source, the frequency content and level of the primary signal, the frequency content and level of the masking signal, and the ambient noise characteristics at the time.

The nature of the mining vessel noise when it is operating in DP mode is that of continual noise over a wide frequency bandwidth which is intense at the source. This represents the worst scenario in terms of masking since it implies there are no time brackets free of masking noise, an animal cannot rely on using a comparatively wide bandwidth signal to avoid masking since the masking noise is also wide bandwidth, and the noise levels are high for relatively long ranges around the source. We have not attempted to calculate

masking ranges for different marine animal sources and receivers around the vessel as there are too many scenarios to consider. However, when analysing long data sets of sea noise it is typical that many more low level signals are detected than high level signals. This is a function of sound transmission in the ocean and the fact that area is proportional to the square of range. As a consequence, if animals are uniformly distributed in space, then there will be four times as many at a range of 2 km than there will be at a range of 1 km. An example of this is shown on Figure 13, where the received level of pygmy blue whale detections in the Perth Canyon is shown (data of McCauley). Assuming that there will be many more long range and thus low level signals transmitted between marine animal groups, then it is probable that for a marine animal 'near' to the mining vessel considerable masking impacts will occur. What is meant by 'near' the vessel depends on the proximity of the transmitting source of interest, but could be into tens of km for, say, a great whale listening for distant (tens km away) con-specifics.

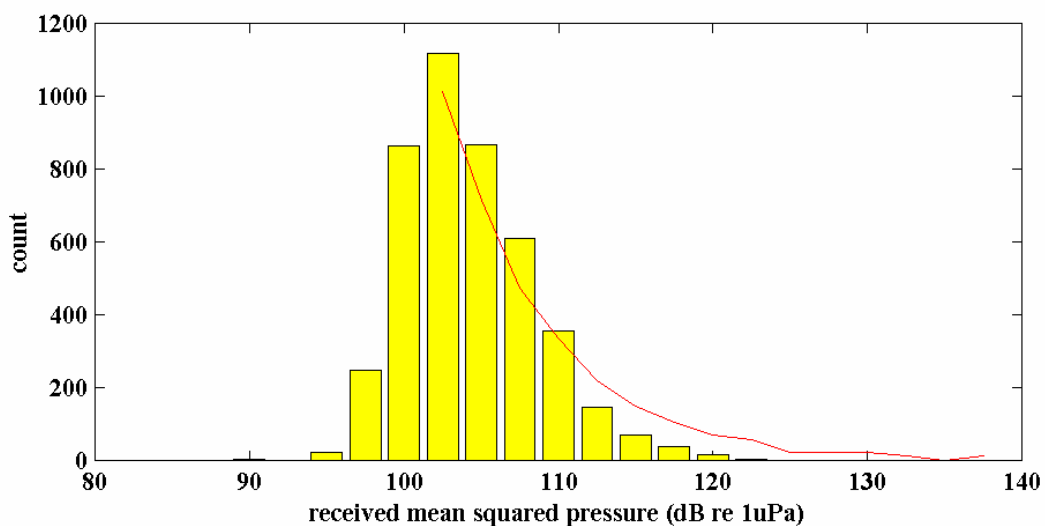


Figure 13. Distribution of received pygmy blue whale call components heard in the Perth Canyon in 2000.

5 Conclusions

Modelling of the underwater propagation of noise produced by the mining vessel's thrusters indicated that received levels will drop rapidly with distance from the vessel out to a horizontal distance of approximately 2 km, after which they will decay more slowly in accordance with cylindrical spreading.

The noise is likely to be audible to marine animals at ranges in excess of 600 km in directions unimpeded by land or shallow water depths (to the west in this case), however levels will be insufficient to produce physiological effects such as temporary threshold shifts at any range, except perhaps in the immediate vicinity of the vessel (within tens of metres). To put this audibility range in context it is important to note that long range sound propagation in the ocean is common for both natural and man-made sounds. For example, low frequency sounds produced by the nearby North Su subsea volcano are likely to be audible for thousands of kilometres, and other seismic events such as earthquakes can produce sounds that are well above ambient noise levels at ranges of thousands to tens of thousands of kilometres. In the case of man-made sources, sounds produced by airgun arrays during seismic surveys have been recorded by the authors at ranges of several thousand kilometres.

Marine mammals are likely to avoid the vessel at ranges of approximately 15 km, and may suffer signal masking effects at similar ranges. However, some animals may also be attracted to the vessel, and the avoidance range is likely to reduce over time as animals habituate to the vessel's presence.

An analysis of the production and propagation of noise from the subsea mining machine and the potential impacts of these noise levels on marine mammals has not been carried out due to a lack of information about the machine's likely source characteristics. The noise produced by this device needs to be considered in the context of the operation being carried out approximately 1 km from an active subsea volcano, which is itself likely to be a major source of low frequency underwater sound.

References

- Fisher, F. H., Simmons, V. P., "Sound absorption in sea water", *J. Acoust. Soc. America*, 62 (3), September 1977.
- Hamilton, E. L. (1980), "Geoacoustic modelling of the sea floor", *J. Acoust. Soc. America*, 68 (5), Nov. 1980, pp 1313-1340.
- Jensen, F. B., Kuperman, W. A., Porter, M. B., Schmidt, H., (2000) *Computational Ocean Acoustics*, Springer-Verlag, N.Y., 2000, ISBN 1-56396-209-8
- McCauley, R. D. (1998), "Radiated Underwater Noise Measured from the Drilling Rig *Ocean General*, Rig Tenders *Pacific Ariki* and *Pacific Frontier*, Fishing Vessel *Reef Venture*, and Natural Sources in the Timor Sea, Northern Australia". Centre for Marine Science and Technology Report C98-20, 1998.
- McCauley, R.D., Cato, D.H., Jeffery, A.F. (1996). "A study of the impacts of vessel noise on humpback whales in Hervey Bay." Prepared for Queensland Department of Environment and Heritage, Maryborough, Queensland, 137 pp.
- McCauley, R.D., Jenner, C., Bannister J.L., Burton, C.L.K., Cato, D.H., Duncan, A. (2001). "Blue whale calling in the Rottnest trench - 2000", Western Australia. Prepared for Environment Australia, from Centre for Marine Science and Technology, Curtin University, R2001-6, 55 pp. 51 fig. Available <http://www.cmst.curtin.edu.au>
- National Research Council, committee on characterising biologically significant marine mammal behaviour (2005), "Marine mammal populations and ocean noise, determining when noise causes biologically significant effects", National Academies Press.
- Richardson, W.J., Greene, Jr., C.R., Malme, C.I., Thomson, D.H. (1995). *Marine mammals and noise*. Academic Press, San Diego
- Ross, D, *Mechanics of Underwater Noise*, Peninsula publishing, 1987, ISBN 0-932146-16-3.
- Simpson, S.D., Meekan, M.G., McCauley, R.D., Jeffs, A. (2005) "Homeward Sound." *Science* 308 p. 221

Watkins, W.A. (1986). Whale reactions to human activities in Cape Cod waters. **Mar. Mamm. Sci.** 2(4):251-262

Appendix 14

The Potential for Natural Disasters Being Triggered by Mineral Extraction at the Solwara 1 Seafloor Hydrothermal Vent Site

**The Potential for Natural Disasters being Triggered by
Mineral Extraction at the Solwara 1 Seafloor Hydrothermal Vent Site
Steve Saunders, Rabaul Volcano Observatory
March 2008**

1. Introduction

1.1 Background

Local communities around the Bismarck Sea, (notably villages and individuals from the Duke of York Islands, east New Ireland, North Coast - East New Britain, and one 'Letter to the Editor' in the Post Courier newspaper from Bagabag Island), have expressed concerns that the extraction of minerals from an active seafloor hydrothermal vent system could trigger a natural disaster in the area. Their concerns have been listed as possible: -

- Volcanic activity
- Earthquakes
- Tsunamis

The first two can be related to concerns that the extraction process could un-roof an extremely shallow magma body or destabilise the local stress regime causing decompression of a deeper magma body and/or activate faults leading to seismic activity. It is perceived that any of these events could then trigger a tsunami.

2. The Perceived Potential Hazards

2.1 Natural Volcanic Activity on the Bismarck Sea Seismic Lineation

Volcanic activity is caused by the rise of magma from depth to the surface of the earth. Magma is a mixture of molten rock and gasses, the violence of an eruption is controlled by the decompression of the dissolved gasses and the ease with which these gases can escape from the magma. Decompression of the magma allows bubbles to start to nucleate at a depth of about 3 km. If the magma continues to ascend these gas bubbles will expand as the ambient lithostatic pressure falls. At very shallow levels the expansion of these bubbles disrupts the molten or semi-molten rock causing subsurface frothing in the conduit and explosions and expulsion of particulate matter (variously known as volcanic ash, dust or tephra, including larger blocks and volcanic bombs) at the surface.

Chemically the BSSL lavas are typical Mid Ocean Ridge Basalts (MORBs) with some arc-like contamination at the eastern end (Woodhead et al., 1998). MORBs are among the most gas poor and fluid of all lava types. Typically a basalt will have dissolved in it about 2% of gas by weight (wt%). Below the earth's surface at depths greater than 3000m (approximate depth below which vesicles (bubbles) are thought unlikely to form) 1m³ of basalt magma weighs ~3,000kg and at 2wt% about 60kg of this mass will be completely dissolved gasses (volatiles).

The Solowara 1 deposits are located on volcanic rocks related to the Bismarck Sea Seismic Lineation (BSSL) the proposed extraction site is on the south side of an area called the East Manus Rifts, located near a senile hydrothermal field. The BSSL represents a spreading axis, the rate of divergence is exceptionally fast being ~110mm/yr at its western end and ~140mm/yr at its eastern end (Wallace et al., 2004). The BSSL marks the divide between the North Bismarck and South Bismarck plates. The extensional forces which have formed the fault zone are thought to be caused by convection cells in the upper mantle due to perturbations related to the subduction of the Solomon Sea Plate below the Bismarck Plate. Along the BSSL three main spreading segments have been identified, the Eastern Rifts, the Manus Spreading Centre (MSC) and a third, apparently unnamed, south of Manus Island. As well as the spreading segments part of the Extensional Transform Zone (ETZ), which connects the western end of the MSC to the end of the Willaumez Transform (WT), is termed

'leaky' and recent lava flows have been observed on the seabed in the area. In addition, there is a volcanically active area, the Southern Rifts, associated with, but displaced from the eastern part of the BSSL.

Being a spreading axis volcanism is probably common along the length of the BSSL. At the Solwara 1 site there are fresh glassy lavas with little or no sediment cover (M.J. White pers. Com.) these are considered of recent origin (a few to less than a couple of hundred years old). As mentioned above several lava fields appear to be associated with the Willaumez Transform, but are somewhat displaced from it (C.McKee, pers. Com.), detailed outcrop data is unavailable for other areas.

Decker and Decker (1981) estimated that on the Mid Atlantic Ridge there is 1 eruption every ten years for each 300km length of the spreading axis. The spreading rate of the Mid Atlantic Ridge is ~1-2 cm a year, the BSSL is spreading at a rate of 11 -14 cm a year. From the Decker's work and the observed spreading rates it can be estimated that for each 300km of the BSSL there may be at least one eruption every year or roughly three eruptions a year somewhere along its ~1000km length.

Despite decades of seismic monitoring of the Bismarck Volcanic Arc, only four episodes of suspected BSSL eruptive activity have been recorded instrumentally. Due to the lack of other evidence it is impossible to confirm these were eruptions, but volcanic activity is the best candidate to fit the seismic signals. In the early 1960's seismic events were detected NW of Rabaul, these were attributed to possible activity on the Eastern Rifts (J. Letter, pers. Com.). In 1972 seismic and acoustic evidence pointed to activity near the termination of the WT-ETZ (Johnson et al. 1981). In 1994 a swarm of earthquakes 50km to the north of Rabaul was thought to be associated with eruptive activity on the eastern end of the Eastern Rifts (C. McKee, pers. Com.), and in 2002 low frequency seismic activity NW of Rabaul may have been due to activity on the Eastern Rifts (I. Itikarai, pers.com.). The seismic arrays mentioned are designed to detect volcanic activity at nearby volcanoes on North Coast New Britain and the Islands off Madang and are not designed for monitoring of the BSSL. As such many BSSL eruptions have probably gone unrecorded.

Despite the strong likelihood of there being frequent deep submarine eruptions along the BSSL human populations on the shores of the Bismarck Sea have never reported any effects, which could be attributed to them, or expressed any awareness of such activity taking place.

2.2 Why do BSSL Eruptions go Unnoticed?

It is possible to calculate the volume of gas in magmas when erupted at sea level pressure and temperature. At sea level 1m^3 of gas weighs about 1.37kg. So it can be calculated that what had been 1m^3 of basalt with 60kg of gas dissolved in it will expand to $\sim 83\text{m}^3$ of fragmental magma/rock and gas. This is if the gas is at surface temperature, if however, magmatic temperatures are taken into account - at 1200°C (typical basalt temperature) this gas volume will be $\sim 722\text{m}^3$ (i.e. gas volume doubles for every 273°C rise in temperature). At the earth's surface this gas can escape easily, as basalts are very fluid, and this massive increase in gas volume usually only leads to gentle to moderately violent eruptions (i.e. 'Hawaiian' type).

To get an idea of gas volumes involved in submarine eruptions we can work downwards from sea level using Boyle's Law. Boyle's Law states that gas volume will half with each 10m increase in water depth. Using this simple formula it is found that between 190-200m water depth 1m^3 of basalt magma at 1200°C will only contain about 1mm^3 of bubbles. At the depth of the Solwara1 extraction area (1500-1700m) the volume of bubbles in any liquid magma would only be 5.06×10^{-43} to $1.51 \times 10^{-50}\text{m}^3$, an infinitesimal amount of expansion, making violent explosions/eruptions impossible.

Because of the fact that high hydrostatic pressures severely restrict bubble growth, as described above, natural eruptions at the BSSL go unnoticed by local populations living on

the coast of the Bismarck Sea. These deep-water eruptions take the form of gentle lava outpourings onto the seabed, with little if any explosive activity. The magma rises from the mantle/crust boundary purely due to the pulling apart of the rift system allowing the relatively buoyant hot material to rise to fill the gap. Due to its passive rise and inability to vesiculate at the ambient pressures encountered these naturally occurring magma ascents pose no hazard to coastal communities or maritime traffic.

2.3 Although Eruptions At The Depth Of The BSSL Are Non-Violent, Is There A Possibility That Mineral Extraction At The Solwara 1 Site Could Initiate Lava Effusion?

The only way that mineral extraction could lead to lava effusion is if excavations unroofed a shallow magma body, or altered the stress regime significantly causing the dilation of faults up which magma could flow. Even if this were to happen, as described above, there would be no noticeable effects at the surface.

The water being expelled at the Solwara 1 site has gained its heat by seawater circulating through a fractured and permeable seabed to deeper hot rocks. The maximum recorded temperature of the fluid being expelled at the Solwara 1 site is at ~340°C (M.J. White pers. Com.). With fluid basalt being typically around 1200°C it can be assumed that magma is at some distance from the point of upwelling water otherwise the water temperature would be significantly higher. Scientific estimates and comparisons with other spreading axis put the magma at a minimum of 1-kilometer depth and probably more from the seabed's surface. The Solwara 1 extraction site is a mound that rises 200m above the surrounding seafloor. The extraction method will involve removing swaths of 1m depth at a time from the top of the mound. The mound may eventually be totally removed to a possible depth of 20m relative to the surrounding seabed. The likelihood of the gradual removal of 220m of low-density porous material depressing magma at 1km, or more, depth is very unlikely, as being an elastic medium all unloading stresses would be relieved in the near surface layers. For the same reason the unloading process is unlikely to induce fault movements opening pathways to the seabed surface for subsurface magmas (see below).

Figure 2. A finite elements model showing strain in the seabed due to the Solwara 1 mound. Because of the material strength of the seabed stress/strain due to the weight of the mound only penetrates to a certain depth.

2.4 Natural Seismic Activity on the Bismarck Sea Seismic Lineation

As its name suggests the Bismarck Sea Seismic Lineation is a zone of frequent seismicity. Most earthquakes produced on the lineation are relatively small and shallow. No damaging earthquakes have originated from here in recorded history. At the spreading centers the crust is pulled apart by naturally occurring tectonic forces. In tension rocks have little strength therefore they break at a very low elastic limits, as such stresses do not build up as the rock is continually failing, giving very weak earthquakes or even aseismic pull apart events.

2.5 Is there a Possibility that Mineral Extraction At The Solwara 1 Site Could Create a Seismic Hazard?

At various sites around the world subaerial mining has induced seismic events (much work has been undertaken in the United States, events at Wasatch Plateau and the Book Cliffs coal mines, Utah, the Trona Mining District, Wyoming are discussed on the Unavercity of Utahs web site). These occur when the local elastic stress regime has been changed by the loading or unloading of large volumes of rock or changing hydrostatic pore-pressures. This is however, extremely unlikely to occur at the Solwara 1 site.

The factors mitigating against induced seismicity occurring at the Solwara 1 site are: -

- i.) The area is naturally very seismically active, so the rocks are not pre-stressed
- ii.) The swaths of material that will be removed will only be 1 m thick

- iii.) Incrementally these 1 m swathes will lead to a maximum depth of only 220m below the current seabed.
- iv.) There are favorable unloading differentials in an aqueous environment
- v.) Changes in hydrostatic pore-pressure is not going to occur at these depths

i.) It has been noted that mining induced seismic events tend to take place in tectonically stable areas. This is because stresses can gradually build up over long time periods as no sudden seismic triggers occur. In seismically active areas the regular regional failures and 'tectonic kneading' tends to relieve stress build up. Thus minor stress modifiers, such as mining, are unlikely to cause seismicity due to triggering of a failure in such an environment. Further, at spreading axis the rocks are under tensional stress. Rocks are weak in tension and will break easily, producing frequent minor and micro-earthquakes rather than allowing stresses to build resulting in major periodic ruptures. So in effect the area of the Solwara 1 site is regularly 'relaxed', there being no major stress build-up, therefore the mining extraction technique is unlikely to cause a catastrophic rock failure.

ii, iii & iv) Although never proven as a single causal mechanism for inducing seismicity at subaerial open cast mines, loading and unloading has been suggested (Kulhanek, 1990) as a minor contributory factor in tectonically stable, highly-stressed areas. At subaerial mines, 1m³ of material removed it is replaced by 1m³ of air. If we assume the mined material to have a density of 2000kg per 1m³ this will be replaced by 1.37kg of atmospheric air; a differential of almost 1500:1. In a subaqueous environment 1m³ of material is replaced by 1000kg of water; leading to a density differential of 2:1. As such if all else is equal a submarine excavation has to be over one thousand times bigger to induce the same stress modification in the local environment as that of an identical subaerial pit. The Solwara 1 mine will be a relatively small-scale operation compared to a terrestrial open cut mines.

v.) Most subaerial mines, pits or wells have water or other fluids pumped from them. This is to enable humans or equipment to operate in areas that are otherwise below the water table and hence flooded. This fluid extraction effects the local hydrostatic pore-pressure and elsewhere has been seen as the main stress modifier leading to mine induced seismicity. As the Solwara 1 mine will be at 1500-1700m below sea level all equipment is designed to operate submerged and at the ambient pressures encountered there. No de-watering will take place until the slurry reaches the surface. As such at the extraction site the hydrostatic pore-pressures will not be effected by mining activities, all pores will have a head of 1500-1700 m of water acting on them, both before and after material has been removed. This source of induced seismicity can be discounted.

2.6 Natural Tsunami Activity in Papua New Guinea

There have been fourteen recorded tsunamis in PNG in the last 150 years. Known by the names of :-

1. Ritter Island, 1888
2. North coast PNG mainland, 1930.
3. Rabaul, 1937.
4. Chile, 1960.
5. Madang, 1970.
6. Solomon Sea, July 14th 1971.
7. Solomon Sea, July 26th 1971.
8. Lae, 1972.
9. Rabaul, Sept 1994.
10. Aitape, July 1998.
11. Southern New Ireland, Nov 2000.
12. Wewak, Sept 2002
13. Rabaul, October 2006
14. Solomon Sea April 2007

None of these were associated with activity on the BSSL.

A tsunami can be generated by any disturbance that displaces a large water mass from its equilibrium position. The largest of the above tsunamis were generated by earthquake at subduction zones (Chile 1960, Solomon Sea 1971, 2007), where plates move vertically relative to each other and hence can displace large quantities of water. These can cause just local effects or regional and even trans-oceanic (such as the 1960 tsunami sourced to Chile). The others were produced by masses of material entering the sea or moving along the sea bed. Such mass movement can be produced by subaerial volcanic eruptions causing pyroclastic flows to enter the sea, these only have a local impact (Rabaul 1937, 1994 and 2006). Volcanic islands have been known to collapse (Ritter 1888) and seabed sediments laying on steep gradients can slump downwards generating tsunamis (Madang, 1970, Lae 1972, Aitape 1998), both of these mechanisms can have effect areas up to a few hundred kilometres away, but are usually much more local.

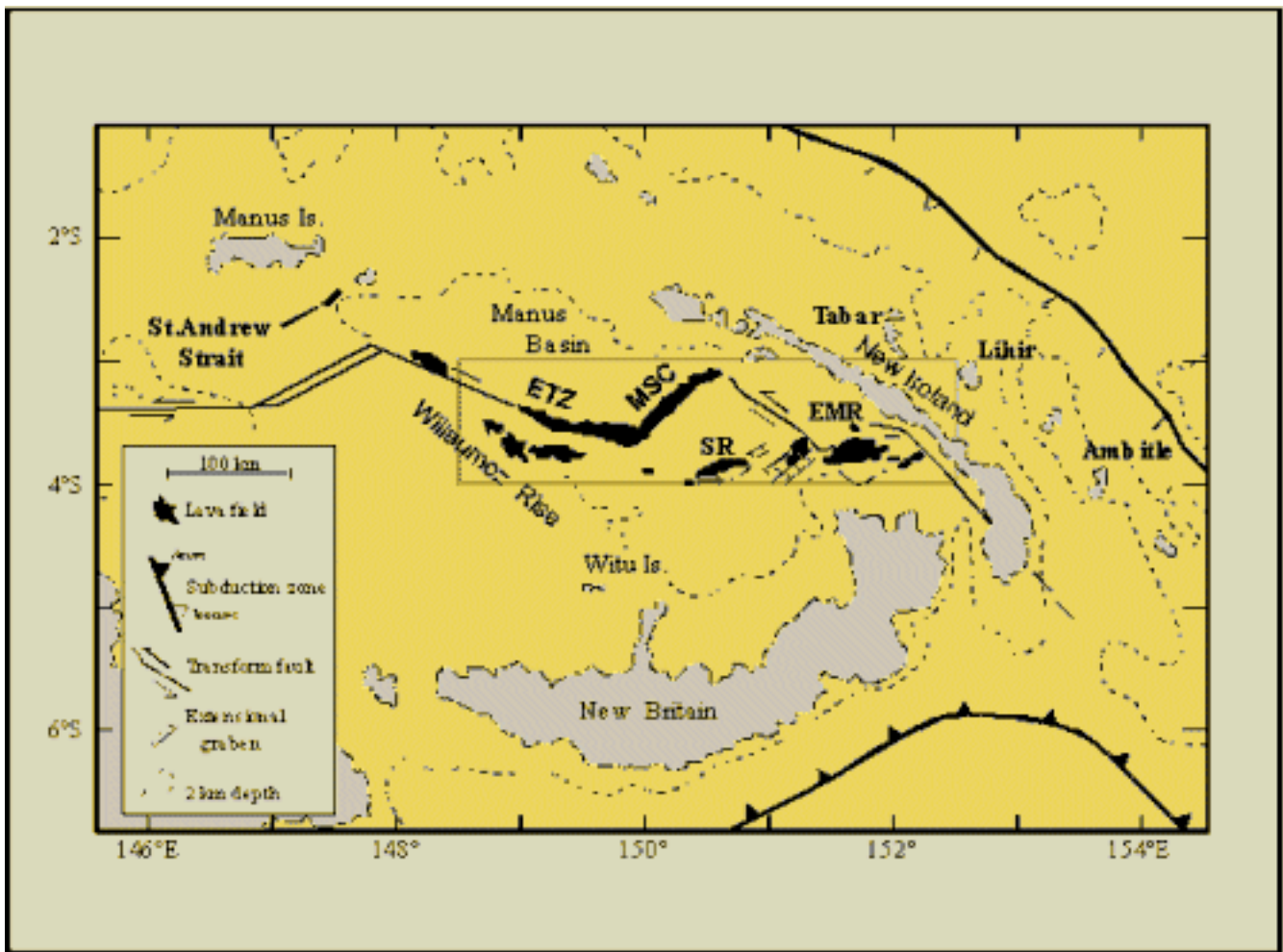
2.7 Linkages Between Volcanic Activity, Earthquakes and Tsunamis and Whether the Project could Trigger a Tsunami

None of the above mechanisms for tsunami generation exist, or can be caused by mineral extraction at the Solwara 1 deposit. As outlined above the mining technique can not generate earthquakes or volcanic eruptions in the environment encountered at the site. The seabed in the area is topographically complex, but no long steep slopes exist and sediment deposits are thin. Therefore there is little sediment to slump and the topography is not conducive to debris flow initiation.

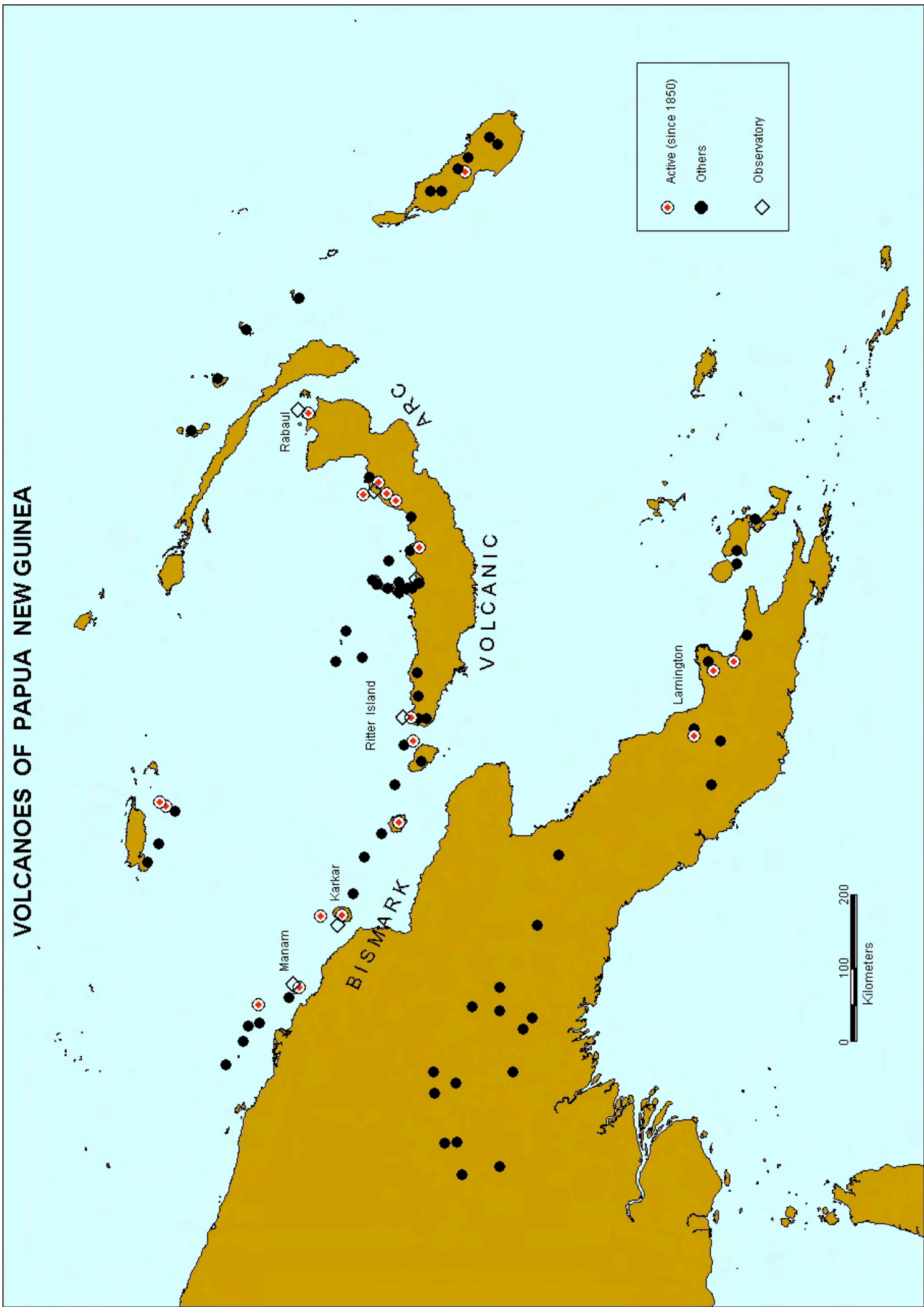
Kulhanek O., (1990) Anatomy of seismograms. Developments in Solid Earth Geophysics, 18. Elsevier

Wallace M.W., Stevens C., Silver E., McCaffrey R., Loratung W., Hasiata S., Stanaway R., Curley R., Rosa R., and Taugaloidi J. (2004) GPS and seismological constraints on active tectonics and arc-continent collision in Papua New Guinea: Implications for mechanics of microplate rotations in a plate boundary zone. J. Geophys. Res. Vol. 109, B05404

Woodhead J. D., Eggins S. M. and Johnson R. W. (1998) Magma Genesis I the New Britain Island Arc: Further Insights into Melting and Mass Transfer Processes. J. Petrology, Vol. 39. No. 9, pages 1641-1668



VOLCANOES OF PAPUA NEW GUINEA



Appendix 15

Stakeholder Consultation

Appendix 15 – Stakeholder Consultation

Church

Kimadan Workshop (6 August 2007)

Participant name	Organisation
Robinson Moses	Minister – A/Bishop, United Church
John Mokis	Literacy Co-ordinator, United Church, Ligga
Stanley Lavo	Minister United Church, Halis
Rev Timothy Gapi	Minister, United Church, Ranmelek
Doreen Buken	Co-ordinator, UCWF
Lina Voklus	Marama, UCWF, Ligga
Alice Sumati	Treasurer, UCWF, Ligga
Rev Eritius Voklus	Chaplain, Manggai High School
Pstr Holbon Todiat	Pastor, United Church, Ligga
Mr Wilfred Semmie	Pastor, United Church, Djual
Junias Darius	Minister, Vutei Circuit
Rev John Vaip	Minister, Samo Sursurunga Circuit
Stanley Emil	Minister, Pinikidu Sub-Circuit
Rev Elias Benson	Minister, United Church
Ben Kapsava	Minister, United Church
Elison Lali	S/S Coordinator, United Church
Noel Paisat	Minister, Pinatgin Church
John Iso	Pastor, Messi Circuit
Tobata Paslain	Delegate, Lelet Circuit
Obed Letaba	Sec/Treasurer, Lelet Circuit
Toirip Birong	Pastor, Hilolon Circuit
Joel Makis	Pastor, Kontu Circuit
Esrom Lamasuk	Pastor, Kontu Circuit
Ekonia Magen	Secretary, Kontu Circuit
Manual Lukar	Secretary, Libba Circuit
Johnathan Bune	S/S Coordinator, Libba Circuit
Robin Suimailik	Pastor, Umbukul Circuit
Spania Vatlom	Div Secretary (NHD), United Church, Tsoi Circuit
Johnson Igua	Pastor, Enang Circuit
Robinson Gomat	Congregation Chairman, Pinikidu Sub-Circuit
Gorwin Oki	Caretaker Pastor Kabakadas, Kabanut Circuit
Misiel Rolley	Secretary, Vutei Circuit
Subul Loma	Pastor, Baso Circuit
Elison Buken	Chairman, Kav., Omo Circuit
Rev Taura Frank	Minister, Libba Circuit

Environmental Impact Statement
Solwara 1 Project

Josin	Galia	H/Pastor, Magam Circuit
Mathew	Pogos	H/Pastor, Ranmelek Circuit
Rev Robin	Buluanis	Delegate, Hilolon Circuit
Sisikim	Hosea	Delegate, Namatanai Town Circuit
Toua	Doura	Circuit Evangelism Coordinator, Pinikidu Sub-Circuit
Michelle	Kapin	Transit Manageress, Iigga
Kolish	Topu	W/F President, Tabar Circuit
Willimaina	Bafun	S/S Coordinator, Panamecho Circuit
Laurel	Vain	W/F President, Kaut Circuit
Linda	Taurikai	President, Fankolak Circuit
Dorothy	Apelis	Secretary, Fankolak Circuit
Helen	Taugrim	Maram, Kabanut Circuit
Anna	Tabu	Vice President, Kabanut Circuit
Sirapi	Judith	W/F President, Panamecho Circuit
Kavisi	Pitalot	W/F Secretary, Ngavalus Circuit
Margaret	Boskey	W/F President, Vutei Circuit
Midia	Togu	W/F President, Namatanai Town Circuit
Ivanie	Johnathan	W/F Coordinator, Metabau Circuit
Margreth	Ben	W/F Coordinator, Kontu Circuit
Agnes	Rangia	SIC Piliwa, Djaul Island
Gethrude	Kapsawa	Marama, Messi Circuit
Margreth	Lavoi	Marama, Halis Circuit
Darlyne	Matalolou	Marama, Djaul Circuit
Susan	Darius	Marama, Vutei Circuit
Suluvet	Igua	Marama, Ngavalus Circuit
Addie	Wilson	Marama, Namatanai Town Circuit
Ethy	Waip	Marama, Samo/Sursurunga Circuit
Ruth	Keka	Marama, Metebau Circuit
Gethrude	Jacob	Div. Secretary, Libba Circuit
Dessie	Malau	W/F President, Lakurumau Circuit
Beki	Kamrai	W/F Secretary, Lakurumau Circuit
Pollen	Boas	W/F President, Kavieng/Omo Circuit
Hellen	Misiang	Marama, Kavieng/Omo Circuit
Esther	Kuam	Div. W/F Secretary, Kavieng/Omo Circuit

Kavieng Workshop (9 August 2007)

Participant name		Organisation
Albert	Lereking	C.E.S., Diocese of Kavieng
Aloysia	Mara	Teacher, Utu High School
Andrew	Topolot	D.Y.C. Diocese of Kavieng

Environmental Impact Statement
Solwara 1 Project

Bernard	Rutmat	Secretary Health, Kavieng
Bis Ambrose	Kiapseni	Bishop, Diocese Kavieng
Bruno	Babala	Waterboard, Kavieng
Catherine	Tude	Teacher, Lelet Primary
Celine	Waningu	KBO, Diocese of Kavieng
Daniel	Lasvut	Teacher, Kavieng
Dennis	Kilion	Farmer, New Hanover
Elison	Kongio	Teacher, Lelet P/School
Felicitas	Funmat	RWO Tanga Health Centre
Florence	Copland	Nursing Officer, Lavongai Health Centre
Fr Ben	Kaleb	Parish Priest, Lihir
Fr Bruno	Junalien	Priest, Anir Parish
Fr Domininc	Maka	Rector, Kokopo
Fr Joc	James	Parish Priest, Lamasong Parish
Fr Mathias	Wel	Father, Diocese Kavieng
Fr Moris	Kitup	Parish Priest, Lemakot
Fr Steven	B	Associate Priest, Namatanai
Fr. Patrick	Funmat	Priest, Patu Parish
Gabriel	Molonges	Nursing Officer, Mapua Health Centre, Tabar
Gerard	Pentecos	P.O.S., (PTB) Works Kavieng
Ignatius	Salbil	Deacon, Lamasong Parish
Jarius	Pariorie	Self employed, Kavieng
Jerry	K	Parish Priest, Puas
Joe	Kolos	Farmer, Puas Villlage
Joe	Lereking	Student, Fissoa Voc. Centre
John	Mara	Manager, Diocese Kavieng
John	Siavan	Secretary Youth, Metemana
Lasi	Benjamin	Teacher, Mapua P/School
Lawrence	Abage	Self employed, Karu Village
Luke	Jangei	CHW – Lipek, South Lavongai
Marius	Soiat	CEO, Local Environment Foundation
Martin Joseph	Harnas	Teacher, Morkon C/School
Moses	Penias	Health Ext Officer, Palie Health Centre, Lihir Island
Nolis	Amos	Farmer, New Hannover
Patrick	Raurang	Teacher, Tukulison Primary School
Relvie	Sionnie	Teacher, Lelet Primary
Ronald	B	Deacon, Mongop
Ronald	Sapak	Teacher, Auto Mart
Roslyne	Sapak	RWO, Bundralis Health Centre, Manus
Sebastian	Langua	Diocese of Kavieng, Tufabi Village
Simon	Kongas	Layman, Kavieng

Solo	Utiak	Farmer, Mapau
Stanley	Sirifave	Lecturer, Kabalco Teachers College
Wanariu	Benjamin	Farmer, Mapua

Awareness Program

West Coast Namatanai meeting (16-18 May 2007)

Participant name	Organisation
Apisai	LLG Manager, Konos Subdistrict, Central New Ireland LLG
Jerry Naime	Acting Director Project Coordination, Department of Mining and newly appointed coordinator of Solwara 1 Project
Gabriel Polut	Acting Mining Coordinator – Mining Coordination Unit of New Ireland Provincial Government
Mesulam Sumlin	Senior Project Officer – Mining Coordination Unit
Mel Togolo	Country Manager, Nautilus Minerals Niugini
Gabriel Towaira	LLG Manager, Namatanai District
Plus nearly 2,000 community members from 11 LLG Wards comprising more than 32 villages	

Southwest Coast New Ireland Meeting (16-18 May 2007)

Approximately 2,000 community members

West Coast New Ireland Province Meeting (16-19 May 2007)

Approximately 1,600 community members from 6 villages

Community meetings

West Coast New Ireland Province Meeting (22 March 2007)

25 community members

Bagabag Meeting (18 August 2007)

Participant name	Organisation
Bagei Gau	Community leader, Matiu 2 village
Bilalu Mait	Community Youth Leader
Dabik Bilau	Sinomber clan leader
Daoi Bunafun	Health Centre Chairman
Dong Nagel	Sinomber clan leader
Dumui Daing	Tador Village
Galun Yamad	Primary School Chairman
Giok Yadai	Elementary School Chairman
Joseph Gumoi	Community based Org – Kuluk village
Kell Balun	Community Youth Leader – Tador village
Long Gulob	Pastor
Mager Gaiam	Sinomber clan leader
Margaret Long	Women's Rep
Mike Miamai	Elementary school teacher

Nag	Kanai	BCDA Zone co-ordinator
Narer	Taut	Tador Village
Ngarer	Taut	Community youth leader – Tador village
Paul	Daing	BCDA Chairman, Tador Village
Shong	Mad	Village Court Chairman
Sibilol	Gines	Tador Village
Stalin	Saluk	Chairman Parents Citizen Association
Steven	Madom	Kiap
Wang	Beb	Tador village clan leader

University of Papua New Guinea Deep Sea Science Seminar (3 July 2008)

Participant name	Organisation
Approximately 200 students	University of Papua New Guinea
Unknown number	PNG Government
Wences Magun	Sea Turtle Restoration Project
Taisha	Mineral Policy Institute

Engagement Workshops

Rabaul (13 December 2007)

Participant name	Organisation
Beddie Jubilee	ENB Provincial Administration
Bongian Bunbun	Doy LLG (Councilor)
Bongian Anis	Doy LLG (Lands Sector)
Boskie Tannos	Doy LLG (Villager)
Cecillia Konie	Provincial Council of Women
Christine Masiu	Community Development
Francis Tike	Commerce Division
Francis Manus	Doy LLG (Villager)
Isimel Kabian	Doy LLG (Villager)
Jack Gphikaine	Doy LLG (Councilor)
Jeremiah Rovo	NGO - Kokopo District, Youth Chairman
John Valex	Doy LLG (Villager)
Leo Benedict	Doy LLG (BOM Chairman)
Linda Passingan	Barefoot
Misiel Jonah	NBC – Radio East New Britain
Nerrie Wilson	NGO – Kokopo District, Women's Rep
Noah Pue	National Development Bank Ltd
Paul Kapa	Community Development
Robin Value	NGO – Kokop District, Bilapaka Youth Rep
Serah Mika	NBC – Radio East New Britain
Steve Saunders	Rabaul Volcano Observatory

Taupa	Lakono	Doy LLG (Villager)
Tio	Likaimt	Doy LLG
Tony	Judas	NGO - Kokopo District, Youth Rep

Kavieng (20 February 2007)

Participant name		Organisation
Aisi	Anas	National Fisheries College, university of Vudal
Alfred	Mungai	C.E.O. Niemac Inc (Environmental Group)
Andrew	Topolot	Kavieng Diocese
Ange	Amon	Lissenung Island Resort/Lissenung Diving
Arthur	Williams	NGO – Environment
Ben	Logai	New Ireland Provincial Administration
Clement	Dardar	NIP Governemnt (Provincial Assembly Member for Lihir)
Dietmar	Amon	Lissenung Island Resort/Lissenung Diving
Frasier	Hartley	Wildlife Conservation Society – PNG Marine
Gabriel	Polut	
Jerry	Sigulogo	Ailan Awareness (Environmental NGO)
John	Aini	Ailan Awareness (Environmental NGO)
John	Mara	Catholic Diocese of Kavieng
Luke	James	Kavieng Surf Club
Marius	Soiat	Ward 8, Lovo, LLG
Mel	Togolo	Nautilus Minerals BNE
Mesulum	Sumlin	NIPA, Kavieng
Mike	Wright	Coffey Natural Systems
Paul	Varom	Lavongai Community
Philomena	Jonah	Diocese of Kavieng
Salot	Taran	United Church
Samantha	Smith	Nautilus Minerals BNE
Shaun	Keane	Nusa Island Retreat
Theophilus	Bulo	Christian Life Church
Tony	Drett	NIPA, Kavieng
Yvonne	Tio	Department of Environment PNG

Mining Warden Hearings

Participant name		Organisation
<i>Kimbe (20 March 2007)</i>		
Joshua	Giru	Provincial Administrator,
Willaimson	Hosea	Acting Deputy Provincial Administrator
Michael	Kiangua	Advisor, Planning

Environmental Impact Statement
Solwara 1 Project

Willie	Waleca	Advisor, Provincial Finance
Philip	Taubuso	Advisor, HR
Gervasius	Rovi	Resources Officer
<i>Kavieng (22 March 2007)</i>		
Not recorded		
<i>Lorengau (24 April 2007)</i>		
Kule'en	Hamou	Deputy Administrator
Kiapin	Tawali	Assistant Administrator – Commerce and Industry
Fenwick	Saliau	Executive Officer – ICE
Koru	Abe	Assistant Administrator – Planning
Obert	Otto	Environment and Conservation Officer – Planning
Pompiran	Kuyei	Assistant Administrator – Education
Oscar	Carol	Assistant Administrator – Finance
Kisapai	Kutan	Chairman LLG/President - Pobuma LLG
Bernhard	Moigah	Assistant Administrator – Infrastructure
Paul	Swere	Supt – Open Learning, Education
Edward	Saleu	Executive Officer – Pomotu, N'drehet, Kuruti, Ardra Local Level Government.
<i>Alotau (23 May 2007)</i>		
Not recorded		
<i>Kimbe (29 May 2007)</i>		
Not recorded		
<i>Madang (19 June 2007)</i>		
Francis	Irara	Lands
Bul	Dulau	Commerce
Jack	Masu	Forest
Joseph	Bande	Community Development
Galun	Kasas	Deputy Prov. Admin
Simon	Simoi	Policy and Planning
John	Bivi	Ramu Nickel Coordinator
Marilyn	Alok	
Fafaeg	Bibin	DOM – Ramu Nickel Liaison Offer
<i>Kavieng (25 July 2007)</i>		
Veronica	Jidege	NIPA, NPA, Corporate Services
Gabriel	Polut	NIPA, Mining Project Coordinator
Posikai	Jonah	NIPA, Provincial Planning Office
Satrek	Taput	NIPA, Fisheries and Marine
Belden	Laia	Finance, District Treasurer – Kavieng
Gabriel	Towaira	Namatani, District Administrator
Simon	Passingan	NIPA, Special Projects
Mesulam	Sumlin	NIPA, Senior Project Officer, Mining Project Coordination Unit

<i>Wewak (22 October 2007)</i>		
Not recorded		
<i>Lorengau, Manus (6 November 2007)</i>		
Not recorded		
<i>Lae (17 January 2008)</i>		
Vincent	Michaels	MP– Member for Tewai-Siasi Electorate
Micah	Yawing	Deputy Prov. Administrator (Health) also rep for Siasi Peoples Association
Gioving	Bilong	a/Deputy Prov. Administrator, Community Affairs
Taikone	Gwakoro	Coordinator Mines
Mai	Banoteng	Prov. Project Officer, Mines
Jackson	Roland	EO Tewai Siasi Electorate
Tarosi	Angori	Community Representative – Siasi Island
Wilson	Waese	Advisor TDF
Robert	Kipi	Tewai-Siasi Community
Tom	Mollo	Tewai-Siasi Community
Mel	Togolo	Nautilus Minerals
Timothy	Kota	Chief Mining Warden
<i>Alotau (23 January 2008)</i>		
Judah	Dickson	Mines Liaison, MBA
Gerega	Kila	Director, Economic Services, MBA
Michael	Ova	Principal Advisor, Education, MBA
Rona	Dobunaba	Secretary, Milne Bay Tourism Bureau
Stephen Paul	Nesai	a/PA Planning, MBA
Nimrod	Mark	Director Governance, MBA
Bobby	Baloiloi	Prov Admin, Lands, MBA
Steven	Gibson	Deputy Administrator, MBA
Alphonse	Morona	a/PA Fisheries, MBA
Timothy	Kota	Chief Mining Warden, MRA
Mel	Togolo	PNG Country Manager, Nautilus

Kavieng (8-15 October 2007)

Participant name	Organisation
Not recorded	

Scientific Workshops

Port Moresby (13-14 March 2007)

Participant name	Organisation
Alison Swaddling	Nautilus Minerals BNE
Anaseini Ban	Mahonia Daria Research Centre
Barbara Roy	Department of Environment & Conservation
Barnabas Wilmott	Department of Environment & Conservation

Environmental Impact Statement
Solwara 1 Project

Chaplan	Kaluwin	University of Papua New Guinea
Cindy	Van Dover	Duke University
David	Gwyther	Enesar Consulting
Doug	Horswill	Teck Comminco
Gaikovina	Kula	Conservation International
Graeme	Hancock	World Bank
Guy	Gilron	Teck Comminco
John	Genolagani	Department of Environment & Conservation / PINBIO
John	Sambeok	Department of Mining
Josephine	Vovore	University of Papua New Guinea
Lasark	Joseph	Department of Mining
Lohi	Matainaho	University of Papua New Guinea / PINBIO
Lynn	Walsh	Professional Facilitators International
Martha	Macintyre	University of Melbourne
Martin	Angel	Southampton University
Maurice	Tivey	Woods Hole Ocean Institute
Mel	Togolo	Nautilus Minerals
Michael	Johnston	Nautilus Minerals BNE
Michael	Wright	Enesar Consulting
Naomi	Boughen	CSIRO
Paul	Lokani	The Nature Conservancy
Samantha	Smith	Nautilus
Shirley	Sombolok	Individual Community Rights Advocacy Forum
Stuart	Jones	Enesar Consulting
Susan	Yakip	Department of Environment & Conservation
Yvonne	Tio	Department of Environment & Conservation

Rabaul (16 March 2007)

Participant name		Organisation
Alison	Swaddling	Nautilus
Carol	Logan	Duke University
Jessica	Wiltshire	Coffey Natural Systems
Michael	Wright	Coffey Natural Systems
Patrick	Collins	Duke University
Samantha	Smith	Nautilus
Talina	Konotchick	Scripps Institution of Oceanography
Tony	O'Sullivan	Nautilus

San Diego (17-18 April 2008)

Participant name	Organisation
Carlos Neira	Scripps Institution of Oceanography
Cindy Lee Van Dover	Duke University
David Gwyther	Coffey Natural Systems
Greg Rouse	Scripps Institution of Oceanography
Guillermo Mendoza	Scripps Institution of Oceanography
Lisa Levin	Scripps Institution of Oceanography
Maurice Tivey	Woods Hole Oceanographic Institution
Mel Togolo	Nautilus Minerals PNG
Michael Wright	Coffey Natural Systems
Patrick Collins	Bangor University
Samantha Smith	Nautilus Minerals BNE
Steve Rogers	Nautilus Minerals BNE (via telephone)
Talina Konotchick	Scripps Institution of Oceanography

Brisbane Workshop (1-2 July 2008)

Participant name	Organisation
5 scientists	Duke University
Alison Swaddling	Nautilus Minerals BNE
Christian Mace	Nautilus Minerals BNE
Samantha Smith	Nautilus Minerals BNE

In addition to the above consultation programs, some groups presented pre-prepared lists of concerns. These groups included:

- New Ireland Environment Monitoring and Awareness Committee (NIEMAC Inc).
- The United Church.
- Utu High School students.



Cyclus is an EMAS certified stock
produced by Dalum Papir A/S, Denmark
Mill registration number DK-000023.

This material is printed on CPI Paper's (CyclusPrint matt/ Cyclus Offset), a 100% post-consumer recycled paper from Dalum Paper an EMAS accredited mill.
EMAS is the European Union's regulated environmental management scheme.